

**Universidad CEU San Pablo
CEINDO – CEU Escuela Internacional de
Doctorado**

PROGRAMA en CIENCIA Y TECNOLOGÍA DE LA SALUD



CEU

*Escuela Internacional
de Doctorado*

**Non-linear reaction and diffusion models
in partial differential equations with
applications to aerospace and
biomedical sciences**

TESIS DOCTORAL

Presentada por:
José Luis Díaz Palencia

Dirigida por:
Mariano Fernández López

MADRID
Año 2020



Este trabajo ha sido realizado en el departamento de Tecnologías de la Información dentro de la Escuela Politécnica Superior de la Universidad San Pablo CEU (Madrid), bajo la dirección del profesor Dr. Mariano Fernández López.

El Dr. Mariano Fernández López, director de este trabajo, expresa su conformidad para la presentación del mismo por considerar que reúne los requisitos necesarios y constituye una aportación original al tema tratado.

Fdo. Dr. Mariano Fernández López

TESIS DOCTORAL

José Luis Díaz Palencia

2020

A mi mujer, Belén, por su comprensión y su paciencia. A mis padres, José y María Jesús, y mi hermana, Esther, por su enorme apoyo en todos los proyectos. Y, a ti Daniel, por servir de luz.

Es imposible ser matemático sin ser un poeta del alma (S. Kovalévskaya).

Agradecimientos

La elaboración de una tesis doctoral es un proceso largo y complejo. Nos pone a prueba a muchos niveles tanto profesionales como personales. Desde los inicios de los planteamientos de los problemas que se tratan en esta tesis, siempre he encontrado el apoyo de muchas personas, y cuando, ha habido circunstancias difíciles siempre he podido contar con el inestimable apoyo de familia, compañeros y directores.

Un especial agradecimiento debo a mi director de tesis, el Doctor Mariano Fernández López, trabajador infatigable e investigador de una brillante inteligencia, quien con sus consejos y soporte, ha sido fundamental para que esta tesis pueda ver la luz y convertirse en una realidad, que espero, nos proporcione aún muchas más charlas.

Dar las gracias a todas las personas de la CEINDO que me han apoyado para llegar a buen puerto. Vuestra entrega y paciencia han sido y son un referente. En especial a las doctoras Coral Barbas, Antonia García y Marta Viana.

Agradecer también su enorme colaboración a mi tutor en la empresa, Juan Garbayo, quien ha sido capaz de ver más allá de su labor cotidiana, para apoyar una tesis doctoral que pretende dar respuesta a algunas de las preguntas de mayor calado en el diseño de sistemas en ingeniería. Gracias por tu excelente trabajo, tu rigurosidad hacia la ingeniería y tu capacidad para empatizar en todos los momentos que hemos tenido que afrontar.

Agradecer a todas las personas que han contribuido a mi formación como investigador, por sus charlas, sus consejos, sus principios y pensamientos. A todos de corazón, un enorme gracias.

Por último, y no menos importante, a mi familia. Ellos han sido el verdadero motor e impulso en los momentos difíciles. No puedo evitar acordarme de mi abuela cuando me decía “hijo no estudies tanto, que te

puedes volver loco”. Desde luego razón llevaba, algo de locura hay en el investigador de matemáticas aplicadas. A ella y a mis abuelos les debo la humildad como principio vital. A mis padres y a mi hermana, por su infatigable labor y paciencia, por educarme y velar por el cumplimiento de mis sueños y objetivos vitales. Un gracias enorme y emotivo a mi mujer, Belén, ella ha sido mi principal valedora y defensora, gracias por confiar en mí, por proporcionarme esa seguridad, serenidad, y ese tiempo, que prometo devolverte. Y a ti hijo, Daniel, darte las gracias por compartir mi tiempo día a día contigo, sin ti, nada sería igual.

Non-linear reaction and diffusion models in partial differential equations with applications to aerospace and biomedical sciences.

October 7, 2020

Resumen a modo de presentación

La modelización en ingeniería constituye un aspecto clave para entender el comportamiento de cualquier realidad. El ingeniero, habitualmente, emplea la lógica científica para la obtención de un modelo que permita predecir modos de funcionamiento en el sistema sujeto a estudio. Para los propósitos de la presente tesis, se referirán sistemas dentro de los ámbitos de la ingeniería biomédica y aeroespacial.

La ingeniería tiene como base epistemológica el acceso a las ciencias puras. En la presente tesis, se desarrollan modelos que otorgan peso a un ejercicio detallado de las matemáticas que los soportan. La descripción de un fenómeno físico en ingeniería es habitualmente complejo. Para el propósito de la tesis, se considera la complejidad en relación con el ser humano [1] como parte principal en la cadena procesual del ejercicio de modelado. Al fin y al cabo, el término complejidad es relativo al sujeto que define, cataloga y clasifica un problema. Sin olvidar esta perspectiva, los procesos de modelado en ingeniería han de clasificarse como, naturalmente, complejos al involucrar una gran cantidad de variables, de las que en muchos casos, se desconoce el comportamiento preciso de su dinámica. Aquí, se introduce el alcance y el contexto de la tesis presentada, entendidos como

el empleo de las ciencias matemáticas para la mejora del conocimiento de fenómenos de complejidad para el ingeniero.

Durante la tesis se ha observado una parcela del mundo exterior de interés, se ha construido un mapa mental del fenómeno observado, se han formado un conjunto de ecuaciones y se han resuelto los modelos en su forma conceptual para, posteriormente, llevar a cabo un ejercicio de calibración con la realidad observada. Además, se han explorado relaciones entre el mundo real y el mundo de las ideas y abstracciones. Al hacerlo, las matemáticas han proporcionado una visión simple, unitaria e intuitiva de la parcela a estudiar. Cualquier modelo matemático, cuyo objetivo sea servir de descripción de un fenómeno, debe ser probado en situaciones y actuaciones propias de su ámbito de aplicación. En la presente tesis se lleva a cabo un análisis de aplicación de las soluciones obtenidas matemáticamente a la realidad a estudiar (Anexo II), permitiendo así, cerrar el bucle de verificación de toda actividad científica aplicada a ingeniería.

Se presentan y analizan dos problemas de diferente naturaleza obtenidos mediante la observación de fenómenos de transporte de masa en los campos de la ingeniería biomédica y aeroespacial. Los modelos presentados están embebidos dentro de la teoría matemática de ecuaciones diferenciales en derivadas parciales con términos de difusión no lineales y de reacción *no lipschitzianos*. Dichos modelos tienen como objetivos arrojar luz en procesos de depredador - presa (especie invasora - especie invadida) en sistemas biológicos, el comportamiento de la dinámica de gases para producir atmósferas inertes en tanques de combustible de aeronaves y en la descripción de los fenómenos dinámicos de transporte en la descarga de agentes extintores para la supresión de fuegos en entornos aeroespaciales.

Una vez que se obtienen y justifican los modelos y sus ecuaciones rectoras, el objetivo se centra en resolver y discutir aspectos relevantes sobre las soluciones, a saber: existencia, unicidad, comportamiento asintótico, características propias y soluciones aproximadas o exactas. Además, para cada uno de los dos modelos planteados, se ha llevado a cabo una colaboración con el grupo Airbus para su aplicación en los sistemas de aeronaves citados.

Durante la elaboración del presente documento, se ha realizado un estudio exhaustivo del estado del arte en modelos de difusión y transporte de masa. Los detalles de tal estudio se mencionan a lo largo de la tesis

con el objetivo de demostrar las mejoras en el conocimiento que supone el ejercicio llevado a cabo. Las ecuaciones que se tratan en cada uno de los apartados correspondientes presentan novedades en el marco de la teoría de ecuaciones en derivadas parciales no lineales. Dichas novedades han surgido de la aplicación de las ciencias formales a la realidad a modelar, es decir, se plantean ecuaciones con un sentido intrínseco de aplicación. Además, se encuentran aproximaciones nuevas en la forma de tratar y modelar los fenómenos de transporte en sistemas de inertización de tanques de combustible y de supresión de fuego en aviones, con el objetivo de soportar procesos más eficientes en las fases de concepción, dimensionado y diseño de aeronaves.

Introduction

During the last century, the Partial Differential Equation theory has been used to model biological systems where reaction and diffusion are relevant [2]. The introduction of the diffusion in the biological models permits describing the random transfer of mass (usually expressed as a mass density or concentration of species per unit of volume) in the domain of interest. Furthermore, the introduction of the reaction term permits to describe the rate of production or vanishing of the involved species (for a definition of a diffusive process see Section 4).

The interaction between diffusion and reaction appears in areas such as chemistry kinetics, fluids engineering or biological population dynamics, where reaction-diffusion models have been used to understand the behaviour of tumor growth, leukemia or atherosclerosis [2]. It is to be highlighted that the work developed in this memory is according to the state of the art and in line with the recent discoveries and researching areas in biomathematics [2]. The main novelty relies on the non-linearities considered, that introduce non-regularity (understood as a lack of the Lipschitz condition or as a generalization of the diffusion through a Porous Medium Equation). This fact can be interpreted as a way to model complex interactions in biology and engineering. The problems review compiled in [2] reflects equations where the Lipschitz condition in the reaction term is met or where the diffusion follows the classical second order Fick law. It is shown that the regularity of the solutions is met under the classical parabolic scope.

In the 1930s, Fisher [6], proposed the first reaction-diffusion model to understand the interaction process of genes. In parallel, Kolmogorov, Petrovskii and Piskunov [7] proposed the same equation in combustion theory. Such proposed equation, referred in the literature as KPP-Fisher, is of the form:

$$\frac{\partial u}{\partial t} = \frac{\partial^2 u}{\partial x^2} + u(1 - u), \quad (0.1)$$

where u represents the genes concentration in the Fisher models and the fuel concentration in the Kolmogorov, Petrovskii and Piskunov combustion theory. The non-linearity is given in the reaction term $u(1 - u)$, while the diffusion ($\partial^2 u / \partial x^2$) is linear. The duple (x, t) represents the classical spatial and temporal independent variables.

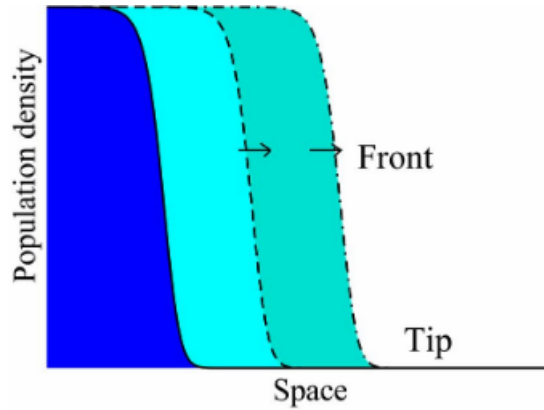


Figure 0.1: Travelling wave (TW) solution description (courtesy of MR Evans [9])

The kind of solutions studied by the cited authors are called Travelling Waves (represented as well by the siglum TW. See Section 4 for a definition of a TW profile solution) and are of the form:

$$u(x, t) = f(\xi), \quad \xi = x - at, \quad (0.2)$$

where a represents the travelling wave speed. This kind of solutions are formed by a front and a tip (Figure 0.1). The front carries the information transition in the media from one state to other. In the case of biological invasion problems, the front shifts the concentration of the populations affected in the media. In addition, the tip constitutes the adaptation of the front solution to the equilibrium state (in Figure 0.1 the equilibrium is given by the solution $u = 0$).

After the paramount formulation by Fisher and Kolmogorov, *et al*, other researchers studied the KPP-Fisher model with applications in biology, chemistry and medicine. As an example we can refer to the study of random movements of biological populations by Skellam [8]. This thesis is heirless of the Fisher theory and the Skellam studies for life sciences, in the sense that we aim to apply partial differential equation techniques to understand the dynamic of biological populations in a given media.

The models provided in this thesis can be applied to other fields of engineering or science. It suffices to consider the searched solutions as concentration of any substance subjected to study: This is the case of the fire prevention and extinguishing systems where gases concentrations are analyzed to avoid the formation and propagation of a fire or the combustion

theory to study the kinetics of the involved substances. In the aerospace sector, the fire prevention and extinguishing technology requires accurate models to ensure the safety of the involved designs.

Practically, the aim of this thesis is to define and obtain results about the solvability of different models to understand, characterize and predict the dynamic of concentration species (either biological agents or gas substances) in a global medium where convection and diffusion or diffusion alone are of importance.

To illustrate the relevancy of our study within the aerospace perimeter, we highlight that there are plenty of general, and relatively simple models in the engineering world dealing with diffusion. Ghadirian *et al.* [10] establish the state-of-the-art for simulating a diffusion process of the fuel vapors in the airspace of a fuel tank, such diffusion is governed by the classical parabolic homogeneous equation:

$$\frac{\partial C_f}{\partial t} = D \frac{\partial^2 C_f}{\partial z^2}, \quad (0.3)$$

where C_f is the fuel concentration in the air, and z is the vertical coordinate. We remark that this problem considers only the diffusion, disregarding the natural convection terms and reaction or absorption phenomena. The diffusion models, given in this thesis, represent an advance; as convection and non-linear (non-Lipschitz) reaction and absorption are considered.

As mentioned, this memory presents several equations, for which, a search of solutions is envisaged under the umbrella of the partial differential equations techniques for parabolic and porous media operators. In addition and for completeness, this thesis does not forget the applications to biology and engineering, which is the main motivation for each fit-for-purpose model derivation. Such derivation is based on the physic principles, the experience and the engineering judgement. In any of the cases, we do not compromise the generality and rigour of the mathematics involved and the ending results; on the contrary, we try to show a synergy between applications and mathematics towards the resolution of complex models of interest for biology and aerospace engineering. The resolutions pay attention to those results of relevancy for the engineers and scientist who are mainly interested in explicit solutions given either in analytical or graphical forms. The scope of this memory is mainly, but not limited, mathematical; in the sense that the

results shall be read considering the potential applications. In each of the problems involved, we will provide evidences and examples (for each of the models in the summary chapter) about the potentialities to serve as a reference for engineers and scientists searching for mathematical results for reaction-diffusion problems in their area of expertise.

We would like to remark the importance of following the approach and the results of this thesis with a real scenario extracted from the aerospace industry: the fire prevention and extinguishing processes are evident for the safety of any aircraft operation. The fire, in an aeroplane, may lead to catastrophic consequences involving human fatalities. One of the most studied accidents happened on July-1996 on a Boeing 747 operating between New York and Paris [11]. After take-off, the aircraft exploded. The American Federal Aviation Administration, through the National Transportation Safety Board, was in charge of the investigations to clarify the origin of such explosion. Four years after, it was concluded that the most probable root cause was related to the explosion of the aircraft centre fuel tank due to the proximity of the heat generated by the air conditioning packs [11].

The results of this investigation changed the mentality of the aerospace designers that, since then and currently, must take into account an aircraft design providing means towards explosion prevention, fire avoidance and fire extinguishing [12]. In addition, it has been promoted the possibility of removing the oxygen from a fuel tank to avoid any hydrocarbon combustion [12]. One of the solutions raised for this purpose, of relatively new implementation in the aerospace sector, is the inerting system that is thought to fall within the category of fire prevention [13]. As a short description, the inerting system consists of a filter that is capable of separating the nitrogen and oxygen present at the air. The nitrogen is introduced into the fuel tank while the oxygen goes outboard. The nitrogen is suitable to produce a inert atmosphere, since it does not support the hydrocarbon combustion reaction, is non-reactive with the materials used in the fuel tanks components and is not toxic neither for maintenance personnel nor passengers. The inerted atmosphere prevents the possibility of nucleating a fire as, in case of an electrical spark in any in-tank equipment, there is not sufficient oxygen concentration to produce and sustain a combustion process. The model to predict the behaviour of the interaction process between the nitrogen and oxygen is dealt in Chapter 1.

Additionally, the aerospace sector has the need of using high power turbomachinery (engines and auxiliary power units) that, in case of a failure, may produce a fire. To avoid any risk to the occupants, any fire shall be extinguished by automatic or manually activated fire suppressors. The areas of fire extinguisher discharge are, typically, very complex with plenty of mechanical equipment, pipes, computers and sensors installed; this is the case of, for instance, the engine nacelles. Currently, the models used in the fire suppressor discharge process employ linear diffusion [14], nonetheless, we try to fit our models to a more realistic approximation through a non-linear diffusion in the form of a Porous Medium Equation. This is the purpose of Chapter 2.

We stress the fact that the model we have developed in Chapter 2, involving a Porous Medium Equation, has been implemented in the aerospace industry (Annex II). The analysis performed based on the PME equation, reflects accurate results in the proximity of complex geometries where the extinguishing agent dynamic is modelled with a non-linear diffusion compared to the frequently used linear diffusion.

Eventually, It is highlighted that this thesis consists of mathematics and the results are oriented to engineering and biological applications. We never lose the mathematical rigour and the application of modern techniques raised to work with non-linear parabolic differential equations.

Contents

1	Coupled System of reaction and absorption with convection and diffusion equations	13
1.1	Description and objectives	13
1.2	Summary	24
1.3	Existence	26
1.4	Global solutions	47
1.5	Uniqueness	50
1.6	Comparison of solutions	54
1.7	On global and local solutions	62
1.8	Evolution of solution profiles	78
1.9	Travelling Waves (TW)	91
1.10	TW profiles	92
2	Existence, evolution of solutions and finite propagation for a PME problem with a reaction of the form $x ^\sigma u^p$, $\sigma > 0$ and $p < 1$	103
2.1	Description and objectives	103
2.2	Summary	111
2.3	Source-type solutions and comparison of the Heat Equation versus the Porous Medium Equation	115
2.3.1	Heat Equation source-solution	115
2.3.2	Porous Medium Equation source-solution	118
2.3.3	Comparison of the fundamentals solutions for the HE and PME	122
2.4	Initial data growing condition	124
2.5	The Lipschitz Problem	126
2.6	The non-Lipschitz problem	133
2.6.1	Discussion about types of solutions	137

2.6.2	Precise minimum order of growth. A selfsimilar approach.	140
2.6.3	Uniqueness	149
2.6.4	Comparison of solutions	162
2.7	Finite Propagation	169
3	Conclusions and future lines of research	174
4	Some Useful Definitions	179

List of Figures

0.1 Travelling wave (TW) solution description (courtesy of MR Evans [9])	5
1.1 Media, where the process occurs, schematic representation .	19
1.2 Travelling Wave evolution for $c + a = 4$ corresponding to $n = 0.9$ and $m = 0.1$. For convenience $d = 2$. The horizontal axis represents the TW independent variable $\xi = x - at$	98
1.3 Travelling Wave evolution for $c + a = 4$ corresponding to $n = 0.9$ and $m = 0.1$. For convenience $d = 2$. It is possible to see the sub-evolution f_{1m} as solution for the problem (1.358). The horizontal axis represents the TW independent variable $\xi = x - at$	98
1.4 Travelling Wave evolution for $c + a = 4$ corresponding to $n = 0.9$ and $m = 0.1$. For convenience $d = 2$. It is possible to see the sub-evolution f_{2m} as solution for the problem (1.358). The horizontal axis represents the TW independent variable $\xi = x - at$	99
1.5 Travelling Wave evolution for $c + a = 4$ corresponding to $n = 0.2$ and $m = 0.9$. For convenience $d = 2$. The horizontal axis represents the TW independent variable $\xi = x - at$	99
1.6 Travelling Wave evolution for $c + a = 4$ corresponding to $n = 0.2$ and $m = 0.9$. For convenience $d = 2$. It is possible to see the sub-evolution f_{1m} as solution for the problem (1.358). The horizontal axis represents the TW independent variable $\xi = x - at$	100
1.7 Travelling Wave evolution for $c + a = 4$ corresponding to $n = 0.2$ and $m = 0.9$. For convenience $d = 2$. It is possible to see the sub-evolution f_{2m} as solution for the problem (1.358). The horizontal axis represents the TW independent variable $\xi = x - at$	100
2.1 The tank 2 is the source of nitrogen concentration u that invades the tank 1 through the interfacing wall.	106

2.2	The source-type evolution solution for the Heat Equation. It is to be highlighted the positivity condition everywhere. (Source reference [33])	118
2.3	The source-type evolution solution for the Homogenous PME. It is to be highlighted the non-negativity everywhere. (Source reference [33])	122
2.4	The function $f_\delta(s)$ is used to approximate the non-Lipschitz problem by a Lipschitz one. Note that in the limit $\delta \rightarrow 0$, we recover the original non-Lipschitz term	134

1 Coupled System of reaction and absorption with convection and diffusion equations

1.1 Description and objectives

Our main objective in this chapter is to derive the set of equations, for which we think about the application to an industrial problem related to the fire prevention technologies and, afterwards, to a biological interaction.

As presented, the fire prevention technology is known as inerting system. This technology consists on removing the oxygen from the fuel tanks and replacing it by nitrogen; this gas is well-known to be non-ignitable.

Let us think on a fuel tank with a certain quantity of fuel and air space. We introduce nitrogen that will evolve in the air space replacing the oxygen and making any combustion process impossible. The nitrogen enters the tank through small nozzles (of the order of 2 cm in diameter) and provokes the oxygen to exit via the fuel tank vents outboard.

We can think, as well, on a invasive-invaded biological system. Let consider a domain in which a specie is living in perfect equilibrium. This means that the rate of life and death and the carrying media capacity are balanced to keep the population constant. At some moment, we introduce a new specie that feeds on the already existing one. In addition, and with a filter or similar device, we remove from the media the death species while we continue introducing the new specie at a given rate, motivating the presence of convection. There are other sources of convection in biological media such us the effect of the gravity or the super-population of cells that may push one cell into the other leading to pressure differences.

Another area of application where the set of equations, derived in this chapter, is applicable is related to the biological invasion problem. According to the Convention of Biological Diversity, the biological invasion is defined as:

"Those alien species which threaten ecosystems, habitats or species."
(page 1, Chapter 1 of [5])

It is particularly relevant, in the biomedical field, to study the cancer invasion or metastasis; both understood as the penetration of the cancer cells

into close organs (invasion) and the propagation of the cells through the circulatory or lymphatic systems (metastasis). Under the cancer study perimeter, we can consider our reaction-diffusion with convection model as a way to understand the physical interaction between healthy and cancer cells.

This kind of described problems with several inputs and several outputs are governed by the so-called mass conservation principle. In our case, the variables involved are the nitrogen quantity and the oxygen quantity (for the fire prevention application) and the new specie, as input, and the old specie, as output, in the biological application. We consider that the involved media, in both cases, has a fixed volume, therefore our searched solutions will be:

- For the industrial application: the nitrogen concentration per unit volume (called u) and the oxygen concentration per unit volume (called v).
- For the biological application: the invasive, new specie or cancerous cells concentration per unit volume (called u) and the invaded existing specie of healthy cells concentration per unit volume (called v).

It is important to consider the following simple dynamic process based on the observation, experience and judgement:

The quantity of nitrogen or invasive specie always increases. At the beginning of the process, the nitrogen or invasive time increasing rate is qualitatively and relatively high, nonetheless, as the time evolves, the saturation of the media, due to the decreasing quantity of oxygen or invaded specie and the increasing quantity of nitrogen or invasive specie, makes the time rate of the nitrogen or invasive concentration to decrease, but still positive. This can be modelled by considering the following rate of change:

$$u_t = hv^n, \quad (1.1)$$

where $n \in (0, 1)$ is a parameter, that shall be tailored for each particular application, and h is a proportionality constant that will be considered as $h = 1$.

Additionally, the oxygen or invaded concentration reduces with the time evolution. This decreasing rate is relatively high at the beginning of the process, nonetheless, when the nitrogen or invasive concentration increases,

the oxygen rate reduces due to the reduction of the nitrogen or invasive rate. Thus, we read:

$$v_t = -j u^m, \quad (1.2)$$

where $m \in (0, 1)$ is an adjustable parameter depending on the application and j is a proportionality constant that will be considered as $j = 1$.

This, a priori, simple dynamic-interaction between species shall be used during our model derivation process in the form of reaction (v^n) and adsorption ($-u^m$). We can positively say that our species to characterize are two functions $u(x, t)$ and $v(x, t)$ where $t \in (0, \infty)$ and $x \in \mathbb{R}^N$ ($N = 1, 2, 3$).

To derive the equations of our model, we employ the conservation law assuming a virtual sub-domain $\Omega \in \mathbb{R}^N$, where we can say that the rate of change of any of the both concentrations, (u, v) , is equal to the flux across the borders of the postulated virtual sub-domain Ω plus or minus the reaction and absorption independent forcing terms.

Let us consider that the vectors $\Phi_u \in \mathbb{R}^N$ and $\Phi_v \in \mathbb{R}^N$ represent the local concentration flux per unit time and per unit area through the borders ($\partial\Omega$) of the sub-domain Ω . Let the vector $\Pi \in \mathbb{R}^N$ to be the local normal vector to the same boundaries $\partial\Omega$ and let consider that the term $S_u(u, v, x, t)$ represents the reaction of nitrogen gas or invasive specie per unit volume and per unit time and $S_v(u, v, x, t)$ the absorption function to characterize the oxygen or invaded specie per unit volume and per unit time.

The engineering and biological applications of this problem accompanied with the observations, make us to consider that the functions Φ_u , Φ_v , S_u and S_v are continuous in the spatio-temporal variables and with continuous derivatives as well. Note that we require the solutions $u(x, t)$ and $v(x, t)$ to be distributed homogeneously in the domain so that any evolution, under the regular parabolic operator is continuous (see Theorems 2.1 and 2.2 in Chapter 7 of [26] for the regularity of the parabolic operator). Thus, we have:

$$\frac{d}{dt} \int_{\Omega \in \mathbb{R}^N} u \, dx = - \int_{\partial\Omega \in \mathbb{R}^{N-1}} \Phi_u \cdot \Pi \, ds + \int_{\Omega \in \mathbb{R}^N} S_u(u, v, x, t) \, dx, \quad (1.3)$$

$$\frac{d}{dt} \int_{\Omega \in \mathbb{R}^N} v \, dx = - \int_{\partial\Omega \in \mathbb{R}^{N-1}} \Phi_v \cdot \Pi \, ds + \int_{\Omega \in \mathbb{R}^N} S_v(u, v, x, t) \, dx. \quad (1.4)$$

Now, we need to relate the vector fluxes with the concentrations u and v . For this purpose, we make use of the Fick law that establishes the functional relation:

$$\Phi_u = -\delta \nabla u - cu, \quad \Phi_v = -\epsilon \nabla v - cv, \quad (1.5)$$

where $\delta = \epsilon$, as they represent the diffusion effect of the interacting species in each other and

$$c \in \mathbb{R}^N, \quad (1.6)$$

represents the forced flow given in the medium.

Therefore, we have:

$$\frac{d}{dt} \int_{\Omega} u \, dx = - \int_{\partial\Omega} (-\delta \nabla u - cu) \cdot \Pi \, ds + \int_{\Omega} S_u(u, v, x, t) \, dx, \quad (1.7)$$

$$\frac{d}{dt} \int_{\Omega} v \, dx = - \int_{\partial\Omega} (-\epsilon \nabla v - cv) \cdot \Pi \, ds + \int_{\Omega} S_v(u, v, x, t) \, dx. \quad (1.8)$$

And making use of the divergence theorem, we have:

$$\begin{aligned} \int_{\partial\Omega} (-\delta \nabla u - cu) \cdot n \, ds &= \int_{\Omega} \nabla \cdot (-\delta \nabla u - cu) \, dx \\ &= \int_{\Omega} (-\delta \nabla \cdot (\nabla u) - c \cdot \nabla u) \, dx, \end{aligned} \quad (1.9)$$

$$\begin{aligned} \int_{\partial\Omega} (-\epsilon \nabla v - cv) \cdot n \, ds &= \int_{\Omega} \nabla \cdot (-\epsilon \nabla v - cv) \, dx \\ &= \int_{\Omega} (-\epsilon \nabla \cdot (\nabla v) - c \cdot \nabla v) \, dx. \end{aligned} \quad (1.10)$$

Then, we have:

$$\frac{d}{dt} \int_{\Omega} u \, dx = - \int_{\Omega} (-\delta \Delta u - c \cdot \nabla u) \, dx + \int_{\Omega} S_u(u, v, x, t) \, dx, \quad (1.11)$$

$$\frac{d}{dt} \int_{\Omega} v \, dx = - \int_{\Omega} (-\epsilon \Delta v - c \cdot \nabla v) \, dx + \int_{\Omega} S_v(u, v, x, t) \, dx. \quad (1.12)$$

Without loss of generality, and for simplification in the problem formulation, we make:

$$\epsilon = \delta = 1. \quad (1.13)$$

Note that, we will recover, later, the diffusion coefficient ϵ and δ at the moment of formally enunciating and naming the problem.

As the integrals in the left hand side are performed considering the spatial domain, we can introduce the d/dt into the integral. In addition, we have shown, in equations (1.1) and (1.2), that $S_u(u, v, x, t) = v^n$ and $S_v(u, v, x, t) = -u^m$ with $n, m \in (0, 1)$; therefore, we arrive to:

$$\begin{aligned} u_t &= \Delta u + c \cdot \nabla u + v^n, \\ v_t &= \Delta v + c \cdot \nabla v - u^m, \end{aligned} \quad (1.14)$$

$$n, m \in (0, 1).$$

It is to be stressed, now, an analysis on the initial conditions. Normally, in the engineering and biological applications in which we want to make use of our model, the initial conditions are positive and given by a constant quantity homogeneously distributed in the domain. We can say:

$$u_0(x) = u_0 > 0, \quad v_0(x) = v_0 > 0, \quad (1.15)$$

which can be generalized by stating:

$$u_0(x), v_0(x) \in \mathbb{L}_{loc}^1(\mathbb{R}^N) \cap \mathbb{L}^\infty(\mathbb{R}^N). \quad (1.16)$$

Given the regularity of the involved parabolic operator (Theorems 2.1 and 2.2 in Chapter 7 of [26]), we proceed considering that the solutions follow a monotone behaviour, increasing or decreasing, in our domain. Nonetheless, the solutions monotone properties, in particular the non-decreasing behaviour of u , are controlled and governed by the sub-linear reaction term $S_u(u, v, x, t) = v^n$, $n \in (0, 1)$. For both reaction terms, the most general

condition that we can require to the solutions is:

$$u(x, t), v(x, t) \in \mathbb{L}_{loc}^1(\mathbb{R}^N). \quad (1.17)$$

Nonetheless, we will show in Chapter 1.3 that solutions can be expressed as continuous functions.

Another important discussion to hold is related to the boundary set of conditions. It may look as lack of rigour to work in the domain \mathbb{R}^N , even when we know that any media (for instance a fuel tank, in the aerospace application) is a finite volume in the space. Nonetheless, we can argue as follows: the kinematic boundary condition related to the non-slip phenomena and slip phenomena suggests that the velocity variations are concentrated in the proximity of the borders, while if we are far from that border, the domain behaves free with minor influence of the boundary conditions. In addition, the kinematic of the species is not of great relevance for us because we admit to know the influence and behaviour of convective effect (thanks to the vector c), and more particularly, the effect of such convection into the concentrations (u, v) constituting our searched solutions. We admit, then, that the concentration of any of the species is supposed to be non-influenced by the tank boundaries. Thus, we can summarize by stating that we are interested in understanding the dynamic associated to the solutions at the core of the domain (sufficiently large as to consider \mathbb{R}^N) not affected by the domain borders.

It is remarkable to highlight that the specific geometry of the media and boundaries affects the convective term. Indeed, it is possible to estimate simply the magnitude of the convection by considering the area of a cross-section of the media (see Figure 1.1) and applying the mass continuity equation to have:

$$c = \frac{dm/dt}{\rho A_T}, \quad (1.18)$$

where dm/dt , ρ and A_T are the mass flow, the density and the media cross-section. The three parameters are known data for any given problem. For the case of an inerting process for a fuel tank, the mass flow is provided by the nitrogen flow entering into the tank, the dimensions are known and the density, ρ , corresponds to the density of each of the gases constituting the gas mixture. In case of air, the predominant components are the nitrogen and the oxygen.

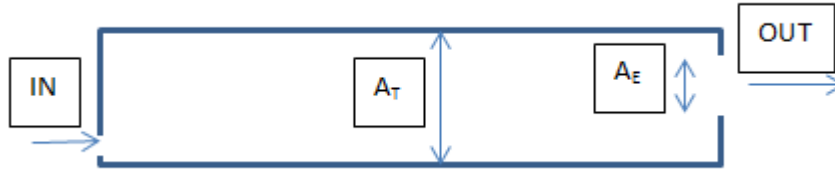


Figure 1.1: Media, where the process occurs, schematic representation

Additionally, we formulate a different, but related model to deal with solutions mainly affected by the evolution or propagation of a profile connecting two stationary solutions (this is the case of the travelling waves [2]). In this sense, we will obtain a tendency of our species to stationary solutions. It is remarkable to say that the solutions shall satisfy the following monotone conditions:

$$u_t \geq 0; \quad v_t \leq 0. \quad (1.19)$$

Therefore and considering the propagation towards stationary solutions, the following system will be analyzed:

$$\begin{aligned} u_t &= \Delta u + c \cdot \nabla u - v^n(u - d), \\ v_t &= \Delta v + c \cdot \nabla v - u^m v, \\ n, m &\in (0, 1), \end{aligned} \quad (1.20)$$

$$u_0(x), v_0(x) \in \mathbb{L}_{loc}^1(\mathbb{R}^N) \cap \mathbb{L}^\infty(\mathbb{R}^N),$$

where $d \geq \max_{x \in \mathbb{R}^N} \{u_0(x)\}$ or $d \geq u_0$ in case of a constant initial data.

One can see that two stationary solutions are:

$$u = d; \quad v = 0. \quad (1.21)$$

Then, starting from a initial condition, the solution u will evolve towards the stationary solution

$$u = d, \quad (1.22)$$

from below, and then, the forcing term

$$-v^n(u - d), \quad (1.23)$$

is positive, while the solution v will decrease towards the stationary solution

$$v = 0, \quad (1.24)$$

as the forcing term given by

$$-u^m v, \quad (1.25)$$

is negative.

In the biological application, the stationary solutions represent a situation in which the invasive (u) wins over the invaded (v) ending in the stationary solutions $u = d$ and $v = 0$. The travelling waves are the connection of the initial conditions to the stationary solutions $u = d$ and $v = 0$. One potential application of this model is related to the cancer evolution in a human organ. If we consider that the function u represents the cancerous cells and v the healthy cells; the evolution starts from a certain quantity of cancerous cells in the organ and ends in a situation in which the concentration of cancerous cells leads to the organ death. This killer concentration can be considered as the stationary solution $u = d$.

In the industrial fuel tank application, the stationary solutions $u = d$ and $v = 0$ are the natural evolution of the problem, since it is known that the quantity of nitrogen cannot increase without any limit as the tank volume is finite and the tank pressure cannot exceed its structural limit by simply adding quantity of nitrogen. Our aim is, then, to study the propagation profile of the travelling waves. The propagation is studied once the system is free to evolve from the initial conditions up or down to the equilibrium solutions.

As already said, this thesis provides the mathematical approach and results that can be used by any engineer or scientist with a mathematical background. In addition and, as an example, we present here the scope of what it can be considered as an engineering problem to be solved with the results of this thesis:

It is known by the aerospace industry (table 5 in [17]) that a level of 93% of Nitrogen (or 7% of oxygen) in a fuel tank is enough to avoid having a risk of fire in case of any spark or extreme heat generated by surrounding

machinery are given. In the military applications, it is allowed up to a level of 9% of oxygen and 91% of nitrogen [18]. We remind that the initial air presented in the fuel tank is a mix mainly form of a 80% of nitrogen and 20% of oxygen. Thus, the problematic to solve is related to the required time to pass from the initial concentration of 80% of nitrogen up to the 93%. The current technology is based on filtering and separating the oxygen from nitrogen introducing the nitrogen in the fuel tank and exiting the oxygen outboard. This technology permits reaching an estimated value of 96% of nitrogen (Figure 5 in [19]). It is not possible to get a value corresponding to the 100% of nitrogen in the fuel tanks with the filtering techniques in use nowadays. Therefore, we can consider, as stationary solutions, the concentrations corresponding to a level of 96% of nitrogen and 4% of oxygen. The question is, then, formulated as:

How much time is required to reach 93% of nitrogen and 7% of oxygen when starting from a initial air mix of 80% of nitrogen and 20% of oxygen?

The answer to this question can be obtained by application of a propagation kind of solution. This is the case of the travelling waves that will be treated in Section 1.10. The travelling waves permit studying the profile evolution from a given initial data up to the stationary conditions. Let consider the intersection of the growing front with a value of 93% of nitrogen when evolving to the stationary condition (see Figures 1.2 and 1.5). Note that the travelling wave independent variable is given by

$$\xi = x \cdot n_d - at, \quad (1.26)$$

where n_d is a unitary vector in \mathbb{R}^N that defines the travelling wave propagation direction, and a is the travelling wave speed. For convenience, we consider that

$$n_d = (1, 0, \dots, 0), \quad (1.27)$$

then

$$x \cdot n_d = x \in \mathbb{R}. \quad (1.28)$$

Operating in the travelling wave variable, we determine the value $\xi = \xi_1$ corresponding to the 93% level of nitrogen evolution. Then, for a travelling wave speed a to be determined (Section 1.10), we have a relation of the

form:

$$\xi_1 = x - at \rightarrow t = \frac{x - \xi_1}{a}. \quad (1.29)$$

Therefore, for each tank location given by the variable $x \in \mathbb{R}$, it is possible to obtain a time t value to ensure the preventive protection against a fire given by the 93% level of nitrogen concentration.

Additionally, we can consider conservatively the largest tank dimension given by the diagonal D of such tank to obtain a simple time estimation:

$$t = \frac{D - \xi_1}{a}. \quad (1.30)$$

This simple example is only to illustrate the mentality that has motivated this thesis. The results are obtained thinking in future applications and it is, in fact, a final objective to implement the results obtained from this memory into engineering problems raised in the industry (Annex II), in biomedical engineering or bio-physics.

Before proceeding further in this work, we summarize the problems that will be studied in this thesis. Note that we recover, the diffusion coefficients ϵ and δ :

Problem P :

$$\begin{aligned} u_t &= \delta \Delta u + c \cdot \nabla u + v^n, \\ v_t &= \epsilon \Delta v + c \cdot \nabla v - u^m, \\ n, m &\in (0, 1), \end{aligned} \quad (1.31)$$

$$u_0(x), v_0(x) \in \mathbb{L}_{loc}^1(\mathbb{R}^N) \cap \mathbb{L}^\infty(\mathbb{R}^N).$$

Problem P_T :

$$\begin{aligned}u_t &= \delta \Delta u + c \cdot \nabla u - v^n(u - d), \\v_t &= \epsilon \Delta v + c \cdot \nabla v - u^m v, \\n, m &\in (0, 1),\end{aligned}\tag{1.32}$$

$$u_0(x), v_0(x) \in \mathbb{L}_{loc}^1(\mathbb{R}^N) \cap \mathbb{L}^\infty(\mathbb{R}^N).$$

1.2 Summary

First of all, we focus our attention on the problem P . We start by studying the associated Cauchy problem, i.e; the existence and uniqueness of solutions as a way to ensure that our equations are capable of producing representative solutions. For this purpose, we define and show the existence of two pairs of solutions, that will be referred as supersolutions or upper solutions (\hat{u}, \hat{v}) and subsolutions or lower solution (\tilde{u}, \tilde{v}) . We require the basic regularity condition for each of the functions, such that

$$\hat{u}, \hat{v}, \tilde{u}, \tilde{v} \in C^{2+\gamma, 1+\gamma/2}(\mathbb{R}^N \times (0, T)), \quad (1.33)$$

where $C^{2+\gamma, 1+\gamma/2}$ refers to the $(2 + \gamma)$ Hölder norm of u , u_x and u_{xx} and the $(1 + \gamma/2)$ Hölder norm of u and u_t (idem for v).

We show that the upper solutions and the lower solutions define a band with smooth boundaries such that any solution is located in.

Afterwards, we define and proof the existence of ordered monotone sequences of upper and lower solutions $(\hat{u}^{(k)}, \hat{v}^{(k)})$ and $(\tilde{u}^{(k)}, \tilde{v}^{(k)})$, so that in the limit with $k \rightarrow \infty$, they converge to a solution for P , in virtue of to the dominated converge theorem (Theorem 1.4.49 in [15]). This analysis is provided in Section 1.3.

Additionally, we show the existence of global solutions to the problem P in Section 1.4 . This proof is relevant to determine the non-existence of blow-up in finite time due to the accumulated effect of the non-linear reaction terms.

Afterwards, we make use of the Duhamel's principle for representing the problem P and the fixed point theorem to proof local existence of a unique point in the operator $\Psi(U)$ defined in accordance with Duhamel. This analysis permits to show the existence of a unique solution to the problem P permitting, then, to conclude the correct mathematical formulation of the set of equations in P . This analysis is shown in Section 1.5.

Another interesting aspect is the existence of a comparison principle locally for single spatial and time variables. The comparison principle permits to ensure that if one solution is higher than the other, it will keep the order during the evolution locally. This analysis is performed in Section 1.6.

We provide evidences about the properties of global and local solutions

in Section 1.7. Firstly, we provide a compatibility condition between the initial data and the convection effects presented in the set of equations for the problem P . Our concern is focused on obtaining solutions that preserve the searched monotony properties with time ($u_t \geq 0$; $v_t \leq 0$) for different levels of convection. It is to be stressed that a strong convection can lead to minimize the effect of the absorption and reactions terms acting over the given initial data, leading to jeopardize the monotony properties.

Afterwards, and in the same Section 1.7, we make use of the self-similar kind of solutions to determine local spatial distributions of the solutions for each given time $t > 0$. For this purpose, we define a subsolution for the concentration u and a supersolution for the concentration v . In addition, we provide a bound for the solution u , locally, for $t \leq \tau$ and $|x| \leq R$. These results are particularly useful for our objectives. The population u represents the concentration of nitrogen, which is required at a certain level to reach a non-ignitable atmosphere in the fuel tank. Indeed, having a subsolution for u implies to have an under-estimation of the quantity of nitrogen. This is overly conservative; we only need to keep the time evolving until the concentration of nitrogen reaches the required values for a non-ignitable condition. Additionally and in the same section, we obtain a maximal bound for u which gives us an indication of the maximum value of nitrogen accepted in our spatial domain. In the same way, we provide a sub-evolution for the concentration of oxygen v .

In Section 1.8, we provide a precise evolution of the solutions, for different approximations to the lower solution for the concentration v . The estimation of the precise evolution is strongly coupled and it is required to postulate a sub-evolution for the concentration v to obtain the searched evolution profiles.

After the study of the problem P , we move on to study the problem P_T in Section 1.9. For the problem P_T , we show the existence of solutions. Afterwards, we study a particular sort of solutions referred as travelling waves (TW), where we show the existence of TW-speeds motivating the propagating wave to be positive and to converge to the stationary solutions $u = d$ and $v = 0$.

1.3 Existence

The existence of solutions may seem to be of mathematical interest only. Nowadays, the numerical analysis permits to solve a wide variety of equations, leading to think that the only representative solution is that derived from the numerical results without questioning if solutions do exist. Indeed and in some cases, solutions may not exist and, hence, numerical analysis does not provide clear results (several examples are provided in [3]). In order to avoid such described situations, we study, firstly, if our proposed model has existence of solutions making use of novel Partial Differential Equations techniques. Conclusively, a consistent and appropriate analysis of any equation and model shall start with an approach to the existence of solutions.

Firstly and before proceeding with the existence related lemmas and theorems, we show the norm in which we are going to operate. Given two functions u and $v \in \mathbb{L}^1(\mathbb{R}^N)$, we define the norm as:

$$\|(u, v)^T\| = \|u\| + \|v\|. \quad (1.34)$$

Let define U_1 and U_2 as:

$$U_i = (u, v)^T \quad i = 1, 2. \quad (1.35)$$

We show that the triangular property is met for the defined norm:

$$\begin{aligned} \|U_1 + U_2\| &= \|(u_1, v_1)^T + (u_2, v_2)^T\| = \|(u_1 + u_2, v_1 + v_2)^T\| \\ &= \|u_1 + u_2\| + \|v_1 + v_2\| \leq \|u_1\| + \|u_2\| + \|v_1\| + \|v_2\| \\ &= \|U_1\| + \|U_2\|. \end{aligned} \quad (1.36)$$

Note that we have requested, for each of the component functions u_i, v_i , to be in the space $\mathbb{L}^1(\mathbb{R}^N)$ although the triangular demonstration remains applicable for any norm in $\mathbb{L}^r(\mathbb{R}^N)$, $r \geq 1$. It is, as well, applicable for any function locally, i.e. in $\mathbb{L}_{loc}^r(\mathbb{R}^N)$, $r \geq 1$. The coming existence lemmas can be shown, without loss of generality, considering the component functions $u_i, v_i \in \mathbb{L}^1(\mathbb{R}^N)$.

In this section, we develop the Cauchy problem for the system P with

the initial values satisfying the condition: $u_0(x); v_0(x) \in \mathbb{L}_{loc}^1(\mathbb{R}^N) \cap \mathbb{L}^\infty(\mathbb{R}^N)$. This is, for example, the case of constant values initial data.

During the evolution of the solutions, in the frame of the Cauchy problem, we consider the functions $u, v : \mathbb{R}^N \times (0, T) \rightarrow \mathbb{R}$ and we denote by $u(t)$ and $v(t)$, the functions evaluated for any given constant x represented by $u(\cdot, t)$ and $v(\cdot, t)$.

Making use of the Duhamel's principle, the problem P can be expressed as:

$$\Phi_1(u)(t) = G_\delta * u_0 + \int_0^t c \cdot \nabla G_\delta(t-s) * u(s) ds + \int_0^t G_\delta(t-s) * v^n(s) ds, \quad (1.37)$$

$$\Phi_2(v)(t) = G_\epsilon * v_0 + \int_0^t c \cdot \nabla G_\epsilon(t-s) * v(s) ds - \int_0^t G_\epsilon(t-s) * u^m(s) ds, \quad (1.38)$$

where G_δ and G_ϵ represent the heat kernel for each of the equations composing the problem P and defined as:

$$G_\delta = \frac{1}{(4\pi\delta t)^{N/2}} e^{-\frac{x^2}{4\delta t}}, \quad (1.39)$$

$$G_\epsilon = \frac{1}{(4\pi\epsilon t)^{N/2}} e^{-\frac{x^2}{4\epsilon t}}. \quad (1.40)$$

The equations (1.37) and (1.38) can be re-written using a matrix symbolic representation as:

$$\begin{aligned} \begin{pmatrix} u \\ v \end{pmatrix} &= \begin{pmatrix} G_\delta & 0 \\ 0 & G_\epsilon \end{pmatrix} * \begin{pmatrix} u_0 \\ v_0 \end{pmatrix} + \int_0^t \begin{pmatrix} c \cdot \nabla G_\delta & 0 \\ 0 & c \cdot \nabla G_\epsilon \end{pmatrix} * \begin{pmatrix} u \\ v \end{pmatrix} ds \\ &+ \underbrace{\int_0^t \begin{pmatrix} 0 & G_\delta \\ -G_\epsilon & 0 \end{pmatrix} * \begin{pmatrix} u^n \\ v^m \end{pmatrix} ds}_{\Psi(u,v)^T = \Psi(U)}. \end{aligned} \quad (1.41)$$

The last expression can be seen as an operator $\Psi(U)$ that, after transformation, provides the required solutions $(u, v)^T$. It is necessary to show that

such operator is bounded and stable; so that, it does not introduce oscillations or solutions going to infinity at any time (phenomena known as finite time blow-up). This is the purpose of the following lemma:

Lemma 1.1. *The operator $\Psi(U)$ is bounded for a given time $t > 0$ in the norm defined by the expression (1.34):*

Proof. Let start by evaluating the magnitude of the expression

$$\left\| \begin{pmatrix} G_\delta & 0 \\ 0 & G_\epsilon \end{pmatrix} * \begin{pmatrix} u_0 \\ v_0 \end{pmatrix} \right\|, \quad (1.42)$$

so that:

$$\begin{aligned} \|(G_\delta * u_0, G_\epsilon * v_0)^T\| &= \|G_\delta * u_0\| + \|G_\epsilon * v_0\| \\ &\leq \|G\|_\infty (\|u_0\| + \|v_0\|), \end{aligned} \quad (1.43)$$

where $G = \max\{G_\delta, G_\epsilon\}$.

It is to be noted that the heat kernel is a bounded function in the domain for any local $t > 0$. Therefore, we can define:

$$\|G\|_\infty = R_1 = \frac{1}{(4\pi dt)^{\frac{N}{2}}}, \quad (1.44)$$

Where $d = \min[\delta, \epsilon]$.

Then, the term to assess results in:

$$\|(G_\delta * u_0, G_\epsilon * v_0)^T\| \leq R_1 (\|u_0\| + \|v_0\|). \quad (1.45)$$

We continue by evaluating the expression:

$$\left\| \int_0^t \begin{pmatrix} c \cdot \nabla G_\delta & 0 \\ 0 & c \cdot \nabla G_\epsilon \end{pmatrix} * \begin{pmatrix} u \\ v \end{pmatrix} ds \right\|. \quad (1.46)$$

For this purpose, we know that:

$$c \cdot \nabla G_\delta = \sum_{i=1}^N c_i (\nabla G_\delta)_i = \sum_{i=1}^N -\frac{c_i}{(4\pi t \delta)^{\frac{N}{2}}} \frac{2x_i}{4\delta t} e^{-\frac{x^2}{4\delta t}}, \quad (1.47)$$

which is bounded function in \mathbb{R}^N . Therefore, we can say $\|c \cdot \nabla G_\delta\|_\infty = R_2$. Analogously, we can say $\|c \cdot \nabla G_\epsilon\|_\infty = R_3$. The introduced parameters R_2 and R_3 are determined some lines forward.

We have, then:

$$\begin{aligned}
& \left\| \int_0^t \begin{pmatrix} c \cdot \nabla G_\delta & 0 \\ 0 & c \cdot \nabla G_\epsilon \end{pmatrix} * \begin{pmatrix} u \\ v \end{pmatrix} ds \right\| \\
& \leq \int_0^t \|(c \cdot \nabla G_\delta * u, c \cdot \nabla G_\epsilon * v)^T\| ds \\
& = \int_0^t (\|c \cdot \nabla G_\delta * u\| + \|c \cdot \nabla G_\epsilon * v\|) ds \tag{1.48} \\
& \leq \int_0^t (\|c \cdot \nabla G_\delta\|_\infty \|u\| + \|c \cdot \nabla G_\epsilon\|_\infty \|v\|) ds \\
& \leq \int_0^t (R_2 \|u\| + R_3 \|v\|) ds.
\end{aligned}$$

It is to be noted that R_2 and R_3 are functions of time, indeed:

$$\begin{aligned}
R_2(t) &= \|c \cdot \nabla G_\delta\|_\infty = \left\| \sum_{i=1}^N c_i (\nabla G_\delta)_i \right\|_\infty \\
&= \left\| \sum_{i=1}^N \frac{c_i}{(4\pi t \delta)^{\frac{N}{2}}} \frac{2x_i}{4\delta t} e^{-\frac{x^2}{4\delta t}} \right\|_\infty \leq \sum_{i=1}^N \frac{c_i}{(4\pi t \delta)^{\frac{N}{2}}} \left\| \frac{2x_i}{4\delta t} e^{-\frac{x^2}{4\delta t}} \right\|_\infty \\
&= N c_M \frac{1}{(4\pi t \delta)^{\frac{N}{2}}} \frac{1}{4\delta t} 2\sqrt{2\delta t} e^{-\frac{1}{2}}. \tag{1.49}
\end{aligned}$$

Where $c_M = \max\{c_i\}$. The assessment $\left\| \frac{2x_i}{4\delta t} e^{-\frac{x^2}{4\delta t}} \right\|_\infty$ leads to a relation between x_i and t of the form

$$x_i = \sqrt{2\delta t}. \tag{1.50}$$

Operating analogously, we can determine the value for R_3 :

$$R_3(t) = N c_M \frac{1}{(4\pi t \epsilon)^{\frac{N}{2}}} \frac{1}{4\epsilon t} 2\sqrt{2\epsilon t} e^{-\frac{1}{2}}. \tag{1.51}$$

Our next objective is to evaluate the term:

$$\left\| \int_0^t \begin{pmatrix} 0 & G_\delta \\ -G_\epsilon & 0 \end{pmatrix} * \begin{pmatrix} u^n \\ v^m \end{pmatrix} ds \right\|. \quad (1.52)$$

For this purpose, we remind that the initial conditions satisfy $u_0(x); v_0(x) \in \mathbb{L}_{loc}^1(\mathbb{R}^N) \cap \mathbb{L}^\infty(\mathbb{R}^N)$. Thus, let assume that $\|u_0\|_\infty \leq R_4$ and $\|v_0\|_\infty \leq R_4$ where:

$$R_4 = \max\left\{ \max_{x \in \mathbb{R}^N} u_0(x), \max_{x \in \mathbb{R}^N} v_0(x) \right\}. \quad (1.53)$$

The regularity conditions of the heat evolution establishes that any solution to the heat equation with bounded initial data will be kept locally bounded, at least, locally in time and for any $x \in \mathbb{R}^N$ (see Theorem 5, Chapter 7 in [23]). Note that we assume implicitly that solutions will be global in case of existence. Even, when admitting global solutions seems to be artificial, the true existence of such solutions is proved in section 1.4. We can, therefore, say that $\|u\| \leq KR_4$ and $\|v\| \leq KR_4$ for a local time $t > 0$. We read:

$$\begin{aligned} \left\| \int_0^t \begin{pmatrix} 0 & G_\delta \\ -G_\epsilon & 0 \end{pmatrix} * \begin{pmatrix} u^n \\ v^m \end{pmatrix} ds \right\| &\leq \int_0^t \|(G_\delta * v^m, -G_\epsilon * u^n)^T\| ds \\ &= \int_0^t (\|G_\delta * v^m\| + \|-G_\epsilon * u^n\|) ds \\ &\leq \int_0^t (\|G_\delta\|_\infty \|v^m\| + \|G_\epsilon\|_\infty \|u^n\|) ds \\ &\leq \int_0^t (R_1 \|u^n\| + R_1 \|v^m\|) ds \\ &\leq \int_0^t (R_1 K^n R_4^n + R_1 K^m R_4^m) ds. \end{aligned} \quad (1.54)$$

We consider the inequality $\|u^n\| \leq \|u\|^n$ and $\|v^m\| \leq \|v\|^m$.

After having assessed each term in the expression (1.41), we can com-

pile as:

$$\begin{aligned} \|\Psi(U)\| &\leq R_1 (R_4 + R_4) + \int_0^t (R_2 K R_4 + R_3 K R_4) ds \\ &+ \int_0^t (R_1 K^n R_4^n + R_1 K^m R_4^m) ds. \end{aligned} \quad (1.55)$$

And operating the associated integrals, taking into account the time dependency of the involved parameters, we arrive to:

$$\begin{aligned} \|\Psi(U)\| &\leq \frac{1}{(4\pi d)^{\frac{N}{2}}} t^{-N/2} (R_4 + R_4) \\ &+ N c_M \frac{1}{(4\pi \delta)^{\frac{N}{2}}} \frac{1}{4\delta} 2\sqrt{2\delta} e^{-\frac{1}{2}} \frac{t^{-N/2+1/2}}{-N/2+1/2} K R_4 \\ &+ N c_M \frac{1}{(4\pi \epsilon)^{\frac{N}{2}}} \frac{1}{4\epsilon} 2\sqrt{2\epsilon} e^{-\frac{1}{2}} \frac{t^{-N/2+1/2}}{-N/2+1/2} K R_4 \\ &+ t^{-N/2+1} (K^n R_4^n + K^m R_4^m) \frac{1}{(4\pi d)^{N/2}}. \end{aligned} \quad (1.56)$$

It is to be noted that R_4 is the bound of the initial data, therefore for any value of R_4 and for any $t > 0$ the operator $\Psi(U)$ is bounded.

□

We have shown the bound of the solutions, through the bound properties of the involved operator, to the problem P locally in time ($0 < t < T$) when involving bound initial data. In addition, the own regularity of the parabolic operator permits to keep the solutions into the space $\mathbb{L}^1(\mathbb{R}^N)$ (based on results from [30]):

$$u, v, \nabla u, \nabla v \in \mathbb{L}^1(\mathbb{R}^N \times (0, T)), \quad (1.57)$$

where $T > 0$ is any finite time.

Additionally and under the regularity conditions for the absorption and reaction terms given by the Hölder definition of continuity (see the definition

1), we can make use of the regularity results contemplated in [27], so that:

$$u, v \in \mathbb{L}^1((0, T); \mathbb{W}^{2,1}(\mathbb{R}^N)) \cap \mathbb{W}^{1,1}((0, T); \mathbb{L}^1(\mathbb{R}^N)), \quad (1.58)$$

where $\mathbb{W}^{2,1}(\mathbb{R}^N)$ refers to functions with the first and the second spatial derivatives in $\mathbb{L}^1(\mathbb{R}^N)$ and $\mathbb{W}^{1,1}$ refers to the first time derivative, that is as well in \mathbb{L}^1 in time within the interval $(0, T)$ and space (\mathbb{R}^N) .

Our next objective is to show the existence of solutions u, v that satisfy the equations and the conditions of the problem P . First of all, we define hereafter, the scope of regularity in the reaction and absorption terms given by the Hölder condition for a continuous function:

Definition 1. *Given a scalar function $f(y)$, we say that such function is Hölder continuous if there exists non-negative constants K and γ , so that:*

$$|f(y_1) - f(y_2)| \leq K \|y_1 - y_2\|^\gamma, \quad (1.59)$$

for any y_1 and $y_2 \in \mathbb{R}$.

Note that if $\gamma = 1$, the function $f(y)$ satisfies the Lipschitz condition.

In addition, we require our solutions to have spatial derivatives up to the second order and time derivatives up to the first order. To characterize the involved functions behaviour, we introduce the Hölder norm, which permits to ensure, at least, a weak continuity in the postulated solutions:

$$|u|_{C^\gamma} = \sup_{u_1, u_2 \in \mathbb{R}} \frac{|f(u_1) - f(u_2)|}{\|u_1 - u_2\|^\gamma}. \quad (1.60)$$

We will refer as $C^{2+\gamma}$ -norm of any function u to the C^γ -norm of u, u_x, u_{xx} . And $C^{1+\gamma/2}$ -norm to any function with the derivative u_t in $C^{\gamma/2}$ -norm. To summarize, we work with functions $u \in C^{2+\gamma, 1+\gamma/2}(\mathbb{R}^N \times (0, T))$; where $C^{2+\gamma, 1+\gamma/2}(\mathbb{R}^N \times (0, T))$ refers to the Hölder norms of u, u_x, u_{xx} and u_t .

Additionally, we can show that the reaction and adsorption terms meet the Hölder condition in $\mathbb{R}^N \times (0, T)$. Indeed:

$$|u_1^m - u_2^m| \leq K \|u_1 - u_2\|^\gamma. \quad (1.61)$$

We know that the function u^m ($m \in (0, 1)$) is a differentiable function as

we have requested $u > 0$. Let consider $\gamma = m$:

$$|u_1^m - u_2^m| \leq \frac{m}{u^{1-m}} \|u_1 - u_2\| \leq K_u \|u_1 - u_2\|^m, \quad (1.62)$$

where

$$K_u = \frac{m}{\min_{u \in \mathbb{R}^+} |u^{1-m}|}. \quad (1.63)$$

Note that the last inequality on the right hand side of (1.62) is met provided that u_1 and u_2 are sufficiently close:

$$\|u_1 - u_2\| < 1. \quad (1.64)$$

The same argument can be applied to the population $v > 0$ to show its Hölder continuity:

$$|v_1^n - v_2^n| \leq \frac{n}{v^{1-n}} \|v_1 - v_2\| \leq K_v \|v_1 - v_2\|^n, \quad (1.65)$$

where

$$K_v = \frac{n}{\min_{v \in \mathbb{R}^+} |v^{1-n}|}. \quad (1.66)$$

The inequality (1.65) holds provided:

$$\|v_1 - v_2\| < 1. \quad (1.67)$$

For a single criteria, we can select the following value of K :

$$K = \max(K_u, K_v), \quad (1.68)$$

so that, the expressions in (1.62) and (1.65) are written simply as:

$$|u_1^m - u_2^m| \leq K \|u_1 - u_2\|^m, \quad (1.69)$$

and

$$|v_1^n - v_2^n| \leq K \|v_1 - v_2\|^n. \quad (1.70)$$

With the intention of having a single value of $\gamma > 0$, we can consider any value of m and n with the same coming conclusions. Thus, we keep the value of:

$$\gamma = m. \quad (1.71)$$

The fact of showing the Hölder continuity of the reaction and absorption terms in our problem is an important aspect to show, afterwards, the existence of solutions. Previously and for this purpose, we use the monotone method to obtain upper and lower solutions for the problem P . To this aim, we remark:

v^n is a monotone increasing function.

$-u^m$ is a monotone decreasing function.

We refer this property as mixed-monotone and is of relevancy for the definition of upper and lower solutions.

For simplification purposes, during the elaboration of this analysis, we define the following linear operator:

Definition 2. Given a function $f \in C^{2+\gamma, 1+\gamma/2}(\mathbb{R}^N \times (0, T))$, the following linear operator is defined:

$$Lf = f_t - \Delta f - c \cdot \nabla f \quad (1.72)$$

We continue by the definition of upper and lower solutions:

Definition 3. Given the pairs of solutions (\hat{u}, \hat{v}) and $(\tilde{u}, \tilde{v}) \in C^{2+\gamma, 1+\gamma/2}(\mathbb{R}^N \times (0, T))$.

We say that the pair (\hat{u}, \hat{v}) is formed of upper solutions if:

$$\begin{aligned} L\hat{u} &\geq \hat{v}^n, \\ L\hat{v} &\geq -\hat{u}^m. \end{aligned} \quad (1.73)$$

We say that the pair (\tilde{u}, \tilde{v}) is formed of lower solutions if:

$$\begin{aligned} L\tilde{u} &\leq \tilde{v}^n, \\ L\tilde{v} &\leq -\tilde{u}^m. \end{aligned} \quad (1.74)$$

Note that the following inequality holds for the initial conditions:

$$\tilde{u}(x, 0) \leq u(x, 0) \leq \hat{u}(x, 0), \quad (1.75)$$

$$\tilde{v}(x, 0) \leq v(x, 0) \leq \hat{v}(x, 0),$$

where:

$$\tilde{u}(x, 0), \hat{u}(x, 0), \tilde{v}(x, 0), \hat{v}(x, 0) \in \mathbf{L}_{loc}^1(\mathbb{R}^N) \cap \mathbf{L}^\infty(\mathbb{R}^N). \quad (1.76)$$

The compliance with the inequalities in the initial conditions can be met by considering:

$$\nu \in \mathbb{R}^+, \quad (1.77)$$

so that:

$$0 < \nu < \min_{x \in \mathbb{R}^N} (u(x, 0), v(x, 0)). \quad (1.78)$$

Note that the superior bound of ν is defined to avoid that the lower solutions may reach zero or negative values. Then, we have:

$$\hat{u}(x, 0) = u(x, 0) + \nu,$$

$$\hat{v}(x, 0) = v(x, 0) + \nu,$$

$$\tilde{u}(x, 0) = u(x, 0) - \nu,$$

$$\tilde{v}(x, 0) = v(x, 0) - \nu. \quad (1.79)$$

According to the above definitions and, as a direct consequence, we enunciate the following lemma:

Lemma 1.2. *Given the pair of upper solutions (\hat{u}, \hat{v}) and the pair of lower solutions (\tilde{u}, \tilde{v}) , where $\hat{u}, \hat{v}, \tilde{u}, \tilde{v} \in C^{2+\gamma, 1+\gamma/2}(\mathbb{R}^N \times (0, T))$, the following order is met:*

$$\hat{u} \geq \tilde{u}, \quad (1.80)$$

$$\hat{v} \geq \tilde{v}.$$

Proof. First of all, we remind the strong positivity of the parabolic operator L (for a complete discussion on the maximum principle and strong positivity of the parabolic operator, we can refer to Section 7 in [23]). As a consequence, if the initial conditions are positive, any evolution resulting as the application of the operator L is positive.

This lemma is shown based on the definitions provided for upper and lower solutions. Indeed:

$$L\hat{u} \geq \hat{v}^n, \quad (1.81)$$

$$L\tilde{u} \leq \tilde{v}^n.$$

And making the subtraction, we read:

$$L(\hat{u} - \tilde{u}) \geq \hat{v}^n - \tilde{v}^n. \quad (1.82)$$

If we proceed analogously for the population v , we have:

$$L\hat{v} \geq -\tilde{u}^m, \quad (1.83)$$

$$L\tilde{v} \leq -\hat{u}^m.$$

And making the subtraction, we read:

$$L(\hat{v} - \tilde{v}) \geq -\tilde{u}^m + \hat{u}^m. \quad (1.84)$$

If we make the assumption that

$$\hat{v}^n \geq \tilde{v}^n, \quad (1.85)$$

we have:

$$L(\hat{u} - \tilde{u}) \geq 0 \rightarrow \hat{u} \geq \tilde{u}. \quad (1.86)$$

And,

$$L(\hat{v} - \tilde{v}) \geq -\tilde{u}^m + \hat{u}^m \geq 0 \rightarrow \hat{v} \geq \tilde{v}. \quad (1.87)$$

This result is in line with the initial assumption in (1.85), showing, then, the correctness of both the initial assumption and the theorem results.

□

It is clear, then, that any solution (u, v) for the problem P is located

within the band defined for the upper and lower solutions; this means that:

$$(\tilde{u}, \tilde{v}) \leq (u, v) \leq (\hat{u}, \hat{v}). \quad (1.88)$$

Where the inequality shall be understood in each component wise.

The lower and upper solutions define a band with smooth bound in $C^{2+\gamma, 1+\gamma/2}(\mathbb{R}^N \times (0, T))$ in which any solution is located in.

Note that we have assumed the existence of such upper and lower solutions. Indeed, those solutions do exist; for this purpose, it is sufficient to highlight the Lipschitz condition of the reaction and absorption terms when dealing with positive solutions:

$$\begin{aligned} |\hat{u}^m - \tilde{u}^m| &\leq K \|\hat{u} - \tilde{u}\|, \\ |\hat{v}^n - \tilde{v}^n| &\leq K \|\hat{v} - \tilde{v}\|, \end{aligned} \quad (1.89)$$

where K is as per (1.68).

These Lipschitz conditions ensure the existence of the upper and lower solutions satisfying the results given by the expression (1.58) under the regular parabolic operator L (see Theorems 2.1 and 2.2 in Chapter 7 of [26]).

The existence of the lower and upper solutions is relevant towards the definition of the monotone sequences associated to the problem P and that will be used to show lately the existence of solutions.

Now, it is our aim to define the monotone sequences referred as

$$(u^{(k)}, v^{(k)})_{k=0,1,2,\dots} \quad (1.90)$$

Such sequences start from an initial data $(u^{(0)}, v^{(0)})$ with an iteration pro-

cess given by:

$$\begin{aligned}
 u_t^{(k)} &= \Delta u^{(k)} + c \cdot \nabla u^{(k)} + (v^{(k-1)})^n, \\
 v_t^{(k)} &= \Delta v^{(k)} + c \cdot \nabla v^{(k)} - (u^{(k-1)})^m, \\
 u^{(k)}(x, 0) &= u_0(x), \\
 v^{(k)}(x, 0) &= v_0(x), \\
 k &= 1, 2, 3 \dots
 \end{aligned} \tag{1.91}$$

For simplification purpose during the writing, by notation, we will consider:

$$\begin{aligned}
 (v^{(k-1)})^n &= v^{(k-1) n}, \quad (u^{(k-1)})^m = u^{(k-1) m}, \\
 k &= 1, 2, 3 \dots
 \end{aligned} \tag{1.92}$$

And, it shall be understood as the $k - 1$ component of the sequence up to n or m for v and u respectively.

Note that the system is now uncoupled with Lipschitz reaction and absorption; therefore, we can ensure the existence of solutions $(u^{(k)}, v^{(k)})$ for each $k = 1, 2, 3, \dots$ based on the regularity of the parabolic operator L (see Theorems 2.1 and 2.2 in Chapter 7 of [26]).

In the following lemma, we establish the monotone properties of the sequence $(u^{(k)}, v^{(k)})$ defined as:

Lemma 1.3. *Given the mixed monotone forcing terms $(v^n, -u^m)$, the sequences defined for the upper solutions $(\hat{u}^{(k)}, \hat{v}^{(k)})_{k=0,1,2,\dots}$ and for the lower solutions $(\tilde{u}^{(k)}, \tilde{v}^{(k)})_{k=0,1,2,\dots}$ possess monotone behaviour.*

Proof. Let assume that the first elements of the upper sequence $(\hat{u}^{(0)}, \hat{v}^{(0)})$

departs from the highest upper solution given by:

$$\begin{aligned}
 \hat{u}_t &= \Delta \hat{u} + c \cdot \nabla \hat{u} + \hat{v}^n, \\
 \hat{v}_t &= \Delta \hat{v} + c \cdot \nabla \hat{v} - \hat{u}^m, \\
 \hat{u}(x, 0) &= u_0(x) + \nu, \\
 \hat{v}(x, 0) &= v_0(x) + \nu, \\
 k &= 1, 2, 3\dots
 \end{aligned} \tag{1.93}$$

And that the first elements of the lower sequence $(\tilde{u}^{(0)}, \tilde{v}^{(0)})$ departs for the lowest solution given by:

$$\begin{aligned}
 \tilde{u}_t &= \Delta \tilde{u} + c \cdot \nabla \tilde{u} + \tilde{v}^n, \\
 \tilde{v}_t &= \Delta \tilde{v} + c \cdot \nabla \tilde{v} - \tilde{u}^m, \\
 \tilde{u}(x, 0) &= u_0(x) - \nu, \\
 \tilde{v}(x, 0) &= v_0(x) - \nu, \\
 k &= 1, 2, 3\dots
 \end{aligned} \tag{1.94}$$

This means that $\hat{u}^{(0)} = \hat{u}$, $\hat{v}^{(0)} = \hat{v}$ and $\tilde{u}^{(0)} = \tilde{u}$, $\tilde{v}^{(0)} = \tilde{v}$. To proof monotony, we start with:

$$\begin{aligned}
 L(\hat{u}) &\geq \hat{v}^n, \\
 L(\hat{u}^{(1)}) &\geq \hat{v}^n.
 \end{aligned} \tag{1.95}$$

And after subtraction:

$$L(\hat{u} - \hat{u}^{(1)}) \geq 0 \rightarrow \hat{u} \geq \hat{u}^{(1)}. \tag{1.96}$$

Analogously for v :

$$L(\hat{v}) \geq -\tilde{u}^m, \quad (1.97)$$

$$L(\hat{v}^{(1)}) \geq -\tilde{u}^m.$$

$$L(\hat{v} - \hat{v}^{(1)}) \geq 0 \rightarrow \hat{v} \geq \hat{v}^{(1)}. \quad (1.98)$$

Operating in the same way for the lower solutions, we have:

$$L(\tilde{u}) \leq \tilde{v}^n, \quad (1.99)$$

$$L(\tilde{u}^{(1)}) \leq \tilde{v}^n.$$

And after subtraction:

$$L(\tilde{u} - \tilde{u}^{(1)}) \leq 0 \rightarrow \tilde{u} \leq \tilde{u}^{(1)}. \quad (1.100)$$

Analogously for v :

$$L(\tilde{v}) \leq -\hat{u}^m, \quad (1.101)$$

$$L(\tilde{v}^{(1)}) \leq -\hat{u}^m.$$

And the difference provides:

$$L(\tilde{v} - \tilde{v}^{(1)}) \leq 0 \rightarrow \tilde{v} \leq \tilde{v}^{(1)}. \quad (1.102)$$

In each step, the upper solutions are above the lower solutions, this can be shown as follows:

$$L(\hat{u}^{(1)}) \geq \hat{v}^n, \quad (1.103)$$

$$L(\tilde{u}^{(1)}) \leq \tilde{v}^n.$$

And after subtraction:

$$L(\hat{u}^{(1)} - \tilde{u}^{(1)}) \geq \hat{v}^n - \tilde{v}^n. \quad (1.104)$$

Analogously for v :

$$L(\hat{v}^{(1)}) \geq -\tilde{u}^m, \quad (1.105)$$

$$L(\tilde{v}^{(1)}) \leq -\hat{u}^m.$$

And after subtraction:

$$L(\hat{v}^{(1)} - \tilde{v}^{(1)}) \geq \hat{u}^m - \tilde{u}^m. \quad (1.106)$$

Assume now that $\hat{v} \geq \tilde{v}$, then we read:

$$\begin{aligned} L(\hat{u}^{(1)} - \tilde{u}^{(1)}) &\geq 0 \rightarrow \hat{u}^{(1)} \geq \tilde{u}^{(1)}, \\ L(\hat{v}^{(1)} - \tilde{v}^{(1)}) &\geq 0 \rightarrow \hat{v}^{(1)} - \tilde{v}^{(1)}. \end{aligned} \quad (1.107)$$

Definitely, we have shown that:

$$\begin{aligned} \tilde{u} &\leq \tilde{u}^{(1)} \leq \hat{u}^{(1)} \leq \tilde{u}, \\ \tilde{v} &\leq \tilde{v}^{(1)} \leq \hat{v}^{(1)} \leq \tilde{v}. \end{aligned} \quad (1.108)$$

By induction, we assume that the last inequalities hold for a generic k :

$$\begin{aligned} \tilde{u} &\leq \tilde{u}^{(k)} \leq \hat{u}^{(k)} \leq \tilde{u}, \\ \tilde{v} &\leq \tilde{v}^{(k)} \leq \hat{v}^{(k)} \leq \tilde{v}. \end{aligned} \quad (1.109)$$

Now, we show that the same inequalities hold for the next step $k + 1$:

$$\begin{aligned} L(\hat{u}^{(k)}) &\geq \hat{v}^{(k-1)} n, \\ L(\hat{u}^{(k+1)}) &\geq \hat{v}^{(k)} n. \end{aligned} \quad (1.110)$$

And after subtraction:

$$L(\hat{u}^{(k)} - \hat{u}^{(k+1)}) \geq \hat{v}^{(k-1)} n - \hat{v}^{(k)} n \geq 0 \rightarrow \hat{u}^{(k)} \geq \hat{u}^{(k+1)}. \quad (1.111)$$

We have assumed in the previous step that $\hat{v}^{(k-1)} n \geq \hat{v}^{(k)} n$, which is a correct assumption in view of the coming results.

Analogously for v :

$$\begin{aligned} L(\hat{v}^{(k)}) &\geq -\tilde{u}^{(k-1)} m, \\ L(\hat{v}^{(k+1)}) &\geq -\tilde{u}^{(k)} m. \end{aligned} \quad (1.112)$$

And after sub-traction:

$$L(\hat{v}^{(k)} - \hat{v}^{(k+1)}) \geq -\tilde{u}^{(k-1)} m + \tilde{u}^{(k)} m \geq 0 \rightarrow \hat{v}^{(k)} \geq \hat{v}^{(k+1)}. \quad (1.113)$$

Operating in the same way for the lower solutions, we have:

$$\begin{aligned} L(\tilde{u}^{(k)}) &\leq \tilde{v}^{(k-1)} n, \\ L(\tilde{u}^{(k+1)}) &\leq \tilde{v}^{(k)} n. \end{aligned} \quad (1.114)$$

And after sub-traction:

$$L(\tilde{u}^{(k)} - \tilde{u}^{(k+1)}) \leq \tilde{v}^{(k-1)} n - \tilde{v}^{(k)} n \leq 0 \rightarrow \tilde{u}^{(k)} \leq \tilde{u}^{(k+1)}. \quad (1.115)$$

From the previous step, we assume that $\tilde{v}^{(k-1)} n \leq \tilde{v}^{(k)} n$.

Analogously for v :

$$\begin{aligned} L(\tilde{v}^{(k)}) &\leq -\hat{u}^{(k-1)} m, \\ L(\tilde{v}^{(k+1)}) &\leq -\hat{u}^{(k)} m. \end{aligned} \quad (1.116)$$

And after subtraction:

$$L(\tilde{v}^{(k)} - \tilde{v}^{(k+1)}) \leq \hat{u}^{(k)} m - \hat{u}^{(k-1)} m \leq 0 \rightarrow \tilde{v}^{(k)} \leq \tilde{v}^{(k+1)}. \quad (1.117)$$

From the previous step, we assume that $\hat{u}^{(k)} m \leq \hat{u}^{(k-1)} m$.

Finally, we show that in the step $k + 1$, the upper solutions are above the lower solutions:

$$\begin{aligned} L(\hat{u}^{(k+1)}) &\geq \hat{v}^{(k)} n, \\ L(\tilde{u}^{(k+1)}) &\leq \tilde{v}^{(k)} n. \end{aligned} \quad (1.118)$$

And after sub-traction:

$$L(\hat{u}^{(k+1)} - \tilde{u}^{(k+1)}) \geq \hat{v}^{(k)} n - \tilde{v}^{(k)} n \geq 0 \rightarrow \hat{u}^{(k+1)} \geq \tilde{u}^{(k+1)}. \quad (1.119)$$

Where it is assumed that in the previous step k : $\hat{v}^{(k)} n \geq \tilde{v}^{(k)} n$.

For the population v :

$$L(\hat{v}^{(k+1)}) \geq -\tilde{u}^{(k)} m, \quad (1.120)$$

$$L(\tilde{v}^{(k+1)}) \leq -\hat{u}^{(k)} m.$$

And after sub-traction:

$$L(\hat{v}^{(k+1)} - \tilde{v}^{(k+1)}) \geq \hat{u}^{(k)} m - \tilde{u}^{(k)} m \geq 0 \rightarrow \hat{v}^{(k+1)} \geq \tilde{v}^{(k+1)}. \quad (1.121)$$

Where it is assumed that in the previous step k : $\hat{u}^{(k)} n \geq \tilde{u}^{(k)} n$.

Finally, we have shown that based on the monotone properties of the reaction and absorption terms, it is possible to write that:

$$\tilde{u} \leq \tilde{u}^{(k+1)} \leq \hat{u}^{(k+1)} \leq \hat{u}, \quad (1.122)$$

$$\tilde{v} \leq \tilde{v}^{(k+1)} \leq \hat{v}^{(k+1)} \leq \hat{v},$$

for $k = 0, 1, 2, \dots$ □

Once the monotone properties of the defined upper and lower solutions sequences have been shown, it is our next intention to determine if the sequences are ordered. For this purpose, we proceed to enunciate the following lemma:

Lemma 1.4. *Given the ordered pairs of solutions (\hat{u}, \hat{v}) and (\tilde{u}, \tilde{v}) , then the iterations resulting upon them, $(\hat{u}^{(k)}, \hat{v}^{(k)})$ and $(\tilde{u}^{(k)}, \tilde{v}^{(k)})$ are ordered:*

Proof.

$$L(\hat{u}^{(k)}) = \hat{v}^{(k-1)} n = \hat{v}^{(k-1)} n - \hat{v}^{(k)} n + \hat{v}^{(k)} n \geq \hat{v}^{(k)} n. \quad (1.123)$$

We have used the shown fact $\hat{v}^{(k-1)} n \geq \hat{v}^{(k)} n$, thus:

$$L(\hat{u}^{(k)}) \geq \hat{v}^{(k)} n. \quad (1.124)$$

Analogously for v , we have:

$$L(\hat{v}^{(k)}) \geq -\tilde{u}^{(k)} m. \quad (1.125)$$

Operating for the lower solutions, we read:

$$L(\tilde{u}^{(k)}) = \tilde{v}^{(k-1) n} = \tilde{v}^{(k-1) n} - \tilde{v}^{(k) n} + \tilde{v}^{(k) n} \leq \tilde{v}^{(k) n}. \quad (1.126)$$

As we know that $\tilde{v}^{(k-1) n} \leq \tilde{v}^{(k) n}$; we, therefore, have:

$$L(\tilde{u}^{(k)}) \leq \tilde{v}^{(k) n}. \quad (1.127)$$

Analogously for v , we have:

$$L(\tilde{v}^{(k)}) \leq -\hat{u}^{(k) m}. \quad (1.128)$$

□

Based on the monotony and ordered properties shown, we are in a position to enunciate a existence theorem:

Theorem 1.3.1. *Let $(\hat{u}^{(k)}, \hat{v}^{(k)})$ and $(\tilde{u}^{(k)}, \tilde{v}^{(k)})$ be ordered upper and lower solutions to the problem P , then there exist a solution (u, v) obtained as the limit of the given sequences:*

$$\begin{aligned} \hat{u}(x, t) &= \lim_{k \rightarrow \infty} \hat{u}^{(k)}(x, t); & \hat{v}(x, t) &= \lim_{k \rightarrow \infty} \hat{v}^{(k)}(x, t), \\ \tilde{u}(x, t) &= \lim_{k \rightarrow \infty} \tilde{u}^{(k)}(x, t); & \tilde{v}(x, t) &= \lim_{k \rightarrow \infty} \tilde{v}^{(k)}(x, t). \end{aligned} \quad (1.129)$$

In addition:

$$\begin{aligned} \hat{u}(x, t) &= \tilde{u}(x, t) = u(x, t), \\ \hat{v}(x, t) &= \tilde{v}(x, t) = v(x, t). \end{aligned} \quad (1.130)$$

Proof. As $(\hat{u}^{(k)}, \hat{v}^{(k)})$ and $(\tilde{u}^{(k)}, \tilde{v}^{(k)})$ are solutions of the problem P , they satisfy the integral representation in virtue of the Duhamel principle:

$$\begin{aligned} \hat{u}^{(k)}(t) &= G_\delta * (u_0 + \nu(k)) + \int_0^t c \cdot \nabla G_\delta(t-s) * \hat{u}^{(k)}(s) ds \\ &\quad + \int_0^t G_\delta(t-s) * \hat{v}^{(k) n}(s) ds, \end{aligned} \quad (1.131)$$

$$\begin{aligned}\tilde{u}^{(k)}(t) &= G_\delta * (u_0 - \nu(k)) + \int_0^t c \cdot \nabla G_\delta(t-s) * \tilde{u}^{(k)}(s) ds \\ &+ \int_0^t G_\delta(t-s) * \tilde{v}^{(k) n}(s) ds,\end{aligned}\tag{1.132}$$

Where $\lim_{k \rightarrow \infty} \nu = 0$.

Considering the limit approximation and in virtue of the dominated-convergence theorem (enunciated in Theorem 1.4.49 of [15]), we have:

$$\begin{aligned}\lim_{k \rightarrow \infty} \hat{u}^{(k)}(t) &= G_\delta * (u_0 + \lim_{k \rightarrow \infty} \nu(k)) \\ &+ \int_0^t c \cdot \nabla G_\delta(t-s) * \lim_{k \rightarrow \infty} \hat{u}^{(k)}(s) ds \\ &+ \int_0^t G_\delta(t-s) * \lim_{k \rightarrow \infty} \hat{v}^{(k) n}(s) ds,\end{aligned}\tag{1.133}$$

$$\begin{aligned}\lim_{k \rightarrow \infty} \tilde{u}^{(k)}(t) &= G_\delta * (u_0 - \lim_{k \rightarrow \infty} \nu(k)) \\ &+ \int_0^t c \cdot \nabla G_\delta(t-s) * \lim_{k \rightarrow \infty} \tilde{u}^{(k)}(s) ds \\ &+ \int_0^t G_\delta(t-s) * \lim_{k \rightarrow \infty} \tilde{v}^{(k) n}(s) ds.\end{aligned}\tag{1.134}$$

We know that:

$$\begin{aligned}\hat{u}(x, t) &= \lim_{k \rightarrow \infty} \hat{u}^{(k)}(x, t); \quad \tilde{u}(x, t) = \lim_{k \rightarrow \infty} \tilde{u}^{(k)}(x, t), \\ \hat{v}(x, t) &= \lim_{k \rightarrow \infty} \hat{v}^{(k)}(x, t); \quad \tilde{v}(x, t) = \lim_{k \rightarrow \infty} \tilde{v}^{(k)}(x, t).\end{aligned}\tag{1.135}$$

Therefore and after substraction:

$$\begin{aligned}\hat{u}(t) - \tilde{u}(t) &= \int_0^t c \cdot \nabla G_\delta(t-s) * (\hat{u} - \tilde{u})(s) ds \\ &+ \int_0^t G_\delta(t-s) * (\hat{v}^n - \tilde{v}^n)(s) ds.\end{aligned}\tag{1.136}$$

In the assumption that $\hat{v} = \tilde{v}$, the last equality holds provided that $\hat{u} = \tilde{u} = u$.

The same steps can be repeated for the population v :

$$\begin{aligned} \hat{v}(t) - \tilde{v}(t) &= \int_0^t c \cdot \nabla G_\delta(t-s) * (\hat{v} - \tilde{v})(s) ds \\ &+ \int_0^t G_\delta(t-s) * (-\hat{u}^m + \tilde{u}^m)(s) ds. \end{aligned} \quad (1.137)$$

Under the assumption that $\hat{v} = \tilde{v}$, we obtained that $\hat{u} = \tilde{u} = u$. Indeed, the last inequality holds if $\hat{v} = \tilde{v}$, proving the correctness of the assumption.

Finally, we have proved the existence of solutions to our problem P :

$$\begin{aligned} \hat{u}(x, t) = \tilde{u}(x, t) &= u(x, t) \in C^{2+\gamma, 1+\gamma/2}(\mathbb{R}^N \times (0, T)), \\ \hat{v}(x, t) = \tilde{v}(x, t) &= v(x, t) \in C^{2+\gamma, 1+\gamma/2}(\mathbb{R}^N \times (0, T)). \end{aligned} \quad (1.138)$$

Additionally, both solutions satisfy the conditions stated in the expression (1.58) by the embedding:

$$\begin{aligned} &C^{2+\gamma, 1+\gamma/2}(\mathbb{R}^N \times (0, T)) \\ &\subset \mathbb{L}^1((0, T); \mathbb{W}^{2,1}(\mathbb{R}^N)) \cap \mathbb{W}^{1,1}((0, T); \mathbb{L}^1(\mathbb{R}^N)) \end{aligned} \quad (1.139)$$

□

1.4 Global solutions

The existence analysis is completed with the analysis of the existence of global solutions. Aguirre and Escobedo [28] showed the existence of global solutions for a reaction term involving an exponent of the form u^p , with $0 < p < 1$. Additionally, Escobedo and Herrero [29] showed the existence of global solutions for a system of the form:

$$\begin{aligned} u_t &= \Delta u + v^p, \quad p > 0, \\ v_t &= \Delta v + u^q, \quad q > 0. \end{aligned} \tag{1.140}$$

Our objective is to extend the existence results, analyzed by the cited authors, to show the existence of global solutions for the problem P . Nonetheless and previously, we need to consider the convective term. Namely, we aim to show that the fact of introducing a convective term does not impact the existence of global solutions so that the results contemplated in [29] apply. For this purpose, we perform the following change of variables in the problem P :

$$\begin{aligned} u(x, t) &= U(\xi(x, t), t), \\ v(x, t) &= V(\xi(x, t), t), \\ \xi &= x + ct. \end{aligned} \tag{1.141}$$

The derivatives are:

$$\begin{aligned} u_t &= \nabla_\xi U \xi_t + U_t, \\ \nabla u &= \nabla_\xi U \xi_x, \\ \Delta u &= \Delta_\xi U \xi_x^2 + \nabla_\xi U \xi_{xx}. \end{aligned} \tag{1.142}$$

And upon substitution into the equation for u in problem P , we have:

$$\begin{aligned} \nabla_\xi U \cdot c + U_t &= \Delta_\xi U + c \cdot \nabla_\xi U + V^n, \\ U_t &= \Delta_\xi U + V^n. \end{aligned} \tag{1.143}$$

The same operations can be developed for the population v , so that the system P adopts the following structure in the independent variables (ξ, t) :

$$\begin{aligned} U_t &= \Delta_\xi U + V^n, \\ V_t &= \Delta_\xi V - U^m. \end{aligned} \tag{1.144}$$

Any global solution to the coupled problem study by Escobedo and Herrero in [29], is a supersolution to our problem P . Indeed, the problem P is scoped by the problem of Escobedo and Herrero pointed out in the expression (1.140) :

$$\begin{aligned} U_t &= \Delta_\xi U + V^n, \\ V_t &= \Delta_\xi V - U^m \leq \Delta_\xi V + U^m. \end{aligned} \tag{1.145}$$

We denote by P_+ to the following problem formed of upper solutions to the problem P :

$$\begin{aligned} \hat{U}_t &= \Delta_\xi \hat{U} + \hat{V}^n, \\ \hat{V}_t &= \Delta_\xi \hat{V} + \hat{U}^m. \end{aligned} \tag{1.146}$$

As discussed, the existence of global solutions to the problem P_+ has been already performed by Escobedo and Herrero in [29], and, as it bounds the problem P , we show, then, the existence of global supersolutions to the problem P .

At this point, we have shown existence of solutions (see Section 1.3) based on an approximation from above, with upper solutions, and from below, with lower solutions existing in $(0, T)$. In addition, and due to the results presented in this section, we can conclude that solutions exist globally and, as a direct consequence, there not exist blow up phenomena for the problem P .

Furthermore, we can make use of the global supersolutions obtained in [29] to postulate exact global bounds for our problem P , given by:

$$\begin{aligned} \hat{U}(t) &= C_1 t^{\frac{n+1}{1-nm}}, \quad C_1^{1-nm} = \frac{(1-nm)^{n+1}}{(1+n)(1+m)^n}, \\ \hat{V}(t) &= C_2 t^{\frac{m+1}{1-nm}}, \quad C_2 = \frac{C_1^m (1-nm)}{m+1}. \end{aligned} \tag{1.147}$$

We can make use of the translation constants $t_{0,1}$ and $t_{0,2}$ to have:

$$\begin{aligned} u(x, t) &\leq C_1(t + t_{0,1})^{\frac{n+1}{1-nm}}, \quad t_{0,1} = (C_1^{-1}\|u_0\|)^{\frac{1-nm}{1+n}}, \\ v(x, t) &\leq C_2(t + t_{0,2})^{\frac{m+1}{1-nm}}, \quad t_{0,2} = (C_2^{-1}\|v_0\|)^{\frac{1-nm}{1+m}}. \end{aligned} \tag{1.148}$$

1.5 Uniqueness

Once we have set the evidences related to existence of solutions and the bound of the solving operator Ψ , we are going to show the uniqueness of the solutions to P making use of the fixed point theorem. For this purpose, we enunciate the following theorem:

Theorem 1.5.1. *Under the conditions $u_0(x) > 0, v_0(x) > 0$ with*

$$u_0(x), v_0(x) \in \mathbb{L}_{loc}^1(\mathbb{R}^N) \cap \mathbb{L}^\infty(\mathbb{R}^N), \quad (1.149)$$

there is a unique solution to the problem P .

Proof. let consider two different functions

$$U_1 = (u_1, v_1)^T, \quad (1.150)$$

$$U_2 = (u_2, v_2)^T,$$

constituting solutions to the problem P and with the same initial data

$$u_0(x); v_0(x) \in \mathbb{L}_{loc}^1(\mathbb{R}^N) \cap \mathbb{L}^\infty(\mathbb{R}^N). \quad (1.151)$$

The uniqueness is shown based on the functional representation as per (1.41). We show that the norm of the difference

$$\Psi(U_1) - \Psi(U_2), \quad (1.152)$$

is bounded for a given constant time T , so that the fixed point theorem can be applied upon:

$$\begin{aligned} \|\Psi(U_1) - \Psi(U_2)\| &\leq \left\| \int_0^t \begin{pmatrix} c \cdot \nabla G_\delta & 0 \\ 0 & c \cdot \nabla G_\epsilon \end{pmatrix} * \begin{pmatrix} u_1 - u_2 \\ v_1 - v_2 \end{pmatrix} ds \right\| \\ &+ \left\| \int_0^t \begin{pmatrix} 0 & G_\delta \\ G_\epsilon & 0 \end{pmatrix} * \begin{pmatrix} -u_1^m + u_2^m \\ v_1^n - v_2^n \end{pmatrix} ds \right\|, \end{aligned} \quad (1.153)$$

$$\begin{aligned} \|\Psi(U_1) - \Psi(U_2)\| &\leq \int_0^t \left\| \begin{pmatrix} (c \cdot \nabla G_\delta) * (u_1 - u_2) \\ (c \cdot \nabla G_\epsilon) * (v_1 - v_2) \end{pmatrix} \right\| ds \\ &\quad + \int_0^t \left\| \begin{pmatrix} G_\delta * (v_1^n - v_2^n) \\ G_\epsilon * (-u_1^m + u_2^m) \end{pmatrix} \right\| ds. \end{aligned} \quad (1.154)$$

We assess the integrals involved on the right hand side of the last inequality in view of the defined norm (1.34):

$$\begin{aligned} &\int_0^t \left\| \begin{pmatrix} (c \cdot \nabla G_\delta) * (u_1 - u_2) \\ (c \cdot \nabla G_\epsilon) * (v_1 - v_2) \end{pmatrix} \right\| ds \\ &= \int_0^t (\|c \cdot \nabla G_\delta * (u_1 - u_2)\| + \|c \cdot \nabla G_\epsilon * (v_1 - v_2)\|) ds \\ &\leq \int_0^t (\|c \cdot \nabla G_\delta\|_\infty \|u_1 - u_2\| + \|c \cdot \nabla G_\epsilon\|_\infty \|v_1 - v_2\|) ds \\ &\leq \int_0^t (R_2 \|u_1 - u_2\| + R_3 \|v_1 - v_2\|) ds \\ &\leq \sup_{0 < t < T} \|u_1 - u_2\| \int_0^{t=T} R_2 ds + \sup_{0 < t < T} \|v_1 - v_2\| \int_0^{t=T} R_3 ds \\ &= \sup_{0 < t < T} \|u_1 - u_2\| \int_0^{t=T} N c_M \frac{1}{(4\pi s \delta)^{\frac{N}{2}}} \frac{1}{4\delta s} 2\sqrt{2\delta s} e^{-\frac{1}{2}} ds \\ &\quad + \sup_{0 < t < T} \|v_1 - v_2\| \int_0^{t=T} N c_M \frac{1}{(4\pi s \epsilon)^{\frac{N}{2}}} \frac{1}{4\epsilon s} 2\sqrt{2\epsilon s} e^{-\frac{1}{2}} ds \\ &= \sup_{0 < t < T} \|u_1 - u_2\| \frac{2}{1-N} T^{\frac{1-N}{2}} N c_M \frac{1}{(4\pi \delta)^{\frac{N}{2}}} \frac{1}{4\delta} 2\sqrt{2\delta} e^{-\frac{1}{2}} \\ &\quad + \sup_{0 < t < T} \|v_1 - v_2\| \frac{2}{1-N} T^{\frac{1-N}{2}} N c_M \frac{1}{(4\pi \epsilon)^{\frac{N}{2}}} \frac{1}{4\epsilon} 2\sqrt{2\epsilon} e^{-\frac{1}{2}}. \end{aligned} \quad (1.155)$$

For the second integral, we have:

$$\begin{aligned}
& \int_0^t \left\| \begin{pmatrix} G_\delta * (v_1^n - v_2^n) \\ G_\epsilon * (-u_1^m + u_2^m) \end{pmatrix} \right\| ds \\
&= \int_0^t (\|G_\delta * (v_1^n - v_2^n)\| + \|G_\epsilon * (u_2^m - u_1^m)\|) ds \\
&\leq \int_0^t (\|G_\delta\|_\infty \|v_1^n - v_2^n\| + \|G_\epsilon\|_\infty \|u_2^m - u_1^m\|) ds \\
&\leq \int_0^t (R_1 \|v_1^n - v_2^n\| + R_1 \|u_2^m - u_1^m\|) ds \\
&\leq \int_0^t \left(R_1 \frac{n}{v_1^{1-n}} \|v_1 - v_2\| + R_1 \frac{m}{u_1^{1-m}} \|u_2 - u_1\| \right) ds \\
&\leq \frac{n}{a} \sup_{0 < t < T} \|v_1 - v_2\| \int_0^{t=T} R_1 ds + \frac{m}{a} \sup_{0 < t < T} \|u_2 - u_1\| \int_0^{t=T} R_1 ds \\
&= \frac{n}{a} \sup_{0 < t < T} \|v_1 - v_2\| \frac{2}{(4\pi d)^{N/2} (N-2)} T^{\frac{2-N}{2}} \\
&+ \frac{m}{a} \sup_{0 < t < T} \|u_2 - u_1\| \frac{2}{(4\pi d)^{N/2} (N-2)} T^{\frac{2-N}{2}},
\end{aligned} \tag{1.156}$$

where

$$a = \min\{v, u\} + \beta, \tag{1.157}$$

and $N = 3$ to consider the space dimensions.

Note that β is a suitable constant to ensure that $a > 0$ and is considered to be $\beta \rightarrow 0$.

The application of the Lipschitz condition to bound the terms $\|u_2^m - u_1^m\|$ and $\|v_1^n - v_2^n\|$ is consistent in the sense that each of the involved functions u_2^m, u_1^m, v_1^n and v_2^n comply the embedding relation:

$$\begin{aligned}
& u_2^n, u_1^n, v_1^m, v_2^m \in C^{2+\gamma, 1+\gamma/2}(\mathbb{R}^N \times (0, T)) \\
& \subset \mathbb{L}^1((0, T); \mathbb{W}^{2,1}(\mathbb{R}^N)) \cap \mathbb{W}^{1,1}((0, T); \mathbb{L}^1(\mathbb{R}^N)),
\end{aligned} \tag{1.158}$$

that has been shown for the solutions in Theorem 1.3.1. Indeed the Lipschitz case corresponds to $\gamma = 1$ in the last relation of inclusion.

After compilation of both assessments, we have:

$$\begin{aligned}
& \|\Psi(U_1) - \Psi(U_2)\| \\
& \leq \sup_{0 < t < T} \|u_1 - u_2\| \frac{2}{1-N} T^{\frac{1-N}{2}} N c_M \frac{1}{(4\pi\delta)^{\frac{N}{2}}} \frac{1}{4\delta} 2\sqrt{2\delta} e^{-\frac{1}{2}} \\
& + \sup_{0 < t < T} \|v_1 - v_2\| \frac{2}{1-N} T^{\frac{1-N}{2}} N c_M \frac{1}{(4\pi\epsilon)^{\frac{N}{2}}} \frac{1}{4\epsilon} 2\sqrt{2\epsilon} e^{-\frac{1}{2}} \\
& + \frac{n}{a} \sup_{0 < t < T} \|v_1 - v_2\| \frac{2}{(4\pi d)^{N/2} (N-2)} T^{\frac{2-N}{2}} \\
& + \frac{m}{a} \sup_{0 < t < T} \|u_2 - u_1\| \frac{2}{(4\pi d)^{N/2} (N-2)} T^{\frac{2-N}{2}}.
\end{aligned} \tag{1.159}$$

For a given $T > 0$ in the space ($N = 3$), the term

$$\|\Psi(U_1) - \Psi(U_2)\|, \tag{1.160}$$

is a contraction (understood in the sense of each component wise) on

$$\begin{aligned}
& C^{2+\gamma, 1+\gamma/2}(\mathbb{R}^N \times (0, T)) \\
& \subset \mathbb{L}^1((0, T); \mathbb{W}^{2,1}(\mathbb{R}^N)) \cap \mathbb{W}^{1,1}((0, T); \mathbb{L}^1(\mathbb{R}^N)).
\end{aligned} \tag{1.161}$$

Indeed, it is enough to make

$$\begin{aligned}
u_1 & \rightarrow u_2, \\
v_1 & \rightarrow v_2,
\end{aligned} \tag{1.162}$$

to ensure that the operator Ψ has a fixed point U , which is a unique solution to the problem P

□

1.6 Comparison of solutions

The comparison of solutions is mainly governed by the reaction and absorption for the equation in u and v respectively. Indeed, given a solution $u_2 > u_1$, the absorption term in the equation in v would lead to have $v_2 < v_1$ that, in turn, will feed the reaction term in the equation for u with a lower magnitude. In the next step, u would be lower, providing a lower absorption in the equation for v , that will result in a higher value for v . Again, this higher value for v feeds the reaction in the u equation, providing a higher value for u . This oscillatory dynamic is quite specific of our problem, given the coupling effect of the reaction and absorption, and introduces difficulties when arising a comparison principle that can be, only, formulated locally.

In order to deal with the dynamic described, and aiming the proof of a comparison principle, we need to control the effect of both reaction and absorption terms. For this purpose; we introduce, in our original problem P , a controlling parameter, κ , that will allow us to establish certain conditions in which comparison holds. Let us define the following problem referred as P_κ :

$$\begin{aligned} u_t &= \delta \Delta u + c \cdot \nabla u + \kappa v^n, \\ v_t &= \epsilon \Delta v + c \cdot \nabla v - \kappa u^m. \end{aligned} \tag{1.163}$$

We postulate the following theorem:

Theorem 1.6.1. *Given two pairs of solutions such that*

$$(u_1, v_1), (u_2, v_2) \in C^{2+\gamma, 1+\gamma/2}(\mathbb{R}^N \times (0, T)), \tag{1.164}$$

understood in each component wise for the problem P_κ and that

$$\begin{aligned} u_{0,1} \geq u_{0,2} > 0 &\in \mathbb{L}_{loc}^1(\mathbb{R}^N) \cap \mathbb{L}^\infty(\mathbb{R}^N), \\ v_{0,1} \geq v_{0,2} > 0 &\in \mathbb{L}_{loc}^1(\mathbb{R}^N) \cap \mathbb{L}^\infty(\mathbb{R}^N), \end{aligned} \tag{1.165}$$

then:

$$u_1 \geq u_2; \quad v_1 \geq v_2, \tag{1.166}$$

locally, for all $(x, t) \in \beta(x_0, t) \times (0, T)$, where:

$$\beta(x_0, t) = \left[x \in (x_0 - B(t), x_0 + B(t)); x_0 \in \mathbb{R}^N \right]. \quad (1.167)$$

And T is sufficiently small (i.e. $T \rightarrow 0$).

Proof. First of all, we define a region $\gamma(x_0, t)$ in the vicinity of x_0 and contained within the set $\beta(x_0, t)$, so that the solutions order is the opposite compared to the results we aim to proof:

$$\gamma(x_0, t) = \left[x \in (x_0 - \sigma(t), x_0 + \sigma(t)); x_0 \in \mathbb{R}^N; u_2 > u_1, v_2 > v_1 \right], \quad (1.168)$$

with

$$\gamma(x_0, t) \subset \beta(x_0, t). \quad (1.169)$$

The transition between the region $\gamma(x_0, t)$ and the region $\beta(x_0, t)$ is located in the border of γ , i. e. $\partial\gamma(x_0, t)$, where the change of order in the solutions between γ and β , requires:

$$u_1 = u_2; v_1 = v_2 \text{ in } \partial\gamma(x_0, t). \quad (1.170)$$

After the definition of the regions, we substitute the solutions into the problem P_κ :

$$\begin{aligned} u_{1t} &= \delta\Delta u_1 + c \cdot \nabla u_1 + \kappa v_1^n, \\ v_{1t} &= \epsilon\Delta v_1 + c \cdot \nabla v_1 - \kappa u_1^m, \\ u_{2t} &= \delta\Delta u_2 + c \cdot \nabla u_2 + \kappa v_2^n, \\ v_{2t} &= \epsilon\Delta v_2 + c \cdot \nabla v_2 - \kappa u_2^m. \end{aligned} \quad (1.171)$$

Making the subtraction, arranging the terms in vectorial form, integrating

over $\gamma(x_0, t)$ and making $\delta = \epsilon = 1$ for the sake of simplicity, we have:

$$\begin{aligned} \frac{d}{dt} \int_{\gamma(t)} \begin{pmatrix} u_2 - u_1 \\ v_2 - v_1 \end{pmatrix} dx &= \int_{\gamma(t)} \begin{pmatrix} \Delta(u_2 - u_1) \\ \Delta(v_2 - v_1) \end{pmatrix} dx \\ &+ \int_{\gamma(t)} \begin{pmatrix} c \cdot \nabla(u_2 - u_1) \\ c \cdot \nabla(v_2 - v_1) \end{pmatrix} dx + \int_{\gamma(t)} \kappa \begin{pmatrix} v_2^n - v_1^n \\ -u_2^m + u_1^m \end{pmatrix} dx. \end{aligned} \quad (1.172)$$

Making use of the divergence theorem, we have:

$$\begin{aligned} &\int_{\gamma(t)} \begin{pmatrix} c \cdot \nabla(u_2 - u_1) \\ c \cdot \nabla(v_2 - v_1) \end{pmatrix} dx \\ &= \int_{\gamma(t)} \begin{pmatrix} \nabla \cdot (c(u_2 - u_1)) - (\nabla \cdot c)(u_2 - u_1) \\ \nabla \cdot (c(v_2 - v_1)) - (\nabla \cdot c)(v_2 - v_1) \end{pmatrix} dx \quad (1.173) \\ &= \int_{\partial\gamma(t)} \begin{pmatrix} \Pi \cdot c(u_2 - u_1) \\ \Pi \cdot c(v_2 - v_1) \end{pmatrix} dx(s), \end{aligned}$$

where Π is the outer normal unit vector to $\partial\gamma(t)$ that is considered to be sufficiently smooth for our purposes and $dx(s)$ represents the integration over a spatial domain $\partial\gamma(t)$ variable with time s .

Note we have required that

$$\begin{aligned} u_1 &= u_2, \\ v_1 &= v_2, \end{aligned} \quad (1.174)$$

in $\partial\gamma(t)$.

Therefore, the last integral is zero:

$$\int_{\partial\gamma(t)} \begin{pmatrix} \Pi \cdot c(u_2 - u_1) \\ \Pi \cdot c(v_2 - v_1) \end{pmatrix} dx(s) = \begin{pmatrix} 0 \\ 0 \end{pmatrix}. \quad (1.175)$$

We proceed, now, by employing the Green's formula to evaluate the term corresponding to the diffusion:

$$\int_{\gamma(t)} \begin{pmatrix} \Delta(u_2 - u_1) \\ \Delta(v_2 - v_1) \end{pmatrix} dx = \int_{\partial\gamma(t)} \begin{pmatrix} \nabla(u_2 - u_1) \cdot \Pi \\ \nabla(v_2 - v_1) \cdot \Pi \end{pmatrix} dx(s). \quad (1.176)$$

Note that when we make the approach to the $\partial\gamma(t)$, the difference $(u_2 - u_1)$ and $(v_2 - v_1)$ approaches to zero. We can consider that this approach is sufficiently smooth in the proximity of $\partial\gamma(t)$ so that in the vicinity of such border, we have

$$\nabla(u_2 - u_1) \leq 0, \quad (1.177)$$

$$\nabla(v_2 - v_1) \leq 0.$$

Therefore, we read:

$$\int_{\partial\gamma(t)} \begin{pmatrix} \nabla(u_2 - u_1) \cdot \Pi \\ \nabla(v_2 - v_1) \cdot \Pi \end{pmatrix} \leq \begin{pmatrix} 0 \\ 0 \end{pmatrix}. \quad (1.178)$$

After the evaluation of the convective and diffusion terms, we arrive to the following expression:

$$\begin{aligned} \frac{d}{dt} \int_{\gamma(t)} \begin{pmatrix} u_2 - u_1 \\ v_2 - v_1 \end{pmatrix} dx &\leq \int_{\gamma(t)} \kappa \begin{pmatrix} v_2^n - v_1^n \\ -u_2^m + u_1^m \end{pmatrix} dx \\ &\leq \int_{\gamma(t)} \kappa \begin{pmatrix} \frac{n}{v_1^{1-n}} |v_2 - v_1| \\ \frac{m}{u_1^{1-m}} |-u_2 + u_1| \end{pmatrix} dx. \end{aligned} \quad (1.179)$$

It is possible to observe that a comparison principle cannot be obtained in case the solutions v or u are equal to zero. This fact is due to the lack of the Lipschitz condition in both, the absorption and reaction terms. Nonetheless, we have required the initial conditions to be positive and based on the regularity of solutions expressed by the condition (1.139) and the positivity of the lower solutions (see expressions (1.288) and (1.79)), we can ensure the positivity of any solution. Thus, in the frame of the comparison theorem, we can only consider positive solutions for which the Lipschitz condition is met.

We define the following Lipschitz constant:

$$K = \max\{m, n\} \frac{1}{\min_{\gamma(t)} \{v_1^{1-n}, u_1^{1-m}\}}. \quad (1.180)$$

Then, returning to the integral assessment, we have:

$$\frac{d}{dt} \int_{\gamma(t)} \begin{pmatrix} u_2 - u_1 \\ v_2 - v_1 \end{pmatrix} dx \leq \kappa K \int_{\gamma(t)} \begin{pmatrix} |v_2 - v_1| \\ |-u_2 + u_1| \end{pmatrix} dx. \quad (1.181)$$

If we apply the Gronwall's inequality:

$$\begin{aligned} \frac{d}{dt} \int_{\gamma(t)} \begin{pmatrix} u_2 - u_1 \\ v_2 - v_1 \end{pmatrix} dx &\leq \kappa K \int_{\gamma(t)} \begin{pmatrix} |v_{0,2} - v_{0,1}| \\ |-u_{0,2} + u_{0,1}| \end{pmatrix} dx + \\ &\quad \kappa K \int_{\gamma(t)} \int_0^t \begin{pmatrix} |v_2 - v_1| \\ |-u_2 + u_1| \end{pmatrix} ds dx. \end{aligned} \quad (1.182)$$

Now, we can make

$$\sigma(t) \rightarrow 0, \quad (1.183)$$

so that the domain $\gamma(t)$ approximates the center point x_0 . We can say that for any time is $B(t) \gg \sigma(t)$:

$$\frac{d}{dt} \int_{\beta(t)} \begin{pmatrix} u_2 - u_1 \\ v_2 - v_1 \end{pmatrix} dx \leq \frac{d}{dt} \int_{\gamma(t)} \begin{pmatrix} u_2 - u_1 \\ v_2 - v_1 \end{pmatrix} dx. \quad (1.184)$$

It is clear that in case of having $\kappa \rightarrow 0$ in the domain $\beta(t)$, the comparison principle applies easily, indeed:

$$\frac{d}{dt} \int_{\beta(t)} \begin{pmatrix} u_2 - u_1 \\ v_2 - v_1 \end{pmatrix} dx \leq \begin{pmatrix} 0 \\ 0 \end{pmatrix} \rightarrow \begin{pmatrix} u_{2t} \leq u_{1t} \\ v_{2t} \leq v_{1t} \end{pmatrix}_{\beta}, \quad (1.185)$$

which means that

$$\begin{pmatrix} du_2 \leq du_1 \\ dv_2 \leq dv_1 \end{pmatrix}_{\beta}. \quad (1.186)$$

This last expression can be evaluated as:

$$\begin{pmatrix} u_2 - u_2(\partial\gamma) \leq u_1 - u_1(\partial\gamma) \\ v_2 - v_2(\partial\gamma) \leq v_1 - v_1(\partial\gamma) \end{pmatrix}_{\beta}, \quad (1.187)$$

where $u_i(\partial\gamma)$ and $v_i(\partial\gamma)$ represent the evaluation of each function in the border of the domain γ . We remind that the expression (1.170) holds, so,

we can conclude:

$$\left(\begin{array}{l} u_2 \leq u_1 \\ v_2 \leq v_1 \end{array} \right)_{\beta}, \quad (1.188)$$

as we are aiming to proof. The index $\beta(t)$ stresses the fact that the comparison holds locally as described in the theorem postulations.

Nonetheless, if we consider that $\kappa > a > 0$ (for example $\kappa = 1$), we can ensure a comparison provided the initial conditions are sufficiently close and that we operate in small time intervals $t = T \rightarrow 0$. Under these assumptions we have, as well:

$$\begin{aligned} u_2 &\leq u_1, \\ v_2 &\leq v_1. \end{aligned} \quad (1.189)$$

Locally in $\beta(x_0, t)$.

□

We have shown that a comparison principle holds provided the absorption and reactions terms are sufficiently small or when the initial conditions are close enough integrating over arbitrary small times. This result is particularly interesting as it reveals that a comparison principle does not hold, in general, due to the dynamic of the coupling between the reaction and absorption terms, and it provides the most general conditions in which comparison between solutions can be ensured.

In addition, we consider for completeness, the following lemma:

Lemma 1.5. *Let consider*

$$u_0 \geq v_0, \quad (1.190)$$

for $x \in \mathbb{R}^N$, then

$$u \geq v, \quad (1.191)$$

for any $(x, t) \in \mathbb{R}^N \times (0, T)$.

Proof. For the shake of convenience and without impacting the final conclusion, we operate making $\epsilon = \delta = 1$ in the diffusion.

After the application of the Duhamel principle and making the subtraction, we read the following expression:

$$\begin{aligned} u - v &= G * (u_0 - v_0) + \int_0^t c \cdot \nabla G(t - s) * (u - v)(s) ds \\ &+ \int_0^t G(t - s) * (v^n + u^m)(s) ds. \end{aligned} \quad (1.192)$$

Under the positivity condition of both solutions (u, v) (see the positivity of the lower solutions in the expressions (1.288) and (1.79)) the term:

$$\int_0^t G_\delta(t - s) * (v^n + u^m)(s) ds, \quad (1.193)$$

is positive, as the integrand G_δ is positive. Therefore, we have:

$$\begin{aligned} (u - v) - \int_0^t c \cdot \nabla G(t - s) * (u - v)(s) ds \\ = G * (u_0 - v_0) + \int_0^t G(t - s) * (v^n + u^m)(s) ds. \end{aligned} \quad (1.194)$$

We know that:

$$c \cdot \nabla G = \sum_{i=1}^N c_i \nabla G_i = \sum_{i=1}^N -\frac{c_i}{(4\pi t)^{\frac{N}{2}}} \frac{2x_i}{4t} e^{-\frac{x^2}{4t}}, \quad (1.195)$$

thus:

$$\begin{aligned} (u - v) + \int_0^t \sum_{i=1}^N \frac{c_i}{(4\pi(t - s))^{\frac{N}{2}}} \frac{2x_i}{4(t - s)} e^{-\frac{x^2}{4(t - s)}} * (u - v)(s) ds \\ = G * (u_0 - v_0) + \int_0^t G(t - s) * (v^n + u^m)(s) ds \geq 0 \end{aligned} \quad (1.196)$$

Therefore, we have that:

$$(u - v) + \int_0^t \sum_{i=1}^N \frac{c_i}{(4\pi(t-s))^{\frac{N}{2}}} \frac{2x_i}{4(t-s)} e^{-\frac{x^2}{4(t-s)}} * (u - v)(s) ds \geq 0. \quad (1.197)$$

Given the positivity of the integrand governed by the exponential term, this last condition holds provided that

$$u \geq v \quad (1.198)$$

□

1.7 On global and local solutions

Our next objective, is to define the conditions to ensure the monotone behaviour of both solutions u, v . Indeed, the physical meaning requires us to have an increasing solution (u) which indicates the predominance of this solution when compared to the decreasing solution (v). For this purpose, we shall enunciate what conditions are required to ensure that $u_t \geq 0$ and $v_t \leq 0$.

When convection is introduced into a diffusion system with absorption and reaction, we shall establish the conditions to avoid the convection to be much predominant over the absorption or reaction. The fact of having a predominant convection can induce the solutions to be governed by it, minimizing, or even extinguishing, the effect of reaction and absorption. Therefore, any compatibility condition shall take into account a comparison between any parameter (mainly through an initial distribution mean value) of the solutions when subjected to reaction and absorption and when subjected, in addition, to the convection.

We stress the fact that diffusion will not be part of the ending comparison between reaction/absorption and convection. The diffusion acts when a initial mass for each of the searched solutions is given motivating the initial concentration to change over the domain when subjected to the forcing terms reaction/absorption. Nonetheless, our concern in this chapter is not related to the behaviour of the diffusion, indeed and independently of diffusion, any strong convection may lead to minimize the effect of the absorption and reaction terms. This is, in fact, the purpose of the following lemma:

Lemma 1.6. *Given a pair of solutions $(u, v) \in C^{2+\gamma, 1+\gamma/2}(\mathbb{R}^N \times (0, T))$ to the problem P , so that $u_t \geq 0$ and $v_t \leq 0$ in $\mathbb{R}^N \times (0, T)$, the following compatibility conditions shall be met to ensure the absorption and reaction terms are predominant over the convection:*

$$v_0^n \geq 2c \cdot \nabla u_0, \tag{1.199}$$

$$\int_{\mathbb{R}^N} u_0^m \geq \|c\| v_0.$$

Proof. We start by the set of equations defined under the scope of the problem P multiplying the first equation by u^2 and the second equation by v^2 .

Note that, we can make $\delta = \epsilon = 1$ in the development below without impacting the ending results:

$$\begin{aligned} u_t u^2 &= \delta \Delta u u^2 + c \cdot \nabla u u^2 + v^n u^2, \\ v_t v^2 &= \epsilon \Delta v v^2 + c \cdot \nabla v v^2 - u^m v^2. \end{aligned} \quad (1.200)$$

And integrating over $\mathbb{R}^N \times (0, T)$, we have:

$$\begin{aligned} \int_{\mathbb{R}^N} \int_0^T u_t u^2 &= \int_{\mathbb{R}^N} \int_0^T \delta \Delta u u^2 \\ &+ \int_{\mathbb{R}^N} \int_0^T c \cdot \nabla u u^2 + \int_{\mathbb{R}^N} \int_0^T v^n u^2, \end{aligned} \quad (1.201)$$

$$\begin{aligned} \int_{\mathbb{R}^N} \int_0^T v_t v^2 &= \int_{\mathbb{R}^N} \int_0^T \epsilon \Delta v v^2 \\ &+ \int_{\mathbb{R}^N} \int_0^T c \cdot \nabla v v^2 - \int_{\mathbb{R}^N} \int_0^T u^m v^2. \end{aligned} \quad (1.202)$$

Integrating by parts, we obtain:

$$\int_{\mathbb{R}^N} \int_0^T \delta \Delta u u^2 = \int_0^T \delta u^2 |\nabla u| - \int_{\mathbb{R}^N} \int_0^T \delta |\nabla u|^2 2u, \quad (1.203)$$

$$\int_{\mathbb{R}^N} \int_0^T c \cdot \nabla u u^2 = \int_0^T \|c\| u^3 - \int_{\mathbb{R}^N} \int_0^T u 2u c \cdot \nabla u. \quad (1.204)$$

Analogously for v :

$$\int_{\mathbb{R}^N} \int_0^T \epsilon \Delta v v^2 = \int_0^T \epsilon v^2 |\nabla v| - \int_{\mathbb{R}^N} \int_0^T \epsilon |\nabla v|^2 2v, \quad (1.205)$$

$$\int_{\mathbb{R}^N} \int_0^T c \cdot \nabla v v^2 = \int_0^T \|c\| v^3 - \int_{\mathbb{R}^N} \int_0^T v 2v c \cdot \nabla v. \quad (1.206)$$

After the integral assessment, we return to the expressions defined in (1.201)

and (1.202):

$$\begin{aligned}
\int_{\mathbb{R}^N} \int_0^T u_t u^2 &= \int_0^T \delta u^2 |\nabla u| - \int_{\mathbb{R}^N} \int_0^T \delta |\nabla u|^2 2u \\
&+ \int_0^T \|c\| u^3 - \int_{\mathbb{R}^N} \int_0^T u 2uc \cdot \nabla u + \int_{\mathbb{R}^N} \int_0^T v^n u^2 \\
&\geq \int_{\mathbb{R}^N} \int_0^T v^n u^2 - \int_{\mathbb{R}^N} \int_0^T \left(\delta |\nabla u|^2 2u + u 2uc \cdot \nabla u \right).
\end{aligned} \tag{1.207}$$

Assuming $u_t \geq 0$, implies to show that the last expression is ≥ 0 :

$$v^n u^2 \geq \delta |\nabla u|^2 2u + u 2uc \cdot \nabla u. \tag{1.208}$$

And performing the similar operations for the equation in v , we arrive at:

$$\begin{aligned}
\int_{\mathbb{R}^N} \int_0^T v_t v^2 &= \int_0^T \epsilon v^2 |\nabla v| - \int_{\mathbb{R}^N} \int_0^T \epsilon |\nabla v|^2 2v \\
&+ \int_0^T \|c\| v^3 - \int_{\mathbb{R}^N} \int_0^T v 2vc \cdot \nabla v - \int_{\mathbb{R}^N} \int_0^T u^m v^2 \tag{1.209} \\
&\leq \int_0^T \epsilon v^2 |\nabla v| + \int_0^T \|c\| v^3 - \int_{\mathbb{R}^N} \int_0^T u^m v^2.
\end{aligned}$$

Showing that $v_t \leq 0$, implies to show that the last expression is ≤ 0 :

$$\int_0^T \epsilon v^2 |\nabla v| + \int_0^T \|c\| v^3 - \int_{\mathbb{R}^N} \int_0^T u^m v^2 \leq 0. \tag{1.210}$$

In summary, we need to determine what conditions are required to be met, so that the inequalities (1.208) and (1.210) are satisfied. For this purpose:

$$v^n u^2 \geq \delta |\nabla u|^2 2u + u 2uc \cdot \nabla u \geq u 2uc \cdot \nabla u. \tag{1.211}$$

In the last expression, we have focused our attention only on the convective terms rather than diffusion, as we are interested on deriving an expression to compare convection with reaction and absorption. Therefore, we have that:

$$v^n \geq 2c \cdot \nabla u. \tag{1.212}$$

And for the solution v , we have:

$$\int_{\mathbb{R}^N} \int_0^T u^m v^2 \geq \int_0^T \epsilon v^2 |\nabla v| + \int_0^T \|c\| v^3, \quad (1.213)$$

so that

$$\int_{\mathbb{R}^N} u^m v^2 \geq \epsilon v^2 |\nabla v| + \|c\| v^3 \geq \|c\| v^3, \quad (1.214)$$

and

$$\int_{\mathbb{R}^N} u^m v^2 \geq \|c\| v^3. \quad (1.215)$$

We disregard the effects of the diffusion; we are interested in comparing the convection with the reaction and absorption. The assessment of the integral can be considered for mean values of v , so that the expressions reads as:

$$\int_{\mathbb{R}^N} u^m \geq \|c\| v. \quad (1.216)$$

The conditions obtained in the expressions (1.212) and (1.216) applies to the initial conditions as well, as both are applicable for any arbitrary small time T :

$$v_0^n \geq 2c \cdot \nabla u_0, \quad (1.217)$$

$$\int_{\mathbb{R}^N} u_0^m \geq \|c\| v_0.$$

□

It is particularly relevant to discuss the conditions shown. For this purpose, we start by considering the second equation of the system given by P and the condition for v given in (1.217). Indeed and in order to have $v_t \leq 0$, the mean integral over the domain of the initial data shall be higher than the magnitude of the convection given by the $\|c\|$. This will ensure that the absorption term is capable of avoiding any possible positive effect of the convection to contribute toward a positive v_t for any $T > 0$.

Additionally, the condition given in (1.217) reflects the fact that the reaction term shall be higher than the convective effects to ensure the increasing condition of the solution $u_t \geq 0$.

Note that the condition (1.217) is expressed as a compatibility condition for the initial data. Nonetheless, they apply to any local $T > 0$ as both

conditions have been obtained integrating between 0 and T .

Once we have shown the relationships between the convection and the forcing terms to meet the monotony properties of the solutions. It is, now, our aim to determine solutions locally for a given time $t > 0$. For this kind of local solutions, it is possible to determine the spatial distributions. This is the objective of the following lemma:

Lemma 1.7. *Given a pair of solutions (u, v) to the problem P in $\mathbb{R}^N \times (0, T)$, the following functions represent an asymptotic evolution (for $T \gg 1$) of the spatial distribution for the concentrations u, v . Both shall be understood, as valid locally for a given $t > 0$, so that the following expressions define the spatial distributions:*

$$u_s = u_0 + D_1 \int_{\mathbb{R}^N} (|x - s|)^{\frac{1}{2} \frac{2+m(1-n)}{1-nm}} C_u(t) e^{-\frac{|s|^2}{4t}} ds, \quad (1.218)$$

$$v_s = v_0 - D_2 \int_{\mathbb{R}^N} (|x - s|)^{\frac{m+1}{1-nm} - 2} C_v(t) e^{-\frac{|s|^2}{4t}} ds, \quad (1.219)$$

where

$$D_1 = \frac{1}{2\Gamma(2\alpha_1+1)}, \quad (1.220)$$

$$D_2 = \frac{1}{2\Gamma(2\alpha_2-1)},$$

being Γ the Gamma function.

In addition:

$$C_u(t) = t^{-\frac{1}{2} \frac{2+m(1-n)}{1-nm}}, \quad (1.221)$$

$$C_v(t) = t^{1-\frac{1}{2} \frac{m+1}{1-nm}}.$$

Proof. We proceed by searching solutions in the self-similar structure, as disposed by Barenblatt in [16] for a wide variety of problems. For this pur-

pose, we consider that the solutions can be expressed as:

$$\begin{aligned}
 u &= u_0 + t^{\alpha_1} \phi \left(|x| t^{-\beta_1} \right), \\
 v &= v_0 - t^{\alpha_2} \psi \left(|x| t^{-\beta_2} \right), \\
 \xi_1 &= |x| t^{-\beta_1}, \\
 \xi_2 &= |x| t^{-\beta_2},
 \end{aligned} \tag{1.222}$$

where $\alpha_1, \alpha_2, \beta_1$ and β_2 are constants to be assessed.

We are interested in determining the asymptotic evolution profile (for $T \gg 1$). Therefore, we operate making $u_0 = v_0 = 0$, i.e. when $T \gg 1$ the effect of the initial conditions are considered to be null or negligible.

Substituting the derivatives into the problem P , we read:

$$\begin{aligned}
 &\alpha_1 t^{\alpha_1-1} \phi \left(|x| t^{-\beta_1} \right) - t^{\alpha_1} |x| \beta_1 t^{-\beta_1-1} \phi_t \left(|x| t^{-\beta_1} \right) \\
 &= t^{\alpha_1-2\beta_1} \phi_{\xi\xi} + t^{\alpha_1} t^{-\beta_1} c \cdot \nabla \phi(\xi) + t^{\alpha_2 n} \psi^n, \\
 &-\alpha_2 t^{\alpha_2-1} \psi \left(|x| t^{-\beta_2} \right) + t^{\alpha_2} |x| \beta_2 t^{-\beta_2-1} \psi_t \left(|x| t^{-\beta_2} \right) \\
 &= t^{\alpha_2-2\beta_2} \psi_{\xi\xi} - t^{\alpha_2} t^{-\beta_2} c \cdot \nabla \psi(\xi) - t^{\alpha_1 m} \phi^m.
 \end{aligned} \tag{1.223}$$

We perform the following equalities in the coefficients:

$$\begin{aligned}
 \alpha_1 - 1 &= \alpha_1 - 2\beta_1 \rightarrow \beta_1 = \frac{1}{2}, \\
 \alpha_1 - \beta_1 &= \alpha_2 n \rightarrow \alpha_1 - \frac{1}{2} = \alpha_2 n, \\
 \alpha_2 - 1 &= \alpha_2 - 2\beta_2 \rightarrow \beta_2 = \frac{1}{2}, \\
 \alpha_2 - \beta_2 &= \alpha_1 m \rightarrow \alpha_2 - \frac{1}{2} = \alpha_1 m.
 \end{aligned} \tag{1.224}$$

An upon resolution:

$$\alpha_1 = \frac{1}{2} \frac{2+m(1-n)}{1-nm}, \quad \beta_1 = \frac{1}{2}, \quad (1.225)$$

$$\alpha_2 = \frac{1}{2} \frac{m+1}{1-nm}, \quad \beta_2 = \frac{1}{2}.$$

The resulting equations are:

$$-\phi'' - \left(\frac{1}{t^{\alpha_1-\beta_1}} c + \frac{1}{t^{\frac{\alpha_1-\beta_1-1}{\alpha_1-1}} \frac{\xi}{2}} \right) \phi' = -\alpha_1 \phi + \frac{1}{t^{\alpha_1-\beta_1}} \psi^n,$$

$$-\psi'' + \left(\frac{1}{t^{\alpha_2-\beta_2}} c + \frac{1}{t^{\frac{\alpha_2-\beta_2-1}{\alpha_2-1}} \frac{\xi}{2}} \right) \psi' = \alpha_2 \psi - \frac{1}{t^{\alpha_2-\beta_2}} \phi^m. \quad (1.226)$$

We can easily check that:

$$\frac{\alpha_i - 1}{\alpha_i - \beta_i} > 0, \quad i = 1, 2. \quad (1.227)$$

Therefore in the asymptotic approach with $t \gg 1$, we have:

$$-\phi'' - K_1(t) \frac{\xi}{2} \phi' = -\alpha_1 \phi, \quad (1.228)$$

$$-\psi'' + K_2(t) \frac{\xi}{2} \psi' = \alpha_2 \psi,$$

where:

$$K_1(t) = \frac{1}{t^{\frac{\alpha_1-\beta_1-1}{\alpha_1-1}}}, \quad K_2(t) = \frac{1}{t^{\frac{\alpha_2-\beta_2-1}{\alpha_2-1}}}. \quad (1.229)$$

As our intention is to obtain a spatial distribution, we can consider t as a parameter, so that the system of equations is solved for a given $t > 0$ providing fixed values for K_1 and K_2 . We obtain a spatial distribution making

$$K_1 = K_2 = 1. \quad (1.230)$$

Note that the spatial distribution structure will no change if we consider other values for K_1 and K_2 .

It is possible to solve, now, any of the equations. Note that we have removed the coupling effects of the system to obtain an asymptotic evolution that will drive the solutions autonomously.

Let operate in the equation for ϕ , naturally and in a similar procedure we can operate in the equation in ψ . Making the Fourier Transformation, we have:

$$-\omega^2\Phi - \frac{1}{2}(\Phi + \omega\Phi') - \alpha_1\Phi = 0, \quad (1.231)$$

so that:

$$\Phi' = \left(-2\omega - \frac{1}{\omega} - \frac{2\alpha_1}{\omega}\right)\Phi. \quad (1.232)$$

Upon resolution, we arrive at the following expression for Φ :

$$\Phi = e^{-\omega^2 + \log \omega^{-1-2\alpha_1}}. \quad (1.233)$$

The anti-transformation is:

$$\Phi = D_1 \xi^{2\alpha_1} * e^{-\frac{\xi^2}{4}}. \quad (1.234)$$

Where $*$ represents the convolution operator and

$$D_1 = \frac{1}{2\Gamma(2\alpha_1 + 1)}, \quad (1.235)$$

being Γ the Gamma function.

Analogously, for the concentration v , we have:

$$\Psi = D_2 \xi^{2\alpha_2-2} * e^{-\frac{\xi^2}{4}}, \quad (1.236)$$

where

$$D_2 = \frac{1}{2\Gamma(2\alpha_2 - 1)}. \quad (1.237)$$

Finally and after compilation, we have:

$$u_s = u_0 + D_1 \left(\frac{|x|}{t^{1/2}} \right)^{2\frac{1}{2} \frac{2+m(1-n)}{1-nm}} * e^{-\frac{|x|^2}{4t}}, \quad (1.238)$$

$$u_s = u_0 + C_u(t) D_1 (|x|)^{\frac{1}{2} \frac{2+m(1-n)}{1-nm}} * e^{-\frac{|x|^2}{4t}}, \quad (1.239)$$

where:

$$C_u(t) = t^{-\frac{1}{2} \frac{2+m(1-n)}{1-nm}}. \quad (1.240)$$

And finally,

$$u_s = u_0 + D_1 \int_{R^N} (|x-s|)^{\frac{1}{2} \frac{2+m(1-n)}{1-nm}} C_u(t) e^{-\frac{|s|^2}{4t}} ds. \quad (1.241)$$

Operating analogously for the population v :

$$v_s = v_0 - D_2 \left(\frac{|x|}{t^{1/2}} \right)^{2 \frac{1}{2} \frac{m+1}{1-nm} - 2} * e^{-\frac{|x|^2}{4t}}, \quad (1.242)$$

$$v_s = v_0 - D_2 C_v(t) (|x|)^{\frac{m+1}{1-nm} - 2} * e^{-\frac{|x|^2}{4t}}. \quad (1.243)$$

where:

$$C_v(t) = t^{1 - \frac{1}{2} \frac{m+1}{1-nm}}. \quad (1.244)$$

Thus:

$$v_M = v_0 - D_2 \int_{R^N} (|x-s|)^{\frac{m+1}{1-nm} - 2} C_v(t) e^{-\frac{|s|^2}{4t}}, \quad (1.245)$$

where

$$D_2 = \frac{1}{2\Gamma(2\alpha_2 - 1)}, \quad (1.246)$$

being Γ the Gamma function. □

The fact of having $v_t < 0$ and $u_t > 0$ shall be considered together with the positivity of solutions. If the solution u grows uncontrollably, it may induce that v goes to negativity and in turn, it may lead to a decreasing evolution for u down to negativity as well. In order to keep the positivity in the solutions, but keeping the order growth to avoid the term $-u^m$ acts toward negativity, the coming lemma shall be taken into account. We stress the fact that the coming maximal solution for u represents a bound that can be considered for assessing the maximum concentration of any of the substances

involved. For example, in the biological application, the following lemma provides the maximum concentration of cancerous cells in the media:

Lemma 1.8. *Let assume $(u_0, v_0) > (0, 0)$ and the parameter n satisfying $0, 5 < n < 1$. For any $\tau > 0$ and $R > 0$ such that $t \leq \tau$ and $|x| \leq R$ and under the condition $(u(x, t), v(x, t)) \geq (0, 0)$, the following upper bound is obtained for u :*

$$\max(u(x, t), t \leq \tau, |x| < R) \leq \frac{1}{k} \left(\frac{1}{2\sqrt{\pi\delta t}} \right)^{\frac{1}{nm}} \int_0^x e^{-\frac{(x-\xi)^2}{4\delta t nm}} * u_0^{\frac{1}{nm}}(\xi). \quad (1.247)$$

where

$$k = -\cos(n\pi). \quad (1.248)$$

Making use of the norm in $\mathbb{L}^1(|x| \leq R)$ we have:

$$\max(u(x, t), t \leq \tau, |x| < R) \leq \frac{1}{k} \|u_0\|^{\frac{1}{nm}}. \quad (1.249)$$

Proof. We start by considering Duhamel principle for our problem:

$$\begin{aligned} u(t) &= G_\delta * u_0 + \int_0^\tau |c \cdot \nabla G_\delta|(t-s) * u(s) ds + \int_0^\tau G_\delta(t-s) * v^n(s) ds, \\ v(t) &= G_\epsilon * v_0 + \int_0^\tau |c \cdot \nabla G_\epsilon|(t-s) * v(s) ds - \int_0^\tau G_\epsilon(t-s) * u^m(s) ds. \end{aligned} \quad (1.250)$$

The term v^n in the first equation can be obtained from the second equation; it can be replaced into the first equation, so that it is possible, after operating, to get an equation only dependant on u . Indeed:

$$\begin{aligned} u(t) &= G_\delta * u_0 + \int_0^\tau |c \cdot \nabla G_\delta|(t-s) * u(s) ds \\ &+ \int_0^\tau G_\delta(t-s) \\ &* \left[G_\epsilon * v_0 + \int_0^s |c \cdot \nabla G_\epsilon|(s-r) * v(r) dr - \int_0^s G_\epsilon(s-r) * u^m(r) dr \right]^n ds \\ &\geq G_\delta * u_0 + \int_0^\tau G_\delta(t-s) * \left[- \int_0^s G_\epsilon(s-r) * u^m(r) dr \right]^n ds \\ &= G_\delta * u_0 + (-1)^n \int_0^\tau G_\delta(t-s) * \left[\int_0^s G_\epsilon(s-r) * u^m(r) dr \right]^n ds. \end{aligned} \quad (1.251)$$

Considering that $0,5 < n < 1$, we read:

$$(-1)^n = -k = \cos(n\pi), \quad (1.252)$$

where consequently

$$0 < k < 1. \quad (1.253)$$

Making use of the Jensen inequality together with the condition (1.252), we have:

$$\begin{aligned} G_\delta * u_0 - k \int_0^\tau G_\delta(t-s) * \left[\int_0^s G_\epsilon(s-r) * u^m(r) dr \right]^n ds \\ \geq G_\delta * u_0 - k \int_0^\tau G_\delta(t-s) * \int_0^s G_\epsilon^n(s-r) * u^{mn}(r) dr ds. \end{aligned} \quad (1.254)$$

Assume that

$$\nu = \max(u(x,t), t \leq \tau, |x| < R), \quad (1.255)$$

then we have:

$$\begin{aligned} G_\delta * u_0 - k \int_0^\tau G_\delta(t-s) * \int_0^s G_\epsilon^n(s-r) * u^{mn}(r) dr ds \\ \geq G_\delta * u_0 - k \int_0^\tau G_\delta(t-s) * \int_0^s G_\epsilon^n(s-r) * \nu^{mn} dr ds \\ = G_\delta * u_0 - \nu^{mn} k \int_0^\tau G_\delta(t-s) * \int_0^s G_\epsilon^n(s-r) dr ds \\ \geq G_\delta * u_0 - \nu^{mn} k \int_0^\tau G_\delta(t-s) * \int_0^s G_\epsilon(s-r) dr ds. \end{aligned} \quad (1.256)$$

The normalization of the Gaussian Kernel leads to:

$$G_\delta * u_0 - \nu^{mn} k \geq 0 \quad (1.257)$$

so that,

$$\nu \leq \frac{1}{k} (G_\delta * u_0)^{\frac{1}{nm}} = \frac{1}{k} \left(\int_0^x \frac{1}{2\sqrt{\pi\delta t}} e^{-\frac{(x-\xi)^2}{4\delta t}} * u_0(\xi) \right)^{\frac{1}{nm}}. \quad (1.258)$$

therefore

$$\nu \leq \frac{1}{k} \left(\frac{1}{2\sqrt{\pi\delta t}} \right)^{\frac{1}{nm}} \int_0^x e^{-\frac{(x-\xi)^2}{4\delta t nm}} * u_0^{\frac{1}{nm}}(\xi). \quad (1.259)$$

In order to account for a magnitude, we can operate in the \mathbb{L}^1 norm, so that the following is get:

$$\max\{u(x, t), t \leq \tau, |x| < R\} \leq \frac{1}{k} \|G_\delta^{\frac{1}{nm}}\| \|u_0^{\frac{1}{nm}}\| \leq \frac{1}{k} \|u_0\|^{\frac{1}{nm}} \quad (1.260)$$

□

Our next intention is to find an estimation to the solution v applicable locally in space. We remind that $v_t < 0$, therefore, the idea is to search for a time-decaying estimation. The following lines are inspired by a procedure (adapted to our conditions and needs) already contemplated in Lemma 2.5 according to [24]. In addition, a similar approach was previously used in [25]. Note that in [24], the proposed estimation was used to obtain a supersolution, nonetheless, and in our case, it will be used to get a subsolution as local estimate. Indeed, this fact will lead to important differences compared to [24]. On top of the mathematical approach, in the biological application, the following lemma provides a minimum local concentration of healthy cells that can keep the organ alive:

Lemma 1.9. *Given a local point x_0 and a positive parameter R :*

$$0 < R < \left(\frac{1}{2} - \epsilon \right) \frac{1}{c} < |x_0|, x_0 \in \mathbb{R}^N. \quad (1.261)$$

There exists a positive T satisfying:

$$T \leq \left[\frac{\alpha}{\nu^m} (2\epsilon + c2R - 1) \right]^{\frac{1}{1-\alpha}}, \quad (1.262)$$

(where ν is the maximum value of u as per (1.255)), such that the following lower local bound for the solution v holds in $0 < t < T$:

$$v(x, t) \geq K \frac{(R^2 + t)^{2\alpha}}{(R^2 - x^2 + t)^\alpha}, \quad 0 < x \leq R, \quad (1.263)$$

where:

$$k \frac{1}{\|u_0\|^{\frac{1-nm}{n}}} \leq K \leq \left(\frac{(R^2 + T)^4}{\epsilon \alpha 4 R^2 (\alpha + 1)} \right)^{\frac{1}{1-m}}, \quad (1.264)$$

note that k is as per (1.252), and

$$\alpha = \frac{2}{m-1}. \quad (1.265)$$

Proof. We start by considering the equation for v :

$$v_t = \epsilon \Delta v + c \cdot \nabla v - u^m \leq \epsilon \Delta v + c \cdot \nabla v - v^m, \quad (1.266)$$

then,

$$v_t - \epsilon \Delta v - c \cdot \nabla v + v^m \leq 0. \quad (1.267)$$

This last inequality holds as we have shown that $u \geq v$ (Lemma 1.5). Therefore, we have an inequality whose approximate resolution will provide a subevolution for the population v . We assume an evolution of the form (according to [24] and [25]):

$$V(x, t) = K \frac{(R^2 + t)^{2\alpha}}{(R^2 - x^2 + t)^\alpha}. \quad (1.268)$$

The associated time derivative is:

$$\begin{aligned} V_t &= K 2\alpha (R^2 + t)^{2\alpha-1} (R^2 - x^2 + t)^{-\alpha} \\ &\quad - K (R^2 + t)^{2\alpha} \alpha (R^2 - x^2 + t)^{-\alpha-1}, \end{aligned} \quad (1.269)$$

The first spatial derivative is:

$$V_x = K (R^2 + t)^{2\alpha} \alpha 2x (R^2 - x^2 + t)^{-\alpha-1}, \quad (1.270)$$

and the second:

$$\begin{aligned} V_{xx} &= K (R^2 + t)^{2\alpha} \alpha 2 (R^2 - x^2 + t)^{-\alpha-1} \\ &\quad + K (R^2 + t)^{2\alpha} \alpha 2x (\alpha + 1) 2x (R^2 - x^2 + t)^{-\alpha-2}. \end{aligned} \quad (1.271)$$

And introducing these last derivatives into the equation (1.267), we have:

$$\begin{aligned}
& K2\alpha(R^2 + t)^{2\alpha-1}(R^2 - x^2 + t)^{-\alpha} \\
& - K(R^2 + t)^{2\alpha}\alpha(R^2 - x^2 + t)^{-\alpha-1} \\
& - \epsilon K(R^2 + t)^{2\alpha}\alpha 2(R^2 - x^2 + t)^{-\alpha-1} \\
& - \epsilon K(R^2 + t)^{2\alpha}\alpha 2x(\alpha + 1)2x(R^2 - x^2 + t)^{-\alpha-2} \quad (1.272) \\
& - cK(R^2 + t)^{2\alpha}\alpha 2x(R^2 - x^2 + t)^{-\alpha-1} \\
& + K^m \frac{(R^2 + t)^{2\alpha m}}{(R^2 - x^2 + t)^{\alpha m}} \leq 0.
\end{aligned}$$

Aiming the easiest comparison, we make:

$$-\alpha m = -\alpha - 2 \rightarrow \alpha = \frac{2}{m-1} < 0. \quad (1.273)$$

To achieve the inequality condition, we shall find an appropriate value of K . For this purpose, we require that:

$$\begin{aligned}
\epsilon K(R^2 + t)^{2\alpha}\alpha 4x^2(\alpha + 1) & \geq K^m(R^2 + t)^{2\alpha m}, \\
\epsilon(R^2 + t)^{-4}\alpha 4x^2(\alpha + 1) & \geq K^{m-1}, \\
K & \leq \left(\frac{\epsilon\alpha 4x^2(\alpha+1)}{(R^2+t)^4} \right)^{\frac{1}{m-1}}, \quad (1.274)
\end{aligned}$$

$$K \leq \left(\frac{(R^2+t)^4}{\epsilon\alpha 4x^2(\alpha+1)} \right)^{\frac{1}{1-m}} \leq \left(\frac{(R^2+T)^4}{\epsilon\alpha 4x^2(\alpha+1)} \right)^{\frac{1}{1-m}}.$$

By replacing $x = x_0$ in this last expression and making the convergence $R \rightarrow |x_0|$, we obtain the following estimation for the parameter K :

$$K \leq \left(\frac{(R^2 + T)^4}{\epsilon\alpha 4R^2(\alpha + 1)} \right)^{\frac{1}{1-m}}. \quad (1.275)$$

Our next intention is to show that (1.268) with the estimations (1.273) and (1.275) is a subsolution for $0 < t < T$. For this purpose we shall show

that:

$$v_t \leq \epsilon \Delta v + c \cdot \nabla v - u^m, \quad (1.276)$$

or, equivalently:

$$v_t - \epsilon \Delta v - c \cdot \nabla v + u^m \leq 0. \quad (1.277)$$

Therefore, we have:

$$\begin{aligned} & K 2\alpha (R^2 + t)^{2\alpha-1} (R^2 - x^2 + t)^{-\alpha} \\ & - K (R^2 + t)^{2\alpha} \alpha (R^2 - x^2 + t)^{-\alpha-1} \\ & - \epsilon K (R^2 + t)^{2\alpha} \alpha 2 (R^2 - x^2 + t)^{-\alpha-1} \\ & - \epsilon K (R^2 + t)^{2\alpha} \alpha 2x (\alpha + 1) 2x (R^2 - x^2 + t)^{-\alpha-2} \\ & - c K (R^2 + t)^{2\alpha} \alpha 2x (R^2 - x^2 + t)^{-\alpha-1} + K \nu^m \leq 0. \end{aligned} \quad (1.278)$$

where u^m has been replaced by $K\nu^m$ in the assumption that ν is sufficiently large to consider

$$K\nu^m \geq u^m. \quad (1.279)$$

Note that ν is given by (1.255). The expression (1.279) holds for a suitable value of K that can be chosen by comparing the initial conditions in accordance with (1.260)

$$K \geq \frac{u^m}{\nu^m} \sim k \frac{\|u_0\|^m}{\|u_0\|^{\frac{m}{nm}}}. \quad (1.280)$$

Upon operation, we have

$$K \geq k \frac{1}{\|u_0\|^{\frac{1-nm}{n}}}. \quad (1.281)$$

where k is as per (1.252).

Now, making $t = T \gg 1$ and considering the leading terms in (1.278), we read:

$$K\alpha + K\nu^m T^{1-\alpha} \leq 2K\alpha\epsilon + cK\alpha 2x. \quad (1.282)$$

Making $x \rightarrow R$ and obtaining T we have:

$$T \leq \left[\frac{\alpha}{\nu^m} (2\epsilon + c2R - 1) \right]^{\frac{1}{1-\alpha}}, \quad (1.283)$$

According to (1.273) $\alpha < 0$, therefore to account for a suitable positive value for the upper bound of T we require:

$$1 > 2\epsilon + c2R, \quad (1.284)$$

which provides the following value for R :

$$R < \left(\frac{1}{2} - \epsilon\right) \frac{1}{c}. \quad (1.285)$$

□

1.8 Evolution of solution profiles

In this section, we use the monotone properties of the reaction and absorption forcing terms to show the behaviour and precise evolutions of an upper solution and a lower solution. In addition, we determine the asymptotic order of growth.

In the industrial application, we are interested on finding a non-decreasing upper solution for the concentration u (i.e. $u_t \geq 0$) and a non-increasing lower solution for the concentration v (i.e. $v_t \leq 0$). This can be explained in view of the following argument:

Within the industrial scope, the set of equations in P has the objective to determine suitable concentrations of nitrogen (represented by u) and oxygen (represented by v) capable of preventing fuel tank ignition in the presence of a spark or hot surfaces. The fact of having a lower solution for u and a upper solution for v will under-estimate the quantity of nitrogen and over-estimate the quantity of oxygen for any given time $t > 0$. These approximations are perfectly valid for our purposes as they are overly conservative. Indeed, consider that at a given time $t > 0$, the upper solution and the lower solution determine the existence of a potentially flammable mixture of oxygen and nitrogen in the presence of a spark or hot surface. It is, thus, required to continue with the evolution to reach and under-estimation of nitrogen (the lower solution for u) and a over-estimation of oxygen (the upper solution for v). Both estimations will be determined at a time $t > 0$ and are values for which we relay that a non-flammable mixture is given.

The following theorem provides a proof about the behaviour and precise evolution of the mentioned upper solution and lower solution:

Theorem 1.8.1. *Assume that:*

$$u(x, 0) > 0, \tag{1.286}$$

$$v(x, 0) > 0.$$

Let consider a variable ν :

$$\nu \in \mathbb{R}^+, \tag{1.287}$$

and

$$0 < \nu < \min_{x \in \mathbb{R}^N} (u(x, 0), v(x, 0)). \quad (1.288)$$

So that, the initial conditions are re-written as:

$$\begin{aligned} u(x, 0) + \nu, \quad v(x, 0) + \nu, \\ u(x, 0) - \nu, \quad v(x, 0) - \nu. \end{aligned} \quad (1.289)$$

Assume the following flow evolutions resulting from the mentioned initial conditions:

$$\begin{aligned} (u(x, 0) + \nu, v(x, 0) + \nu) &\rightarrow \text{evol} \rightarrow (\hat{U}(x, t), \hat{V}(x, t)), \\ (u(x, 0) - \nu, v(x, 0) - \nu) &\rightarrow \text{evol} \rightarrow (\tilde{U}(x, t), \tilde{V}(x, t)). \end{aligned} \quad (1.290)$$

The upper solutions $(\hat{U}(x, t), \hat{V}(x, t))$ are time monotone non-increasing and the lower solutions $(\tilde{U}(x, t), \tilde{V}(x, t))$ are time monotone non-decreasing for $t \in (0, T)$.

Additionally, we have that for any $t \in (0, T)$,

$$((\hat{U}(x, t), \hat{V}(x, t)) \geq ((\tilde{U}(x, t), \tilde{V}(x, t)), \quad (1.291)$$

and the following limit apply:

$$\begin{aligned} \lim_{\nu \rightarrow 0} (\hat{U}(x, t), \hat{V}(x, t)) &= (\hat{U}(x, t)_a, \hat{V}(x, t)_a), \\ \lim_{\nu \rightarrow 0} (\tilde{U}(x, t), \tilde{V}(x, t)) &= (\tilde{U}(x, t)_a, \tilde{V}(x, t)_a). \end{aligned} \quad (1.292)$$

such that:

$$\begin{aligned} \hat{U}(x, t)_a &\geq \tilde{U}(x, t)_a, \\ \hat{V}(x, t)_a &\geq \tilde{V}(x, t)_a. \end{aligned} \quad (1.293)$$

In addition, the upper solutions $(\hat{U}_a(x, t), \hat{V}_a(x, t))$ are monotone non-increasing and the lower solutions $(\tilde{U}_a(x, t), \tilde{V}_a(x, t))$ are monotone non-decreasing for $t \in (0, T)$

Proof. We, firstly, show the order between the upper and lower solutions.

For this purpose, we define:

$$w_1 = \hat{U} - \tilde{U}, \quad (1.294)$$

$$w_2 = \hat{V} - \tilde{V},$$

and the initial conditions:

$$w_1(x, 0) = \hat{U}(x, 0) - \tilde{U}(x, 0) = u_0 + \nu - u_0 + \nu = 2\nu > 0,$$

$$w_2(x, 0) = \hat{V}(x, 0) - \tilde{V}(x, 0) = v_0 + \nu - v_0 + \nu = 2\nu > 0. \quad (1.295)$$

Now, we focus on the operator:

$$L(\hat{U}) = \hat{V}^n; \quad L(\tilde{U}) = \tilde{V}^n. \quad (1.296)$$

And making the subtraction:

$$L(w_1) = \hat{V}^n - \tilde{V}^n. \quad (1.297)$$

Analogously:

$$L(\hat{V}) = -\tilde{U}^m; \quad L(\tilde{V}) = -\hat{U}^m. \quad (1.298)$$

Again, making the subtraction, we have:

$$L(w_2) = \hat{U}^m - \tilde{U}^m. \quad (1.299)$$

In summary, we have the following problem:

$$L(w_1) = \hat{V}^n - \tilde{V}^n,$$

$$L(w_2) = \hat{U}^m - \tilde{U}^m, \quad (1.300)$$

$$w_1(x, 0), \quad w_2(x, 0) > 0.$$

If we assume that $\hat{V}^n \geq \tilde{V}^n$ for $t \in (0, T)$, we have:

$$L(w_1) = \hat{V}^n - \tilde{V}^n \geq 0, \quad (1.301)$$

$$w_1 \geq 0 \rightarrow \hat{U} \geq \tilde{U}.$$

Therefore, we can consider that in the w_2 equation, the following is met:

$$L(w_2) = \hat{U}^m - \tilde{U}^m \geq 0, \quad (1.302)$$

$$w_2 \geq 0 \rightarrow \hat{V} \geq \tilde{V},$$

for any $t \in (0, T)$. The same results can be obtained by considering the strong positivity of the parabolic operator L (for a complete discussion on the maximum principle and strong positivity of the parabolic operator, we can refer to Section 7 in [23]). If the initial conditions w_1 and w_2 are positive, any flow subjected to L is positive, i.e:

$$L(w_1) \geq 0, \quad (1.303)$$

$$L(w_2) \geq 0.$$

Our next intention is to show the time monotone properties of each of the defined solutions, namely, $\hat{U}, \tilde{U}, \hat{V}$ and \tilde{V} . For this purpose, we consider two fixed real parameters $\sigma_1, \sigma_2 > 0$, such that, we make the following differences:

$$\begin{aligned} \tilde{U}_{\sigma_1}(x, t) &= \tilde{U}(x, t + \sigma_1) - \tilde{U}(x, t), \\ \tilde{V}_{\sigma_1}(x, t) &= \tilde{V}(x, t + \sigma_1) - \tilde{V}(x, t), \\ \hat{U}_{\sigma_2}(x, t) &= \hat{U}(x, t + \sigma_2) - \hat{U}(x, t), \\ \hat{V}_{\sigma_2}(x, t) &= \hat{V}(x, t + \sigma_2) - \hat{V}(x, t). \end{aligned} \quad (1.304)$$

For $t = 0$, we have:

$$\begin{aligned} \tilde{U}_{\sigma_1}(x, 0) &= \tilde{U}(x, \sigma_1) - u(x, 0) + \nu, \\ \tilde{V}_{\sigma_1}(x, 0) &= \tilde{V}(x, \sigma_1) - v(x, 0) + \nu, \\ \hat{U}_{\sigma_2}(x, 0) &= \hat{U}(x, \sigma_2) - u(x, 0) - \nu, \\ \hat{V}_{\sigma_2}(x, 0) &= \hat{V}(x, \sigma_2) - v(x, 0) - \nu. \end{aligned} \quad (1.305)$$

We can select a sufficiently large ν or a sufficiently small and positive values

for the parameters σ_1 and σ_2 so that:

$$\tilde{U}_{\sigma_1}(x, 0) \geq 0; \quad \tilde{V}_{\sigma_1}(x, 0) \geq 0; \quad \hat{U}_{\sigma_2}(x, 0) \leq 0; \quad \hat{V}_{\sigma_2}(x, 0) \leq 0. \quad (1.306)$$

The defined solutions $\hat{U}_{\sigma_2}, \tilde{U}_{\sigma_1}, \hat{V}_{\sigma_2}$ and \tilde{V}_{σ_1} satisfy the given equations in P . For this purpose, we submit such solutions to the operator L :

$$\begin{aligned} L(\tilde{U}_{\sigma_1}) &= \tilde{V}(x, t + \sigma_1)^n - \tilde{V}(x, t)^n, \\ L(\tilde{V}_{\sigma_1}) &= \hat{U}(x, t)^m - \hat{U}(x, t + \sigma_2)^m, \\ L(\hat{U}_{\sigma_2}) &= \hat{V}(x, t + \sigma_2)^n - \hat{V}(x, t)^n, \\ L(\hat{V}_{\sigma_2}) &= \tilde{U}(x, t)^m - \tilde{U}(x, t + \sigma_1)^m. \end{aligned} \quad (1.307)$$

Assume that for $t \in (0, T)$:

$$\tilde{V}(x, t + \sigma_1)^n \geq \tilde{V}(x, t)^n, \quad (1.308)$$

then we have:

$$L(\tilde{U}_{\sigma_1}) \geq 0 \rightarrow \tilde{U}_{\sigma_1} \geq 0 \rightarrow \tilde{U}(x, t + \sigma_1) \geq \tilde{U}(x, t). \quad (1.309)$$

As

$$L(\hat{V}_{\sigma_2}) = \tilde{U}(x, t)^m - \tilde{U}(x, t + \sigma_1)^m, \quad (1.310)$$

we read:

$$L(\hat{V}_{\sigma_2}) \leq 0 \rightarrow \hat{V}(x, t + \sigma_2) \leq \hat{V}(x, t). \quad (1.311)$$

And again, as

$$L(\hat{U}_{\sigma_2}) = \hat{V}(x, t + \sigma_2)^n - \hat{V}(x, t)^n, \quad (1.312)$$

we read:

$$L(\hat{U}_{\sigma_2}) \leq 0 \rightarrow \hat{U}_{\sigma_2} \leq 0 \rightarrow \hat{U}(x, t + \sigma_2) \leq \hat{U}(x, t). \quad (1.313)$$

And finally, we repeat the process for

$$L(\tilde{V}_{\sigma_1}) = \hat{U}(x, t)^m - \hat{U}(x, t + \sigma_2)^m, \quad (1.314)$$

so that:

$$L(\tilde{V}_{\sigma_1}) \geq 0 \rightarrow \tilde{V}_{\sigma_1} \geq 0 \rightarrow \tilde{V}(x, t + \sigma_1) \geq \tilde{V}(x, t). \quad (1.315)$$

Initially, we assumed that $\tilde{V}(x, t + \sigma_1)^n \geq \tilde{V}(x, t)^n$. In the last expression, we have reached a condition that satisfies the initial assumption, showing, thus, its validity.

Summarizing the conditions obtained, we have:

$$\begin{aligned} \tilde{V}(x, t + \sigma_1) &\geq \tilde{V}(x, t), \\ \tilde{U}(x, t + \sigma_1) &\geq \tilde{U}(x, t), \\ \hat{V}(x, t + \sigma_2) &\leq \hat{V}(x, t), \\ \hat{U}(x, t + \sigma_2) &\leq \hat{U}(x, t), \end{aligned} \quad (1.316)$$

which permit to show that the upper solutions are time monotone non-increasing and that the lower solutions are time monotone non-decreasing as postulated in the theorem enunciation.

The upper and lower solutions can be defined for any arbitrary small $\nu > 0$ approaching the initial conditions as $\nu \rightarrow 0$. For any ν , the monotony properties of the upper and lower solutions sequences (as defined in lemma 1.3) holds, permitting to ensure the existence of a limit solution such that:

$$\begin{aligned} \lim_{\nu \rightarrow 0}(\hat{U}(x, t), \hat{V}(x, t)) &= (\hat{U}(x, t)_a, \hat{V}(x, t)_a), \\ \lim_{\nu \rightarrow 0}(\tilde{U}(x, t), \tilde{V}(x, t)) &= (\tilde{U}(x, t)_a, \tilde{V}(x, t)_a). \end{aligned} \quad (1.317)$$

In addition, the limit solutions when $\nu \rightarrow 0$ preserves the ordered properties between upper and lower solutions and the time monotony properties.

Indeed, when passing to the limit, we can say that:

$$\begin{aligned}
\tilde{V}_a(x, t + \sigma_1) &\geq \tilde{V}_a(x, t), \\
\tilde{U}_a(x, t + \sigma_1) &\geq \tilde{U}_a(x, t), \\
\hat{V}_a(x, t + \sigma_2) &\leq \hat{V}_a(x, t), \\
\hat{U}_a(x, t + \sigma_2) &\leq \hat{U}_a(x, t).
\end{aligned}
\tag{1.318}$$

We have shown the theorem postulation stating that the upper solutions $(\hat{U}_a(x, t), \hat{V}_a(x, t))$ are monotone non-increasing and the lower solutions $(\tilde{U}_a(x, t), \tilde{V}_a(x, t))$ are monotone non-decreasing for $t \in (0, T)$.

Furthermore:

$$\begin{aligned}
\hat{U}_a &\geq \tilde{U}_a, \\
\hat{V}_a &\geq \tilde{V}_a.
\end{aligned}
\tag{1.319}$$

□

We are interested on finding a lower solution for the concentration u and a upper solution for v . We have shown, in the previous section, that any lower solution is monotone non-decreasing and any upper solution is monotone non-increasing. Our next intention is to find a upper and lower solutions complying with the time monotone properties described. In particular, we are going to search only for spatially homogeneous distributed solutions (also known as flat solutions) so that we only take into account the time variable.

It is to be stressed that the forcing terms are only functions of the solutions, there are not explicit dependency with the spatial term. Therefore, we do not need to take the supreme of the forcing term for the variable x . This means that the time evolution profile for the expected upper and lower solutions are given by the initial data shift $\tilde{U}(x, 0) = u(x, 0) - \nu$ and $\hat{V}(x, 0) = v(x, 0) + \nu$ together with the linear first derivative in the operator L

The problem to study is, therefore:

$$\begin{aligned}\tilde{U}_t &= \tilde{V}^n, \\ \hat{V}_t &= -\tilde{U}^m, \\ \tilde{U}(x, 0) &= u(x, 0) - \nu, \\ \hat{V}(x, 0) &= v(x, 0) + \nu.\end{aligned}\tag{1.320}$$

Any solution to this problem shall satisfy the time monotony properties given in the expressions (1.318).

With the aim of solving the problem (1.320), we shall perform an assumption for the lower solution \tilde{V} . We know that such solution shall be time monotone non-decreasing in virtue of the conditions obtained in (1.318). Let assume that we can know a lower threshold for the solution v . This lower threshold cannot be trespass by any solution in virtue of the uniqueness properties of our problem obtained in Section 1.5. Therefore, let consider:

$$\tilde{V} = \mu^{1/n}\tag{1.321}$$

So that, the problem in (1.320) reads:

$$\begin{aligned}\tilde{U}_t &= \mu, \\ \hat{V}_t &= -\tilde{U}^m, \\ \tilde{U}(x, 0) &= u(x, 0) - \nu, \\ \hat{V}(x, 0) &= v(x, 0) + \nu.\end{aligned}\tag{1.322}$$

Upon integration, we have a linear evolution for the lower solution of u that can be used for obtaining the upper solutions to v :

$$\begin{aligned}\tilde{U}(t) &= \tilde{U}_0 + \mu t, \\ \hat{V}(t) &= \hat{V}_0 - \frac{1}{\mu(m+1)}(\tilde{U}_0 + \mu t)^{m+1}.\end{aligned}\tag{1.323}$$

For the initial data, we have required

$$u_0(x), v_0(x) \in \mathbb{L}_{loc}^1(\mathbb{R}^N) \cap \mathbb{L}^\infty(\mathbb{R}^N), \quad (1.324)$$

which is the case when the initial data are given constants (see problem P in (1.318))

For all other case in which the initial data is not constant, and to account for a close solution search, we require:

$$u(x, 0), v(x, 0) \in \mathbb{L}^1(\mathbb{R}^N), \quad (1.325)$$

Thus, we define:

$$\|\tilde{U}_0\|_{\mathbb{L}^1} = \|u(x, 0)\|_{\mathbb{L}^1} - \nu_n. \quad (1.326)$$

And analogously for the concentration v :

$$\|\hat{V}_0\|_{\mathbb{L}^1} = \|v(x, 0)\|_{\mathbb{L}^1} + \nu_n. \quad (1.327)$$

The value of ν_n may be different compared to ν so that the Schwarz inequality turns to equality:

$$\|u(x, 0) - \nu\|_{\mathbb{L}^1} = \|u(x, 0)\|_{\mathbb{L}^1} - \nu_n \leq \|u(x, 0)\|_{\mathbb{L}^1} + \nu, \quad (1.328)$$

analogously for v :

$$\|v(x, 0) + \nu\|_{\mathbb{L}^1} = \|v(x, 0)\|_{\mathbb{L}^1} + \nu_n \leq \|v(x, 0)\|_{\mathbb{L}^1} + \nu, \quad (1.329)$$

We can choose $\nu_n \rightarrow 0$ (idem for ν), so that the solutions adopt the following form:

$$\begin{aligned} \tilde{U}_a(t) &= \|u(x, 0)\|_{\mathbb{L}^1} + \mu t, \\ \hat{V}_a(t) &= \|v(x, 0)\|_{\mathbb{L}^1} - \frac{1}{\mu(m+1)} (\|u(x, 0)\|_{\mathbb{L}^1} + \mu t)^{m+1}. \end{aligned} \quad (1.330)$$

It is remarkable to say that the solutions are valid in a interval $(0, T)$ in which we can ensure that the postulated lower solution in (1.321) for v applies. Indeed, the decreasing rate of the solution v will lead to intersect the constant lower solution given by $\tilde{V} = \mu^{1/n}$. It is, then, required to obtain

the upper limit T in which the spatially homogeneous solutions are valid:

$$\mu^{1/n} = \|v(x, 0)\|_{\mathbb{L}^1} - \frac{1}{\mu(m+1)} (\|u(x, 0)\|_{\mathbb{L}^1} + \mu T)^{m+1}. \quad (1.331)$$

We can, now, obtain T as:

$$T = \frac{(\mu(m+1))^{\frac{1}{m+1}} (\|v(x, 0)\|_{\mathbb{L}^1} - \mu^{1/n})^{\frac{1}{m+1}} - \|u(x, 0)\|_{\mathbb{L}^1}}{\mu}. \quad (1.332)$$

In the assumption that $\|v(x, 0)\|_{\mathbb{L}^1} \gg \mu^{1/n}$, we have that solutions will exist provided:

$$\mu(m+1) (\|v(x, 0)\|_{\mathbb{L}^1}) \geq \|u(x, 0)\|_{\mathbb{L}^1}^{m+1}. \quad (1.333)$$

So that the value of μ shall be selected under the condition:

$$\mu \geq \frac{\|u(x, 0)\|_{\mathbb{L}^1}^{m+1}}{(m+1) \|v(x, 0)\|_{\mathbb{L}^1}}. \quad (1.334)$$

Another assumption that we can make for the lower solution \tilde{V} , towards solving the problem in (1.320), is to consider a monotone non-decreasing logistic evolution in the form:

$$\tilde{V} = \frac{\mu}{1 + e^{-\beta t}}. \quad (1.335)$$

And making $\nu \rightarrow 0$, the system (1.320) adopts the form:

$$\begin{aligned} \tilde{U}_t &= \frac{\mu}{1 + e^{-\beta t}}, \\ \hat{V}_t &= -\tilde{U}^m, \end{aligned} \quad (1.336)$$

$$\tilde{U}(x, 0) = u(x, 0) - (\nu \rightarrow 0),$$

$$\hat{V}(x, 0) = v(x, 0) + (\nu \rightarrow 0).$$

The solutions to this system are:

$$\tilde{U}_a = \|u(x, 0)\|_{\mathbb{L}^1} + \frac{\sigma}{\beta} \log \left(\frac{1+e^{-\beta t}}{e^{-\beta t}} \right),$$

$$\hat{V}_a = \|v(x, 0)\|_{\mathbb{L}^1} - \int_0^T \left(\|u(x, 0)\|_{\mathbb{L}^1} + \frac{\sigma}{\beta} \log \left(\frac{1+e^{-\beta t}}{e^{-\beta t}} \right) \right)^m dt. \quad (1.337)$$

And making use of the mean value theorem for the solution \hat{V}_a , we read:

$$\hat{V}_a = \|v(x, 0)\|_{\mathbb{L}^1} - \left(\|u(x, 0)\|_{\mathbb{L}^1} + \frac{\sigma}{\beta} \log \left(\frac{1+e^{-\beta t_m}}{e^{-\beta t_m}} \right) \right)^m T, \quad (1.338)$$

where $0 < t_m < T$.

The solutions given in (1.337) exist provided the asymptotic value of the logistic growth (μ), admitted for \tilde{V} , satisfies the condition derived in (1.334).

Our next intention is to show the stability of the solutions \tilde{U}_a and \hat{V}_a . We enunciate the following lemma:

Lemma 1.10. *The solutions $(\tilde{U}_a, \tilde{V}_a)$ and (\hat{U}_a, \hat{V}_a) satisfy the following conditions in $\mathbb{R}^N \times (0, T)$:*

$$(u_0, v_0) \leq (\hat{U}_a, \hat{V}_a) \leq (\tilde{U}, \tilde{V}), \quad (1.339)$$

and

$$(\tilde{U}, \tilde{V}) \leq (\tilde{U}_a, \tilde{V}_a) \leq (\hat{U}_a, \hat{V}_a), \quad (1.340)$$

where,

$$\hat{U}_a, \hat{V}_a, \tilde{U}_a, \tilde{V}_a \in C^{2+\gamma, 1+\gamma/2}(\mathbb{R}^N \times (0, T)). \quad (1.341)$$

Proof. Let define the following variables:

$$\begin{aligned}
 w_1 &= \hat{U}_a - \hat{U}, \\
 W_1 &= \tilde{U}_a - \tilde{U}, \\
 w_2 &= \hat{V}_a - \hat{V}, \\
 W_2 &= \tilde{V}_a - \tilde{V}.
 \end{aligned}
 \tag{1.342}$$

And introducing the above expression in the operator evolution, we read:

$$\begin{aligned}
 L(w_1) &= \hat{V}_a^n - \hat{V}^n, \\
 L(W_1) &= \tilde{V}_a^n - \tilde{V}^n, \\
 L(w_2) &= -\tilde{U}_a^m + \tilde{U}^m, \\
 L(W_2) &= -\hat{U}_a^m + \hat{U}^m.
 \end{aligned}
 \tag{1.343}$$

The time monotony properties of each of the terms in the right hand side of the last expressions are the same between the elements involved in the difference (See inequalities in (1.316) and (1.318)). In addition, each of the terms with sub-index a were defined as a limit solutions in the expressions (1.317).

The non-increasing condition of the upper solutions permits to write $\hat{V}_a \leq \hat{V}$, therefore we have:

$$L(w_1) \leq 0 \rightarrow w_1 \leq 0 \rightarrow \hat{U}_a \leq \hat{U}. \tag{1.344}$$

In the same way we can say:

$$L(W_2) = -\hat{U}_a^m + \hat{U}^m \geq 0 \rightarrow W_1 \geq 0 \rightarrow \tilde{V}_a \geq \tilde{V}. \tag{1.345}$$

We repeat the process for W_1 :

$$L(W_2) = \tilde{V}_a^n - \tilde{V}^n \geq 0 \rightarrow W_2 \geq 0 \rightarrow \tilde{U}_a \geq \tilde{U}. \tag{1.346}$$

Eventually, a similar argument applies to w_2 :

$$L(w_2) = -\tilde{U}_a^m + \tilde{U}^n \leq 0 \rightarrow w_2 \leq 0 \rightarrow \tilde{V}_a \geq \tilde{V}. \quad (1.347)$$

Then, we can write the following bounds based on the ordered properties obtained between the solutions:

$$\begin{aligned} (u_0, v_0) &\leq (\hat{U}_a, \hat{V}_a) \leq (\hat{U}, \hat{V}), \\ (\tilde{U}, \tilde{V}) &\leq (\tilde{U}_a, \tilde{V}_a) \leq (\hat{U}_a, \hat{V}_a). \end{aligned} \quad (1.348)$$

As it was our aim to proof.

Note that this condition ensures a band for the the limit solutions $\hat{U}_a, \hat{V}_a, \tilde{U}_a$ and \tilde{V}_a . In addition, the involved functions in the borders of the band satisfy the regularity condition in the expression (1.139), therefore we can say that:

$$\hat{U}_a, \hat{V}_a, \tilde{U}_a, \tilde{V}_a \in C^{2+\gamma, 1+\gamma/2}(\mathbb{R}^N \times (0, T)). \quad (1.349)$$

Note that the solutions described in the expressions (1.330) and (1.337) satisfy to be in $C^{2+\gamma, 1+\gamma/2}(\mathbb{R}^N \times (0, T))$ \square

1.9 Travelling Waves (TW)

In the kind of the physical reality, we aim to characterize, it is common to have stationary solutions towards the evolution tends for a sufficiently large time. In our case, we have $u_t > 0$ and $v_t < 0$, thus, the long time behaviour of solutions suggests that the population u will tend to a value such that:

$$u = d > \max_{x \in \mathbb{R}^N} u_0(x). \quad (1.350)$$

And the population v will tend to a value close to zero:

$$v \rightarrow 0^+ \quad (1.351)$$

The problem P is now rewritten as:

$$\begin{aligned} u_t &= \delta \Delta u + c \cdot \nabla u - v^n (u - d), \\ v_t &= \epsilon \Delta v + c \cdot \nabla v - u^m v, \end{aligned} \quad (1.352)$$

$$m, n < 1.$$

For convenience, and aiming the understanding of the system dynamic in the Travelling Wave (TW) domain, we require the initial conditions to be the opposite Heaviside function:

$$\begin{aligned} u_0(x) = v_0(x) &= H(-x) \in \mathbb{L}_{loc}^1(\mathbb{R}^N) \cap \mathbb{L}^\infty(\mathbb{R}^N), \\ x &\in \mathbb{R}^N. \end{aligned} \quad (1.353)$$

The equations (1.352) and (1.353) will be referred as the problem P_T .

We are interested on understanding the dynamics when the solutions starts from the initial data to the stationary solutions asymptotically; showing a non-decreasing behaviour for u (as $0 < u < d$) and a non-increasing condition for v (as $v > 0$). The initial function given in (1.353) defines two parts; one part constitutes a positive function in $(-\infty, 0)$ and, another part exhibits a null function in $(0, \infty)$. Both different behaviours are connected by a step at the origin. If we introduce the opposite Heaviside initial condition into the problem P_T , we can understand the evolution of the positive mass

and the null one. Furthermore, we can determine a precise evolution for the TW kind of solutions. (1.353).

The existence and uniqueness of solutions will become apparent during the analysis in the travelling waves domain. In addition, we provide numerical evidences of the solutions (see Figures 1.2 to 1.7).

1.10 TW profiles

The TW profiles are of the form:

$$u(x, t) = f(\xi), \tag{1.354}$$

$$\xi = x \cdot n_d - at \in \mathbb{R}.$$

Where n_d is a unitary vector in \mathbb{R}^N that defines the TW-propagation direction. a is the TW-speed and $f : \mathbb{R} \rightarrow (0, \infty)$ is a function in $\mathbb{L}_{loc}^1(\mathbb{R}^N) \cap \mathbb{L}^\infty(\mathbb{R}^N)$.

We consider that two TW are equivalent if they are different by translation $\xi \rightarrow \xi + \xi_0$ or by symmetry $\xi \rightarrow -\xi$. Both changes do not affect the nature of the TW solution. Without loss of generality, our study is, then, based on a TW propagating from $-\infty$ to ∞ .

We study only one propagating direction of the TW-profile. Thus, we require the vector n_d to adopt the value $n_d = (1, 0, \dots, 0)$; then, we have:

$$u(x, t) = f_1(\xi), \quad \xi = x - at \in \mathbb{R}, \tag{1.355}$$

$$v(x, t) = f_2(\xi), \quad \xi = x - at \in \mathbb{R}.$$

The problem P_T can be transformed into the TW-domain by considering the

following derivatives:

$$\begin{aligned}
u_x &= \xi_x f'_1, \\
u_{xx} &= \xi_{xx} f'_1 + \xi_x^2 f''_1, \\
u_t &= \xi_t f'_1, \\
v_x &= \xi_x f'_2, \\
v_{xx} &= \xi_{xx} f'_2 + \xi_x^2 f''_2, \\
v_t &= \xi_t f'_2.
\end{aligned} \tag{1.356}$$

And after substitution into the problem P_T :

$$\begin{aligned}
u_t &= f''_1 + c f'_1 - f_2^n (f_1 - d) = f''_1 + c f'_1 + f_2^n (d - f_1), \\
v_t &= f''_2 + c f'_2 - f_1^m f_2, \\
f_{1,0} &= f_{2,0} = H(-x) \quad x \in \mathbb{R}, \\
u_t &= -a f'_1; \quad v_t = -a f'_2.
\end{aligned} \tag{1.357}$$

H corresponds to the Heaviside function. It is remarkable to say that the model is postulated so that the concentration of f_2 can go to zero from above; while the concentration of f_1 tends to $d > H(-x)$ from below, so that we have $(d - f_1) > 0$.

Note that a linearization of the problem (1.357) in the proximity of the critical point ($f_1 = d, f_2 = 0$) is not possible as the term f_2^n is not Lipschitz in the proximity of zero. Nonetheless, in such proximity, we know that $f_2^n > f_2$, therefore, the problem analyzed replacing the term f_2^n by f_2 is below the solution corresponding to the the problem P_T . In addition, and as the solution $f_1 \rightarrow d$, we can consider $f_1 = d$ in the second equation in (1.357). The set of equations (1.357) are, then, uncoupled, and after making $f_1 = d$, we have a subsolution for the second equation in (1.357). Hence, we operate in the following problem whose solutions are lower than

the solutions for the set of equations (1.357):

$$\begin{aligned} f_1'' + (c + a)f_1' + f_2(d - f_1) &= 0, \\ f_2'' + (c + a)f_2' - d^m f_2 &= 0, \\ f_{1,0} = f_{2,0} &= H(-x) \quad x \in \mathbb{R}. \end{aligned} \tag{1.358}$$

Any solution to (1.358) is a subsolution to (1.357). Therefore, if we ensure the positivity of the TW solutions for the problem (1.358), we can postulate that the solutions for the problem (1.357) are, indeed, positive in the TW domain. This is the purpose of the coming results.

We perform now the following change of variables:

$$d - f_1 = \hat{f}_1. \tag{1.359}$$

So that, the system reads:

$$\begin{aligned} -\hat{f}_1'' - (c + a)\hat{f}_1' + f_2\hat{f}_1 &= 0, \\ f_2'' + (c + a)f_2' - d^m f_2 &= 0, \\ \hat{f}_{1,0} &= d - H(-x) \quad x \in \mathbb{R}, \\ f_{2,0} &= H(-x) \quad x \in \mathbb{R}. \end{aligned} \tag{1.360}$$

This problem is considered together with the following boundary like conditions:

$$\begin{aligned} (\hat{f}_1, f_2) &\rightarrow (0, 0), \quad \xi \rightarrow \infty, \\ (\hat{f}_1, f_2) &\rightarrow (d - 1, 1), \quad d > 1, \quad \xi \rightarrow -\infty. \end{aligned} \tag{1.361}$$

Our intention is to find a suitable (non-oscillating) exponential behaviour of the TW-tail related to the profile speed. In the proximity of the equilibrium set $(\hat{f}_1 = 0, f_2 = 0)$, we can consider the moving tail within a linearized frame. Note that the solutions have a non-increasing behaviour when connecting heteroclinically the boundary-like conditions reflected in (1.361). Thus we

require an exponential behaviour of the form:

$$\begin{aligned} \hat{f}_1 &= Ae^{-\lambda_1 \xi}, \\ f_2 &= Be^{-\lambda_2 \xi}. \end{aligned} \tag{1.362}$$

And replacing into the system (1.360):

$$\begin{aligned} -A\lambda_1^2 e^{-\lambda_1 \xi} + (c+a)\lambda_1 A e^{-\lambda_1 \xi} + B A e^{-(\lambda_1 + \lambda_2) \xi} &= 0, \\ B\lambda_2^2 e^{-\lambda_2 \xi} - (c+a)\lambda_2 B e^{-\lambda_2 \xi} - B d^m e^{-\lambda_2 \xi} &= 0. \end{aligned} \tag{1.363}$$

As the second equation is uncoupled, we can obtain a relation between the exponential decay rate and the TW-speed together with the convection ($c+a$). This value is given by:

$$\lambda_2 = \frac{c+a + \sqrt{(c+a)^2 + 4d^m}}{2}. \tag{1.364}$$

If we operate analogously, we can obtain a similar relation for the decay rate λ_1 :

$$\lambda_1 = \frac{c+a + \sqrt{(c+a)^2 + 4B e^{-\lambda_2 \xi}}}{2}. \tag{1.365}$$

In the limit with $\xi \rightarrow \infty$, we can consider that the term $4B e^{-\lambda_2 \xi}$ is a positive infinitesimal ϵ . So that, we have the asymptotic speed $\lambda_{1,a}$:

$$\begin{aligned} \lambda_{1,a} &= \frac{c+a + \sqrt{(c+a)^2 + 4B\epsilon}}{2}, \\ \epsilon &\rightarrow 0^+. \end{aligned} \tag{1.366}$$

It is particularly interesting to observe, in view of the results obtained for λ_1 and λ_2 , that the decaying rate is higher than the convection-moving terms ($c+a$). This behaviours explains that an effective decaying moving TW-tail shall be able to compensate the convection effect of the media (c) and the own moving frame of the TW (a).

The following theorem is a characterization of the TW involved in our problem and aims to compile the relevant results. We compare the linearized

solutions obtained for the problem (1.358) with the solutions for the original problem (1.357):

Theorem 1.10.0.1. *The system of equations P_T (1.357) admits TW profiles as solutions. In addition, the solutions of (1.358), provided in the proximity of the equilibrium $(f_1 = d, f_2 = 0)$, are subsolutions of (1.357).*

Note: The bundle of TW moving to the opposite direction can be obtained by spatial reflection without impacting the exponential rate of the TW and the smoothness-regularity of the TW trail.

Proof. The condition of the exponential decaying rate has been obtained under a linearization, that in turn, provided a subsolution. Our aim is, now, to show that the solutions to the problem (1.358) are subsolutions to the problem (1.357) and then, the monotony is ensured during the whole evolution to the equilibrium $(f_1 = d, f_2 = 0)$.

To support our analysis, we provide numerical evidences (see Annex I for the code definition). The numerical approach has the following properties:

- The integration domain for the computation is $(0, 100)$. The upper limit is sufficiently large to avoid the effect of the pseudo-boundary conditions. The domain is divided into sub-domains for representation purposes.
- The error tolerances have been adjusted according to the integration sub-domain. For the computation over the interval $(0, 100)$, the considered tolerance is 10^{-6} .
- The number of nodes for the integration is $N = 100000$.
- The first assessment for the solution to start the numerical analysis is considered to be a "step-like" function given by the initial conditions $f_{1,0} = f_{2,0} = H(-x)$.
- The system has different parameters that need to be defined previous to the numerical proposal. We run the exercise considering the value for $d = 2$ and the value for $(c + a) = 4$. Both values have been selected for simplicity sake of convenience; nonetheless, there is not

loss of generality in the final conclusions. Additionally, the numerical evidences are given for different combination of the parameters $n, m \in (0, 1)$

The results are as follows:

- $n = 0.9; m = 0.1$. We have considered $m = 0.1$ to account for sufficient margin to avoid encountering a singular Jacobian during the numerical exercise, due to the strong non-lipschitz condition of f_1^m when m approaches zero. For this case, and assuming that $c+a = 4$, we can observe in Figures 1.2, 1.3 and 1.4 that the solutions for the problem (1.358) are indeed subsolutions for the problem (1.357). We can see in the pointed figures that the function f_{2m} (representing the solution f_2 to the problem (1.358)) is positive everywhere (note that for simplification and better picture resolution we have selected a reduced interval for $\xi \in [0, 2]$). Therefore, when moving with decaying rate given by the expression of λ_2 in (1.364), we can ensure the asymptotic positivity of the TW-tail. Even further, one can check that the solutions to the original problem (1.357) evolve closely to the linearized problem (1.358).
- $n = 0.2; m = 0.9$. We have considered $n = 0.2$ to account for sufficient margin to avoid encountering a singular Jacobian during the numerical exercise, due to the strong non-lipschitz condition of f_2^n when n approaches zero. We can observe in Figures 1.5, 1.6 and 1.7 that the solutions for the problem (1.358) are indeed subsolutions for the problem (1.357). We can see in the pointed figures that the function f_{2m} (representing the solution f_2 to the problem (1.358)) is positive everywhere (note that for simplification and better picture resolution we have selected a reduced interval for $\xi \in [0, 2]$). Therefore, when moving with decaying rate given by the expression of λ_2 in (1.364), we can ensure the asymptotic positivity of the TW-tail. Even further, one can check that the solutions to the original problem (1.357) evolve closely to the linearized problem (1.358).

We have shown that the postulated travelling wave speed given by the expressions (1.364) and (1.365) provides a subevolution to the problem P_T

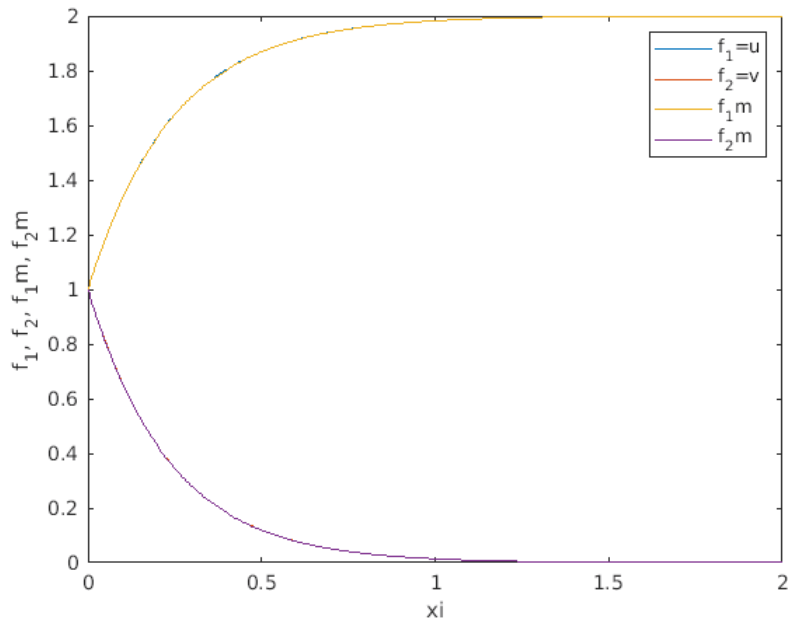


Figure 1.2: Travelling Wave evolution for $c + a = 4$ corresponding to $n = 0.9$ and $m = 0.1$. For convenience $d = 2$. The horizontal axis represents the TW independent variable $\xi = x - at$.

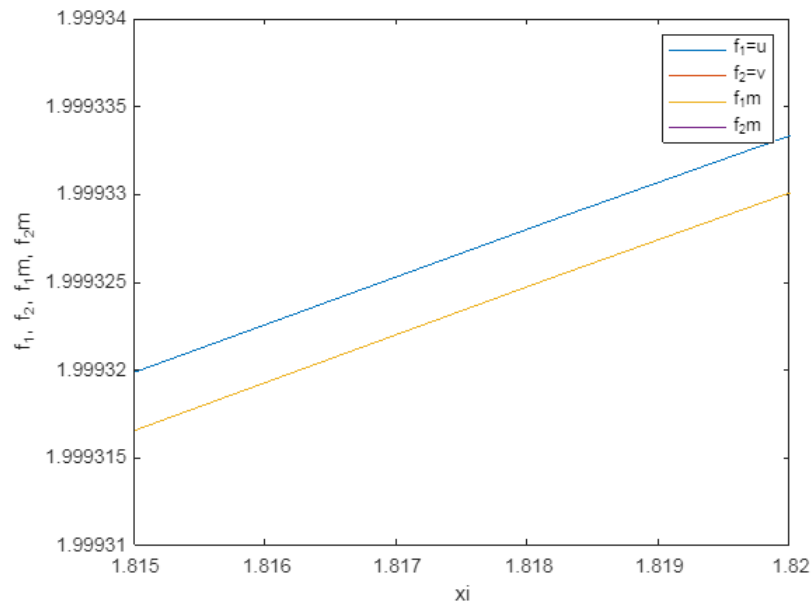


Figure 1.3: Travelling Wave evolution for $c + a = 4$ corresponding to $n = 0.9$ and $m = 0.1$. For convenience $d = 2$. It is possible to see the sub-evolution f_{1m} as solution for the problem (1.358). The horizontal axis represents the TW independent variable $\xi = x - at$.

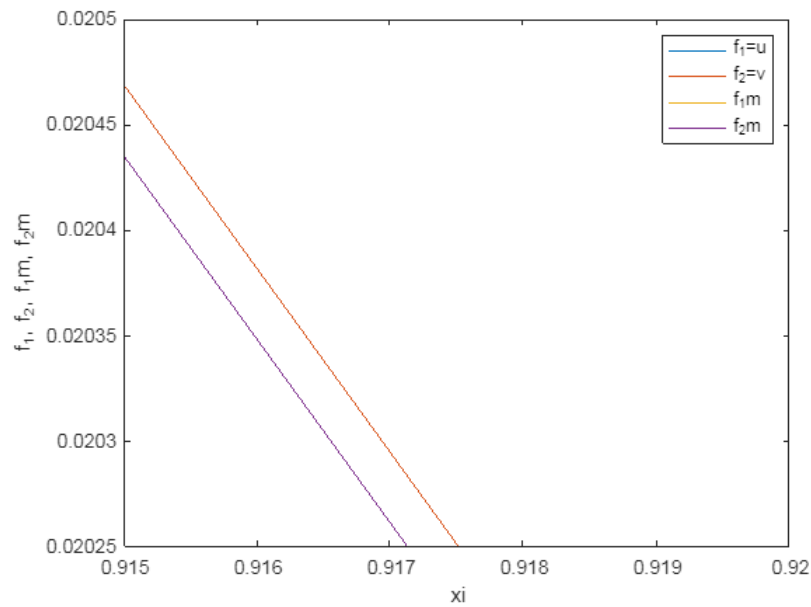


Figure 1.4: Travelling Wave evolution for $c + a = 4$ corresponding to $n = 0.9$ and $m = 0.1$. For convenience $d = 2$. It is possible to see the sub-evolution f_{2m} as solution for the problem (1.358). The horizontal axis represents the TW independent variable $\xi = x - at$.

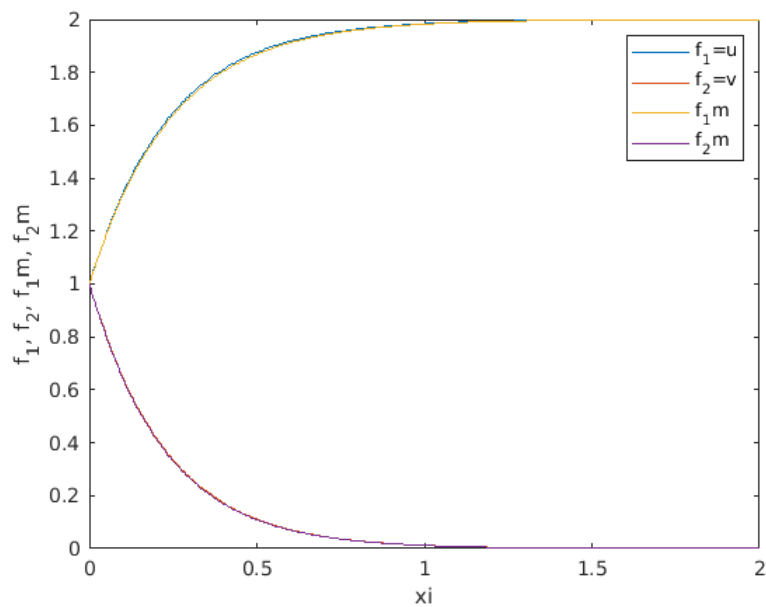


Figure 1.5: Travelling Wave evolution for $c + a = 4$ corresponding to $n = 0.2$ and $m = 0.9$. For convenience $d = 2$. The horizontal axis represents the TW independent variable $\xi = x - at$.

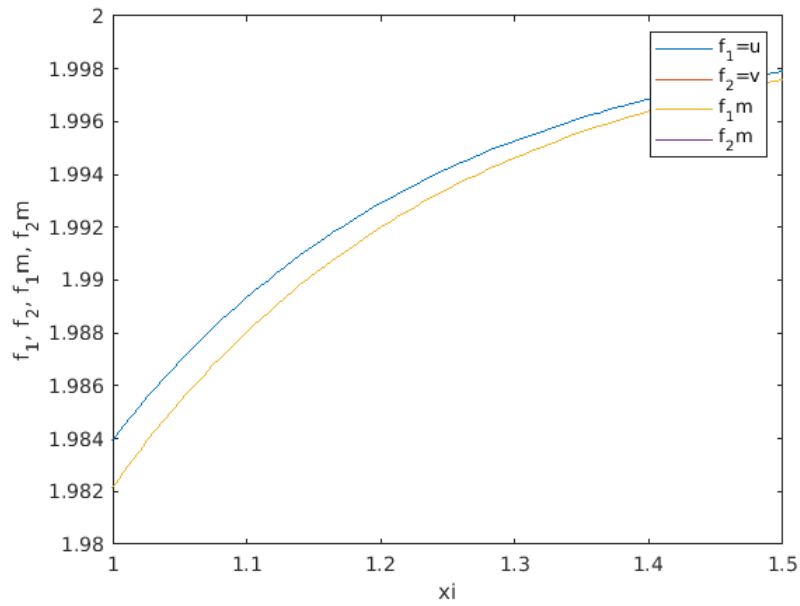


Figure 1.6: Travelling Wave evolution for $c + a = 4$ corresponding to $n = 0.2$ and $m = 0.9$. For convenience $d = 2$. It is possible to see the sub-evolution f_{1m} as solution for the problem (1.358). The horizontal axis represents the TW independent variable $\xi = x - at$.

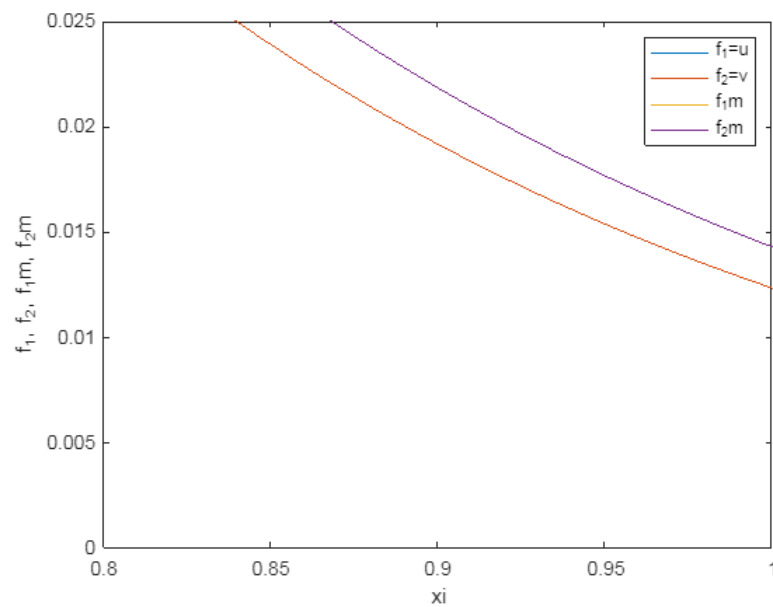


Figure 1.7: Travelling Wave evolution for $c + a = 4$ corresponding to $n = 0.2$ and $m = 0.9$. For convenience $d = 2$. It is possible to see the sub-evolution f_{2m} as solution for the problem (1.358). The horizontal axis represents the TW independent variable $\xi = x - at$.

(1.357) that ensures the positivity of the involved solutions (u, v) . Indeed the TW-profiles in the problem (1.358) have been obtained by replacing f_2^n by f_2 in the proximity of $f_2 = 0$ where we know that $f_2 < f_2^n$; and by making $f_1 = d$; so that the problem (1.358) provides subsolutions to the problem P_T (1.357). As the TW-profiles do not oscillate for TW-speed complying with (1.364) and (1.365), the solutions of the problem P_T will be positive when propagating toward the stationary solutions $u = d$ and $v = 0$.

□

2 Existence, evolution of solutions and finite propagation for a PME problem with a reaction of the form $|x|^\sigma u^p$, $\sigma > 0$ and $p < 1$

2.1 Description and objectives

The Porous Medium Equation (PME) is classified within the nonlinear parabolic partial differential equations scope (see the page 85 of [33] for a discussion on the regularity conditions associated to the parabolic PME) . Unlike in the previous studied diffusion problem, in a PME, the non-linearity is given in the diffusion term which introduces a set of properties differing from the classical order two diffusion. It has application on mechanical and physical problems where slow diffusion is important or where the pressure due to the over-population (in case of biological applications) induces diffusion in the media. The PME main key features depart from the Heat Equation (HE) and derive into a complete set of novelties of relevance in applied sciences that we will specify in this memory.

To illustrate the relevancy and novelties of the PME compared to the HE, we can think on a simple mechanical problem in which a small particle with a high temperature (much higher than the ambient temperature) is set fixed in the space. The physics establishes a precise heat transfer evolution problem that derives into the classical HE. Even when this equation is capable of precisely predicting the behaviour of the solution, it provides positivity everywhere in the domain; in the sense that the points located at a infinite location will increase its temperature instantaneously. This HE feature is usually referred as infinite propagation speed in the literature (see the remarks in page 49 of [23]) . On the contrary, the PME exhibits a non-linear diffusion which turns out on a finite propagation speed. This is one of the main key features of the PME and indicates that upon evolution, a diffusion front carries the information from zero to non-zero and, hence, positivity is not given at all places in the domain instantaneously, as predicted by the HE. In section 2.3, we provide a comparison of the infinite speed versus a finite speed of propagation and the advantages derive upon.

But not only the heat transfer process can be modelled by the PME by

replacing the classical HE. Another sort of important problems is related to the mass diffusion in a given media. Here is where we introduce the potentialities of the PME to model problems in biology and engineering.

Bertsch and Gurtin employed a PME in [20] to simulate a biological interaction in which the diffusion coefficient depends on each biological agent, i.e., the population gradient $(u + v)_x$ is proportional to u and v , being such variables the corresponding population densities:

$$\begin{aligned} u_t &= k_1 \{u(u + v)_x\}_x, \\ v_t &= k_2 \{v(u + v)_x\}_x, \end{aligned} \tag{2.1}$$

where,

$$k_1, k_2 > 0. \tag{2.2}$$

This biological model is relevant when the diffusion in the medium is affected by the over-population pressure. In other words, the crowding effects in one part of the domain provokes the population to invade other areas with a finite speed propagation.

In our case, we purport to model the population evolution when the crowding makes the biological agents to travel. To explain our purposes, let consider a sub-region of the domain where the biological specie starts to increase. The pressure acting on the population makes the specie to move towards other sub-region with a finite propagation speed. This phenomena can be simulated by the homogeneous Porous Medium Equation [33]:

$$\begin{aligned} u_t &= \nabla \cdot (u^{m-1} \nabla u), \\ m &> 1, \end{aligned} \tag{2.3}$$

where u^{m-1} is known as the pressure term.

Additionally, we propose a reaction term of the form $|x|^\sigma u^p$, $\sigma > 0$ and $p < 1$, that can be justified as follows:

When any biological specie starts to populate any region, this medium is rich in nutrients, therefore, we can expect that the time growing rate is high and positive at the beginning, but with less growing rate when the population

increases due to the saturation of the overcrowding in the media:

$$u_t = u^p, \quad (2.4)$$

$$p < 1.$$

Additionally, we consider that the nutrients are not homogeneous spatially distributed. This leads to the further increasing of the biological individuals in certain locations. Mathematically speaking, we can think on:

$$u_t = F(x)u^p, \quad (2.5)$$

where $F(x)$ is a smooth function that permits to characterize the time growing rate depending on the location. In our case, we are going to consider:

$$F(x) = |x|^\sigma, \quad (2.6)$$

$$\sigma > 0.$$

The selection of $F(x)$ responds to:

$$u_t \rightarrow \infty, \quad (2.7)$$

whenever:

$$|x| \rightarrow \infty, \quad (2.8)$$

to model a heterogeneous distributed population which overcrowding effect comes from a location sufficiently far in the domain.

One key question that will arise during our study is the finite time blow-up phenomena. We will proof if such property can be given in certain locations; Indeed, if the specie concentration growing rate goes to infinity with the space variable, it may induce the own concentration to go to infinity in a finite time.

In the engineering scope, and as discussed in the introduction to this thesis, one of our purposes is to model accurately the dynamics of the fire extinguishing agent in areas where equipment capable of originating a fire exists, particularly aircraft areas where engines and auxiliary power units are working. In addition, it is our aim to model the dynamic of nitrogen evolution when the nitrogen invades the tank from an adjacent inerted tank

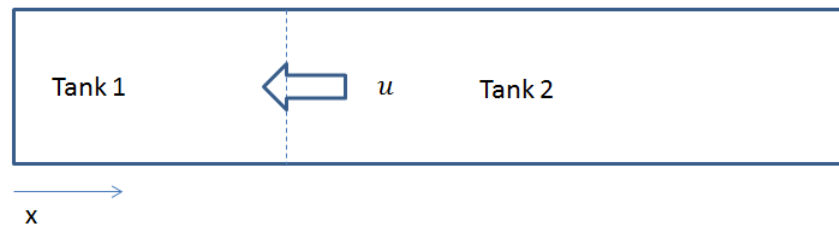


Figure 2.1: The tank 2 is the source of nitrogen concentration u that invades the tank 1 through the interfacing wall.

interfacing through one wall (Figure 2.1).

As a piece of background in relation with the fire extinguishing systems in aircrafts, it is remarkable to remember, at this point, that plenty of ground and flight testing campaigns have been performed in the aerospace sector regarding fire extinguishing agents discharge processes in areas where the turbomachinery is hosted. The observations reveal that the predicted positivity everywhere of the heat equation is not given in a real scenario. Indeed, the positivity property would lead us to think that the concentration of the discharged agent distributes everywhere leading to the fire extinguishing almost since the beginning. However, this is not completely true. Indeed, once the discharging process is initiated, the agent propagates with a finite speed, i.e., the propagation front carries the positivity in the media, switching the solution from zero to positive. In addition, the concentration of fire extinguisher agent is much higher in certain locations of the environment than in others. This last observed behaviour is related to the complexity of the engine nacelles and auxiliary power units compartments where plenty of electromechanical equipment and computers are hosted. In certain areas of these compartments, mainly zones with complex geometry close to the discharging area, the diffusion and the reaction terms interact to increase the concentration of the discharging agent unexpectedly. One can think that this growth, in certain locations, can be modelled by considering a finite time blow-up in the equations. As discussed, the simulation of this growth would be one of our purposes.

In relation with the modelling exercises currently being followed by the industry, we can highlight that engineers have tried to simulate appropriately the environment with digital mock-ups using advanced software techniques. After this digitalization exercise, the discharge process is simulated using a classical linear order two diffusion under numerical algorithms based on a

discretization of equations [14]. Nonetheless, the results may not fit closely the observations obtained during posterior testing activities in the aircraft either on ground or in flight. This potential mismatch between predictions and observations leads to incorporate important modifications in the model (but without modifying the linear diffusion) that implies a significant reduction of the scope of the model. Eventually, the model modifications are only carried out for the particular testing conditions, thus losing the possibility of employing the model for designing in the complete aircraft operational envelope.

The fact of following a testing and model tuning handmade process is costly in terms of human efforts, leading to high time-consuming, even, endless works. We propose, instead, to model the discharge process by a PME equation of the form:

$$u_t = \Delta u^m + |x|^\sigma u^p, \quad (2.9)$$

where:

$$m > 1, \sigma > 0, p < 1.$$

As discussed, the diffusion term, Δu^m , induces finite propagation of the fire extinguisher agent while the reaction term, $R(x, u) = |x|^\sigma u^p$, will be proved to provide blow-up properties for certain values of σ to be characterized upon. The term $|x|^\sigma$ is introduced as a location variable that can be adapted, based on observations, to the location where the extinguishing agent concentration grows unexpectedly. Mathematically speaking, we can abstract by considering that in such locations finite time blow-up is given. The results obtained in this thesis have been applied to a real scenario to model the fire extinguisher discharge in the Annex II.

We focus our attention, now, to understand the term u^p ($p < 1$). This term aims to model the effect of the discharge process. Indeed, if we make the first derivative, we have

$$\frac{1}{u^{1-p}}, \quad (2.10)$$

where we can see that for low concentration values ($u \rightarrow 0$), the derivative increases asymptotically. Nonetheless, when the concentration starts to develop and follows a monotone increasing evolution during the discharge, the derivative decreases (but still positive) due to the own saturation of the media by the discharged agent.

The PME equation can be applied to model the inerting process of a fuel tank as well (Figure 2.1). For this purpose, we shall consider a situation, in which, the growing rate of nitrogen (u_t) increases with $|x|$. This phenomena can be associated with an invading nitrogen concentration located at the tank 2, so that:

$$|x| \gg 1, \quad (2.11)$$

and then:

$$u_t \gg 1. \quad (2.12)$$

The growing rate decreases when $|x| \rightarrow 0$. In addition, the term u^p intends to introduce the saturation effect of the nitrogen in the tank 1. This process is simulated with a PME related diffusion, so that the invading nitrogen moves with a finite speed down to reach the tank wall located at $x = 0$.

One of the main aspects of the equation (2.9), to be characterized, is the existence of finite time blow-up. In our models, such phenomena expresses the effect of a massive invasion (from the biological agent, the discharged fire extinguisher or the nitrogen gas concentration) that leads the solution to increase randomly to infinity in a certain finite time. We shall notice that the existence of such finite time blow-up may no be given in a real scenario. In fact, in the application compiled in the Annex II, finite time blow-up is not a feature given during the discharge of an engine fire extinguisher. The non-existence of finite time blow-up, in this case, is established by the parameters involved in the PME and determined for the application in Annex II, this means that we have not imposed any *ad hoc* condition.

Working with a PME equation of the form (2.9) implies to consider significant novelties. To illustrate the differences, in terms of results, compared to the assessments performed up to now in related studies, we stress that a similar equation (but with a reaction term not depending on $|x|^\sigma$) was studied by De Pablo and Vázquez in [31]. In particular, the authors showed that solutions to the problem:

$$u_t = \Delta u^m + u^p, \quad (2.13)$$

$$p < 1,$$

does not exhibit local blow-up.

Additionally, R. Ferreira *et al.* showed in [37] the existence of blow up

for a equation of the form:

$$u_t = \Delta u^m + u^{p(x)}, \quad (2.14)$$

where $p(x)$ is a smooth function with bounds (p_-, p_+) . They showed that when the integration domain $\Omega = \mathbb{R}^N$, there exists local (finite in time) blow-up provided that the following condition is met:

$$1 < p_- \leq p_+ \leq 1 + 2/N. \quad (2.15)$$

The coefficient $p^* = 1 + 2/N$ is denoted as Fujita exponent and is well known to be a boundary between values of p motivating finite time blow-up (as expressed under the condition (2.15)) and values of p providing global blow up, for which the following condition is shown:

$$p_- > 1 + 2/N. \quad (2.16)$$

Nonetheless, in our case, we show the existence of blow-up in finite time, due to the introduction of the term $|x|^\sigma$, for certain values of σ and in the condition with $p < 1$ (which according to [31], no finite time blow up is given). Eventually, we formulate a new value of the critical exponent to segregate between the existence of local in time blow-up and the existence of global solutions. In a physical intuition, this means:

- Finite time Blow-up: The solutions goes to infinity for a given finite time due to the cumulative effect of the reaction term. This phenomena is well known in the study of parabolic operators and has become a source of investigations [39]. Considering that the blow-up is given at $t = T$, we can express the finite time blow-up phenomena as:

$$|u(x, T)| \rightarrow \infty. \quad (2.17)$$

In a physical sense, a finite time blow-up corresponds to an extreme invasion, either from a biological agent or from a gas substance, that provokes the solutions to increase suddenly up to a theoretical infinity.

- Global solutions: The solutions evolve with no blow-up in finite time. This means, that solutions can go to infinity, nonetheless, this will hap-

pen in a infinite time as well. Then, we can read:

$$u(x, T \rightarrow \infty) \rightarrow \infty. \quad (2.18)$$

In this case, the physical intuition suggests that the solutions are not bounded unless we limit the exposure time (i.e. we make T finite).

2.2 Summary

This work starts by determining and comparing the so-called source-type solution for the HE and for the PME. The source-type solution for the PME is also known as Zeldovich, Kompaneets and Barenblatt (ZKB) solution in honour to the first authors investigating the properties of the PME (page 6 in [33]). Afterwards, we proceed to discuss topics related to existence and uniqueness of solutions. We characterize solutions through the analysis of uniqueness, a comparison principle and a precise evolution of them. Eventually, we finish with finite propagation for a reaction problem with a non-Lipschitz term. The fact of having a non-Lipschitz term makes useless the available techniques for existence of solutions contemplated only for Lipschitz reaction (see the different problems provided in Chapter 4 of [33]). Therefore, we proceed firstly to convert our original problem P into a Lipschitz problem referred as P' , so that we show existence and uniqueness of solutions. Lately, we show existence of solutions for the non-Lipschitz problem (P) by making the limit of an appropriate parameter involved in the Lipschitz approach.

We discuss, now, some aspects about the PME pressure term (also known as diffusivity). For a PME, the pressure term is of the form:

$$D(u) = m|u|^{m-1}, \quad (2.19)$$

with $m > 1$.

To show this, it suffices to re-write the Laplacian term as:

$$\Delta u^m = \nabla \cdot (m u^{m-1} \nabla u), \quad (2.20)$$

where:

$$D(u) = m|u|^{m-1}. \quad (2.21)$$

Alternatively, the diffusivity for HE equation is:

$$D(u) = 1, \quad (2.22)$$

Indeed

$$\Delta u = \nabla \cdot (1 \nabla u), \quad (2.23)$$

which is positive for any value of u . Nonetheless, the diffusivity introduced

by the PME, called degenerate diffusivity, leads to the fact that whenever $u = 0$, the diffusion coefficient is null ($D(u) = 0$). This particular behaviour of the PME introduces relevant properties related to finite speed propagation in a local ball B_R in which the solution $u(x, t) \rightarrow 0$ for $x \in B_R$ and $0 \leq t \leq \tau$ (with τ sufficiently small).

As discussed and to complete our problem, we introduce a reaction term of the form

$$|x|^\sigma u^p. \quad (2.24)$$

In this case, the reaction term does not satisfy the Lipschitz condition (hence introduces non-uniqueness) whenever $u = 0$ or $u \rightarrow 0$ locally. It is important to highlight that, even when non-Lipschitz, the forcing reaction term is considered to be positive at some moment during the finite propagation. Additionally, it satisfies the condition:

$$R(x, u) \in \mathbb{L}_{loc}^\infty(\mathbb{R}^N). \quad (2.25)$$

The existence of solutions for a Lipschitz problem discussion employs already known results compiled in [31] and [32]. Nonetheless, the differences of our problem compared to that in the cited references are notable and will introduce novelties in the development of a consistent theory. The main differences compared to the already known problems are summarized as:

- The introduction of a non-Lipschitz reaction with a term depending on $|x|$. This means that the reaction is

$$R(x, u) \in \mathbb{L}_{loc}^\infty(\mathbb{R}^N). \quad (2.26)$$

- A generalization on the growth condition for the initial data.

Due to the degeneracy of the diffusion coefficient ($D(u)$), any solution cannot be classically defined, in case it is locally null for a certain time. This is the case of compact support initial conditions and solutions. As a consequence, the theory developed in this work employs a generalization on the way solutions are defined, i.e. we focus our attention in weak solutions.

We will say

$$u \in Q_T = \mathbb{R}^N \times (0, T), \quad (2.27)$$

is a weak solution to the problem P , if for every t , such that $0 \leq t \leq T$; and for every test function

$$\phi \in C^\infty(Q_T), \quad (2.28)$$

with compact support, the following identity holds:

$$\int_{\mathbb{R}^N} u(t) \phi(t) = \int_{\mathbb{R}^N} u(0) \phi(0) + \int_0^t \int_{\mathbb{R}^N} [u \phi_t + u^m \Delta \phi + |x|^\sigma u^p \phi] ds. \quad (2.29)$$

Note that when we refer to a subsolution (minimal) or a supersolution (maximal), the " = " in the last equation is replaced by " \leq " and " \geq " respectively.

One of the intentions of this work is to analyze the existence and to determine a characterization of maximal and minimal solutions for the problem P . Such study does not prevent us to analyze uniqueness of solutions.

We will see that the sign of the parameter

$$\gamma = m\sigma + 2(1 - \sigma)p + \sigma, \quad (2.30)$$

plays an important role to understand the applicable solutions:

- When $\gamma < 2$, the non-Lipschitz reaction is relevant. Thus, the existence of solutions is guaranteed whenever the initial data $u_0(x) > 0$. While in the case of $u_0 \equiv 0$, the proof of existence is more subtle and, in general, we will show that there exist two particular solutions (the maximal and minimal solutions) that are key to demonstrate existence and to bound the family of possible solutions.
- When $\gamma \geq 2$, the existence of solutions is shown with the help of the so-called self-similar solution which is obtained as a minimal asymptotic behavior. Additionally, the degeneracy of the diffusion implies that uniqueness cannot be guaranteed in case $u = 0$ in a ball B_R . In this case, a minimal solution can be proved to exist with the property of finite speed propagation and a maximal solution positive for each time $0 \leq t \leq T$ and all $x \in \mathbb{R}^N$

One of the main features studied in a non-linear PDE evolution is the existence of a blow up pattern. Blow up can be given for a finite time, in which

solutions tend very fast to infinity in a local spatial ball within the integration domain. The finite time blow-up has its own designation to segregate it from the case in which blow-up is given as a evolution problem whose solution tends to infinity when $t \rightarrow \infty$. This last case is usually referred as global existence or global blow up. This work proves that there exists a critical exponent p^* defined as:

$$p^* = \text{sign}_+ \left(1 - \frac{\sigma(m-1)}{2} \right). \quad (2.31)$$

Such that for $p > p^*$, there exists blow up in finite time while for $p \leq p^*$ there exist global solutions.

In summary, the most general problem (P) we aim to study throughout the present work is:

$$\begin{aligned} u_t &= \Delta u^m + |x|^\sigma u^p, \\ u(x, 0) &= u_0(x), \end{aligned} \quad (2.32)$$

$$u_0(x) \geq 0,$$

where

$$\begin{aligned} m &> 1, \sigma > 0, p < 1, \\ (x, t) &\in Q_T = \mathbb{R}^N \times (0, T). \end{aligned}$$

Without losing generality and in virtue of typical applied sciences problems, we will consider that any solution is $u \geq 0$.

The work for the problem P starts by a generalization of the maximal required growing condition for the initial data to support the study of existence of solutions. Later on, the original problem P is replaced by a Lipschitz continuous problem for which existence, uniqueness and a comparison principle can be established. Finally, we contemplate the limit of such Lipschitz problem to convert it into a non-Lipschitz problem with the intention to derive the existence of the maximal and minimal solutions to the problem P , and what conditions are required for unique solutions. In addition, this work provides exact evolution profiles for the maximal and minimal solutions solved as part of an asymptotic approximation.

2.3 Source-type solutions and comparison of the Heat Equation versus the Porous Medium Equation

This section has the aim of setting the fundamental (or source-type) solutions for the HE firstly and for the PME secondly. In both cases, the initial condition is given in the form of a finite pulsed mass (M):

$$u(x, 0) = M\delta(x), \quad (2.33)$$

where $\delta(x)$ represents the Dirac pulse at the spatial coordinate origin.

The homogeneous equation to solve for the HE is of the form:

$$u_t = \Delta u, \quad (2.34)$$

and for the PME:

$$u_t = \Delta u^m. \quad (2.35)$$

The role of the source-type solution is to find a basic evolution that acts as a representative example of the typical behaviour expected once the HE or the PME are solved. We develop the theory with special emphasis in the strong positivity, which is the main feature of the HE source evolution; and the finite propagation speed, which constitutes the paramount difference of the PME source solution when compared with the HE.

2.3.1 Heat Equation source-solution

The process of obtaining a fundamental solution for the HE outlined in this section is based on the theory developed in the page 45 of [23]. It is deemed adequate to reproduce such theory as it stresses the main aspects required for the source-type solution of the PME.

We study the class of solutions that are invariant under the scaling group in the variables (x, t, u) which give the so-called self-similar form:

$$u(x, t) = t^{-\alpha} f(\eta), \quad (2.36)$$

where

$$\eta = xt^{-\beta}. \quad (2.37)$$

The exponents α and β are called self-similarity exponents and the function f is called the self-similar profile.

Now, if we insert the expression (2.36) into the HE equation (2.34), we have:

$$\underbrace{-\alpha t^{-(\alpha+1)} f(\eta) + t^{-\alpha} (-\beta) x t^{-(\beta+1)} f_{\eta}(\eta)}_{u_t} = \underbrace{t^{-(\alpha+2\beta)} f_{\eta\eta}(\eta)}_{\Delta u}. \quad (2.38)$$

Upon operation, we have:

$$-\alpha t^{-(\alpha+1)} f(\eta) - t^{-(\alpha+1)} \beta \underbrace{x t^{-\beta}}_{\eta} f_{\eta}(\eta) - t^{-(\alpha+2\beta)} f_{\eta\eta}(\eta) = 0. \quad (2.39)$$

We require the exponents in the time variable to be equal with the aim of involving an elliptic differential equation in the variable η , while keeping the equation invariant:

$$\alpha + 1 = \alpha + 2\beta \rightarrow \beta = \frac{1}{2}. \quad (2.40)$$

Therefore the elliptic equation reads as:

$$\alpha f + \frac{1}{2} \eta f_{\eta} + f_{\eta\eta} = 0. \quad (2.41)$$

To simplify the resolution, we require the function $f(\eta)$ to be radial in the variable η . From now on, the reader shall understand the variable η as the radial variable r . In the radial restriction, the second derivative is read as expressed by the following expression:

$$\alpha f + \frac{1}{2} r f_r + \underbrace{f_{rr} + \frac{N-1}{r} f_r}_{f_{\eta\eta}} = 0. \quad (2.42)$$

For convenience, we choose the exponent α as:

$$\alpha = \frac{N}{2}, \quad (2.43)$$

and upon substitution in the expression (2.42) and multiplying such equation

by r^{N-1} , we read:

$$r^{N-1} \frac{N}{2} f + \frac{1}{2} r^N f_r + r^{N-1} f_{rr} + (N-1) r^{N-2} f_r = 0, \quad (2.44)$$

we know that:

$$r^{N-1} \frac{N}{2} f + \frac{1}{2} r^N f_r = \frac{1}{2} (r^N f)_r, \quad (2.45)$$

and

$$r^{N-1} f_{rr} + (N-1) r^{N-2} f_r = (r^{N-1} f_r)_r, \quad (2.46)$$

so that, the expression in (2.42) adopts the following form:

$$(r^{N-1} f_r)_r + \frac{1}{2} (r^N f)_r = 0. \quad (2.47)$$

Thus, we can solve making a simple first integral:

$$r^{N-1} f_r + \frac{1}{2} r^N f = K. \quad (2.48)$$

for some constant K. We can consider

$$K = 0, \quad (2.49)$$

under the assumption that

$$\lim_{r \rightarrow \infty} f = 0, \quad (2.50)$$

hence:

$$f_r = -\frac{1}{2} r f. \quad (2.51)$$

Upon integration and for some arbitrary constant M :

$$f = M e^{-\frac{r^2}{4}}. \quad (2.52)$$

And finally upon substitution of the involved variables in the equation (2.36) to recover the original (x, t) as independent, we have:

$$f(x, t) = M \frac{1}{t^{N/2}} e^{-\frac{|x|^2}{4t}}. \quad (2.53)$$

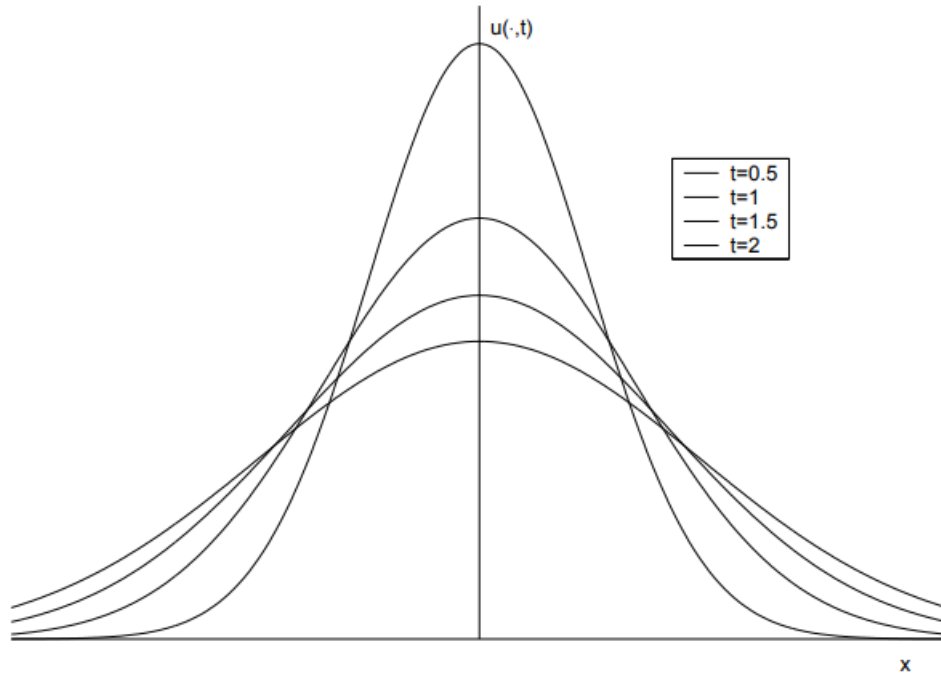


Figure 2.2: The source-type evolution solution for the Heat Equation. It is to be highlighted the positivity condition everywhere. (Source reference [33])

This fundamental or source-type solution is normally named as Gaussian kernel and is represented in Figure 2.2.

Figure 2.2 is a visual representation of the property referred as infinite speed of propagation that naturally appears as a consequence of the HE resolution. Starting from a single and finite mass at an isolated spacial point ($u(x, 0) = M\delta(x)$), the solution evolves towards positivity everywhere in the domain. This property is the basis for a certain comparison with the PME source-type solution to come up in the following chapter.

2.3.2 Porous Medium Equation source-solution

The scaling of the variables, typically performed in the search of a fundamental solution, applies to the PME analogously as we did for the previous HE.

We proceed with the following self-similar solution:

$$u(x, t) = t^{-\alpha} f(\eta) , \quad \eta = xt^{-\beta}. \quad (2.54)$$

$$\underbrace{-\alpha t^{-(\alpha+1)} f(\eta) + t^{-\alpha} (-\beta) t^{-(\beta+1)} x \cdot f_{\eta}(\eta)}_{u_t} = \underbrace{t^{-(\alpha m+2\beta)} f_{\eta\eta}^m(\eta)}_{\Delta u^m}. \quad (2.55)$$

$$-\alpha t^{-(\alpha+1)} f(\eta) - t^{-(\alpha+1)} \beta \eta \cdot f_{\eta}(\eta) - t^{-(\alpha m+2\beta)} f_{\eta\eta}^m(\eta) = 0. \quad (2.56)$$

The elliptic differential equation for the self-similar profile is set after removing the time dependence in the equation (2.56). Hence, we have:

$$\alpha + 1 = \alpha m + 2\beta, \quad (2.57)$$

so that:

$$\alpha(m - 1) + 2\beta = 1. \quad (2.58)$$

We arrive at one equation expressing a relation between the self-similar exponents α and β ; Therefore, another relation is required to determine two particular values for each exponent. This second relation is given by the energy conservation during the evolution:

$$\int_{\mathbb{R}^N} t^{-\alpha} f(xt^{-\beta}) dx = M. \quad (2.59)$$

If we make the following change of variable:

$$\eta = xt^{-\beta}, \quad (2.60)$$

we shall take into account that the term dx is a volume magnitude to represent a differential in the whole space \mathbb{R}^N , therefore operating with volumes, we have:

$$\|x\|_{\mathbb{R}^N}^N = \|\eta\|_{\mathbb{R}^N}^N t^{N\beta}. \quad (2.61)$$

Then, we have that the differential in volumes are given by:

$$d\|x\|_{\mathbb{R}^N}^N = d\|\eta\|_{\mathbb{R}^N}^N t^{N\beta}. \quad (2.62)$$

Note that it is usual to simply write:

$$dx = d\eta t^{N\beta}, \quad (2.63)$$

to represent the volume integral, so that we have:

$$\int_{\mathbb{R}^N} t^{-\alpha} f(xt^{-\beta}) dx = t^{-\alpha+\beta N} \int_{\mathbb{R}^N} f(\eta) d\eta = M. \quad (2.64)$$

If we remove the time-dependency in the previous equation, we have $\alpha = \beta N$, so that we read the following set of algebraic equations:

$$\alpha(m-1) + 2\beta = 1, \quad (2.65)$$

$$\alpha = \beta N. \quad (2.66)$$

After resolution for the variables α and β , we have:

$$\alpha = \frac{N}{N(m-1) + 2}, \quad (2.67)$$

$$\beta = \frac{1}{N(m-1) + 2}. \quad (2.68)$$

It is still pending to solve the following elliptic differential equation for the self-similar profile f :

$$f_{\eta\eta}^m(\eta) + \beta\eta \cdot f_{\eta}(\eta) + \alpha f(\eta) = 0. \quad (2.69)$$

As we did in the previous section, we search for non-negative solutions with a radial symmetric profile. After the substitution of the Laplacian by its corresponding radial coordinates, we arrive at the following expression:

$$\frac{1}{r^{N-1}} [(r^{N-1}(f^m)')' + \beta r^N f' + r^{N-1} N \beta f] = 0. \quad (2.70)$$

Which can be re-written as:

$$\frac{1}{r^{N-1}} [(r^{N-1}(f^m)')' + (\beta r^N f)'] = 0 \rightarrow (r^{N-1}(f^m)')' + \beta r^N f' = 0. \quad (2.71)$$

We can solve the first integral to have:

$$r^{d-1}(f^m)' + \beta r^d f = C. \quad (2.72)$$

As we did with the HE we require that $f \rightarrow 0$, whenever $r \rightarrow \infty$. Hence,

we determine $C = 0$ and the equation (2.72) reads as:

$$(f^m)' + \beta r f = 0. \quad (2.73)$$

The equation (2.73) can be solved using ordinary differential equations techniques:

$$\begin{aligned} \frac{df^m}{f} &= -\beta r dr; \\ \frac{m f^{m-1} df}{f} &= -\beta r dr, \\ m f^{m-2} df &= -\beta r dr, \\ \frac{m}{m-1} f^{m-1} &= -\frac{\beta}{2} r^2 + C. \end{aligned} \quad (2.74)$$

The profile solution is:

$$f(r) = \left(A - \frac{\beta(m-1)}{2m} r^2 \right)^{\frac{1}{m-1}}, \quad (2.75)$$

and in the variable η :

$$f(\eta) = \left(A - \frac{\beta(m-1)}{2m} |\eta|^2 \right)^{\frac{1}{m-1}}. \quad (2.76)$$

Finally, the source-type solution adopts the following expression after substitution in the expression (2.54):

$$u(x, t) = t^\alpha \left(A - \frac{\beta(m-1)}{2m} |x|^2 t^{-2\beta} \right)^{\frac{1}{m-1}}, \quad (2.77)$$

where:

$$\alpha = \frac{N}{N(m-1) + 2}, \quad (2.78)$$

and

$$\beta = \frac{1}{N(m-1) + 2}. \quad (2.79)$$

We can make the graphical representation of the self-similar solution (Figure 2.3) with the aim of comparing with the same graphic obtained in the HE

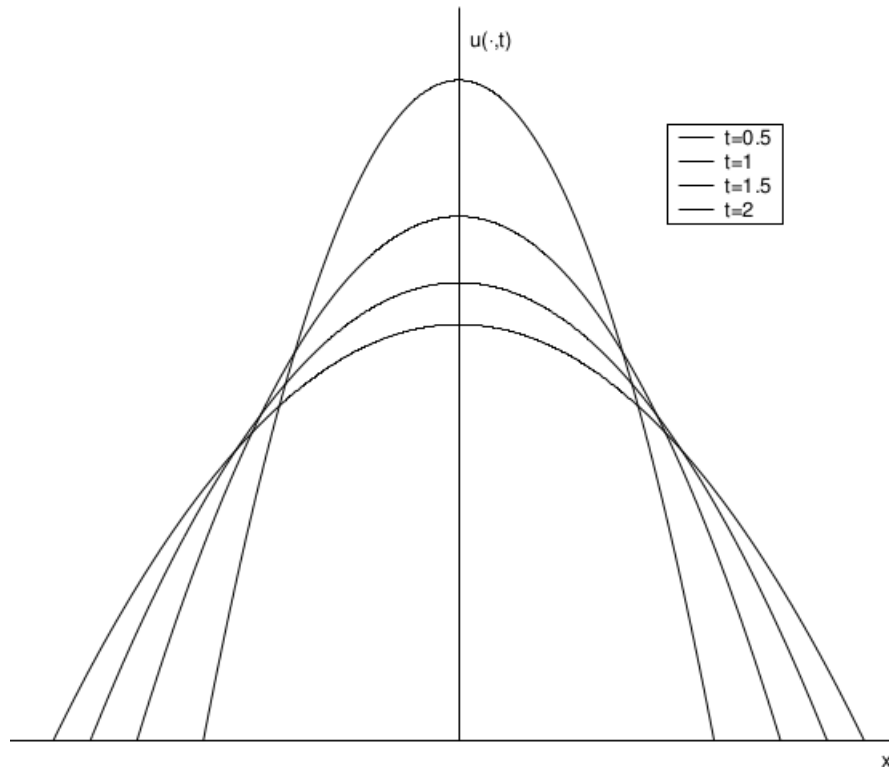


Figure 2.3: The source-type evolution solution for the Homogenous PME. It is to be highlighted the non-negativity everywhere. (Source reference [33])

case. The graphical representation for the PME manifests a relevant difference in the character of the fundamental profile. Namely, the fundamental profile of the PME is not positive everywhere in the domain as we had with the HE.

2.3.3 Comparison of the fundamentals solutions for the HE and PME

The contrast between both solutions of the HE and PME can be summarized as follows:

- HE: A non-negative solution of the heat equation is automatically positive everywhere in its domain of definition.
- PME: Disturbances from the level $u = 0$ propagate in time with finite speed.

To make the comparison more intuitive, we can think how the initial and finite mass evolves in the HE and in the PME. For the HE the initial mass

provides positivity everywhere as the gaussian kernel is positive for any $t > 0$. Nonetheless, the evolution of the PME is not positive everywhere; indeed the support of the solution in the spatial domain propagates with a finite speed introducing a propagation front that turns the domain from zero to positivity. This propagating support evolves precisely in the (x, t) space following the expression:

$$t = \left(\frac{A2m}{\beta(m-1)} \right)^{\frac{1}{\beta}}. \quad (2.80)$$

The finite propagation feature of the PME is very important in the development of this work and shall be considered as a property that will appear when solving the PME with a forcing-reaction term. This property permits to model diffusion problems in which a propagating front appears as a result of the evolution. In the biological application, a specie, invading the domain, moves with finite propagation speed until it covers the whole domain. This principle can be applied, as well, to the aerospace industry related to fire extinguishing and tank inerting. In both cases, a substance (the fire extinguisher agent and the nitrogen respectively) propagates through the media with a finite speed. In the PME, the finite speed is given by the propagation of the function support that shifts the null state to positivity or existence of substance.

2.4 Initial data growing condition

The whole theory developed in this part of the thesis to solve the problem P (2.32) can be perfectly developed considering the following condition for the initial data:

$$u_0(x) \geq 0 \in \mathbb{L}_{loc}^1(\mathbb{R}^{\mathbb{N}}) \cap \mathbb{L}^\infty(\mathbb{R}^{\mathbb{N}}). \quad (2.81)$$

In fact and for convenience, we will refer to the condition (2.81) in some cases that we will specify.

A generalization to consider functions of the form:

$$u_0(x) \geq 0 \in \mathbb{L}_{loc}^1(\mathbb{R}^{\mathbb{N}}) \cap \mathbb{L}_{loc}^\infty(\mathbb{R}^{\mathbb{N}}), \quad (2.82)$$

can be considered provided a condition is set for the growing behavior of the initial data in the spirit of [31] and [32].

The baseline integrability condition requires to introduce the following Banach space:

$$E_0 = \left\{ \phi \in \mathbb{L}_{loc}^1(\mathbb{R}^{\mathbb{N}}) : \|\phi\|_r < \infty \right\}, \quad (2.83)$$

where the norm $\|\phi\|_r (r \geq 1)$ is defined by:

$$\|\phi\|_r = \sup_{R \geq r} R^{-N-a_\sigma} \int_{\mathbb{R}^{\mathbb{N}}} |\phi(x)| dx, \quad (2.84)$$

with

$$a_\sigma = \max \left\{ \frac{\sigma}{1-p}, \frac{2}{m-1} \right\}. \quad (2.85)$$

Considering:

$$B_R = \left\{ x \in \mathbb{R}^{\mathbb{N}}; |x| < R \right\}, \quad (2.86)$$

and

$$\|\phi\|_* = \lim_{r \rightarrow \infty} \|\phi\|_r. \quad (2.87)$$

The reason for the a_σ expression in (2.85) can be understood if we consider two separated problems with different growing conditions in $\mathbb{R}^{\mathbb{N}}$. The first problem is the homogeneous problem that we solved in (2.77). If we

consider a constant time, the evolution in \mathbb{R}^N is given by

$$u \sim |x|^{\frac{2}{m-1}}, \quad (2.88)$$

for

$$|x| \gg 1. \quad (2.89)$$

The mentioned second problem is related to the forcing term solved independently of the diffusion:

$$u_t = |x|^\sigma u^p. \quad (2.90)$$

Upon resolution and for a fixed time we have:

$$u \sim |x|^{\frac{\sigma}{1-p}}. \quad (2.91)$$

Thus, any initial data needs to be weighted and compare to any of the two solutions with the aim to ensure that any growing initial data condition does not jeopardize the existence of solutions.

2.5 The Lipschitz Problem

Firstly, we remark that the reaction term in the problem P (2.32) is not Lipschitz due to the term u^p ($p < 1$). This can be shown by considering two functions

$$u_1 > u_2, \quad (2.92)$$

such that:

$$|u_1^p - u_2^p| \leq \frac{p}{u_2^{1-p}} |u_1 - u_2| \leq L |u_1 - u_2|. \quad (2.93)$$

In case of

$$u_2 \rightarrow 0 \text{ or } u_2 = 0, \quad (2.94)$$

it is not possible to define a finite Lipschitz constant L .

As part of our strategy to show existence of solutions, firstly we proceed to study a equivalent Lipschitz problem referred as P' :

$$\begin{aligned} u_t &= \Delta u^m + f_{lip}(x, u) \text{ in } Q_T = \mathbb{R}^N \times [0, T], \\ u(x, 0) &= u_0(x), \\ u_0(x) &\geq 0 \in E_0, \end{aligned} \quad (2.95)$$

where T is a time value in $0 < T \leq \infty$ and $f_{lip}(x, u)$ is a Lipschitz function on the u variable; $f_{lip}(u) : [0, \infty) \rightarrow [0, \infty)$ with Lipschitz constant L :

$$|f_{lip}(u_1) - f_{lip}(u_2)| \leq L |u_1 - u_2|. \quad (2.96)$$

To show existence based on already available techniques contemplated by de Pablo in [36] and by de Pablo and Vázquez in [31] and [32], we perform a truncation to bound the $|x|^\sigma$ term globally in \mathbb{R}^N . Indeed, this step allows us to show existence for a forcing term that has been already discussed by the cited authors:

$$|x|_\epsilon^\sigma = \begin{cases} |x|^\sigma & \text{when } 0 \leq |x| < \epsilon \\ \epsilon^\sigma & \text{when } |x| \geq \epsilon \end{cases}. \quad (2.97)$$

The following problem P'_ϵ is defined in accordance with the truncation in

(2.97):

$$\begin{aligned}
 u_t &= \Delta u^m + |x|_\epsilon^\sigma f(u) \leq \Delta u^m + \epsilon^\sigma f(u) \text{ in } Q_{T_\epsilon} = \mathbb{R}^N \times [0, T_\epsilon], \\
 u(x, 0) &= u_0(x), \\
 u_0(x) &\geq 0 \in E_0,
 \end{aligned} \tag{2.98}$$

where,

$$f : [0, \infty) \rightarrow [0, \infty), \tag{2.99}$$

is a Lipschitz function and

$$|x|_\epsilon^\sigma \in \mathbb{L}^\infty(\mathbb{R}^N). \tag{2.100}$$

Our intention is to show existence and a comparison principle for the problem P'_ϵ based on already available results [31], [32] and [36]. It is to be highlighted that the novelty is provided by the the introduction of the term $|x|^\sigma$ that has not been treated previously.

Theorem 2.5.1. *For a given $\epsilon > 0$ and if $u_0 \in E_0$, there exists a unique u^ϵ in Q_{T_ϵ} (existing for each ϵ) continuous weak solution to the problem P'_ϵ in a time interval $(0, T_\epsilon)$.*

Proof. De Pablo and Vázquez, [32], showed existence of solutions for the problem

$$u_t = (u^m)_{xx} + \lambda u^n, \tag{2.101}$$

with

$$\lambda > 0, m > 1, n \in \mathbb{R}. \tag{2.102}$$

In our case the truncated term $|x|_\epsilon^\sigma$, bounded by ϵ^σ , plays the role of the parameter λ . Thus, the aim is to proof the existence of solution(s) for the problem P'_ϵ within the time interval $(0, T_\epsilon)$ to be determined.

It is our aim to operate with bounded initial data, therefore and firstly, we define the truncation for $u_0 \in E_0$ and $n \geq 1$ as:

$$u_{0n}(x) = \left\{ \begin{array}{l} u_0(x) \text{ when } |x| \leq n, u_0(x) < n, \\ n \text{ when } |x| \leq n, u_0(x) \geq n, \\ 0 \text{ when } |x| > n \end{array} \right\}. \tag{2.103}$$

It is necessary to remark that, at this point, we have the problem P'_ϵ with a Lipschitz forcing term and with bounded initial data given by the truncation in (2.103).

Summing up:

$$u_{0n}(x) \in \mathbb{L}^1(\mathbb{R}^{\mathbb{N}}) \cap \mathbb{L}^\infty(\mathbb{R}^{\mathbb{N}}). \quad (2.104)$$

The defined problem P'_ϵ is of Lipschitz type with

$$|x|_\epsilon^\sigma \in \mathbb{L}^\infty(\mathbb{R}^{\mathbb{N}}). \quad (2.105)$$

Under these conditions, we can make use of already available results to ensure the existence and uniqueness of solutions. The reader can consult Theorem 3.1 in [35].

The intention is, now, to have a global bound for a subsolution (w) of the problem P'_ϵ that will permit the determination of a value for the time T_ϵ . For this purpose, de Pablo and Vázquez [32] proposed to perform the following change of variables:

$$\begin{aligned} x &\rightarrow x, \\ t &\rightarrow \tau = \frac{e^{k(m-1)t} - 1}{k(m-1)}, \end{aligned} \quad (2.106)$$

$$u(x, t) \rightarrow w(x, \tau).$$

In our case, it is convenient to use a similar change of variables, but with a modification to account for the Lipschitz constant L and the bound ϵ^σ :

$$\begin{aligned} x &\rightarrow x, \\ t &\rightarrow \tau = \frac{e^{\epsilon^\sigma L(m-1)t} - 1}{\epsilon^\sigma L(m-1)}, \end{aligned} \quad (2.107)$$

$$u(x, t) \rightarrow w(x, \tau).$$

This change of variables is very useful as it transforms the PME for the u variable into a problem where w is a subsolution given by an exponential

decay. Indeed, if we make the operations we have:

$$\begin{aligned}
 u_t &= w_\tau \tau_t = w_\tau e^{\epsilon^\sigma L(m-1)t}, \\
 e^{\epsilon^\sigma L(m-1)t} w_\tau &= \Delta w^m, \\
 w_\tau &= e^{-\epsilon^\sigma L(m-1)t} \underbrace{\Delta w^m}_{\Delta u^m}.
 \end{aligned} \tag{2.108}$$

The temporal evolution of the problem in the function w is driven by the decaying exponential term that was not part of the original problem in u . Given a particular value for the Δu^m , the evolution of u is given by:

$$u_t = \Delta u^m, \tag{2.109}$$

while the evolution of w is given by:

$$w_\tau = e^{-\epsilon^\sigma L(m-1)t} \Delta u^m. \tag{2.110}$$

Thus, for a time sufficiently large we can say that w is indeed a subsolution:

$$w_\tau \leq \Delta u^m. \tag{2.111}$$

Note that to recover the original solution for the PME, it suffices to consider:

$$u(x, t) = e^{\epsilon^\sigma L(m-1)t} w(x, \tau(t)). \tag{2.112}$$

The fact of having such exponential decrease rate in (2.110) allows us to bound the function w by an already known estimation [34] of the form:

$$w(x, \tau) \leq cR^{2/(m-1)} \tau^{-\alpha} \|w(\cdot, 0)\|_r^{2\alpha/N}, \tag{2.113}$$

where,

$$\begin{aligned}\alpha &= \frac{N}{N(m-1)+2}, \\ |x| &< R, \\ 1 &\leq r \leq R,\end{aligned}\tag{2.114}$$

$$0 < \tau = \frac{e^{\epsilon^\sigma L(m-1)t} - 1}{\epsilon^\sigma L(m-1)} \leq c \|w(\cdot, 0)\|_r^{(1-m)},$$

and $c \in \mathbb{R}^+$ is a suitable constant that ensures the compliance of the last inequality.

It is convenient to remember that our intention is to determine the existence time T_ϵ based on the bound estimation of the solution for the Lipschitz problem in (2.113).

From now on, we will refer our solution for the PME as $u_n^\epsilon(x, t)$. Indeed such solution is obtained for a given n in the truncation of the initial data and for a given ϵ in the truncation for the term $|x|^\sigma$.

Based on the expression (2.113), the following estimation applies for $u_n^\epsilon(x, t)$ considering that for t sufficiently large we have:

$$u(x, t) \sim e^{\epsilon^\sigma Lmt} w(x, \tau(t)),\tag{2.115}$$

so that,

$$u_n^\epsilon(x, t) \leq cR^{2/(m-1)} e^{Lm\epsilon^\sigma t} \tau^{-\alpha} \|u_n(\cdot, 0)\|_r^{2\alpha/N}.\tag{2.116}$$

The expression (2.116) can be re-written as:

$$u_n^\epsilon(x, t) \leq cR^{2/(m-1)} e^{Lm\epsilon^\sigma t} \left(\frac{e^{L\epsilon^\sigma(m-1)t} - 1}{L\epsilon^\sigma(m-1)} \right)^{-\alpha} \|u_n(\cdot, 0)\|_r^{2\alpha/N},\tag{2.117}$$

where:

$$|x| < R, \quad 1 \leq r \leq R, \quad 0 < t \leq T_{r,\epsilon}.\tag{2.118}$$

The time $T_{r,\epsilon}$ can be obtained operating the expression:

$$\tau = \frac{e^{\epsilon^\sigma L(m-1)t} - 1}{\epsilon^\sigma L(m-1)} \leq c \|u_n(\cdot, 0)\|_r^{(1-m)}. \quad (2.119)$$

And upon operation in the last expression, we arrive at:

$$T_{r,\epsilon} = \frac{1}{L\epsilon^\sigma(m-1)} \log \left(1 + cL\epsilon^\sigma(m-1) \|u_{0,n}\|_r^{1-m} \right). \quad (2.120)$$

Now, for a given ϵ , we can take the limit $n \rightarrow \infty$ to consider the whole initial data. This operation is permitted as we are controlling the initial data by the norm $\|u_{0,n}\|_r$. This means that we can eliminate the truncation in the initial data whenever we control the increasing rate of u_0 thanks to the weighting function in R (implicitly $|x|$) used to define the norm $\|\cdot\|_r$ as per (2.84). Thus, we can write:

$$0 < t \leq T_\epsilon = \frac{1}{L\epsilon^\sigma(m-1)} \log \left(1 + cL\epsilon^\sigma(m-1) \|u_0\|_*^{1-m} \right), \quad (2.121)$$

where $r \rightarrow \infty$.

Finally, we have arrived at the estimation of a time interval where the Lipschitz problem with spacial-bounded forcing term (through the truncation in (2.97)) and with initial data whose increasing rate is controlled by the norm $\|u_0\|_*$ has existence of solutions.

□

It is interesting to observe two cases of time existence:

- $\epsilon \rightarrow 0 \Rightarrow \frac{cL\epsilon^\sigma(m-1) \|u_0\|_*^{1-m}}{L\epsilon^\sigma(m-1)} = c \|u_0\|_*^{1-m}.$

This case corresponds to a time where solutions exist for a finite time given by growing norm of the initial data.

- $\epsilon \rightarrow \infty \Rightarrow \frac{\log(cL\epsilon^\sigma(m-1) \|u_0\|_*^{1-m})}{L\epsilon^\sigma(m-1)} \rightarrow 0.$

This case does not provide information about the existence time due to the globally not bounded evolution of the term $|x|^\sigma$ in the whole space domain. In this case and for a particular value of $|x| = \epsilon$, it

is possible to ensure existence of solutions, as the expression (2.121) provides a dedicated value for T_ϵ . Then and at least, we can ensure the local existence of solutions for finite values of $|x|$ in the proximity of ϵ . Note that the fact of losing an existence criteria when $\epsilon \rightarrow \infty$ can be considered as a condition in which blow-up may be given. The blow-up behaviour is characterized in Section. 2.6.2.

2.6 The non-Lipschitz problem

In this section, we consider the following non-Lipschitz problem, named as P_ϵ :

$$u_t = \Delta u^m + |x|_\epsilon^\sigma u^p \leq \Delta u^m + \epsilon^\sigma u^p \text{ in } Q_{T_\epsilon} = \mathbb{R}^N \times [0, T_\epsilon],$$

$$u(x, 0) = u_0(x),$$

$$u_0(x) \geq 0 \in E_0,$$

$$p < 1; m > 1 N \geq 1$$

(2.122)

The condition of a non-Lipschitz reaction term has implications on the study of existence of solutions. One of them is the impossibility to show uniqueness for any value of u , particularly when $u = 0$ or when u increases from zero to positivity. Our effort is, hence, focused on determining the existence and characterizing two particular solutions, named as the maximal and the minimal solutions, so that any other solution will exist between them.

Theorem 2.6.1. *There exist two particular solutions to the problem P_ϵ referred as maximal solution u^M and minimal solution u_m existing in $[0, T_\epsilon]$ with $T_\epsilon(\epsilon, \|u_0\|_*)$ such that any solution to problem P_ϵ satisfies:*

$$u_m \leq u^\epsilon \leq u^M.$$

Proof. With the objective of applying Theorem 2.5.1, we firstly construct a Lipschitz function depending on a parameter δ :

$$f_\delta(s) = \begin{cases} \epsilon^\sigma \delta^{(p-1)} s & \text{for } 0 \leq s < \delta \\ \epsilon^\sigma s^p & \text{for } s \geq \delta \end{cases}, \quad (2.123)$$

so that in the limit for $\delta \rightarrow 0$, we recover the original term u^p ($p < 1$) (see Figure 2.4 together with the equation (2.123)).

For building the maximal solution, we consider the following problem

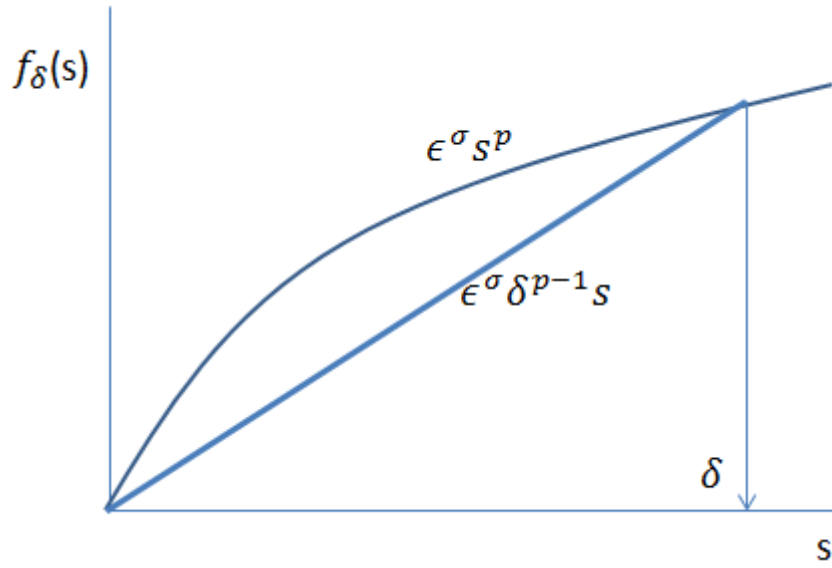


Figure 2.4: The function $f_\delta(s)$ is used to approximate the non-Lipschitz problem by a Lipschitz one. Note that in the limit $\delta \rightarrow 0$, we recover the original non-Lipschitz term

P_ϵ^M :

$$u_t = \Delta u^m + f_\delta(u) \text{ in } Q_{T_{\epsilon,\delta}} = \mathbb{R}^N \times [0, T_{\epsilon,\delta}], \quad (2.124)$$

$$u(x, 0) = u_0(x) + \nu \text{ for } x \in \mathbb{R}^N \text{ and } \nu > 0.$$

ν is selected such that:

$$f_\delta(u_0 + \nu) > f(u_0), \quad (2.125)$$

which gives:

$$\nu > |f_\delta^{-1} f(u_0) - u_0|. \quad (2.126)$$

The Lipschitz constant for the expression $f_\delta(s)$ can be obtained as follows:

$$\epsilon^\sigma (s_1^p - s_2^p) \leq \epsilon^\sigma L (s_1 - s_2) \leq \epsilon^\sigma \delta^{(p-1)} L (s_1 - s_2).$$

We remind that $p < 1$, therefore the last inequality make sense for $|\delta| < 1$.

We shall consider the Lipschitz constant as:

$$\epsilon^\sigma L \delta^{(p-1)} \quad (2.127)$$

The problem P_ϵ^M has a unique solution, in virtue of Theorem 2.5.1, existing

for a time interval $T_{\epsilon,\delta}$ given by the following expression:

$$T_{\epsilon,\delta} \geq \frac{1}{L\delta^{(p-1)}\epsilon^\sigma(m-1)} \log \left(1 + Lc\delta^{(p-1)}\epsilon^\sigma(m-1)\|u_0 + \nu\|_*^{1-m} \right). \quad (2.128)$$

The problem has, now, three different parameters: ϵ used to bound the forcing term, δ used to approximate the non-Lipschitz problem by a Lipschitz one and the parameter ν that shall be chosen to ensure the maximality of u^M .

For a given ϵ , we can make $\delta \rightarrow 0$, to recover the non-Lipschitz problem. Then, it is possible to determine the following condition for the existence time:

$$T_{\epsilon,\delta \rightarrow 0} \geq 0. \quad (2.129)$$

Or explicitly with δ :

$$T_{\epsilon,\delta \rightarrow 0} \geq \frac{1}{L\epsilon^\sigma(m-1)}\delta^{1-p}. \quad (2.130)$$

This condition means that the existence time is given in the proximity of any δ .

To recover the forcing term $|x|^\sigma$, we shall impose $\epsilon \rightarrow \infty$ while to recover the non-Lipschitz problem we shall impose $\delta \rightarrow 0$. To account for both effects, we can take:

$$\epsilon = \frac{1}{\delta^a}, \quad a > 0, \quad (2.131)$$

to jointly evaluate both parameters, ϵ and δ , in the limit with $\delta \rightarrow 0$ and $\epsilon \rightarrow \infty$.

Previously and first of all, we make $\delta \rightarrow \infty$ and $\epsilon \rightarrow 0$. We show that in this case, we recover the result obtained in the Lipschitz case (we remind that $\sigma > 0$).

$$T_{\epsilon,\delta} \geq \frac{\delta^{(1-p)}\delta^{a\sigma}}{L(m-1)} \log \left(1 + c \frac{1}{\delta^{(1-p)}\delta^{a\sigma}} L(m-1)\|u_0 + \nu\|_*^{1-m} \right), \quad (2.132)$$

$$T_{\epsilon \rightarrow 0, \delta \rightarrow \infty} \geq c\|u_0 + \nu\|_*^{1-m}, \quad (2.133)$$

for any $a > 0$.

Even when the value for $T_{\epsilon, \delta}$ has been obtained in the limit for $\epsilon \rightarrow 0$, it can be applied for any positive ϵ and by extension for any local single point in $x \in \mathbb{R}^{\mathbb{N}}$ as the function $|x|^\sigma \in \mathbb{L}_{loc}^\infty$.

Nonetheless, to recover the original problem we shall require $\delta \rightarrow 0$ and $\epsilon \rightarrow \infty$. In this case, we operate with the term $\delta \rightarrow 0$:

$$T_{\epsilon, \delta} \geq \frac{\delta^{(1-p)} \delta^{a\sigma}}{L(m-1)} \log \left(c \frac{1}{\delta^{(1-p)} \delta^{a\sigma}} L(m-1) \|u_0 + \nu\|_*^{1-m} \right), \quad (2.134)$$

$$T_{\epsilon, \delta} \geq 0, \quad (2.135)$$

Or explicitly with δ :

$$T_{\epsilon, \delta \rightarrow 0} \geq \frac{1}{L(m-1)} \delta^{1-p+a\sigma}. \quad (2.136)$$

for any $a > 0$.

This case corresponds to the existence of global blow-up as it will be shown afterwards in section 2.6.2. This global blow-up prevents us of getting a definite and clean conclusion about the existence of a maximal solution. Nonetheless, we can, at least, think on a maximal solution existing for arbitrary and fixed values of δ and ϵ . This implies that, if we select two values, one arbitrary for δ sufficiently small and other one for ϵ sufficiently large; we are in a position to calculate a value for $T_{\epsilon, \delta}$ and, therefore, to ensure the existence of a local maximal solution, not hidden by the global blow-up that seems, previous to any formal proof, to be an inherent feature of our problem. The existence of a maximal solution is supported by the precise calculation of such solution performed in Section 2.6.1.

For building the minimal solution, we consider the following problem P_ϵ^m :

$$u_t = \Delta u^m + f_\delta(u) \quad Q_{T_{\epsilon, \delta}} = \mathbb{R}^{\mathbb{N}} \times [0, T_{\epsilon, \delta}], \quad (2.137)$$

$$u(x, 0) = u_0(x) \quad \text{for } x \in \mathbb{R}^{\mathbb{N}} \text{ and } \delta > 0.$$

The problem P_ϵ^m has a unique solution in virtue of Theorem 2.5.1 existing for a time interval $(0, T_{\epsilon, \delta})$. Any solution, u_δ^m , to the problem P_ϵ^m is a

subsolution to the problem P_ϵ and to the original problem P . Indeed the approximation $f_\delta(u)$ of the non-Lipschitz function u^p satisfies:

$$f_\delta(u) \leq \epsilon^\sigma u^p \leq |x|^\sigma u^p, \quad (2.138)$$

$$u_\delta^m \leq u.$$

Given $\delta_1 > \delta_2$ we have that $f_{\delta_1}(u) < f_{\delta_2}(u)$ for an arbitrary decreasing sequence of δ 's, we have a non-decreasing sequence of u_δ^m that satisfies $u_\delta^m \leq u$, such that in the limit with $\delta \rightarrow 0$ we can establish:

$$u^m = \lim_{\delta \rightarrow 0} u_\delta^m. \quad (2.139)$$

Each element of the sequence u_δ^m does exist in virtue of Theorem 2.5.1, therefore, u^m is a minimal solution to the problem P_ϵ and to the problem P (in virtue of the ordered property in (2.138)). Indeed, u^m has been obtained under the change of the reaction original term u^p by a Lipschitz function from below $f_\delta(u)$. \square

The provided proof of Theorem 2.6.1 is based on the approximation to a Non-Lipschitz problem from a Lipschitz one. The Non-Lipschitz condition of the reaction term implies that uniqueness cannot hold. It has been proved that two particular solutions, maximal and minimal, exist. The determination of both solutions, with a classification in accordance with the problem data, is done in the immediate following sections.

2.6.1 Discussion about types of solutions

We have shown the existence of a maximal and a minimal solution, when the non-Lipschitz reaction imposes non-uniqueness. It is, now, the intention to obtain such solution profiles together with the expected types of solutions depending on the problem P data. This is especially relevant for the maximal solution, where it was not possible to obtain a general existence criteria (according to expression (2.134)), due to the highly suspected global blow-up (see Section 2.6.2 for a characterization of the blow-up phenomena).

We consider the initial condition of the form:

$$u_0 \equiv 0, \quad (2.140)$$

or,

$$u_0 = 0, \quad (2.141)$$

in

$$B_R = \{|x - x_0| < R\}. \quad (2.142)$$

In this case, and whenever $u_0 \rightarrow 0$, the reaction term predominates over the diffusive term (indeed the reaction term has $p < 1$ while the diffusion $m > 1$). Based on the fact that the non-Lipschitz reaction is predominant, we can think on two different solutions: The minimal solution to the problem P of the elementary form

$$u_m = 0, \quad (2.143)$$

and a maximal positive solution that can be shown to be:

$$u_\tau^M = |x|^{\sigma/(1-p)}(1-p)^{1/(1-p)}(t-\tau)^{1/(1-p)}, \quad (2.144)$$

for any $\tau > 0$.

To show the structure of such maximal solution, we start by a function of the form:

$$u_\tau^M = |x|^\theta k(t-\tau)^\alpha. \quad (2.145)$$

Introducing the expression (2.145) into the problem P , we have:

$$|x|^\theta k \alpha (t-\tau)^{\alpha-1} = m\theta(m\theta-1)|x|^{m\theta-2} k^m (t-\tau)^{m\alpha} + |x|^{p\theta+\sigma} k^p (t-\tau)^{p\alpha}. \quad (2.146)$$

The above expression determines the following values for θ and α , provided the reaction term predominates over the diffusion:

$$\theta = \frac{\sigma}{1-p},$$

$$\alpha = \frac{1}{1-p}, \quad (2.147)$$

$$k = (1-p)^{\frac{1}{1-p}}.$$

The postulated maximal solution adopts the following form:

$$u_{\tau \rightarrow 0^+}^M = |x|^{\sigma/(1-p)} (1-p)^{\frac{1}{1-p}} (t)^{1/(1-p)}. \quad (2.148)$$

In Theorem 2.6.3.2 , we will show that any maximal solution is positive.

In addition, we can take benefit of the development in the expression (2.146) to deduce a parameter condition to determine when the reaction predominates. As we start by a null initial condition, either in the whole domain or in B_R , the reaction shall be relevant in the proximity of $u = 0$. For this purpose, we make:

$$t \rightarrow \tau \rightarrow 0^+, \quad (2.149)$$

and the reaction predominates if:

$$p\alpha < m\alpha, \quad (2.150)$$

in the right hand side term of the expression (2.146); meaning that:

$$p < m. \quad (2.151)$$

We have, then, recovered the initial data as per the original problem, in which we made the requirement $0 < p < m$.

Once the solution starts to be positive, the local time evolution provides a positive and growing solution. Therefore, we shall require that the spatial term does not contradict such condition when the reaction predominates over the diffusion by the imposition of the following requirement (see the exponents of $|x|$ in the right hand side of the expression (2.146)):

$$p\theta + \sigma > m\theta - 2, \quad (2.152)$$

$$m\sigma + 2(1 - \sigma)p + \sigma < 2,$$

which shall be met for a maximal solution of the form (2.148). In fact, this condition can be used to state the following results to understand the expected type of solutions depending on the data parameters for P :

- $m\sigma + 2(1 - \sigma)p + \sigma \geq 2$.

The diffusion predominates and finite speed of propagation shall be considered whenever the solution is null in a certain ball B_R . This kind of solutions, where finite speed is given, are characterized in Theorem 2.6.2.2.

- $m\sigma + 2(1 - \sigma)p + \sigma < 2$.

The reaction is relevant, and particularly, the non-Lipschitz condition provides non-uniqueness. Two particular solutions, $u^m = 0$ and $u_{\tau \rightarrow 0}^M$ have been proved to exist (Theorem 2.6.1). In this case, the finite speed is not a predominant feature. This means that the non-uniqueness of solutions is the inherent behaviour to expect. We highlight that the two solutions, $u^m = 0$ and $u_{\tau \rightarrow 0}^M$, have been obtained based on the reaction term properties.

2.6.2 Precise minimum order of growth. A selfsimilar approach.

The intention, now, is to establish a minimum order of growth for the positive solutions to the problem P . During the development of this section and for complete understanding of the solution, we consider that the initial condition is a compactly supported function. This fact will permit to obtain the precise evolution of the support. The interest of a compactly supported function is focused on understanding the evolution of a smooth function whose support is null, and therefore, we can expect finite propagation speed due to the degeneracy of the diffusivity when $u \rightarrow 0$ in accordance with the parameters conditions derived in Section 2.6.1.

This kind of solution can be used to model a biological invasion in which the solution propagates with finite speed. In addition, the propagation of gas substances (either in the fire extinguishing application or the nitrogen invasion from one tank to another with a interfacing wall) can be modelled with a compactly supported function to understand the dynamic of the propagation.

For the purpose of dealing with a compactly supported function evolution, we firstly develop a self-similar solution to the problem P . We are going to see that we need to distinguish between the global evolution problem and the blow-up in finite time case; defining, thus, a critical parameter p^* . This result is compiled in the following theorem:

Theorem 2.6.2.1. *There exist a critical exponent p^* defined as:*

$$p^* = \text{sign}_+ \left(1 - \frac{\sigma(m-1)}{2} \right), \quad (2.153)$$

such that for:

$$p > p^*, \quad (2.154)$$

there exists blow up in finite time, while for:

$$p \leq p^*, \quad (2.155)$$

there exists a global solution.

Proof. We look for self-similar profiles of the form:

$$E(x, t) = t^{-\alpha} f(|x|t^\beta), \quad \chi = |x|t^\beta. \quad (2.156)$$

We make $N = 1$ for simplification purposes. The involved components, in the problem P , adopt the following forms:

$$\begin{aligned} u_t &= -\alpha t^{-\alpha-1} f + \beta \underbrace{|x|t^\beta}_\chi t^{-\alpha-1} f', \\ \Delta u^m &= t^{-\alpha m} t^{2\beta} f_{xx}^m, \\ |x|^\sigma u^p &= \chi^\sigma t^{-\sigma\beta - \alpha p} f^p. \end{aligned} \quad (2.157)$$

Upon substitution into P

$$-\alpha t^{-\alpha-1} f + \beta \underbrace{|x|t^\beta}_\chi t^{-\alpha-1} f' = t^{-\alpha m} t^{2\beta} f_{xx}^m + \chi^\sigma t^{-\sigma\beta - \alpha p} f^p. \quad (2.158)$$

And comparing the exponents of each variable t in the expression (2.158), we arrive at:

$$\begin{aligned} -\alpha - 1 &= -\alpha m + 2\beta, \\ \alpha m - 2\beta &= \alpha p + \beta\sigma. \end{aligned} \quad (2.159)$$

The solutions for α and β are:

$$\alpha = \frac{\sigma+2}{\sigma(m-1)+2(p-1)}, \quad (2.160)$$

$$\beta = \frac{m-p}{\sigma(m-1)+2(p-1)}.$$

Note that the term:

$$\sigma(m-1) + 2(p-1), \quad (2.161)$$

is common to α and β and in the blow-up in finite time case, it must be positive; while for the existence of a global solution, it must be negative (refer to the form of the self-similar profile in (2.156) where the time exponent is $-\alpha$). This two qualitative different behaviour of the solutions to the problem P can be clearly separated thanks to the definition of the critical exponent

$$0 < p^* < 1. \quad (2.162)$$

For the finite time blow up case, we have:

$$\begin{aligned} \sigma(m-1) + 2(p-1) &> 0, \\ p > p^* &= \text{sign}_+ \left(1 - \frac{\sigma(m-1)}{2} \right). \end{aligned} \quad (2.163)$$

Where the function sign_+ returns zero whenever:

$$\left(1 - \frac{\sigma(m-1)}{2} \right) < 0. \quad (2.164)$$

The complementary case provides the criteria for the existence of global in time solutions in Q_T : $p \leq p^*$.

□

The following theorem provides us with the evolution of a positive point $u(x_0, t_0) > 0$ and the evolution of the support, given a compactly supported initial data. It can be stated as:

Theorem 2.6.2.2. *Let u be a solution to problem P , such that $u(x_0, t_0) > 0$ for a given point in Q_T , then the following evolutions hold:*

- $u(x_0, t) \geq c_1(x_0)(t - t_0)^{-\alpha}$ for any

$$t > t_0, \quad (2.165)$$

and

$$\alpha = \frac{\sigma + 2}{\sigma(m - 1) + 2(p - 1)}. \quad (2.166)$$

- $u(x, t) > 0$ for any

$$t > t_0, \quad (2.167)$$

such that

$$|x - x_0| < c_2(x)(t - t_0)^\beta, \quad (2.168)$$

where

$$\beta = \frac{p - m}{\sigma(m - 1) + 2(p - 1)}. \quad (2.169)$$

And where:

$$c_1(x_0) = |x_0|^{\frac{\sigma}{1-p}} (-\alpha + \beta N)^{\frac{1}{p-1}}. \quad (2.170)$$

$$c_2(x) = c_{supp} |x|^{\frac{\sigma(m-1)}{2(1-p)}}, \quad (2.171)$$

being,

$$c_{supp} = \frac{(-\alpha + \beta N)^{\frac{m-1}{2(p-1)}}}{\left(\frac{(m-1)\beta}{2m}\right)^{1/2}}. \quad (2.172)$$

Proof. The stated results are obtained from a lower estimation to the reaction term (see the coming term $h_{\epsilon,n}$ to be characterized), so that comparison can be applied with an explicit subsolution.

The proof of the theorem starts by considering the following problem P_s :

$$u_t = \Delta u^m + h_{\epsilon,n}, \quad (2.173)$$

where:

$$h_{\epsilon,n} = n^\sigma \min \left[u^p, \epsilon^{p-1} u \right], \quad (2.174)$$

for:

$$n > 0 \text{ and } \epsilon > 0, \quad (2.175)$$

understood as parameters such that in the limit with:

$$n \rightarrow \infty \text{ and } \epsilon \rightarrow 0, \quad (2.176)$$

we recover the original term $|x|^\sigma u^p$.

The function $h_{\epsilon,n}$ satisfies the Lipschitz condition and, as a consequence, solutions exist under the scope of Theorem 2.5.1 .

The solution to the problem P_s can be obtained using a self-similar structure. The self-similar form is as per (2.156). The following equation holds for the determination of an exact solution profile for the term $f(|x|t^\beta)$, being $\chi = |x|t^\beta$ in the case of $x \in \mathbb{R}^N$:

$$-\alpha t^{-\alpha-1} f + \beta \chi t^{-\alpha-1} f' = t^{-\alpha m} (f^m)'' + \frac{N-1}{\chi} (f^m)' + h_{\epsilon,n}, \quad (2.177)$$

where:

$$h_{\epsilon,n}(f, t) = n^\sigma \min \left[f^p, \epsilon^{p-1} t^{\alpha(p-1)} f \right]. \quad (2.178)$$

Note that we write

$$h_{\epsilon,n}(f, t) = n^\sigma \min \left[t^{-\alpha p} f^p, \epsilon^{p-1} t^{-\alpha} f \right]. \quad (2.179)$$

This last expression and the expression in (2.178) have exactly the same intersection $f = t^\alpha \epsilon$. For simplification purposes, we make the calculations with the expression in (2.178) operating with the linear term:

$$\epsilon^{p-1} t^{\alpha(p-1)} f. \quad (2.180)$$

We can select a time t (to be determined), such that we have:

$$h_{\epsilon,n}(f, t) \geq n^\sigma c f \quad (2.181)$$

and c can be chosen as

$$c = n^{-\sigma} (-\alpha + \beta N) \quad (2.182)$$

, for simplification during the resolution of (2.177).

The profile $f(\chi)$ must satisfy the coming equation in (2.185) for each time (we assume $t = 1$). We consider that:

$$h_{\epsilon,n}(f, t) = n^\sigma c f, \quad (2.183)$$

such that, the equation reads:

$$-\alpha f + \beta \chi f' = (f^m)'' + \frac{N-1}{\chi} (f^m)' + (-\alpha + \beta N) f. \quad (2.184)$$

$$\beta \chi f' = (f^m)'' + \frac{N-1}{\chi} (f^m)' + \beta N f. \quad (2.185)$$

We have an elliptic equation with a known treatment [36]:

$$f(\chi) = (A - B\chi^2)^{\frac{1}{m-1}}, \quad (2.186)$$

where:

$$A > 0, \quad (2.187)$$

$$B = \frac{(m-1)\beta}{2m}.$$

This solution is valid for a sufficiently large time to hold the inequality (2.181) and to be determined as:

$$n^\sigma \min \left[f^p, \epsilon^{p-1} t^{\alpha(p-1)} f \right] \geq n^\sigma c f, \quad (2.188)$$

$$\min \left[f^p, \epsilon^{p-1} t^{\alpha(p-1)} f \right] \geq c f.$$

And in the sublinear case:

$$\epsilon^{p-1} t^{\alpha(p-1)} \geq n^{-\sigma} (-\alpha + \beta N). \quad (2.189)$$

We perform, now, the change of variable:

$$n = \frac{1}{\epsilon}, \quad (2.190)$$

to jointly evaluate the effect of both ϵ and n^σ . Indeed, we recover the original problem P when we make $\epsilon \rightarrow 0$ and $n^\sigma \rightarrow \infty$.

We can obtain an explicit value of t_ϵ from the expression (2.189):

$$t_\epsilon = (-\alpha + \beta N)^{\frac{-1}{\alpha(1-p)}} \epsilon^{-1/\alpha} \left(\frac{1}{\epsilon}\right)^{\frac{\sigma}{\alpha(1-p)}}, \quad (2.191)$$

such that the solution in (2.186) is a subsolution provided that:

$$t \geq t_\epsilon. \quad (2.192)$$

It is particularly interesting to make the limit with $\epsilon \rightarrow 0$. In this case, we have two cases to distinguish:

- Blow up case $\alpha > 0$:

$$t_\epsilon = (-\alpha + \beta N)^{\frac{-1}{\alpha(1-p)}} \frac{1}{\epsilon^{\frac{\sigma}{\alpha(1-p)} + \frac{1}{\alpha}}} \rightarrow \infty. \quad (2.193)$$

- Global solution case $\alpha < 0$:

$$t_\epsilon = (-\alpha + \beta N)^{\frac{1}{|\alpha|(1-p)}} \epsilon^{\frac{\sigma}{|\alpha|(1-p)} + \frac{1}{|\alpha|}} \rightarrow 0. \quad (2.194)$$

The self-similar solution is a subsolution for $t \geq t_\epsilon$ as it has been obtained by approximating the reaction term by the function $h_{\epsilon,n}$. Note that, on one side, the blow up case represents a singularity as the self-similar structure blows-up in a finite time. On the other side, the self-similar solution is a subsolution for any $t \geq t_\epsilon$ in case a global solution exists.

Any solution to the problem P_s is, indeed, a subsolution to the problem P as $h_{\epsilon,n} \leq n^\sigma u^p$. We can further assess this condition by letting y to be a solution to the problem P and u a solution to the problem P_s , starting at $t = t_\epsilon$. For any $\tau > t_\epsilon$, we have:

$$y(x, \tau) \geq u(x, t_\epsilon) \quad x \in \mathbb{R}^N, \quad (2.195)$$

for any $t \geq 0$, we have:

$$y(x, \tau + t) \geq u(x, t_\epsilon + t) \quad x \in \mathbb{R}^N, \quad (2.196)$$

and in the limit with $\tau \rightarrow 0$:

$$y(x, t) \geq u(x, t) \quad x \in \mathbb{R}^N. \quad (2.197)$$

Showing that $u(x, t)$ solution of the problem P_s is indeed a subsolution to the problem P .

Coming back to the expression (2.186): The precise evolution of the global solutions is given by directly obtaining the evolution of the maximum value in the function (2.186) for $\chi = 0$. The intention is to have a growing evolution starting at the positive A .

$$u(x, t) = A^{\frac{1}{m-1}} t^{-\alpha}, \quad (2.198)$$

$$\alpha = \frac{\sigma+2}{\sigma(m-1)+2(p-1)}.$$

A value for A can be determined from the expression (2.188):

$$\min \left[f^{p-1}, \epsilon^{p-1} t^{\alpha(p-1)} \right] \geq n^{-\sigma} (-\alpha + \beta N). \quad (2.199)$$

To obtain A , we make $\chi = 0$:

$$\min \left[A^{\frac{p-1}{m-1}}, \epsilon^{p-1} t^{\alpha(p-1)} \right] \geq n^{-\sigma} (-\alpha + \beta N). \quad (2.200)$$

Our solution departs from the point $f(\chi = 0)$, which is the minimum point as the time evolves due to the increasing behaviour of the global solution as per the expression (2.198) with $\alpha < 0$. Therefore we can determine A considering the following expression:

$$A^{\frac{p-1}{m-1}} = n^{-\sigma} (-\alpha + \beta N), \quad (2.201)$$

$$A = n^{\frac{\sigma(m-1)}{1-p}} (-\alpha + \beta N)^{\frac{m-1}{p-1}} = c(\alpha, \beta, N, m, p) n^{\frac{\sigma(m-1)}{1-p}}. \quad (2.202)$$

Upon recovering of the independent variable $|x|$:

$$A(x) = c(\alpha, \beta, N, m, p)|x|^{\frac{\sigma(m-1)}{1-p}}. \quad (2.203)$$

Eventually, the minimum growing evolution of the point with $f(\chi = 0)$ is:

$$y_m(x, t) = |x|^{\frac{\sigma}{1-p}}(-\alpha + \beta N)^{\frac{1}{p-1}}t^{-\alpha}. \quad (2.204)$$

This last expression provides the proof of the first part of the enunciated theorem considering that:

$$c_1(x) = |x|^{\frac{\sigma}{1-p}}(-\alpha + \beta N)^{\frac{1}{p-1}}. \quad (2.205)$$

Now, our intention is to determine the time evolution of the support of $f(\chi)$. For this purpose, we firstly calculate the χ values determining such support of f :

$$\begin{aligned} f(\chi) = 0 &\Rightarrow \chi = \left(\frac{A}{B}\right)^{(1/2)}, \\ \chi_{supp} &= \frac{1}{\left(\frac{(m-1)\beta}{2m}\right)^{1/2}} c^{(1/2)}(\alpha, \beta, N, m, p)|x|^{\frac{\sigma(m-1)}{2(1-p)}} \\ &= c_{supp}|x|^{\frac{\sigma(m-1)}{2(1-p)}}. \end{aligned} \quad (2.206)$$

We can easily determine the evolution of the self-similar solution support in the (x, t) hiperspace:

$$|x|_{supp} = \frac{1}{c_{supp}} t^{\frac{2(m-p)(1-p)}{(\sigma(m-1)+2(p-1))^2}}. \quad (2.207)$$

Coming back to the second bullet of the theorem enunciation, we can calculate the value of $c_2(x)$ as:

$$c_2(x) = c_{supp}|x|^{\frac{\sigma(m-1)}{2(1-p)}}. \quad (2.208)$$

The theorem is, therefore, shown and the final results are as per the following expressions:

- $u(x_0, t) \geq c(\alpha, \beta, N, m, p)|x_0|^{\frac{\sigma(m-1)}{1-p}}(t - t_0)^{-\alpha}$ for any $t > t_0$
and

$$\alpha = \frac{\sigma + 2}{\sigma(m - 1) + 2(p - 1)}. \quad (2.209)$$

- $u(x, t) > 0$ for any $t > t_0$ and

$$|x - x_0| < c_{supp}|x|^{\frac{\sigma(m-1)}{2(1-p)}}(t - t_0)^\beta, \quad (2.210)$$

where

$$\beta = \frac{m - p}{\sigma(m - 1) + 2(p - 1)}. \quad (2.211)$$

In addition, note that:

$$c_{supp} = \frac{(-\alpha + \beta N)^{\frac{m-1}{2(p-1)}}}{\left(\frac{(m-1)\beta}{2m}\right)^{1/2}}, \quad (2.212)$$

and,

$$c(\alpha, \beta, N, m, p) = (-\alpha + \beta N)^{\frac{m-1}{2(p-1)}} \quad (2.213)$$

□

Once we have shown the evolution of the solutions for the problem P with compactly supported initial data, we proceed to enunciate the conditions required for a unique solution. This is the purpose of the following section.

2.6.3 Uniqueness

As already discussed, the non-Lipschitz reaction term induces non uniqueness if the initial condition has compact support, as well as, if the initial condition is null ($u_0 = 0$). In Sections 2.6.1 and 2.6.2, we obtained two

particular solutions, maximal and minimal, whose existence was shown in Theorem 2.6.1. Both solutions were obtained under the condition that the initial data is null, at least in a ball B_R , and were of the form (note that for the minimal solutions, we consider the trivial case):

$$\begin{aligned} u_m &= 0, \\ u^M &= |x|^{\sigma/(1-p)}(1-p)^{\frac{1}{1-p}}(t)^{1/(1-p)}. \end{aligned} \tag{2.214}$$

Our objective is, now, to establish the required conditions, so that there exists only one solution to the problem P . Essentially, uniqueness of solutions leads to consider only positive initial data:

$$u_0 \geq \phi > 0, \tag{2.215}$$

so that the reaction term, $R(x, u) = |x|^\sigma u^p$, is Lipschitz in the interval $[\phi, \infty)$. We remind that the existence of solutions for a reaction term of the Lipschitz type has been already shown in Section 2.5. Thus, we enunciate the following lemma:

Theorem 2.6.3.1. *Let consider:*

$$u_0 \geq \phi > 0, \tag{2.216}$$

and let consider that the reaction term is Lipschitz with constant:

$$\frac{p}{\phi^{1-p}}. \tag{2.217}$$

Under these conditions, uniqueness of solutions holds in the interval given by Q_T

Proof. The non-linear diffusion term is associated to a degenerate diffusivity ($D(u) = mu^{m-1}$). In case of $u \rightarrow 0$, for example if $\phi \rightarrow 0$, the degeneracy does not lead to positivity, and thus, solutions cannot be classical locally in time as $u(x, t \rightarrow 0) \rightarrow 0$.

We shall proceed with the definition of a weak solution, as per the expression (2.29), for a given test function $\psi(x, t) \in C^\infty(Q_T)$ with compact support.

Let consider the existence of two solutions $u_1(x, t)$ and $u_2(x, t)$. By initial assumption, and without losing of generality, we consider that

$$u_1 \geq u_2. \quad (2.218)$$

Both solutions have the same initial positive data:

$$u_1(x, 0) = u_2(x, 0) = u_0(x) \geq \phi > 0. \quad (2.219)$$

By the definition of a weak solution, we mean:

$$\begin{aligned} \int_{\mathbb{R}^N} u_1(t) \psi(t) dx &= \int_{\mathbb{R}^N} u(0) \psi(0) dx \\ &+ \int_0^t \int_{\mathbb{R}^N} [u_1 \psi_t + u_1^m \Delta \psi + |x|^\sigma u_1^p \psi] dx ds, \end{aligned} \quad (2.220)$$

$$\begin{aligned} \int_{\mathbb{R}^N} u_2(t) \psi(t) dx &= \int_{\mathbb{R}^N} u(0) \psi(0) dx \\ &+ \int_0^t \int_{\mathbb{R}^N} [u_2 \psi_t + u_2^m \Delta \psi + |x|^\sigma u_2^p \psi] dx ds, \end{aligned} \quad (2.221)$$

and making the subtraction:

$$\begin{aligned} &\int_{\mathbb{R}^N} (u_1 - u_2)(t) \psi(t) dx \\ &= \int_0^t \int_{\mathbb{R}^N} [(u_1 - u_2) \psi_t + (u_1^m - u_2^m) \Delta \psi + |x|^\sigma (u_1^p - u_2^p) \psi] dx ds. \end{aligned} \quad (2.222)$$

Under the Lipschitz condition we have:

$$(u_1^p - u_2^p) \leq |u_1^p - u_2^p| \leq \frac{p}{\phi^{1-p}} |u_1 - u_2|. \quad (2.223)$$

Where the Lipschitz constant is obtained as:

$$K_l = pu^{p-1} = p \frac{1}{u^{1-p}} \leq \frac{p}{\phi^{1-p}}. \quad (2.224)$$

Analogously:

$$(u_1^m - u_2^m) \leq m u_1^{m-1} |u_1 - u_2| \leq \kappa^{m-1} |u_1 - u_2|. \quad (2.225)$$

Where:

$$\kappa = \max_{(x,t) \in Q_T} \{u_1\}. \quad (2.226)$$

We continue by considering a particular value for the test function, so that, the involved integrals can be solved.

$$\psi(x, s) = \frac{e^{-ls}}{(1 + |x|^2)^\gamma}. \quad (2.227)$$

We notice that

$$\psi(x, t) \in C^\infty(Q_T), \quad (2.228)$$

and where γ is such that:

$$e^{ls} \int_{\mathbb{R}^N} |x|^\sigma \psi(x, s) dx < \infty. \quad (2.229)$$

Without impacting the ending conclusions and aiming the easiest way forward during the proof, we require

$$e^{ls} \int_{\mathbb{R}^N} |x|^\sigma \psi(x, s) dx = 1. \quad (2.230)$$

For this purpose, we shall impose the condition that the mass of the integrand shall be null when $|x| \rightarrow \infty$. This can be expressed considering that for a $R \gg 1$, the following is met:

$$\int_{(|x|-R) \rightarrow \infty} |x|^\sigma \psi(x, s) dx = 0. \quad (2.231)$$

Which is equivalent to say, in the asymptotic condition, $|x| \rightarrow \infty$, that:

$$|x|^{-2\gamma} |x|^\sigma |x|^N \rightarrow 0. \quad (2.232)$$

Then:

$$\begin{aligned} -2\gamma + \sigma + N &< 0, \\ \gamma &> \frac{\sigma + N}{2} > 0. \end{aligned} \quad (2.233)$$

We define:

$$\int_{\mathbb{R}^N} \psi(x, s) dx = e^{-ls} \int_{\mathbb{R}^N} \frac{1}{(1 + |x|^2)^\gamma} dx = e^{-ls} \Psi(x), \quad (2.234)$$

where $\Psi(x)$ is the integral defined as:

$$\Psi(x) = \int_{(x \in \mathbb{R}^N) \rightarrow \infty} \frac{1}{(1 + |\beta|^2)^\gamma} d\beta, \quad (2.235)$$

where

$$\beta \in \mathbb{R}^N. \quad (2.236)$$

The integral (2.235) is finite in virtue of the condition for γ in the expression (2.233) and the ∞ for the vector x shall be understood in a component wise.

In the same way:

$$\int_{\mathbb{R}^N} \Delta \psi(x, s) dx \leq \int_{\mathbb{R}^N} K_1(\gamma) \psi(x, s) dx = K_1(\gamma) e^{-ls} \Psi(x). \quad (2.237)$$

Where $K_1(\gamma)$ is obtained as:

$$\begin{aligned} e^{-ls} \Delta \psi &= e^{-ls} \gamma(\gamma + 1) 4x^2 \frac{1}{(1 + |x|^2)^{\gamma+2}} - 2\gamma \frac{1}{(1 + |x|^2)^{\gamma+1}} \\ &\leq e^{-ls} \gamma(\gamma + 1) 4x^2 \frac{1}{(1 + |x|^2)^{\gamma+2}}. \end{aligned} \quad (2.238)$$

In the limit with $|x| \rightarrow \infty$:

$$\begin{aligned} e^{-ls} \gamma(\gamma + 1) 4x^2 \frac{1}{(1 + |x|^2)^{\gamma+2}} &\sim e^{-ls} \frac{\gamma(\gamma + 1) 4}{(1 + |x|^2)^\gamma} \frac{1}{|x|^2} \\ &\leq e^{-ls} \frac{\gamma(\gamma + 1) 4}{(1 + |x|^2)^\gamma} = \gamma(\gamma + 1) 4\psi(x). \end{aligned} \quad (2.239)$$

Then:

$$K_1 = \gamma(\gamma + 1)4. \quad (2.240)$$

The next step is to evaluate the involved integrals in the expression (2.222):

$$\begin{aligned} \int_0^t \int_{\mathbb{R}^N} (u_1 - u_2) \psi_t dx ds &= \int_0^t \int_{\mathbb{R}^N} -l(u_1 - u_2) \psi dx ds \\ &= \int_0^t \int_{\mathbb{R}^N} l(u_2 - u_1) \psi dx ds \\ &\leq l \sup |u_2 - u_1| \Psi(x) \int_0^t e^{-ls} ds \\ &= l \sup |u_2 - u_1| \Psi(x) \left(\frac{1}{l} \right) (1 - e^{-lt}). \end{aligned} \quad (2.241)$$

$$\begin{aligned} \int_0^t \int_{\mathbb{R}^N} (u_1^m - u_2^m) \Delta \psi dx ds &\leq \sup |u_1 - u_2| \int_0^t \kappa^{m-1} K_1(\gamma) \int_{\mathbb{R}^N} \psi(x, s) dx ds \\ &= \sup |u_1 - u_2| \int_0^t \kappa^{m-1} K_1(\gamma) e^{-ls} \Psi(x) \\ &= \sup |u_1 - u_2| \kappa^{m-1} K_1(\gamma) (1 - e^{-lt}). \end{aligned} \quad (2.242)$$

$$\begin{aligned} \int_0^t \int_{\mathbb{R}^N} |x|^\sigma (u_1^p - u_2^p) \psi(x, s) dx ds &\leq \frac{p}{\phi^{1-p}} \sup |u_1 - u_2| \int_0^t e^{-ls} \int_{\mathbb{R}^N} e^{ls} |x|^\sigma \psi(x, s) dx ds \\ &= \frac{p}{\phi^{1-p}} \sup |u_1 - u_2| (1 - e^{-lt}). \end{aligned} \quad (2.243)$$

Compiling the assessments on the integrals in the expression (2.222), we

have:

$$\begin{aligned} \int_{\mathbb{R}^N} (u_1 - u_2)(t) \psi(t) dx &\leq \sup |u_2 - u_1| \Psi(x) (1 - e^{-lt}) \\ &\quad + \sup |u_1 - u_2| \kappa^{m-1} K_1(\gamma) (1 - e^{-lt}) \\ &\quad + \frac{p}{\phi^{1-p}} \sup |u_1 - u_2| (1 - e^{-lt}). \end{aligned} \quad (2.244)$$

For a given $t > 0$, let consider that for the two functions u_1 and u_2 , we determine the supremum of their difference. Then, if we require that:

$$\sup |u_1 - u_2| \rightarrow 0, \quad (2.245)$$

and knowing that:

$$\phi > 0, \quad (2.246)$$

$$|\Psi(x)| < \infty.$$

We conclude:

$$\int_{\mathbb{R}^N} (u_1 - u_2)(t) \psi(t) dx \leq 0. \quad (2.247)$$

The integral preserves the ordered monotony properties (p. 338 in [21]), thus, we have

$$u_1(t) \leq u_2(t). \quad (2.248)$$

As we have initially assumed that

$$u_1(t) \geq u_2(t), \quad (2.249)$$

the only compatible result is to consider:

$$u_1(t) = u_2(t), \quad (2.250)$$

showing, then, the uniqueness of solutions. \square

The following theorem aims to show the evolution of the unique solution.

Theorem 2.6.3.2. *Let u be a solution to problem P , such that*

$$u_0(x) \in E_0, \quad (2.251)$$

and $\nu \in \mathbb{R}^+$ with:

$$u \geq \nu, \quad (2.252)$$

for all $0 \leq t < T$. Then u coincides with the maximal solution to problem P .

Proof. Firstly, we perform the usual truncation to the term $|x|^\sigma$ as follows:

$$|x|_\epsilon^\sigma = \begin{cases} |x|^\sigma & \text{for } 0 \leq x \leq \epsilon \\ \epsilon^\sigma & \text{for } x > \epsilon \end{cases}. \quad (2.253)$$

If we consider v as the maximal solution to the problem P_ϵ in $0 \leq t < T$ and $x \in \mathbb{R}^{\mathbb{N}}$, we have that the following expression holds for every test function $\phi \in C^\infty(Q_T)$ with compact support in x :

$$\begin{aligned} 0 &\leq \int_{\mathbb{R}^{\mathbb{N}}} (v - u)(t) \phi(t) \\ &= \int_0^t \int_{\mathbb{R}^{\mathbb{N}}} [(v - u) \phi_t + (v^m - u^m) \Delta \phi + |x|_\epsilon^\sigma (v^p - u^p) \phi] ds. \end{aligned} \quad (2.254)$$

The bound of any solution to problem P_ϵ is necessary during the proof of the theorem to ensure the correct convergence of the integrals. For this purpose, the truncation in (2.253) is used whenever the term $|x|$ appears during the involved integrals assessments.

$$\begin{aligned} 0 &\leq \int_{\mathbb{R}^{\mathbb{N}}} (v - u)(t) \phi(t) \\ &\leq \int_0^t \int_{\mathbb{R}^{\mathbb{N}}} [(v - u) \phi_t + (v^m - u^m) \Delta \phi + \epsilon^\sigma (v^p - u^p) \phi] ds. \end{aligned} \quad (2.255)$$

To ensure the convergence of the integrals in (2.255), we require

$$\phi \in C^\infty(Q_T) \cap \mathbb{L}^1(Q_T). \quad (2.256)$$

The following function will be of help during the integral assessment:

$$a(\epsilon, s) = \begin{cases} \frac{v(\epsilon, s)^m - u(\epsilon, s)^m}{v(\epsilon, s) - u(\epsilon, s)} & \text{for } v \neq u \\ mv^{m-1} & \text{otherwise} \end{cases}. \quad (2.257)$$

Given two fixed values for ϵ and $s = T$, the last expression is bounded satisfying that:

$$0 \leq a(\epsilon, s) \leq c_0(m, \|u_0\|_\infty, T). \quad (2.258)$$

We try the following test function:

$$\phi(|x|, s) = e^{k(T-s)}(1 + |x|^2)^{-\gamma}, \quad (2.259)$$

for some constant k and γ .

The determination for γ is given by the condition related to the compact support and integral convergence in \mathbb{R}^N . Indeed:

$$\begin{aligned} & \int_{\mathbb{R}^N; |x| \rightarrow \infty} e^{k(T-s)}(1 + |x|^2)^{-\gamma} |x|^\sigma dx \\ & \sim e^{k(T-s)} \int_{\mathbb{R}^N; |x| \rightarrow \infty} (|x|)^{-2\gamma+\sigma} dx \sim e^{k(T-s)} (|x|)^{-2\gamma+\sigma} x^N \rightarrow 0 \end{aligned} \quad (2.260)$$

when $|x| \rightarrow \infty$.

The condition in (2.260) holds for

$$\gamma > \frac{\sigma + N}{2}. \quad (2.261)$$

In addition, the test function satisfies the following expressions:

$$\phi_t = -k\phi, \quad (2.262)$$

$$\Delta_{|x|}\phi \leq c_1(\gamma, N)\phi,$$

we have:

$$\phi_t + a\Delta\phi \leq (-k + a(\epsilon, s) c_1(\gamma, N))\phi. \quad (2.263)$$

We are particularly interested in making:

$$\phi_t + a\Delta\phi \leq 0, \quad (2.264)$$

as it will be shown shortly.

For this purpose, we can consider a k sufficiently large satisfying:

$$k > a(\epsilon, s) c_1(\gamma, N). \quad (2.265)$$

In such a case, the inequality in (2.255) can be rewritten as:

$$\begin{aligned} 0 &\leq \int_{\mathbb{R}^N} (v - u)(t) \phi(t) \\ &\leq \int_0^t \int_{\mathbb{R}^N} [(v - u) \phi_t + a(v - u) \Delta \phi + \epsilon^\sigma (v^p - u^p) \phi] ds, \end{aligned} \quad (2.266)$$

and

$$\begin{aligned} 0 &\leq \int_{\mathbb{R}^N} (v - u)(t) \phi(t) \\ &\leq \int_0^t \int_{\mathbb{R}^N} [(v - u) [\phi_t + a \Delta \phi] + \epsilon^\sigma (v^p - u^p) \phi] ds. \end{aligned} \quad (2.267)$$

Considering that:

$$\phi_t + a \Delta \phi \leq 0, \quad (2.268)$$

we have:

$$\begin{aligned} 0 &\leq \int_{\mathbb{R}^N} (v - u)(t) \phi(t) \\ &\leq \int_0^t \int_{\mathbb{R}^N} \epsilon^\sigma (v(|x|_\epsilon, s)^p - u(|x|_\epsilon, s)^p) \phi(|x|_\epsilon, s) ds. \end{aligned} \quad (2.269)$$

The proof of Theorem 2.6.3.2 will succeed if we demonstrate that the right hand side of the inequality in (2.269) is zero or tends to zero under certain suitable conditions that involve making $\epsilon \rightarrow \infty$.

Given a positive initial data, de Pablo and Vázquez showed in [31] that:

$$u(\epsilon, s) = \epsilon^{\sigma/(1-p)} (1-p)^{(1-p)} (t)^{1/(1-p)}, \quad (2.270)$$

is the minimum solution of the positive solutions. This expression is used to perform the following truncation:

$$0 \leq \epsilon^\sigma (v^p - u^p)(|x|_\epsilon, s) \leq \epsilon^\sigma \frac{p(v-u)}{u^{1-p}} \leq \frac{p}{1-p} \frac{v-u}{s}. \quad (2.271)$$

Therefore, we can write:

$$\begin{aligned} & \int_{\mathbb{R}^N} (v - u)(t) \phi(t) \\ & \leq \frac{p}{1-p} \int_0^t \int_{\mathbb{R}^N} (v(|x|_\epsilon, s) - u(|x|_\epsilon, s)) \phi(|x|_\epsilon, s) s^{-1} ds. \end{aligned} \quad (2.272)$$

We define now the following function:

$$f(t) = \int_\nu^t \int_{\mathbb{R}^N} (v - u) \phi s^{-1} ds, \quad (2.273)$$

where $\nu \rightarrow 0$.

This ν can be considered as the one mentioned in the postulations of the theorem, when we established $u \geq \nu > 0$, as it is a free parameter that we can make positive and tending to zero. The derivative is as follows:

$$\dot{f}(t) = t^{-1} \int_{\mathbb{R}^N} (v - u)(t) \phi(t) dx; \quad t\dot{f}(t) = \int_{\mathbb{R}^N} (v - u)(t) \phi(t) dx. \quad (2.274)$$

The inequality (2.272) can be expressed as:

$$t\dot{f}(t) \leq \frac{p}{1-p} f(t) \quad (2.275)$$

The ordinary differential equation in (2.275) has the solution:

$$f(t) = ct^{p/(1-p)}, \quad (2.276)$$

for a constant c to be determined.

Given $\epsilon > 0$ such that $\nu < t < T$ we have:

$$f(\nu) = c\nu^{p/(1-p)} \rightarrow c = \frac{f(\nu)}{\nu^{p/(1-p)}}. \quad (2.277)$$

Finally, the solution to (2.275) is:

$$f(t) \leq f(\nu) \left(\frac{t}{\nu} \right)^{p/(1-p)}. \quad (2.278)$$

In the limit $t \rightarrow \nu$, we have $f(t) \rightarrow 0$ whenever $f(\nu) \rightarrow 0$. Therefore, our problem has resulted in the searching of a suitable function, such that

$$f(\nu) \rightarrow 0, \quad (2.279)$$

whenever $t \rightarrow \nu$.

In order to find the suitable $f(\nu)$, we can arrange the inequality (2.272) aiming to obtain another upper estimation that after comparison with the expression in (2.278), will support the finding of that suitable $f(\nu)$.

$$\begin{aligned} \int_{\mathbb{R}^{\mathbb{N}}} (v - u)(t) \phi(t) &\leq \int_0^t \int_{\mathbb{R}^{\mathbb{N}}} (v^p - u^p)(\tau) \phi(\tau) \epsilon^\sigma dx d\tau \\ &\leq \int_0^t \left(\int_{\mathbb{R}^{\mathbb{N}}} \phi(\tau) \epsilon^\sigma dx \right)^{1-p} \left(\int_{\mathbb{R}^{\mathbb{N}}} (v - u) \phi(\tau) \epsilon^\sigma dx \right)^p d\tau. \end{aligned} \quad (2.280)$$

Note that the integral:

$$\int_{\mathbb{R}^{\mathbb{N}}} \phi(\tau) \epsilon^\sigma dx, \quad (2.281)$$

is bounded in $\mathbb{R}^{\mathbb{N}}$:

$$\int_0^t \left(\int_{\mathbb{R}^{\mathbb{N}}} \phi(\tau) \epsilon^\sigma dx \right)^{1-p} \leq c(t \rightarrow T). \quad (2.282)$$

And the inequality in (2.280) is expressed as:

$$\begin{aligned} \int_{\mathbb{R}^{\mathbb{N}}} (v - u)(t) \phi(t) &\leq \int_0^t \int_{\mathbb{R}^{\mathbb{N}}} (v^p - u^p)(\tau) \phi(\tau) \epsilon^\sigma dx d\tau \\ &\leq c(T) \int_0^t \left(\int_{\mathbb{R}^{\mathbb{N}}} (v - u) \phi(\tau) \epsilon^\sigma dx \right)^p d\tau. \end{aligned} \quad (2.283)$$

We have obtained two upper estimates for every $0 \leq s = \tau \leq T$ and $x \in \mathbb{R}^{\mathbb{N}}$ in (2.272) and (2.283). Making both of them coincide and obtaining the value for the integrand $v - u$ we arrive at:

$$\int_{\mathbb{R}^{\mathbb{N}}} (v - u)(s) \phi(s) dx = \left(c(T) \frac{1-p}{p} \tau \right)^{1/(1-p)} \epsilon^{\frac{\sigma p}{1-p}}. \quad (2.284)$$

And now considering any of the two upper bounds (in this case (2.272)) we

have:

$$\frac{p}{1-p} \int_0^t \left(c(T) \frac{1-p}{p} \tau \right)^{1/(1-p)} \epsilon^{\frac{\sigma p}{1-p}} \tau^{-1} d\tau. \quad (2.285)$$

The integral in (2.285) can be solved considering that after integration the $|x|$ variable is introduced within the truncation in (2.253) to obtain:

$$\frac{p}{1-p} \int_0^t \left(c(T) \frac{1-p}{p} \tau \right)^{1/(1-p)} \epsilon^{\frac{\sigma p}{1-p}} \tau^{-1} d\tau = c(T, p, \sigma) \epsilon^{\frac{p\sigma}{1-p}} t^{\frac{1}{1-p}}. \quad (2.286)$$

Now we approximate $t \rightarrow \nu \rightarrow 0$ and $\epsilon \rightarrow \infty$. To simplify the balance between both conflicting parts of the integral, we consider

$$\epsilon = \frac{1}{\nu^a}, \quad (2.287)$$

for any $a > 0 \in \mathbb{R}$ to be chosen. Hence, the expression (2.286) can be reformulated in terms of ν only:

$$c(T, p, \sigma) \epsilon^{\frac{p\sigma}{1-p}} t^{\frac{1}{1-p}} = c(T, p, \sigma) \left(\frac{1}{\nu^a} \right)^{\frac{p\sigma}{1-p}} \nu^{\frac{1}{1-p}}, \quad (2.288)$$

for

$$a < \frac{1}{p\sigma}. \quad (2.289)$$

and making $\nu \rightarrow 0$, we finally arrive at:

$$\int_{\mathbb{R}^N} (v - u)(t) \phi(t) \leq c(T, p, \sigma) \left(\frac{1}{\nu^a} \right)^{\frac{p\sigma}{1-p}} \nu^{\frac{1}{1-p}} \rightarrow 0. \quad (2.290)$$

In virtue of the expression in (2.290), we ensure, hence, that $u \equiv v$ in Q_T for any $T > 0$.

□

We can use the conclusions of this theorem to show, *a priori*, the uniqueness of positive solutions considering the initial data positive as well. if in a certain time τ , the solution is positive then the solution will be unique for any $t \geq \tau$.

2.6.4 Comparison of solutions

The PME implies a degenerate diffusivity. This means that whenever $u \rightarrow 0$, the diffusivity tends to zero as well; additionally, the reaction term is not Lipschitz when $u \rightarrow 0$. Therefore, we cannot make use of monotone properties of the forcing terms to compare solutions as we did in Section 1.3 for the coupled system. Indeed:

- PME: $\Delta u^m = \nabla \cdot (m u^{m-1} \nabla u)$ where $D(u) = m |u|^{m-1}$, with $m > 1$.
- HE: $\Delta u = \nabla \cdot (\nabla u)$ where $D(u) = 1$.

If $u \rightarrow 0$, the PME defines the divergence of an infinitesimal function, $D(u)$, whose derivatives may not be classically defined. Thus, we have to refer to the weak solution definition (2.29) for showing a comparison theorem:

Theorem 2.6.4.1. *Let u and v be two solutions to the problem P in Q_T , such that $0 < u_0 \leq v_0$ in \mathbb{R}^N and $u_0, v_0 \in E_0$, then the following comparison principle holds:*

$$0 < u \leq v \text{ in } Q_T \quad (2.291)$$

Proof. The proof of this theorem starts by considering the definition of a weak solution as per the equation (2.29) for $0 \leq \tau < t < T$:

$$\begin{aligned} \int_{\mathbb{R}^N} u(t) \phi(t) dx &= \int_{\mathbb{R}^N} u_0(\tau) \phi(\tau) dx \\ &+ \int_{\tau}^t \int_{\mathbb{R}^N} [(u) \phi_t + (u^m) \Delta \phi + |x|^\sigma u^p \phi] dx ds. \end{aligned} \quad (2.292)$$

$$\begin{aligned} \int_{\mathbb{R}^N} v(t) \phi(t) dx &= \int_{\mathbb{R}^N} v_0(\tau) \phi(\tau) dx \\ &+ \int_{\tau}^t \int_{\mathbb{R}^N} [(v) \phi_t + (v^m) \Delta \phi + |x|^\sigma v^p \phi] dx ds, \end{aligned} \quad (2.293)$$

where $u_0(\tau)$ and $v_0(\tau)$ represent the time translation in τ units of the initial data u_0 and v_0

After performing the subtraction, we have:

$$\begin{aligned} \int_{\mathbb{R}^N} (u - v)(t) \phi(t) dx &= \int_{\mathbb{R}^N} (u_0 - v_0)(\tau) \phi(\tau) dx \\ &+ \int_{\tau}^t \int_{\mathbb{R}^N} [(u - v) \phi_t + (u^m - v^m) \Delta \phi + |x|^\sigma (u^p - v^p) \phi] dx ds, \end{aligned} \quad (2.294)$$

for every test function $\phi \in C^\infty(Q_T)$ with compact support.

Note that the functions u^p, v^p , in the reaction term, are Lipschitz, as we assume that both will be always positive to derive the comparison statement.

Our next intention is to assess each of the integrals involved in the expression (2.294), making use of the norm defined in (2.84) and using the same test function structure than in (2.227), but probably with a different exponent γ , namely:

$$\phi(x, s) = \frac{e^{-ls}}{(1 + |x|^2)^\gamma}. \quad (2.295)$$

Then, the evaluation of the first integral in the right hand side of (2.294) reads:

$$\int_{\mathbb{R}^N} (u_0 - v_0)(\tau) \phi(\tau) dx \leq \|u_0 - v_0\|_* \cdot \|\phi\|_*, \quad (2.296)$$

where:

$$\begin{aligned} \|\phi\|_* &= \lim_{R \rightarrow \infty} R^{-N-a\sigma} \int_{\mathbb{R}^N} |\phi(x)| dx \\ &\sim |x|^{-N-a\sigma} \int_{\mathbb{R}^N} \frac{e^{-ls}}{(1 + |x|^2)^\gamma} dx. \end{aligned} \quad (2.297)$$

In this last expression, we evaluate the integral asymptotically when

$$|x| \rightarrow \infty, \quad (2.298)$$

and γ is selected so that:

$$|x|^{-N-a_\sigma} \int_{\mathbb{R}^N; |x| \rightarrow \infty} \frac{dx}{(1+|x|^2)^\gamma} = 0. \quad (2.299)$$

For this purpose:

$$|x|^{-N-a_\sigma} |x|^{-2\gamma} |x|^N = 0, \quad (2.300)$$

when $|x| \rightarrow \infty$.

This condition implies that:

$$-N - a_\sigma - 2\gamma + N < 0, \quad (2.301)$$

for which it suffices to consider:

$$\gamma > -\frac{a_\sigma}{2}, \quad (2.302)$$

where $a_\sigma > 0$ as shown in (2.85).

With the intention of preserving the decreasing behaviour with $|x|$ of the test function (2.295), we can, then, simply require that:

$$\gamma > 0, \quad (2.303)$$

so that this condition satisfies (2.302) as well.

As the function $\phi(x)$ is monotone decreasing with $|x|$, we can ensure that the maximum value of ϕ corresponds to $|x| = 0$:

$$\max_{x \in \mathbb{R}^N} \phi(x, s) = e^{-ls}. \quad (2.304)$$

And returning to the integral (2.296):

$$\begin{aligned} \int_{\mathbb{R}^N} (u_0 - v_0)(\tau) \phi(\tau) dx &\leq \|u_0 - v_0\|_* \cdot \|\phi\|_* \\ &= \|u_0 - v_0\|_* \lim_{R \rightarrow \infty} R^{-N-a_\sigma} \int_{\mathbb{R}^N} |\phi(x)| dx \\ &\leq \|u_0 - v_0\|_* \lim_{R \rightarrow \infty} R^{-N-a_\sigma} \max |\phi(x)| R^N \\ &= \|u_0 - v_0\|_* e^{-l\tau} \lim_{R \rightarrow \infty} R^{-a_\sigma}, \end{aligned} \quad (2.305)$$

where $a_\sigma > 0$.

We continue by assessing the rest of the integrals involved on the right hand side of (2.294):

$$\begin{aligned}
\int_\tau^t \int_{\mathbb{R}^N} [(u - v) \phi_t] dx ds &= \int_\tau^t \int_{\mathbb{R}^N} (u - v) (-l) \phi \\
&\leq \int_\tau^t |-l| \|u - v\|_* \cdot \|\phi\|_* ds \\
&\leq \|u - v\|_* (e^{-l\tau} - e^{-lt}) \lim_{R \rightarrow \infty} R^{-a\sigma}.
\end{aligned} \tag{2.306}$$

Let continue, now, with the integral associated to the diffusion term for which we make use of the already known calculation in (2.242):

$$\begin{aligned}
\int_\tau^t \int_{\mathbb{R}^N} (u^m - v^m) \Delta \phi &\leq \int_\tau^t \kappa^{m-1} \|u - v\|_* K_1(\gamma) \|\phi\|_* ds \\
&\leq \int_\tau^t \kappa^{m-1} \|u - v\|_* K_1(\gamma) e^{-ls} ds \lim_{R \rightarrow \infty} R^{-a\sigma} \\
&= \kappa^{m-1} \|u - v\|_* K_1(\gamma) \frac{1}{l} (e^{-l\tau} - e^{-lt}) \lim_{R \rightarrow \infty} R^{-a\sigma}.
\end{aligned} \tag{2.307}$$

Before proceeding with the assessment of the integral related to the reaction term, we firstly show the convergence of the integrals involved in \mathbb{R}^N , for which we make $|x| \rightarrow \infty$. Indeed, we have:

$$\begin{aligned}
\int_{\mathbb{R}^N} |x|^\sigma \phi(x) dx &\leq \|\phi\|_* \int_{\mathbb{R}^N} |x|^\sigma dx \\
&= \lim_{R \rightarrow \infty} R^{-N-a\sigma} \int_{\mathbb{R}^N} |\phi(x)| dx \int_{\mathbb{R}^N} |x|^\sigma dx \\
&\sim \lim_{R \rightarrow \infty} R^{-N-a\sigma} e^{-ls} \int_{\mathbb{R}^N} |x|^{-2\gamma} dx \int_{\mathbb{R}^N} |x|^\sigma dx \\
&\sim e^{-ls} \frac{1}{\sigma + 1} \frac{1}{(-2\gamma + 1)} \lim_{R \rightarrow \infty} R^{-N-a\sigma} R^{-2\gamma+1} R^{\sigma+1}.
\end{aligned} \tag{2.308}$$

Therefore, we require γ to satisfy the following inequality to ensure the con-

vergence of the integral:

$$-N - a_\sigma + \sigma + 2 - 2\gamma < 0, \quad (2.309)$$

so that,

$$\gamma > \frac{-N - a_\sigma + \sigma + 2}{2}. \quad (2.310)$$

In order to have a single value of γ considering the expressions (2.302) and (2.310), we use the following condition:

$$\gamma > \max \left\{ \frac{-N - a_\sigma + \sigma + 2}{2}, -\frac{a_\sigma}{2}, 0 \right\}. \quad (2.311)$$

We are in a position, now, to determine the integral related to the reaction term, for which we make use of the definition for the Lipschitz constant provided in (2.224)

$$\begin{aligned} & \int_\tau^t \int_{\mathbb{R}^N} (u^p - v^p) \phi dx ds \leq K_l \int_\tau^t \|u - v\|_* \int_{\mathbb{R}^N} |x|^\sigma \phi ds \\ & \leq K_l \|u - v\|_* \frac{1}{\sigma + 1} \frac{1}{(-2\gamma + 1)} \lim_{R \rightarrow \infty} R^{-N - a_\sigma} R^{-2\gamma + 1} R^{\sigma + 1} \\ & \int_\tau^t e^{-ls} ds \\ & \leq K_l \|u - v\|_* \frac{1}{l} \frac{1}{\sigma + 1} \frac{1}{|-2\gamma + 1|} \lim_{R \rightarrow \infty} R^{-N - a_\sigma} R^{-2\gamma + 1} R^{\sigma + 1} \\ & (e^{-l\tau} - e^{-lt}) \end{aligned} \quad (2.312)$$

Finally, and after compilation of the assessments, we have:

$$\begin{aligned}
& \int_{\mathbb{R}^N} (u - v)(t) \phi(t) dx \\
& \leq \|u_0 - v_0\|_* e^{-l\tau} \lim_{R \rightarrow \infty} R^{-a\sigma} \\
& + \|u - v\|_* (e^{-l\tau} - e^{-lt}) \lim_{R \rightarrow \infty} R^{-a\sigma} \\
& + \kappa^{m-1} \|u - v\|_* K_1(\gamma) \frac{1}{l} (e^{-l\tau} - e^{-lt}) \lim_{R \rightarrow \infty} R^{-a\sigma} \\
& + K_l \|u - v\|_* \frac{1}{l} \frac{1}{\sigma + 1} \frac{1}{|-2\gamma + 1|} \lim_{R \rightarrow \infty} R^{-N-a\sigma} R^{-2\gamma+1} R^{\sigma+1} \\
& (e^{-l\tau} - e^{-lt}).
\end{aligned} \tag{2.313}$$

Note that:

$$\lim_{R \rightarrow \infty} R^{-a\sigma} = 0, \tag{2.314}$$

$$\lim_{R \rightarrow \infty} R^{-N-a\sigma} R^{-2\gamma+1} R^{\sigma+1} = 0. \tag{2.315}$$

Where γ is as per expression (2.311).

In terms of the time variable, If we consider that $\tau \rightarrow \infty$, we have:

$$\tau \rightarrow \infty < s < t, \tag{2.316}$$

Then:

$$s, t \rightarrow \infty. \tag{2.317}$$

Under this condition for the time variables, we have:

$$\int_{\mathbb{R}^N} (u - v)(t) \phi(t) dx \leq 0. \tag{2.318}$$

We obtain, then:

$$u(t) \leq v(t), t \rightarrow \infty. \tag{2.319}$$

Note that we have started in the assumption of $0 < u_0 \leq v_0$ and we have obtained that, when the time progresses to infinity, the same order condition is met as expressed by (2.319).

We have shown that given a solution with positive initial data, the solu-

tion is unique (see Theorem 2.6.3.1). Therefore, the solutions u and v keeps the monotone behaviour between them, without intersecting during the evolution. Thus, we can conclude that the ordered properties expressed at the initial conditions and at infinite time in (2.319), together with the uniqueness of solutions, permits to write that:

$$u(t) \leq v(t), \quad t > 0, \quad \text{in } Q_T \quad (2.320)$$

□

2.7 Finite Propagation

The finite propagation is a well known property of the PME equation [33] (see the discussion in Section 2.1). Our intention, now, is to show that finite propagation holds. This is remarkable for the case when the diffusion is relevant compared to reaction, nonetheless, it will appear, in a less extent, when reaction predominates over diffusion due to the introduction of the PME operator.

The following theorem is shown in [31] for a PME equation with a reaction term not a function of the independent variable $|x|$. Alternatively, in this work, it is shown for a more general reaction term depending on $|x|$. Additionally, we introduce certain improvements in the proof compared to that in [31] for a wider generality.

Theorem 2.7.1. *For the case when the diffusion is important, i.e.:*

$$m\sigma + 2(1 - \sigma)p + \sigma \geq 2, \quad (2.321)$$

with

$$u_0(x) \in \mathbb{L}^1(\mathbb{R}^N) \cap \mathbb{L}^\infty(\mathbb{R}^N), \quad (2.322)$$

and

$$u_0 \equiv 0, \quad (2.323)$$

in some ball $B(x_0, R)$. Then, any minimal solution to the problem P satisfies:

$u(x, t) \equiv 0$ for some ball $B\left(x_0, \frac{R}{2n}\right)$ for any $n \in \mathbb{N}^+$ and t between $0 < t < \tau$ (τ sufficiently small)

Proof. For simplicity, we make $x_0 = 0$ and $R = 1$. The proof of the theorem relies upon finding a local supersolution whose behaviour in the selected ball determines the local behaviour of the postulated minimal solution.

Firstly, we define the following change of variable to work with the pressure term:

$$v = \frac{m}{m-1} u^{m-1}. \quad (2.324)$$

So that:

$$u_t = \left(\frac{m-1}{m} \right)^{\frac{1}{m-1}} v^{\frac{2-m}{m-1}} v_t, \quad (2.325)$$

$$\Delta u^m = \left(\frac{m-1}{m} \right)^{\frac{1}{m-1}} \left(v^{\frac{2-m}{m-1}} |\nabla v|^2 + v^{\frac{1}{m-1}} \Delta v \right). \quad (2.326)$$

Upon substitution, the problem P is, then, transformed into:

$$v_t = (m-1)v\Delta v + |\nabla v|^2 + \mu|x|^\sigma v^\delta, \quad (2.327)$$

$$\delta = \frac{p+m-2}{m-1}, \quad (2.328)$$

$$\mu = m \left(\frac{m-1}{m} \right)^\delta.$$

When $v \rightarrow 0$, the laplacian term in equation (2.327) vanishes leading to a first order spatial equation:

$$v_t \sim |\nabla v|^2 + \mu|x|^\sigma v^\delta. \quad (2.329)$$

This equation is of the first order type that propagates along characteristics. Therefore, in the search of potential solutions, we will search for linear distributions involving the time and spatial variables, i.e. solutions of the form:

$$v(x, t) = g(x + ct), \quad (2.330)$$

where g is a suitable function and c is the propagation speed along characteristics.

The intention now is to find a suitable maximal solution for the equation (2.327) in the assumption that diffusion is relevant, solutions will not blow-up and will preserve the bound condition given at the initial data. A formal proof of this statement is out of the scope of this section, nonetheless, the bound condition of the PME operator, when starting with bound initial data, has been shown in Lemma 3.3 of [33].

we consider the following function in the search of a maximal solution:

$$w(x, t) = a \left(ct + r - \frac{1}{n} \right)_+, \quad (2.331)$$

$$r = |x|; \quad n \in \mathbb{N}.$$

Both a and $c > 0$ are constants to be determined. In particular, given $0 \leq \tau \leq 1$, we can impose:

$$c\tau = \frac{1}{2n}, \quad (2.332)$$

Where c shall be determined.

Under this condition, we have:

$$w(x, t) \equiv 0 \quad \text{for } r < \frac{1}{2n} \quad \text{and } 0 \leq t \leq \tau. \quad (2.333)$$

It is clear that any solution to the equation (2.327) is bounded for

$$0 \leq t \leq \tau, \quad (2.334)$$

because u_0 is bounded according to the theorem condition

$$u_0(x) \in \mathbb{L}^1(\mathbb{R}^{\mathbb{N}}) \cap \mathbb{L}^\infty(\mathbb{R}^{\mathbb{N}}), \quad (2.335)$$

and the diffusion is relevant compared to reaction. Then, we have:

$$v(x, t) \leq K \quad \text{for } x \in \mathbb{R}^{\mathbb{N}} \quad 0 \leq t \leq \tau \quad \text{and } K(\sigma, p, \|u_0\|_\infty). \quad (2.336)$$

Our intention is to make $w(x, t)$ as a maximal solution:

$$w(x, t) \geq v(x, t), \quad (2.337)$$

$$a \left(ct + r - \frac{1}{n} \right)_+ \geq K. \quad (2.338)$$

We can select any $r > \frac{1}{n}$, for example we establish:

$$r = \frac{2}{n}. \quad (2.339)$$

Thus, for $t = 0$ we have:

$$a \left(\frac{2}{n} - \frac{1}{n} \right)_+ \geq K, \quad (2.340)$$

$$a \geq nK. \quad (2.341)$$

We have built a supersolution, such that:

$$w(x, t) \geq v(x, t), \quad (2.342)$$

in $r = \frac{2}{n}$ and $0 \leq t \leq \tau$. Once we have established a suitable condition for the constant a , the next intention is to precise another criteria for c . The value of c shall be chosen in such a way that $w(x, t)$ is a supersolution not only for:

$$r = \frac{2}{n}, \quad (2.343)$$

but for the range:

$$0 < r < \frac{2}{n}, \quad (2.344)$$

and in the time interval:

$$0 \leq t \leq \tau. \quad (2.345)$$

$w(x, t)$ is a supersolution if it satisfies:

$$w_t \geq (m - 1)w\Delta w + |\nabla w|^2 + \mu|x|^\sigma w^\delta, \quad (2.346)$$

and considering that:

$$w_t = ac; \quad w_r = a; \quad w_{rr} = 0, \quad (2.347)$$

the following value for c is obtained:

$$c \geq a + \mu \left(\frac{2}{n} \right)^\sigma a^{\delta-1} \left(c\tau + \frac{1}{n} \right)^\delta. \quad (2.348)$$

For the values of a and c derived in expressions (2.341) and (2.348) respectively, the function $w(x, t)$ is a supersolution locally:

$$w(x, t) \geq u(x, t), \quad (2.349)$$

for

$$0 < |x| < \frac{2}{n}, \quad (2.350)$$

and

$$0 \leq t \leq \tau. \quad (2.351)$$

This inequality (2.349) permits to conclude on the proof of the theorem, as any maximal local solution satisfies the null criteria in a region of the selected ball. By direct argument, any minimal solution $u(x, t)$ satisfies the theorem postulations.

□

3 Conclusions and future lines of research

The main objectives outlined in the *Introduction* section of this thesis have been fulfilled in accordance with the development and resolution of each of the problems described in Sections 1.1 and 2.1. We remark that our top level aim, consisting on following a process to solve a problem coming from the specialty areas in biomedical and aerospace engineering, has been achieved. Each selected problematic has been modelled making use of the physical laws. Afterwards, each of the problems has been solved thanks to relevant advances in Partial Differential Equations. Once each problem has been solved, the different parameters involved in the solutions have been determined by testing activities, particularly related to fire prevention in aircrafts fuel tanks and fire extinguishing in engine nacelles (Annex II). The results obtained, after the mathematical analysis, have been shown to be accurate enough to support the physics concept phase related to any design process in the engineering fields scoping this thesis, i.e. fire prevention and extinguishing in aircrafts and biological predator-prey (invasive-invaded) models.

We remark that each of the problems solved are of reaction and diffusion type. The diffusion has been considered as the classical linear for the problem in Section 1.1 and non-linear for the problem in Section 2.1. Additionally and in both cases, the reaction considered is of non-lipschitz which brought some novel discussions to ensure the existence and uniqueness of solutions for each diffusion operator. For both cases, solutions have been obtained and, as discussed, such solutions have been deemed as precise due to the mathematical treatment related to the searching of exact solutions and to the real engineering applications in which such solutions have been applied (Annex II).

The mathematical work developed in this thesis has been in line with the current advances in Partial Differential Equations. Beyond this, we can stress some future researching lines: In relation to the first problem described in Section 1.1, the considered diffusion has been as the classical linear obtained after the application of the basic Fick law (Section 1.1). This fact is an approximation to a well-proven diffusion, as most of the physical and engineering models formulated with diffusion principles are based on the Fick law. Nonetheless, further aspects about diffusion can be postu-

lated by the introduction of a non-linear concept, for instance of the PME type. This kind of diffusion would allow us to explore the possibility of having a diffusive front with finite propagating speed. In such case, the problem described in 1.1 would adopt the following form:

$$\begin{aligned} u_t &= \delta \Delta u^d + c \cdot \nabla u + v^n, \\ v_t &= \epsilon \Delta v^d + c \cdot \nabla v - u^m, \\ n, m &\in (0, 1), \\ d &> 1, \end{aligned} \tag{3.1}$$

$$u_0(x), v_0(x) \in \mathbb{L}_{loc}^1(\mathbb{R}^N) \cap \mathbb{L}^\infty(\mathbb{R}^N).$$

And for the problem solved making use of a TW approach, the formulation with a PME would lead to:

$$\begin{aligned} u_t &= \delta \Delta u^d + c \cdot \nabla u - v^n(u - d), \\ v_t &= \epsilon \Delta v^d + c \cdot \nabla v - u^m v, \\ n, m &\in (0, 1), \\ d &> 1, \end{aligned} \tag{3.2}$$

$$u_0(x), v_0(x) \in \mathbb{L}_{loc}^1(\mathbb{R}^N) \cap \mathbb{L}^\infty(\mathbb{R}^N).$$

Additionally, further related problems can be formulated in light of a high order diffusion. High order diffusion involves high order spatial derivatives, so that the operator adopts the following form:

$$u_t = -(-\Delta^m)u. \tag{3.3}$$

where $m \in \mathbb{N}$ represents the derivative index. In case of $m = 1$, we recover the classical heat equation. In case of $m = 2$, the involved derivatives are of the fourth order.

High order diffusion appears in areas such as lubrication theory, flame

propagation, phase transition and bistable systems [47].

For our case, we can consider that the diffusion involves spatial derivatives of fourth order:

$$\begin{aligned} u_t &= -\delta\Delta^2u + c \cdot \nabla u + v^n, \\ v_t &= -\epsilon\Delta^2v + c \cdot \nabla v - u^m, \\ n, m &\in (0, 1), \end{aligned} \tag{3.4}$$

$$u_0(x), v_0(x) \in \mathbb{L}_{loc}^1(\mathbb{R}^N) \cap \mathbb{L}^\infty(\mathbb{R}^N).$$

And for the problem solved with TW solutions:

$$\begin{aligned} u_t &= -\delta\Delta^2u + c \cdot \nabla u - v^n(u - d), \\ v_t &= -\epsilon\Delta^2v + c \cdot \nabla v - u^m v, \\ n, m &\in (0, 1), \end{aligned} \tag{3.5}$$

$$u_0(x), v_0(x) \in \mathbb{L}_{loc}^1(\mathbb{R}^N) \cap \mathbb{L}^\infty(\mathbb{R}^N).$$

where

$$\Delta^2 = \frac{\partial^4}{\partial x^4}. \tag{3.6}$$

The minus sign in the bi-laplacian term ($-\delta\Delta^2$ and $-\epsilon\Delta^2$) is set to account for a regular asymptotic stable equation.

For the case of dealing with the high order operator, we would like to introduce some relevant aspects in the spirit of providing a background to guide future works:

The Fisher-Kolmogorov equation was proposed to study the interaction of different populations in a biological environment. Initially, the Fisher-Kolmogorov equation was of a second order type with classical diffusion, and the regularity of the gaussian kernel was intended to provide accurate model results. The equation is of the form:

$$u_t = \Delta u + u - u^3. \tag{3.7}$$

The predictions resulting from the Fisher-Kolmogorov equation have been questioned. In particular, physicians have observed an onset of instabilities near degenerate points given by the Fisher-Kolmogorov equation [43]. This fact led to a reformulation ending in the extended Fisher Kolmogorov equation (3.8). In addition, other authors proposed the Extended Fisher-Kolmogorov equation to model the behaviour of bi-stable systems, which can be defined as those systems with only two uniform states and a solution travelling between stable solutions, either forming a heteroclinic or homoclinic orbit [45]. Peletier and Troy [44], on one hand, and Bonheure [46] in the other hand, showed the existence of oscillatory spatial patterns for the Extended Fisher-Kolmogorov equation. Additionally, they exhibited examples of oscillating heteroclinic (the authors also called it kinks) and homoclinic orbits (pulses) in the spatial domain. In any of the examples mentioned, the instabilities were found to be permanent oscillations, leading to think that there shall be evolution flows hidden by the regularity of the second order diffusion. The studied problem was of the form:

$$u_t = -\gamma \Delta^2 u + \Delta u + u - u^3, \quad (3.8)$$

where

$$\gamma \ll 1. \quad (3.9)$$

In the classical sense, the Extended Fisher-Kolmogorov equation requires solutions to have continuous derivatives up to the fourth order. One can think, very preliminary, that oscillation functions (such as sine, cosine or a combination of both) may have potential to constitute solutions that will explain the permanent instabilities that the Extended Fisher-Kolmogorov equation aims to characterize. On top of the work by Peletier and Troy [44], Rottschäfer and Doelman [43] showed the nature of the oscillations making use of a development in the exponential bundles of solutions.

In relation to the PME problem discussed in Section 2.1, a future researching line would consist on adding a convective term, so that the problem would adopt the following form:

$$u_t = \Delta u^m + c \cdot \nabla u + |x|^\sigma u^p, \quad (3.10)$$

where:

$$m > 1, \sigma > 0, p < 1, c \in \mathbb{R}^N.$$

The fact of adding a convective term would not affect, a priori, the existence and uniqueness of solutions already discussed in Section 2.6. Nonetheless, it would modify substantially the structure of the solutions obtained in Section 2.6.

Another aspect for future discussions would consist on adding a higher order-PME diffusion of the form:

$$u_t = -\Delta^2 u^m + |x|^\sigma u^p, \quad (3.11)$$

where:

$$m > 1, \sigma > 0, p < 1.$$

In this case, we shall assess the finite propagation features in combination with the natural oscillations brought by the bi-laplacian term in the proximity of the null solution. We postulate that finite propagation features will be kept and that the speed of propagation in the support (in the sense of Figure 2.3 where the propagating support shifts the solution from null to positivity) would be lower as a positivity principle cannot hold when dealing with high order operators.

4 Some Useful Definitions

The following terms are deemed as useful for the reader:

Convection: The convection refers to the general motion of a fluid. It encompasses the diffusion and the forced flow due to external agents such as media flow, boundary layer flow or buoyant flow.

Diffusion: In fluid motion, the diffusion refers to the random flow due to the differences of concentrations in the media. The flowing particles go from the zones with higher concentration to the zones with lower concentration.

Finite Speed of Propagation: This definition is based on the information provided in Chapter 1.2 of [33]. The finite propagation refers to the speed of the moving front constituting the Porous Medium Equation. The finite propagation supports the physical soundness of the Porous Medium Equation to model diffusion or heat propagation. The property of finite propagation implies the appearance of a free boundary, that separates the regions where the solution is positive, from the empty regions, where $u = 0$

Finite time blow-up: This definition is based on the information in [40]. When a solution to an initial value problem reaches infinity in finite time, the solution is said to blow up. That is, if $P(t)$ is a solution to the problem:

$$\frac{dP}{dt} = f(t, P), \quad (4.1)$$

with initial condition:

$$P(t_0) = P_0. \quad (4.2)$$

then, the solution blows-up in finite time if:

$$\lim_{t \rightarrow T^-} P(t) = +\infty. \quad (4.3)$$

In Latin languages, the term blow-up is usually referred as explosion.

Kernel: The Kernel of a partial differential equation refers to the fundamental solution given in the integration domain. The Kernel permits to study the main features of the under-study equation.

Lipschitz function: The Lipschitz condition represents the regularity

of a function. It is relevant when studying the uniqueness of differential equations, that in general, can be shown by calling to the Lipschitz condition.

Porous Medium Equation: The PME is a way to model diffusion when speed of propagation is expected in our area of study. It is usually referred as the Darcy's law, and was firstly derived for flows in porous media.

We can derive the PME by departing from the flow of gas in a porous medium:

$$\rho_t + \nabla \cdot (\rho v) = 0, \quad (4.4)$$

where ρ is the gas density and v is the flow speed expressed as:

$$v = -\nabla p, \quad (4.5)$$

where p reflects the pressure of the gas.

If we consider the isentropic evolution to relate the pressure and density of a gas, we have:

$$p = p_0 \rho^\gamma, \quad (4.6)$$

where γ is the isotropic coefficient.

Coming back to equation (4.4):

$$\rho_t = \nabla \cdot (\rho \nabla p) = \nabla \cdot (\rho \nabla (p_0 \rho^\gamma)) = c \Delta \rho^{\gamma+1}, \quad (4.7)$$

$$\rho_t = c \Delta \rho^{\gamma+1}.$$

Considering an isothermal expansion:

$$\gamma = 1, \quad (4.8)$$

then, we have:

$$\rho_t = \Delta \rho^m, \quad (4.9)$$

for $m = 2$.

Self-similar Profile: This definition is based on the information provided in the introduction of [41]. Selfsimilarity results when the symmetry of a physical problem leads to a reduction in the number of the independent variables. In this way a considerable simplification is achieved, that frequently allows the analytical treatment of the problem. This simplification

usually transforms a partial differential problem into an ordinary differential one. The self-similar behavior appears in the intermediate asymptotics of phenomena, when certain details of the initial or boundary conditions are no longer relevant, so that the corresponding parameters can be ignored.

Travelling Wave: This definition is based on the information provided in Chapter 2 of [42]. A travelling wave is a wave that advances in a particular direction, with the addition of retaining a fixed shape. Moreover, a travelling wave is associated to having a constant velocity throughout its course of propagation. Such waves are observed in many areas of science, like in combustion, which may occur as a result of a chemical reaction. In mathematical biology, the impulses that are apparent in nerve fibres are represented as travelling waves.

References

- [1] Magee, C. and Weck, O. (2004). *Complex system classification*. International Council On System Engineering (INCOSE). San Diego (California).
- [2] Volpert, V. and Petrovskii, S. (2009). Reaction-diffusion waves in biology. *Physics of life*, 6, 267-310.
- [3] Petrovskii, S.V and Li, B. L. (2006). *Exactly solvable models of biological invasion*. Champman Hall/CRC Press.
- [4] Petrovskii, S. and Shigesada, N. (2001). Some exact solutions for a generalized Fisher Equation related to the problem of biological invasion. *Mathematical Biosciences*, 172, 73-94.
- [5] Mooney, H. and Williamson, M. (2010). *The problem of Biological Invasions*. Oxford Scholarship Online.
- [6] Fisher, R.A. (1937). The wave of advance of advantageous gene. *Annals of Eugenics*.
- [7] Kolmogorov; Pretrovski and Piskunov (1988). Study of the diffusion equation with growth of the quantity of matter and its application to a biological problem. *Dynamics of curve fronts*. 105-130.
- [8] Skellam, J.G. (1951). Random dispersals in theoretical populations. *Biometrika*, 38, 196-218.
- [9] Martin R. Evans (2013). *Speed Selection in coupled Fisher Waves*. Congress at the School of Physics and Astronomy. University of Edinburgh.

- [10] Ghadirian, E.; Brown, J. and Wahiduzzaman, S. (2019). A quasy-steady diffusion based model for design and analysis of fuel tank evaporate emissions. *SAE Technical Paper ref. 2019-01-0947*.
- [11] National Transportation Safety Board (1996). *In-flight Breakup over the Atlantic Ocean Trans World Airlines Flight 800 , Boeing 747-141. Ref. N93119*. Washington D.C.
- [12] Federal Aviation Administration (2008). *Advisory Circular Ref. 25.981-1C. Fuel Tank Ignition Source Prevention Guidelines*. Washington D.C.
- [13] SAE International (2012). *Aircraft Fuel Tank Inerting Systems. SAE ref ARP6078*. United States of America.
- [14] Faeth, G. (1997). *Combustion Fluid Mechanics: Tools and Methods*. The National Academies Press. University of Michigan.
- [15] Tao, T. (2011). *An introduction to Measure Theory*. American Mathematical Society.
- [16] Barenblatt (1996). *Scaling, self-similarity, and intermediate asymptotics*. Cambridge Texts in Applied Mathematics.
- [17] European Aviation Safety Agency (2008). *Fuel Tank Flammability Reduction. Notice of Proposed Amendment, No 2008-19*. Cologne.
- [18] Federal Aviation Administration (1999). *Mass loading effects on fuel vapor concentration in an aircraft fuel tank ullage. Summer SM. Atlantic (NJ): . Report No.: DOT/FAA/AR-TN99/65.*. United States of America.
- [19] Cai Yan (2015). Experimental study of an aircraft fuel tank inerting system. *Chinese Journal of Aeronautics*. China

- [20] Bertsch; Gurtin; Hilhorst and Peletier (1984). On interacting Populations that disperse to avoid crowding: Preservation of Segregation. *University of Wisconsin - Madison Mathematics Research Center. Technical Summary Report N^o 2767.*
- [21] Lynn; Loomis and Shlomost (1990). *Advanced Calculus.* Jones and Bartlett Publishers.
- [22] Kolmogorov, A. N.; Petrovskii, I.G. and Piskunov, N.S. (1937). Study of the diffusion equation with growth of the quantity of matter and its application to a biological problem. *Byull. Moskov. Gos. Univ., Sect. A, 1.*
- [23] Evans, L. (2010). *Partial Differential Equations.* Advanced Mathematical Society. United States of America.
- [24] Wenxiong, L. (1992). Singular Solutions for a convection diffusion equation with absorption. *Journal of Mathematical Analysis and Applications, 163, 200-219.*
- [25] Brezis, H. and Friedman, A. (1983). Non-linear parabolic equations involving measures as initial conditions. *Journal of Mathematics Pures and Applications, 62, 73-97.*
- [26] Pao, C. (2012). *Nonlinear Parabolic and Elliptic Equations.* Springer Science+Business Media. North Carolina, United States of America.
- [27] Aguirre, J. and Escobedo, M. (1993). On the blow-up of solutions of a convective reaction diffusion equation. *Proceeding of the Royal Society of Edinburg, 123A, 433-460.*
- [28] Aguirre, J. and Escobedo, M. (1987). A Cauchy problem for $u_t - \Delta u = u^p$ with $0 < p < 1$. Asymptotic behaviour of solu-

- tions. *Annales Faculté des Sciences de Toulouse. Vol VIII*, number 2.
- [29] Escobedo, M. and Herrero, M. (1991). A uniqueness result for a semilinear reaction-diffusion system. *Proceedings of the American Mathematical Society. Volume 112*, number 1.
- [30] Jones, B.F. (1963). *Singular integrals and parabolic equations*. American Mathematical Society. United States of America.
- [31] Arturo, P. and Vázquez, J.L. (1990). The balance between strong reaction and slow diffusion. *Communications in Partial Differential Equations, 15*, 159-183.
- [32] Arturo, P. and Vázquez, J.L. (1991). Travelling Waves and Finite Propagation in a Reaction-Diffusion Equation. *Journal of Differential Equations, 93*, 19-61.
- [33] Vázquez, J.L. (2006). *The Porous Medium Equation, mathematical theory*. Oxford Mathematical Monographs. Oxford.
- [34] Bénilan, Crandall and Pierre (1984). Solutions of the porous medium equation in \mathbb{R}^N under optimal conditions on initial values. *Indiana Univ Math Journal, 33*, 51-87.
- [35] Brézis and Crandall (1979). Uniqueness of solution of the initial value problem for $u_t - \Delta\phi(u) = 0$. *Journal Mathematics Pures and Applied, 58*, 153-163.
- [36] De Pablo, A. (1989). *Doctoral Thesis. Estudio de una ecuación de reacción - difusión* Universidad Autónoma de Madrid.
- [37] Ferreira, R.; de Pablo, A.; Pérez-Llanos, M. and Rossi, J.D. (2012). Critical exponents for a semilinear parabolic equation with variable

reaction. *Proceeding of the Royal society of Edinburgh*, 142 A.

- [38] Barenblatt and Zeldovich (1957). On stability of flame propagation. . *Prikl Mat Mekh*, 21, 856-9 (This article is written in russian).
- [39] Galaktionov, V.A. and Vázquez, J.L. (2002). *Discrete and continuous dynamical systems*, 8, 399-434.
- [40] Campbel, D. and Williams, J. (2003). Exploring finite time Blow-up. *Pi Mu Epsilon Journal Vol. 11, No. 8*, 423-428.
- [41] Gratton, J. and Canula, V.M. (1991). *Similarity and Self Similarity in Fluid Dynamics*. NASA. Institute for Space Studies. New York. United States of America.
- [42] Achouri, R. (2016). *Travelling Waves solutions. A dissertation in the University of Manchester*. Manchester. UK.
- [43] Rottschäfer, V. and Doelman, A. (1998). On the transition from the Ginzburg-Landau equation to the extended Fisher-Kolmogorov equation. *Physica D* 118. 261 - 292.
- [44] Peletier, L. and Troy W. (2001). Spatial Patterns. Higher order models in Physics and Mechanics. *Progress in non linear differential equations and their applications. Volume 45. Université Pierre et Maire Curie*.
- [45] Dee, G. and Van Sarloos, V. (1988). Bistable systems with propagating fronts leading to pattern formation. *Physical Review Letter* 60.
- [46] Bonheure, D. *Heteroclinics Orbits for some classes of second and fourth order differential equations. Handbook of differential equations*. Université Libre de Bruxelles.

- [47] Hocking, L.M., Stewartson, K. and Stuart, J.T. (1972). A nonlinear instability burst in plane parallel flow. *Journal of Fluid Mechanics* 51, 702-735.

Annex I

This annex contains the Matlab codes (ODE45 Modulus) used to determine the solutions represented from Figure 1.2 to Figure 1.7:

```

function CRD

    xinit = linspace (0, 60, 10000);
    options = bvpset('RelTol', 10^(-6), 'Abstol', 10^(-6), 'Nmax',
10000, 'Stats', 'off');
    solinit = bvpinit (xinit, @fguess);
    sol = bvp4c(@dEqs, @res, solinit, options);
    f = deval(sol, xinit);
    plot(xinit,f(1,:), xinit,f(3,:), xinit,f(5,:), xinit,f(7,:))
    xlim([1 1.5])
    ylim([1.98 2])
    xlabel('xi') % Etiqueta el eje horizontal
    ylabel('f_1, f_2, f_1m, f_2m') % Etiqueta el eje vertical
    legend('f_1=u', 'f_2=v', 'f_1m', 'f_2m') % Pune una leyenda

```

```

function F = dEqs( x, f )
%Differential equationsco

```

```

F = [f(2); -4*f(2)-(2-f(1))*f(3)^(0.2); f(4); -
4*f(4)+f(3)*f(1)^(0.9); f(6); -4*f(6)-(2-f(5))*f(7); f(8); -
4*f(8)+f(7)*2^(0.9)];

```

```

function r = res( fa, fb )
r = [fa(1)-1; fa(3)-1; fb(1)-2; fb(3); fa(5)-1; fa(7)-1; fb(5)-2;
fb(7)];

```

```

function finit = fguess (x)

```

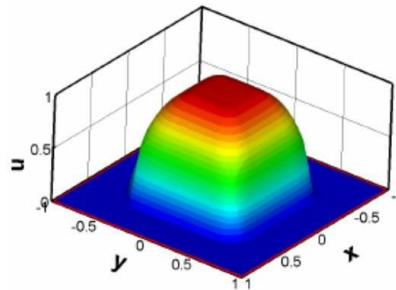
```

finit = [heaviside(-x);0; heaviside(-x); 0; heaviside(-x);0;
heaviside(-x); 0]

```

Annex II

This annex contains the industrial applications of the solutions in this thesis with the collaboration of Airbus Group.



Doctoral thesis applications to industrial problems

Doctoral thesis title: Non-linear reaction and diffusion models in partial differential equations, with application to aerospace and biomedical technologies

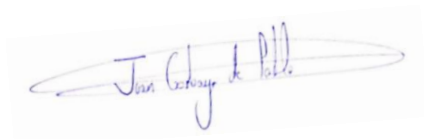
Aplicaciones industriales de la tesis doctoral bajo título “Non-linear reaction and diffusion models in partial differential equations, with application to aerospace and biomedical technologies”

Memoria presentada para optar a la mención de doctorado industrial

Autor/Author: José Luis Díaz Palencia



Company tutor/ Tutor en la empresa: Juan Garbayo de Pablo



"The earliest models of products had the same form as the larger thing to be created". Eckert and Stacey. MATHEMATICAL modelling.

Scope of this memory

The use of mathematical models to optimize the design in engineering for, both products and processes, has been one of the most active motivation for advances in mathematics.

The engineering models for product design rely on the basis of the physical laws [12]. Any model, aiming to describe the sort of reality we pretend to characterize, shall be based on the universal laws of physics. This fact provides the confident for a solid problem understanding, since its formulation to the resolution path.

Even when the physical laws are universal, any set of equations, describing an engineering design process or product; shall contain a certain number of parameters. The parameters are the key for applying the abstract vision of a problem to a particular situation we aim to understand.

The process followed in this memory consists on modelling within the scope of the Partial Differential Equation (PDE) theory. The resulting PDEs are based on the physics and the engineering based experience. The set of equations is solved analytically making use of advanced PDE techniques originally developed for the thesis [2]. Finally, the model parameters are calibrated with data coming from real processes to derive the set of solutions of analytical interest that involves the physics behind.

This memory is formed of two different parts in line with the results in [2]. The first part is devoted to the calibration of the reaction-diffusion coupled system (Section 1 in [2]) for an application related with the Aircraft inerting system. The second part is focused on calibrating the Porous Medium Equation model (Section 2 in [2]) for modelling an aircraft engine fire extinguishing process.

Index

PART I. The Inerting Model through a coupled reaction-diffusion system

I. 1. Background	6
I. 2. Introduction	9
I. 3. Justification.....	10
I. 4. Model parameters calibration with flight test data.....	13
I. 5. Compatibility conditions.	18
I. 6. Solutions calibration.....	19
I. 7. Solutions in the Travelling Waves domain	21

PART II: The Fire Extinguishing model through a Porous Medium Equation (PME)

II.1. Background.....	26
II. 2. Justification.....	28
II. 3. A400M Engine cowl description	31
II. 4. Flight test data.....	37
II.5. Model calibration	39
III. Conclusion.....	48
References.....	50
ANNEX I.....	51

I. 1. Background

On July 17, 1996, the Flight 800 of the Trans World Airlines (TWA) carried out by a Boeing 747-131, crashed in the Atlantic Ocean when approaching New York, having departure from Paris. The accident involved a high number of passenger's deaths and injuries.

The US National Transportation Safety Board determined that the most probable cause of the TWA flight 800 accident was an explosion in the Center Wing Tank that was empty of fuel, but full of fuel vapors in combination with air and a potential instant spark. The fuel vapor/air mixture could ignite provided enough ignition energy is given either by external or internal heating components or internal sparks generated by in-tank components.



Figure 1a. Fuselage status after the accident and accident computational simulation. Both pictures are extracted from [11].

The Fuel Centre Wing Tank on a Boeing 747-131 is located aft of the forward cargo compartment and forward of the main landing gear bay in the lower fuselage. The Centre Wing Tank is below the main cabin floor and the dimensions are about 6,5 m wide and 6 m long and the height varies from about 1,37m to 1,82 m (see the next figure extracted from [1]).

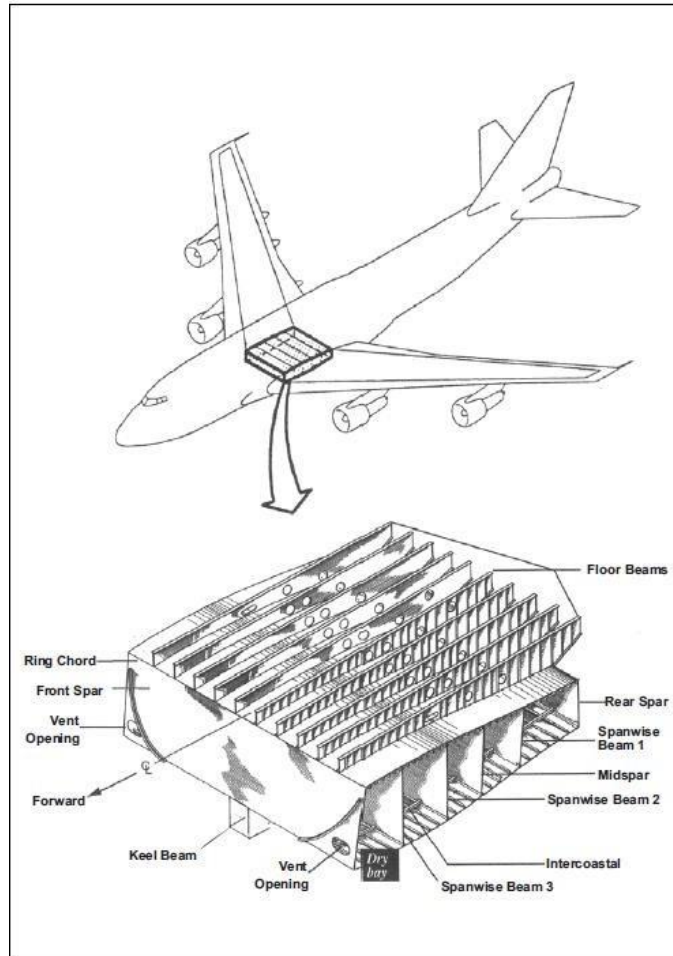


Figure 1b. Cross-section of the Boeing 747-100 Wing center section

During the accident investigation [1], it was concluded that one of the most probable root causes, explaining the accident, was related with the proximity of the heat generated by the air conditioning packs to the Centre Wing Tank. In the following figure, the relative position of both components is provided:

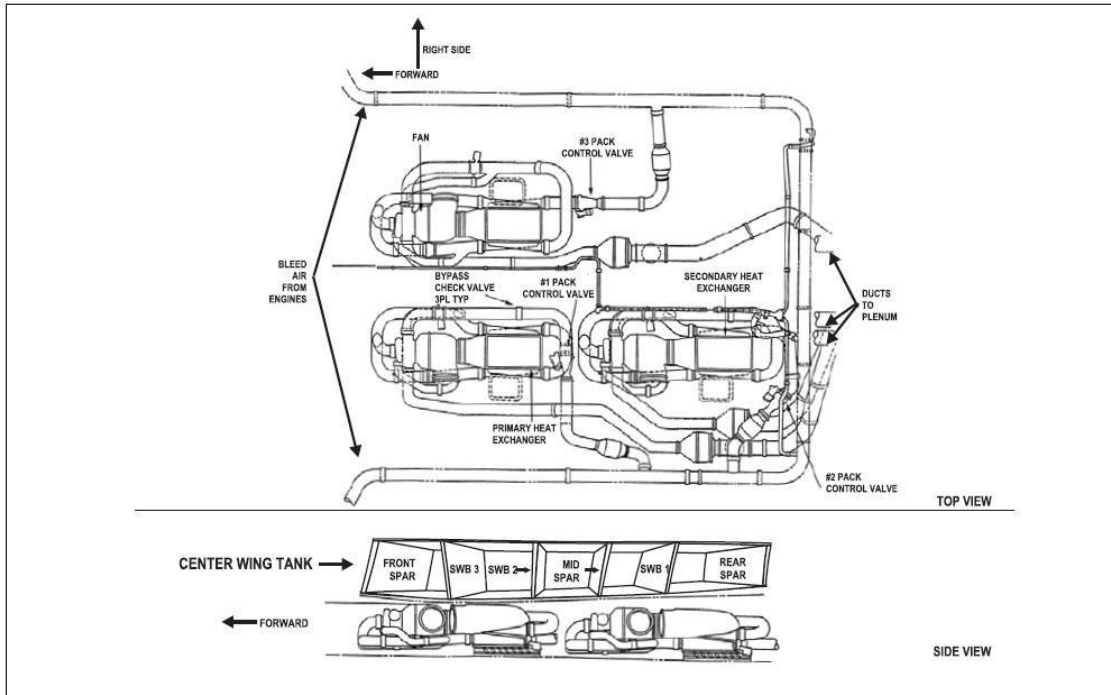


Figure 2. Top and side view of the Centre Wing Tank and Air Conditioning packs.

I. 2. Introduction

As a result of the investigation on the TWA 800 flight accident [1], several design solutions were defined to avoid a similar event. One of these solutions, precluded in [11] and referred as inerting system, was envisaged to provide means for removing the oxygen presented in the Centre Tank ullage.

The Inerting System is installed to reduce the probability of Fuel Tank fires and explosions should any heat or spark sources are given. In addition, and in military applications, the Inerting System is used to reduce the probability of explosions should the aircraft suffers battle damage (such as impact/structural penetration from bullets, or other high energy shrapnel).

The inert condition, within the considered tank, is achieved by using a chemically unreactive gas, i.e. nitrogen, to reduce the oxygen concentration. As a piece of example, the oxygen level of an atmosphere considered inert for military applications is <9% by volume, while for civil applications; the maximum level of oxygen concentration is reduced to <7% by volume.

The component within the Inerting system, that facilitates the separation of the oxygen and nitrogen, is a component known as Air Separation Module (ASM). An ASM consists of a canister that houses hollow semi-permeable fibers sealed in place at each end with an epoxy. The ASM contains an inlet chamber, nitrogen outlet chamber, and an oxygen exhaust chamber. Pressurized air is ported from the inlet duct to the inlet chamber where it is directed into thousands of very small diameter hollow fibres. The inlet air is, then, separated by the fiber membrane; the oxygen passes through the fiber wall radially, and is exhausted outboard. The nitrogen flow continues through the fiber membranes axially and exists the ASM (see the following figure) toward a pipe network ending in the fuel tank.

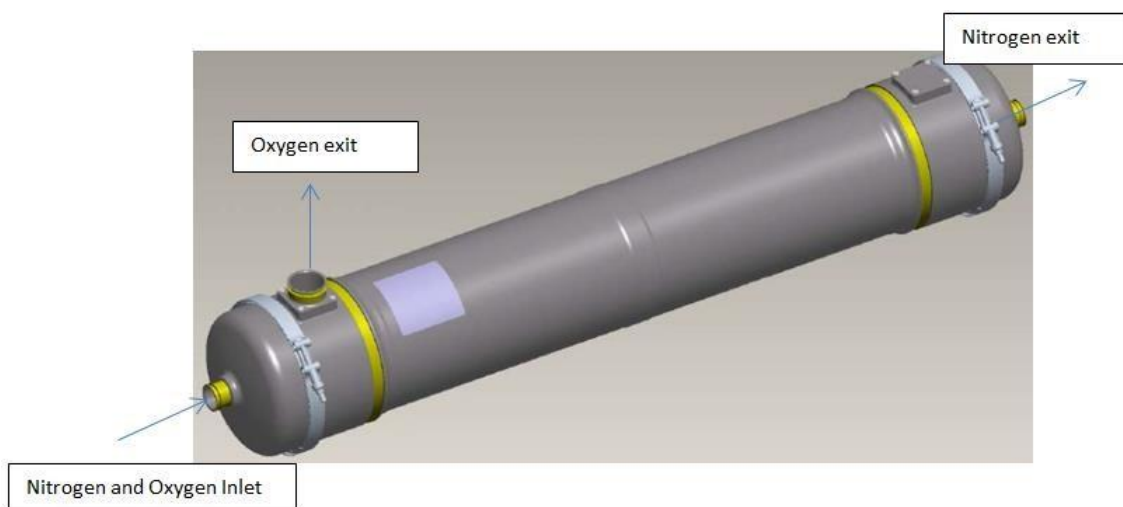


Figure 3. Air Separation Module representation.

I. 3. Justification

This document provides a new baseline modelization exercise, based on an original work [2], aiming to get further views, simplification and accuracy on the tank inerting process.

The phenomena under study is related with the interaction between substances, i.e. the Oxygen and the Nitrogen, so that, an inert gas ullage is obtained to avoid tank fires and explosions.

A simple model to determine the oxygen quantity in the fuel tank, when subjected to variable flight conditions and system performance schedules is provided in [1]. The model is one-dimensional and based on a discrete and algebraic mass balance for each time step considering the oxygen mass quantity going in and out the tank and the changing pressure and temperature in the ullage due to the variable flight conditions:

$$m_{O_2}(t) = m_{O_2}(t-1) + \dot{m}_i \cdot IGOF - \dot{m}_i \cdot UGOF(t-1) - (\Delta\rho \cdot V_{tank}) \cdot UGOF(t-1) + (\Delta\rho \cdot V_{tank}) \cdot 0.21. \quad (Eq. 1)$$

Where:

$UGOF(t-1)$ is the fraction of oxygen in the ullage gas. It is calculated by dividing the mass of oxygen in the tank at $(t-1)$ by the mass of gas in the tank ullage:

$$UGOF(t-1) = \frac{m_{O_2}(t-1)}{m_{tank}(t-1)} \quad (Eq. 2)$$

In addition:

$m_{O_2}(t)$ = Mass of oxygen in the tank at time t .

\dot{m}_i = Mass flow rate of inerting gas (in terms of t).

IGOF = Fraction of Oxygen in inerting gas.

$\Delta\rho$ = Change in ullage density due to altitude change.

V_{tank} = Volume of tank ullage.

The model in *(Eq. 1)* considers the oxygen mass per unit of time. Nonetheless, it disregards the substances diffusion process, which constitutes an important feature for a more realistic picture of the gas interacting phenomenon.

In order to account for the mass diffusion, we consider the classical Fickian approximation. The fact of considering diffusion leads to deal the problem using differential equation techniques. This means that the algebraic equation in *(Eq. 1)* is replaced by a differential continuum problem, in which we pretend to determine each substance concentration. In [2], the

following model has been obtained to simulate the interacting behavior of nitrogen (u) and oxygen (v):

$$\begin{aligned} u_t &= \delta \Delta u + c \cdot \nabla u + v^n \\ v_t &= \varepsilon \Delta v + c \cdot \nabla v - u^m \end{aligned} \quad (\text{Eq. 3})$$

$$n, m \in (0,1)$$

Where:

u = Nitrogen concentration per unit of volume, expressed between (0,1).

v = Oxygen concentration per unit of volume, expressed between (0,1).

And where δ and ε represent the diffusion coefficients between the interacting substances. They can be considered as constants, and can be determined according to the data provided in [3]:

$$\delta = \varepsilon = 0,219 \text{ cm}^2/\text{s} \text{ at } 20^\circ\text{C}$$

The diffusion coefficient varies with the gas temperature. During flight the tank ullage can be considered to have a similar temperature with the Outside Air Temperature (OAT). This temperature value has not been provided in [1], nonetheless, we consider the following data obtained from an A400M flight, and considering similar tank dimensions compared to that in Figure 1b), in which the OAT reaches a value of -7°C .

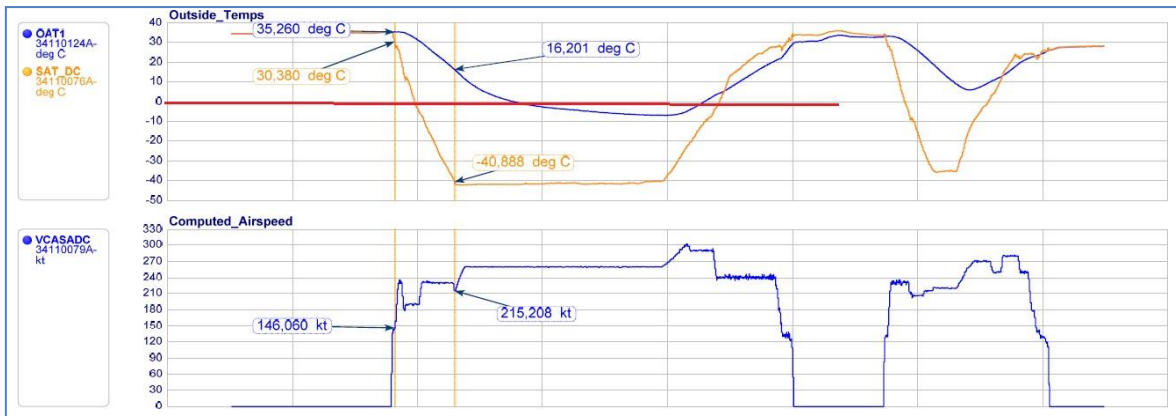


Figure 4. The Outside Air Temperature (OAT) is close to 0°C (red line) and reaches a value of -7°C during a typical flight on an A400M.

We highlight the fact that the Boeing 747 aircraft operates as a higher airspeed compared to the A400M which, in turns, provides a recovery temperature of approximately 3°C . Therefore, it is deemed as a sensible hypothesis to continue discussions to assume that the diffusion coefficients can be determined at 0°C , in accordance with the following expression extracted from [3]:

$$\frac{D_{T_1}}{D_{T_2}} = \left(\frac{T_1}{T_2} \right)^{3/2}$$

Where:

$$D_{T_1} = 0,219 \frac{cm^2}{s}; T_1 = 20^\circ C = 293 K; T_2 = 0^\circ C = 273 K$$

So that:

$$D_{T_2} = 0,196 \frac{cm^2}{s} = \delta = \varepsilon$$

In addition, we shall discuss the importance of modelling with a differential equation (as the *(Eq.3)*) instead of an algebraic one (as proposed by *(Eq.1)*):

The differential equation permits to consider the physics involved in the inerting process, constituted by the gas substances movement due to diffusion, convection and gases in and out. A complete discussion of the physics involved, together with the required mathematical background, is provided in Section 1.1 of [2]. It is relevant to highlight that the algebraic model in *(Eq.1)* is simple and based on a mass balance that disregards the main physics involved for the basic modelization.

I. 4. Model parameters calibration with flight test data.

The model in (Eq. 3) is constituted of three different parameters (n, m, c) that need to be determined making use of real flight testing activities. For this purpose, we consider the flight test data compiled in Figure 19 of [5], and that is summarized in the following figure:

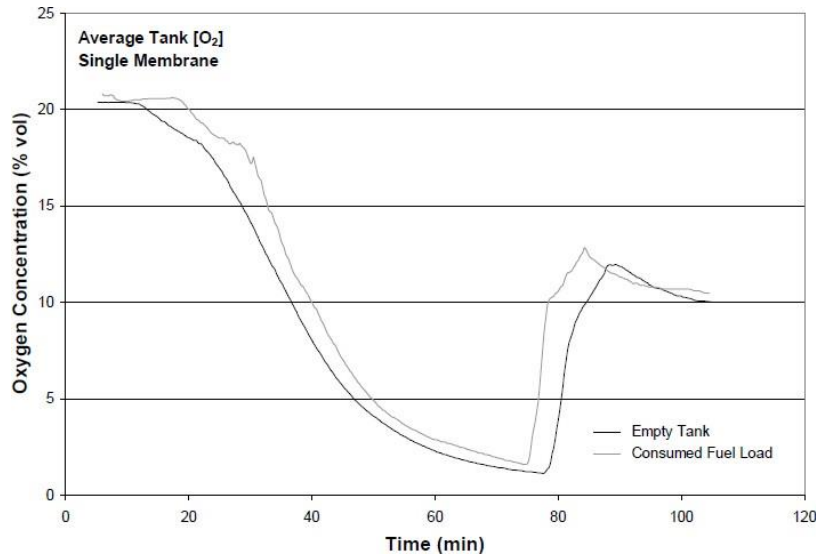


Figure 5. Single membrane (or ASM) inerting flight test average tank oxygen concentration for both empty tank test and consumed fuel load.

For the model parameters obtaining process, we consider the case of an empty tank in view of the following rationale:

An empty tank is defined as that with low level of fuel and high level of fuel vapors. It is usual that the inerting system is constituted by several ASMs to increase the inerting capacity and reduce risk times. An empty tank has higher level of oxygen that shall be replaced by nitrogen to ensure the inert condition. In addition, we consider a test case with a single ASM acting, which means that only one ASM is available to filter the nitrogen and remove the oxygen. This is, indeed, conservative and will lead to the most demanding configuration for the single inerting ASM that, in turn, will lead to provide higher times to get the inert condition.

The flight test data in Figure 5 considers only homogeneous mean oxygen values, therefore this data is useful to define the values of the parameters n and m . Hence, the system in (Eq.3) is reduced to:

$$\begin{aligned} u_t &= v^n \\ v_t &= -u^m \quad (\text{Eq. 4}) \\ n, m &\in (0,1) \end{aligned}$$

For this purpose and for each time step, the time derivatives (u_t, v_t) are determined considering that the substances concentration are expressed between the interval $(0,1)$ and the time is expressed in minutes. The time derivatives are determined for different discrete times and represented versus the value of each substance, with the intention to determine the optimal curve fitting. The results comparing u_t with v are compiled in the following figure:

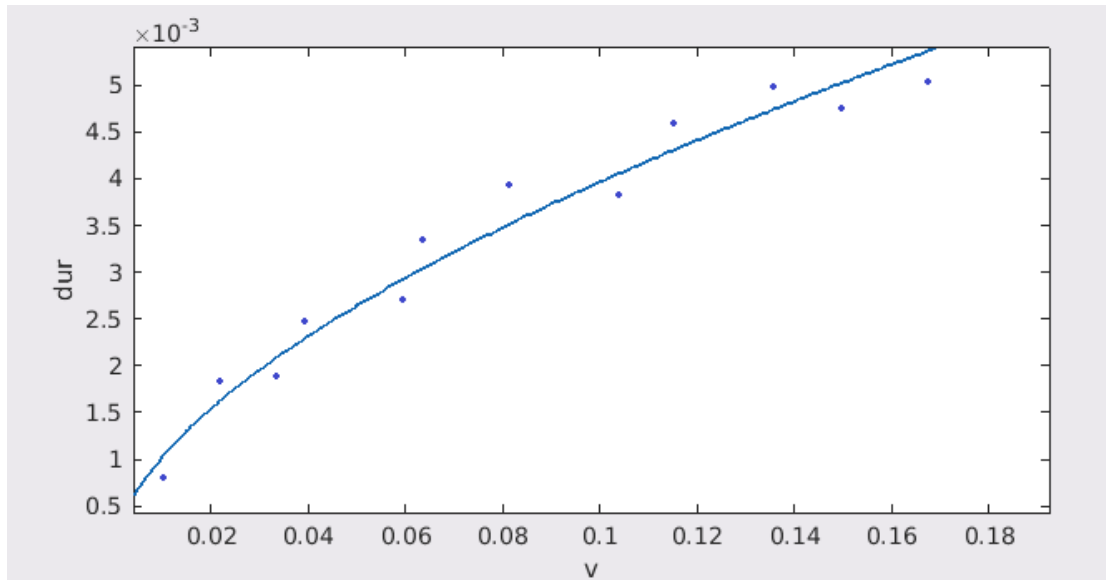


Figure 6. Representation of u_t (nitrogen time derivative) with v (oxygen concentration) for a total of 12 different times extracted from the flight test data compiled in Figure 5 and extracted from [5].

The optimal curve fitting adjusting the proposed data is of the form:

$$u_t \sim v^{0.586}$$

Then, we conclude that:

$$n = 0.586$$

The same representation can be performed to compare v_t with u . Note that $v_t < 0$ as the oxygen concentration decreases during the tank inerting process:

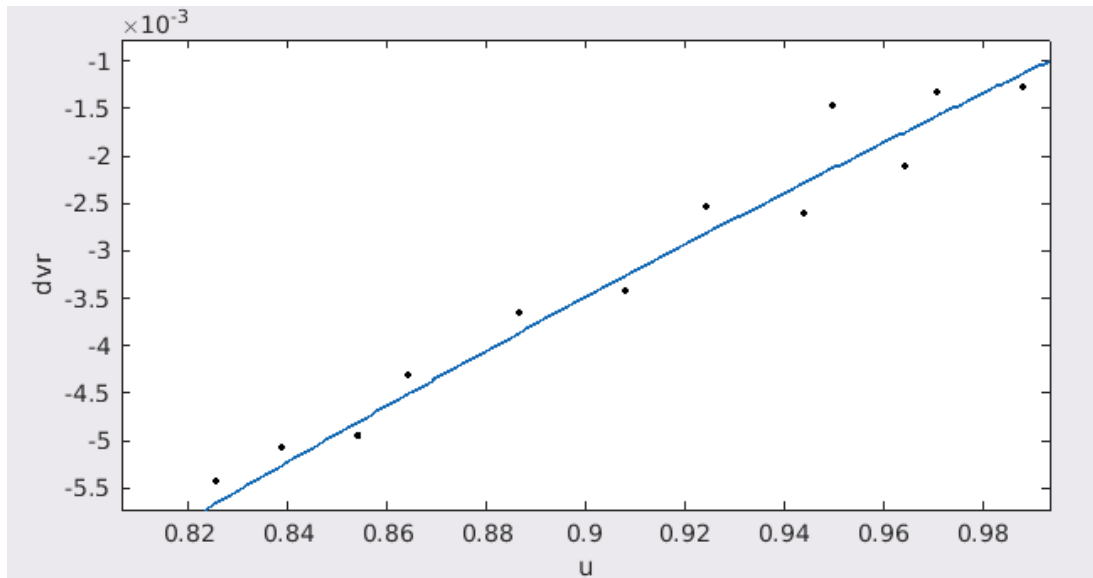


Figure 7. Representation of v_t (oxygen time derivative) with u (nitrogen concentration) for a total of 12 different times extracted from the flight test data compiled in Figure 5 and extracted from [5].

In this case, the optimal curve fitting provides the following value:

$$v_t \sim -u^{0.025}$$

Then:

$$m = 0.025$$

It is particularly relevant to observe that the parameters obtained (n , m), based on flight test data extracted from [6], are indeed between (0,1) as initially appointed in the model conditions expressed in (Eq.3).

The next parameter to obtain is the convective term, c . For this purpose we shall consider the expression outlined in Section 1.1 of [2]

$$c = \frac{\dot{m}}{\rho A_T}$$

Where:

A_T = Transversal area of the fuel tank.

\dot{m} = inerted gas flow rich in nitrogen that is pour into the tank.

ρ = gas density in the fuel tank which mainly constitute of nitrogen at the selected altitude and temperature.

The Nitrogen Enriched Air (NEA) reaching the fuel tank can be extracted from [5] (see the following figure):

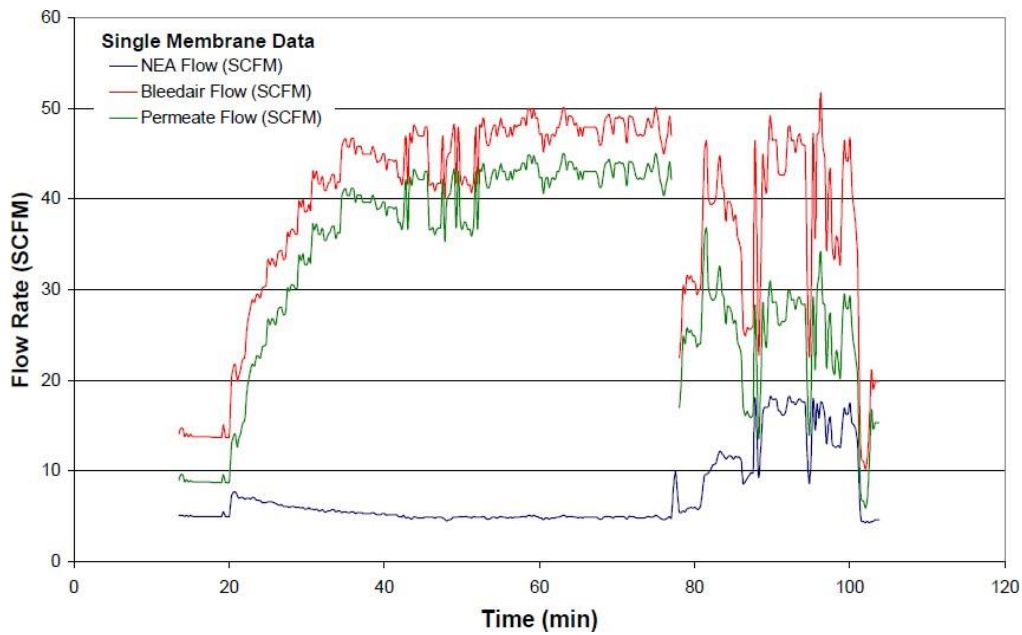


Figure 8. Involved mass flows for the single membrane test. The cruise phase (stabilized flight) is get at $t = 40$ min and the descend phase starts at $t = 78$ min. (see figure 14 in [5]).

It is to be noted that the NEA flow is kept stable during the flight and increases during the descend phase. For our purposes, we can consider the flight cruising phase (which is get at $t = 40$ min), in which the NEA flow value is given by:

$$NEA\ flow = 4,5\ SCFM = 0,044\ kg/min$$

The substance density is a mixture of the predominant nitrogen and remaining oxygen. For our estimation we consider an average value of 95% of nitrogen and 5% of oxygen during the cruise phase (stabilized flight)

$$\rho = 0,95\ \rho_{nitrogen} + 0,05\ \rho_{oxygen} = 0,343\ kg/m^3$$

For the determination of the area A_T , we consider that the fuel tank is almost of rectangular shape, as discussed and represented in the figure 1a, with the a mean height of 1,5 m and a mean wide of 6 m:

$$A_T = 1,5\ m \times 6\ m = 9\ m^2$$

Then and finally, c can be determined as:

$$c = 0,014\ m/min$$

Summing-up, the postulated set of equation compiled in (Eq.3) and demonstrated in Section 1.1 of [2] to model the interaction process between nitrogen and oxygen in a fuel tank, when submitted to the introduction of NEA flow, adopts the form:

$$\begin{aligned} u_t &= \delta \Delta u + c \cdot \nabla u + v^n & (Eq. 5) \\ v_t &= \varepsilon \Delta v + c \cdot \nabla v - u^m \end{aligned}$$

Where:

$$\begin{aligned} n &= 0,586; \quad m = 0,025; \quad c = 0,014 \frac{m}{min}; \\ \varepsilon &= \delta = 0,196 \text{ cm}^2/s \end{aligned}$$

The existence and uniqueness of regular solutions to the problem (Eq.5) has been proof in Sections 1.3, 1.4 and 1.5 of [2].

I. 5. Compatibility conditions.

The Lemma 1.6 in [2] provides a compatibility condition to ensure that the convection will not jeopardize the condition of having an increasing function for the nitrogen concentration (u) and a decreasing concentration of oxygen (v). The conditions to be met are:

$$v_0^n \geq 2c \cdot \nabla u_0$$

$$\int u_0^m \geq \|c\|v_0$$

Where the sub-index "0" represents the initial condition. We notice that, initially, the air is a homogeneous mixture of 80% of nitrogen and 20% of oxygen; therefore:

$$\nabla u_0 = 0$$

then, we have:

$$v_0^n \geq 2c \cdot \nabla u_0 = 0$$

In addition: $v_0^n = 0.2^{0.586} = 0,389$, so that we meet the first compatibility condition, as:

$$0,389 \geq 0$$

Operating for the second compatibility condition and considering that the integral is extended to the wing tank volume we have:

$$\int u_0^m = 0,80^{0,025} \cdot V_{tank} = 0,80^{0,025} \cdot 6,5 \cdot 6 \cdot 1,5 = 58,17$$

In addition, $\|c\|v_0 = 0,014 \cdot 0,2 = 0,0028$

Then:

$$\int u_0^m = 58,17 \geq \|c\|v_0 = 0,0028$$

As both compatibility conditions are met, we can ensure that the convection is relatively weak and will allow the diffusion and reaction/absorption terms to interact during the gas evolution process while complying with:

$$u_t \geq 0, \quad v_t \leq 0$$

During the complete evolution process.

I. 6. Solutions calibration

It is, now, our aim to provide a clear view of the solutions obtained in [2] for the model set in (Eq. 5) subjected to constant initial data:

$$u_0 = 0,8; \quad v_0 = 0,2$$

The initial concentrations correspond to the level of nitrogen and oxygen in the standard atmosphere.

The Section 1.8 in [2] provides a set of solutions for the (Eq.5) independently of the spatial variable and, hence, under the hypothesis of homogeneous distribution of solutions. Previously, we shall recall that the provided solutions are a sub-solution for the nitrogen concentration and a super-solution for the oxygen concentration:

$$u_s = u_0 + \mu t$$

$$v_s = v_0 - \frac{K}{\mu(m+1)} (u_0 + \mu t)^{m+1}$$

Where the parameter μ is obtained based on a sub-evolution bound for the oxygen concentration:

$$v_s = \mu^{1/n}$$

And K is a scaling factor to be assessed.

v_s can be determined based on the data from Figure 5. Previously, we remark that in case the flight would have continued in the cruising phase, the oxygen concentration would have reached an asymptote at a level of 2% of tank volume, in view of the curvature in Figure 5 in the proximity of $t = 70 \text{ min}$. The sudden growth in the oxygen concentration experienced at $t = 80 \text{ min}$ is due to the descend phase, in which the atmospheric air, rich in oxygen, enters into the tank via the tank venting system due to the increasing pressure conditions during a constant descend.

Then, and considering $v_s = 0.02$, we have:

$$\mu = 0,1$$

The solutions adopt the form:

$$u_s = 0,8 + 0,1t$$

$$v_s = 0,2 - 9,75 K (0,8 + 0,1 * t)^{1,025} \quad (\text{Eq.6})$$

The scaling constant K is determined based on one single data in Figure 5. For example, we consider the following point:

$$t = 40 \text{ min}$$

$$v_s = 0,08$$

Then,

$$K = \frac{0,08 - 0,2}{-9,75(0,8 + 0,1 * 40)^{1,025}} = 2,465 \cdot 10^{-3}$$

These postulated solutions are valid for a time interval $(0, T)$, where:

$$T = \left| \frac{(\mu(m + 1))^{\frac{1}{m+1}}(v_0 - \mu^{1/n})^{\frac{1}{m+1}} - u_0}{\mu} \right| = 7,8 \text{ seconds} = 0,13 \text{ min} \quad (Eq. 7)$$

Therefore, the solutions are applicable in time steps of $7,8 \text{ seconds}$ length. To permit the application of the solutions to the complete time domain (*up to $t=80 \text{ min}$*) the solutions shall be applicable in a timely discrete manner with sept amplitudes of $0,13 \text{ min}$.

The following figure represents the solution obtained in *(Eq.6)* compared to actual discretized values obtained from Figure 5.

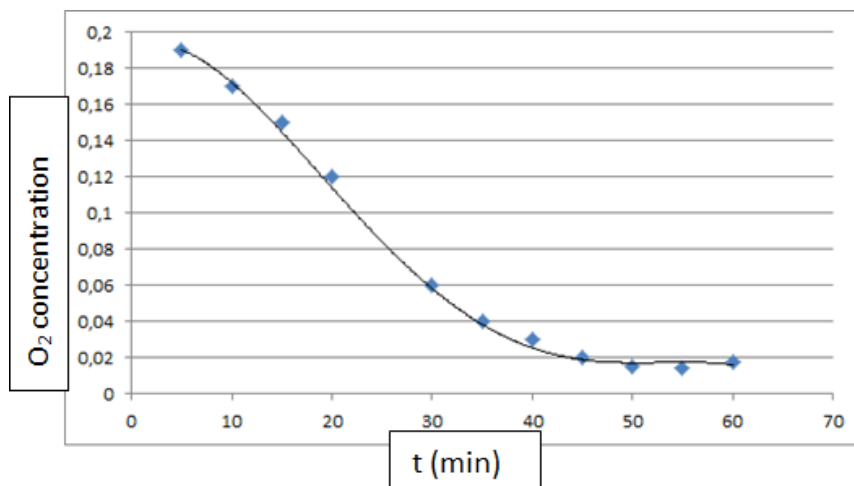


Figure 9 The black line represents the *(Eq.6)* discretized every $0,13 \text{ min}$ as per *(Eq.7)*. The blue points are discrete from Figure 5. It can be observed that the *(Eq.6)* fits very closely the flight test data in Figure 5.

From Figure 9, it is possible to check that the *(Eq.6)*, represented by the black line, fits closely the flight test data represented by the blue dots. This result permits to validate our approach and to confirm that the set of solutions obtained in Section 1.8 of [2] are, indeed, suitable solutions for the fuel tank inerting process described in the Sections I.1 and I.2 of this memory.

I. 7. Solutions in the Travelling Waves domain

The solutions named as Travelling Waves are formed of a front and a tip (see Figure 10). The front carries the information transition in the media from one state to other. This kind of behavior exhibited by the travelling wave solutions can be applied to the propagation of the NEA gas within the fuel tank. Indeed, we can think that the NEA constitutes a propagating front that shifts the tank ullage concentration by reducing the oxygen and increasing the nitrogen.

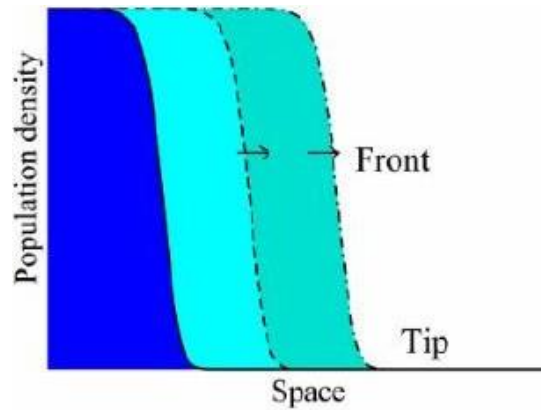


Figure 10. Travelling wave propagating in the media

In the inerting problem, we aim to modelize, we have a stationary solution towards the evolution tends for sufficiently large time; in our case, we consider 80 minutes (according to Figure 5 and previous to start the descend phase) as sufficiently large time to consider the stationary solutions:

$$u = 0,98$$

$$v = 0,02$$

The model, in the travelling wave domain, has been obtained in Section 1.9 of [2]. In addition, we make use of the calibrated model parameters obtained along this memory:

$$\begin{aligned} u_t &= \varepsilon \Delta u + c \cdot \nabla u - v^n (u - 0,98) \\ v_t &= \delta \Delta v + c \cdot \nabla v - u^m v \end{aligned}$$

Where:

$$n = 0,586; \quad m = 0,025; \quad c = 0,014 \text{ m/min}$$

The diffusion coefficients are expressed in terms of m^2/min instead of cm^2/s as reflected in (Eq.5):

$$\varepsilon = \delta = 13,14 \cdot 10^{-4} \frac{m^2}{min}$$

The travelling wave problem results from the following change of the independent variable:

$$\xi = x - at$$

Where “a” represents the travelling wave propagation speed.

In the case of study, the convection can be interpreted as a flow in the same direction of the travelling wave propagation, then the change of variables adopt the form:

$$\xi = x - (a + c) \quad (Eq.8)$$

It is our intention, now, to determine the travelling wave propagation speed. For that purpose, we shall consider that, when the variable $\xi = 0$, the travelling wave has completed the propagation in the tank domain. To understand this approach, we propose the following argument in view of Figure 12:

The front and the tip of the wave moves according to the propagation speed $(a + c)$, therefore, when the variable $\xi = 0$, the wave has run the completed domain:

$$0 = x - (a + c)t$$

$$x = (a + c)t$$

Then, the travelling wave speed can be determined as:

$$a = \frac{x}{t} - c$$

Once the travelling wave has completed the propagation in the tank, we shall reach an inerted level. We can, then, make use of the data in Figure 5. In particular, we consider that at $t = 80 \text{ min}$, the travelling wave has reached all tank areas to provide the lowest value, measured in flight, for the oxygen concentration. In addition, we consider that “x” is a typical tank dimension obtained as the geometric mean of the tank shape:

$$x = \sqrt[3]{6,5 \cdot 6 \cdot 1,5} = 3,88 \text{ m}$$

$$a = \frac{x}{t} - c = \frac{3,88}{80} - 0.014 = 0,061 \frac{\text{m}}{\text{min}}$$

Once the travelling wave speed has been established, the travelling wave model is run in a Matlab code making use of the ODE45 module. The code can be consulted in Annex I. The results in the travelling waves variable ξ are compiled in the following graph:

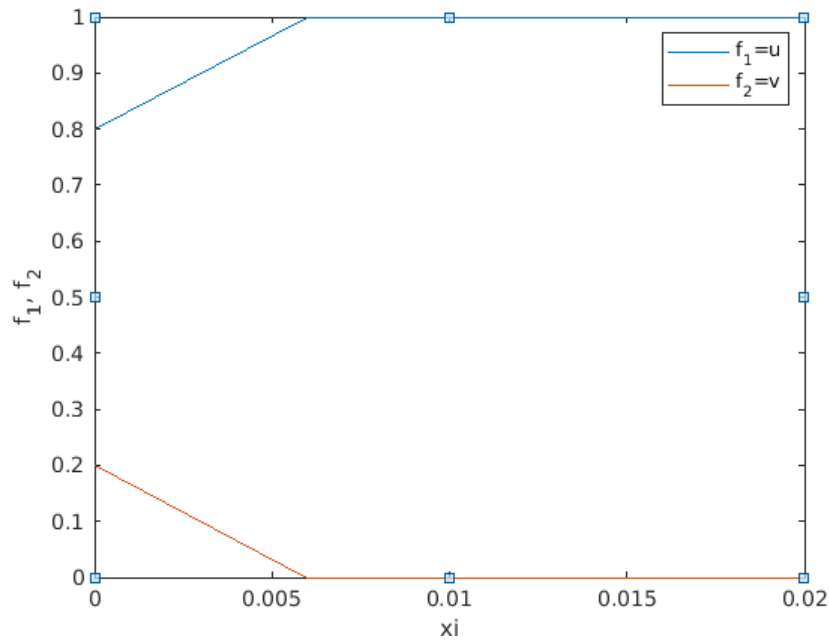


Figure 11. Travelling wave structure. The blue solution represents the evolution of the nitrogen within the tank evolving from 0,8 (80% in volume) up to filling the whole tank 1 (100%). The red solution represents the oxygen density that evolves from 0,2 (20% in volume) down to zero. Note that the horizontal axis represents the variable ξ , while $f_1=u$ and $f_2 = v$.

The main advantage when modelling in the travelling wave domain is the consideration of the diffusion given by the wave front and tip. This is a positive approach compared to the model based on a massic balance (Eq 1).

Based on the results in Figure 11, it is possible to determine the time required to inert at any level in the figure.

Let assume a military aircraft with a similar fuel tank and flying under similar operational conditions compared to the A320 used for our model calibration as per [5]. It is allowed a level up to 9% of oxygen to ensure that military aircrafts operating in a conflictive area do not explode as a consequence of a high energy bullet impacting the wing. A value of 0.09 of oxygen corresponds, according to Figure 11:

$$\xi = 0,004 \text{ meters}$$

Then, the time to get the inerted condition under the similar operational conditions compared to the A320 can be get as:

$$t = \frac{x - \xi}{a + c} = \frac{(3,88 - 0,004)m}{(0,061 + 0,014)\frac{m}{min}} \approx 52 \text{ min}$$

Globally, we can ensure that a time of $t = 52 \text{ min}$, the tank will reach a value of 9% of oxygen in all place area. This value is overly pessimistic compared to the value provided in Figure 5, in which the value of 9% of oxygen is get at $t = 44 \text{ min}$. Nonetheless, we shall argue that the value of oxygen in Figure 5 is only provided for a single location where the oxygen sensor is

placed. Therefore, the modeled value of $t = 52 \text{ min}$, shall be seen as an approximation in which the diffusion acts as per the travelling wave front and tip and in which scattering is considered to reach a homogeneous oxygen concentration of 9% in the tank.

It is particularly relevant to observe that the scale for the tank dimension is much higher than the scale of the travelling wave spatial variable ξ . This fact can be explained in view of the travelling wave features as expressed in Figure 12. The front and the tip represent the diffusion acting along the wave, so that ξ represents a dimension of the wave interface where the front and the tip are confined. This interpretation is based on the change of variable in (Eq.8) where ξ is the difference between the tank dimension x and the moving wave $(a + c)t$:

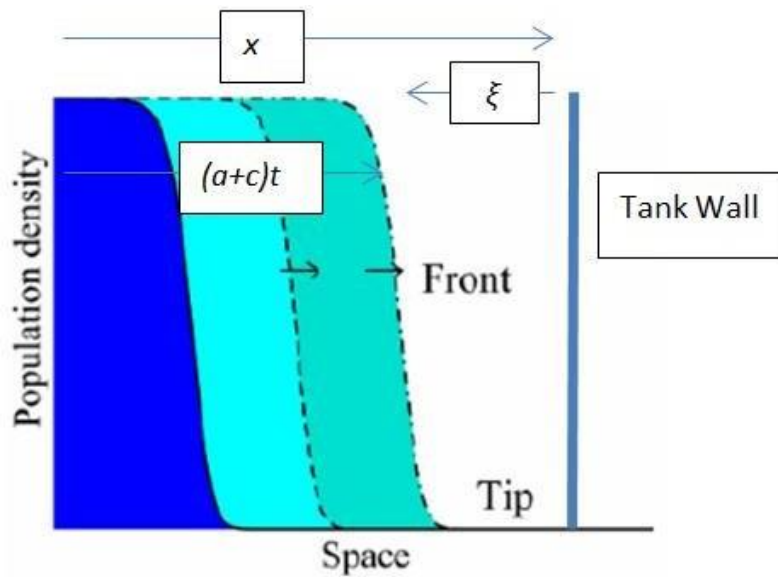


Figure 12: When the travelling wave completes the spatial domain the variable ξ locates a small fraction of the space where the wave front and tip are confined. This space area is of the order of 10^{-3} m .

PART II: The Fire Extinguishing model through a Porous Medium Equation (PME)

II. 1. Background

The aircraft turbomachinery, used as propellant and to produce energy or air, are the main source of aircraft fires as a result of one or multiples failures [6]. The following figure illustrates the aircraft zones where fire ignition is more likely to occur. Engine failures are found to be the most frequent cause of flammable fluid ignition.

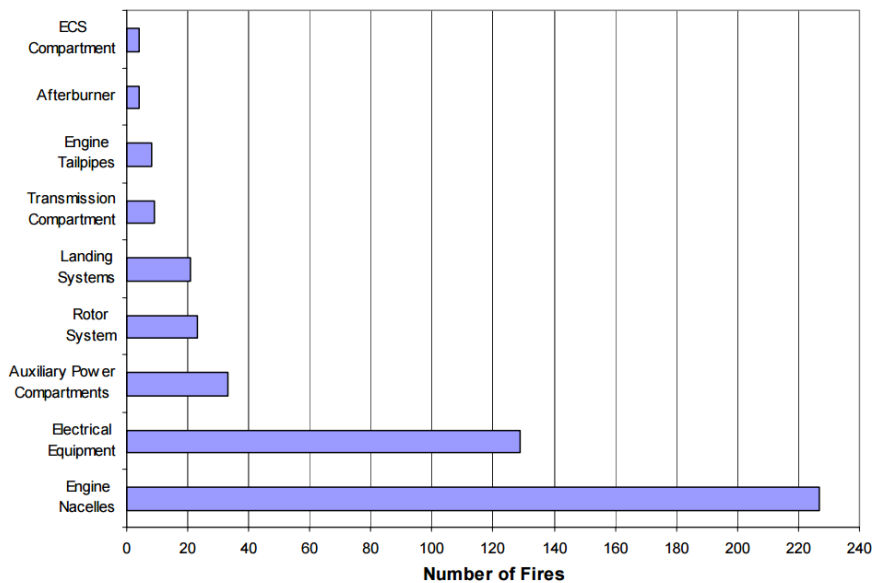


Figure 13. Fires in aircraft split by zones in non-combat aircrafts on the U.S. Navy between 1977 and 1993 [6].

As illustrated, it is obvious that the control of engine and auxiliary power units fires are very relevant to ensure the survivability of the accidental aircraft and the minimization of hazards.

The engine nacelles are very complex areas full of bleed and hydraulic pipes, electrical harnesses and computers. Figures 14 and 15 aim to provide a simple view to illustrate the tightness of the nacelle area where the discharge agent flows.



Figure 14. Engine nacelle of a typical fighter aircraft.

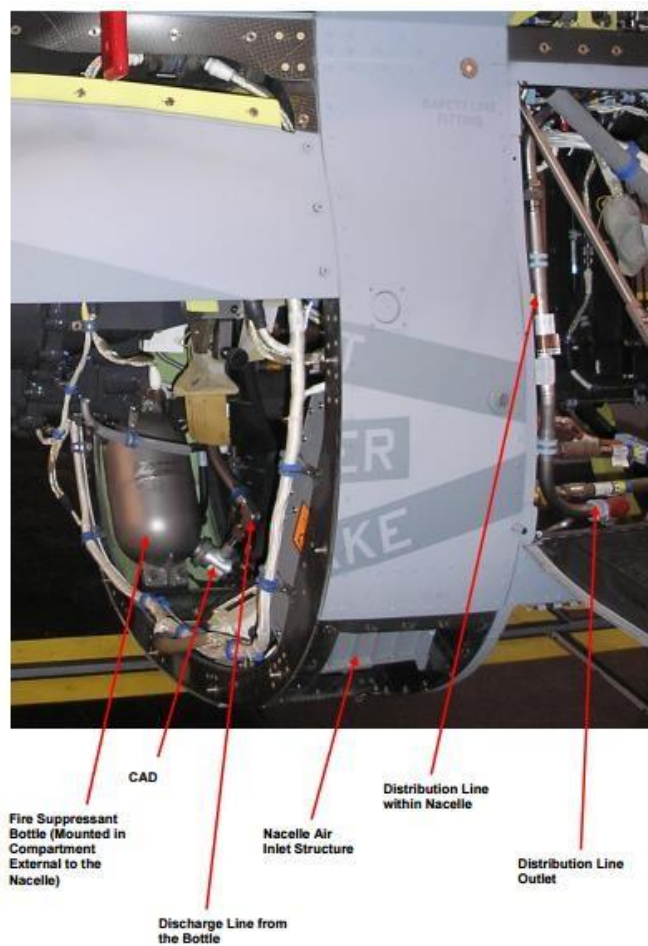


Figure 15. Aircraft engine nacelle fire suppression system installation and fire extinguisher bottle.

II. 2. Justification

One of the most frequently used models for fire extinguishing certification in aircrafts is provided by the Part 1/6 Section 4 (leaflet 86) in [8], and is based on a purely time evolution with no spatial dependency:

$$c(t) = \frac{B}{B + A} [1 - e^{-t(A+B)}], \quad (Eq. 9)$$

where:

$$A = \frac{W_a}{V \cdot \rho}$$

$$B = \frac{W_h/t_d}{V \cdot \varphi}$$

W_a = Air flow rate,

V = fire zone volume,

ρ = Air Density,

W_h = Weight of the agent,

t_d = Time required to discharge,

φ = Discharge agent Density.

A pure time evolution process is a hard simplification. Intuitively, we can think that the complex configuration of the engine nacelles, together with the discharge nozzle located at fixed positions, lead us to consider the spatial distributions as relevant. Unfortunately, the model provided in (Eq. 9) does not consider the space as a variable.

Our intention is to make use of the Porous Medium Equation (PME), as derived in Section 2.1 of [2], to model with a non-linear spatial diffusion. This approach aims to be representative of the real physics involved in the discharging process. The PME is particularly interesting as it presents a finite propagation speed in the diffusion front, this feature can be used to model the propagating agent in the domain of interest (see Section 2.3.2 in [2] for a discussion about the finite propagation induced by a PME).

Our modelization efforts are focused on the Airbus military aircraft A400M and, in particular, our aim is to use flight test data to calibrate the model parameters according to the following governing expression (see Section 2.1 in [2]):

$$u_t = \Delta u^m + |x|^\sigma u^p \text{ (Eq 10)}$$

Where:

$$m > 1; \sigma > 0; 0 < p < 1.$$

Modelling with a non-linear diffusion (Δu^m) and a non-linear reaction ($|x|^\sigma u^p$) makes the process more complex, nonetheless it provides a unique form of modelling considering the physics, that shall be interpreted as a previous step to correctly scope the engineering activities.

The homogeneous PME equation:

$$u_t = \Delta u^m$$

exhibits a set of properties that are particularly useful to model the nature of a fire extinguishing process. The exercise presented along this document consists on modelling the propagation of the extinguishing agent to determine the concentration of the agent in each part of our domain of interest. One the most relevant properties is the non-existence of the positivity condition that is typical when modelling with the classical Gaussian diffusion given by the expression:

$$u_t = \Delta u$$

A complete discussion about the novelties of the PME is provided in Section 2.3 of [2].

In addition to the non-linear diffusion, the governing equation presents a reaction term of the form

$$|x|^\sigma u^p$$

which pretends to introduce the following realistic aspects:

- Agent saturation: Once the extinguisher agent discharges into the domain, the process is fast due to the fact that no agent exists in the media; nonetheless, during the discharge the agent concentration increases leading to reduce the rate of change in the concentration. This fundamental principle is introduced by the term u^p ($p < 1$).
- Agent heterogeneous distribution: The discharge nozzles are located in different places all over the engine cowl and nacelle, the discharging process is far from an homogeneous process. Therefore, we shall consider that the rate of time-change in the agent concentration varies with the position. This is the objective when introducing the term $|x|^\sigma$, $\sigma > 0$.

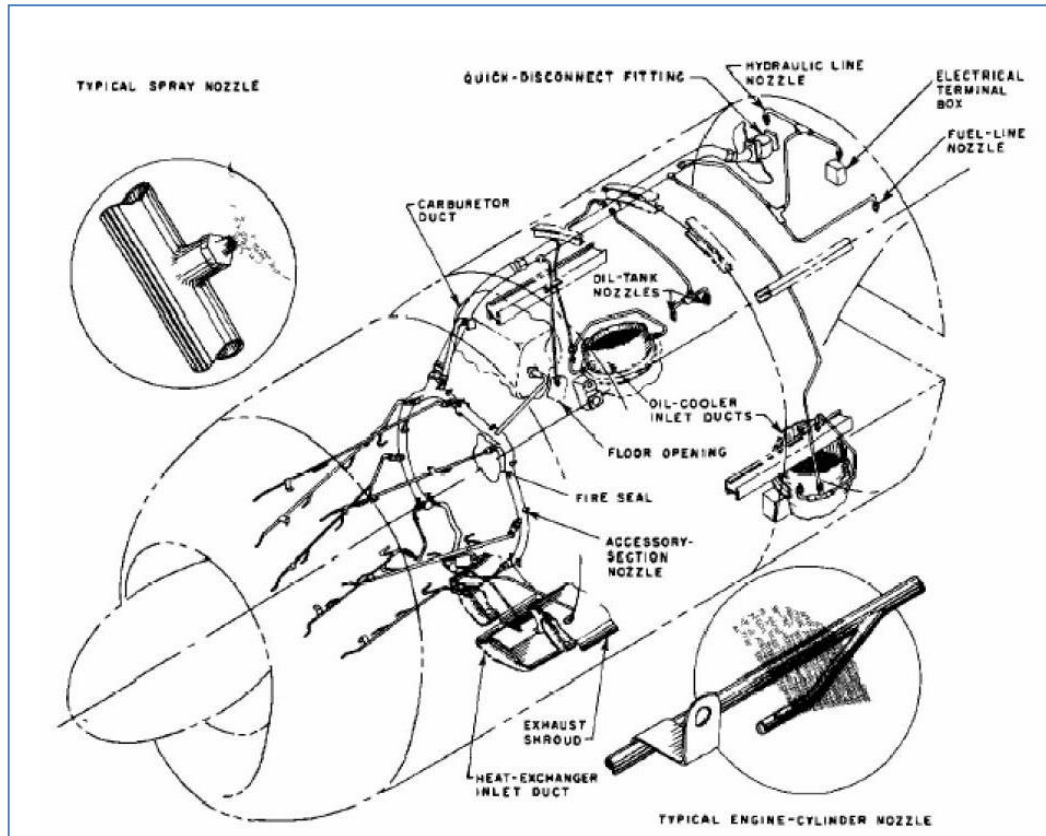


Figure 16. Example of a typical Fire extinguisher lay-out. Note that the nozzles are located heterogeneously.

II. 3. A400M Engine cowl description

The A400M aircraft has four propeller driven engines:



Figure 17. A400M aircraft. We can see the four propellers.

The engine shall be protected against fire hazards for which a fire detector and extinguishing system is provided.

The engine declared fire zones is divided into four sections. The division criterion responds to the following simple conceptions:

- Areas where sensible equipment are installed.
- The number of sections is homogeneously distributed along the domain.

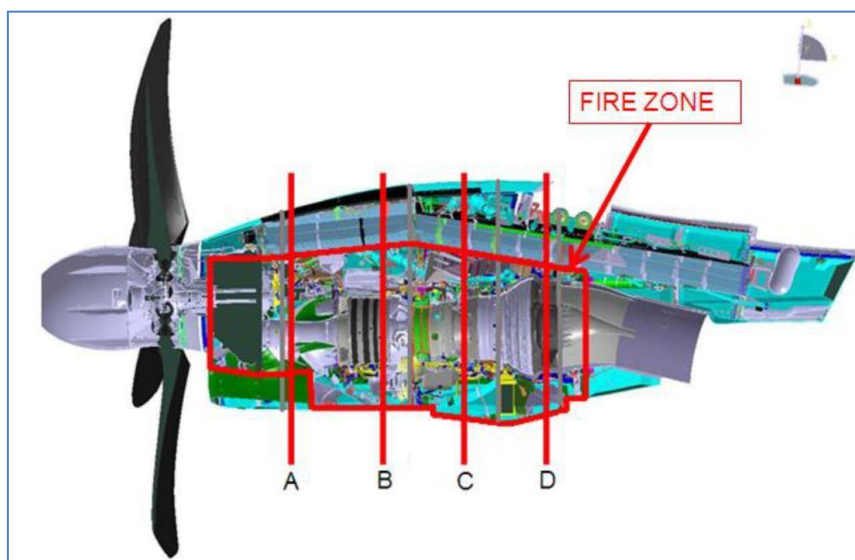


Figure 18. A400M propeller driven engine representation. The fire zone is split into four areas.

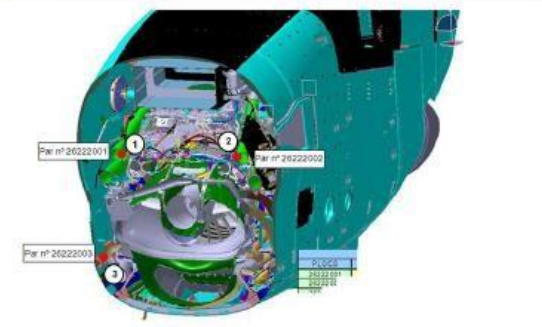
The following table provides a list of the sensitive equipment installed in each section area:

Parameter	Section	Areas covered by the parameter
1	A	<ul style="list-style-type: none"> • Propeller brake unit • Brake oil pipes • PGB
2	A	<ul style="list-style-type: none"> • PGB Oil Filter • PGB
3	A	<ul style="list-style-type: none"> • Rear PGB • Intake drainage (fluid accumulation point)
4	B	<ul style="list-style-type: none"> • Upper part for Engine Oil Tank • Fuel Cooled Oil Cooler
5	B	<ul style="list-style-type: none"> • Handling Bleed Valve – Intermediate Pressure Compressor • Starter • Rear nacelle (fluid accumulation point)
6	B	<ul style="list-style-type: none"> • Rear Engine Oil Tank • Shut Off Valve • Fuel Metering Unit • Main Fuel Filter • Turbo Machinery Oil Pump/Filter • Rear nacelle (fluid accumulation point)
7	C	<ul style="list-style-type: none"> • Upper Fuel Injection • Bleed Hot Ducts
8	C	<ul style="list-style-type: none"> • Upper Fuel Injection
9	C	<ul style="list-style-type: none"> • Fuel Main Pump • Fuel Metering Unit • Main Fuel Filter • Rear nacelle (fluid accumulation point)
10	D	<ul style="list-style-type: none"> • Upper-rear fire zone. Expected low ventilation and concentration point.
11	D	<ul style="list-style-type: none"> • Air Cooled Oil Cooled • Rear nacelle (fluid accumulation point)
12	D	<ul style="list-style-type: none"> • Air Cooled Oil Cooled • Rear nacelle (fluid accumulation point)

Table 1. Engine areas covered by the section. PGB stands for Propeller Gear Box. Each of the parameters (from 1 to 12) corresponds to the position of the entry to the sensors used to measure the extinguishing agent volumetric concentration.

The following figures provide the details of each sensor location per section:

Section A-A (Offset 1200 mm.)



Section A-A (Offset 1200 mm.)

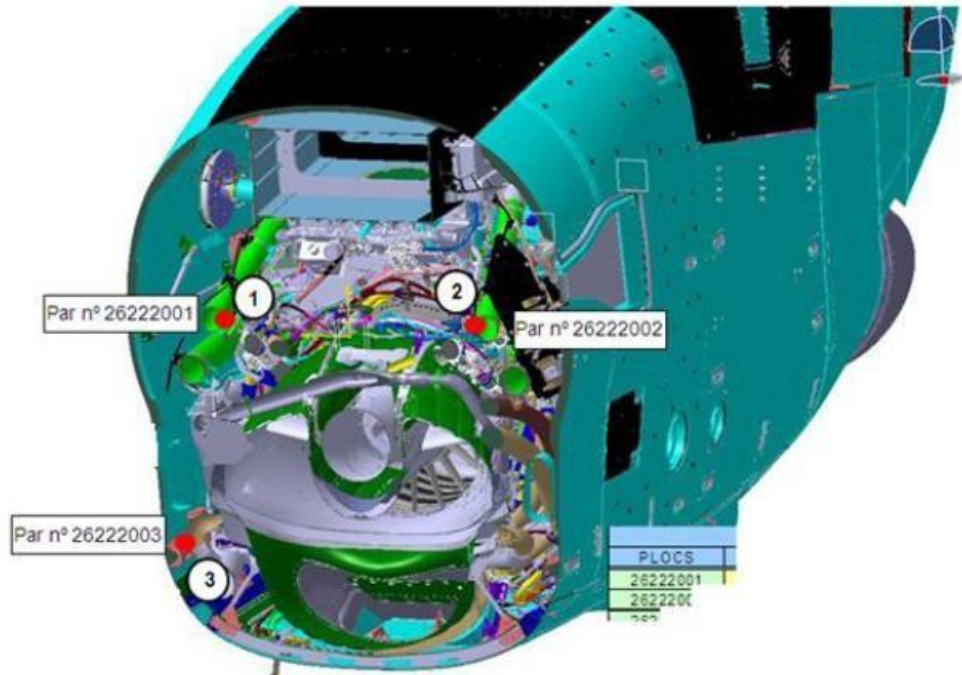
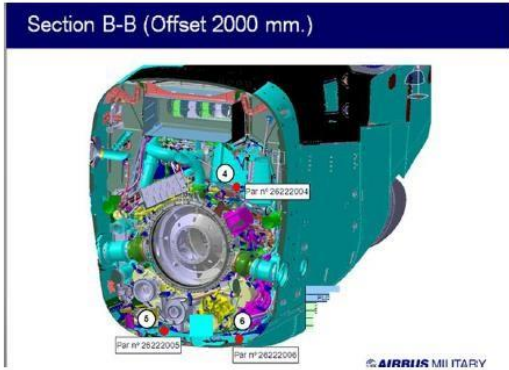


Figure 19. Section A sensors entry positions



Section B-B (Offset 2000 mm.)

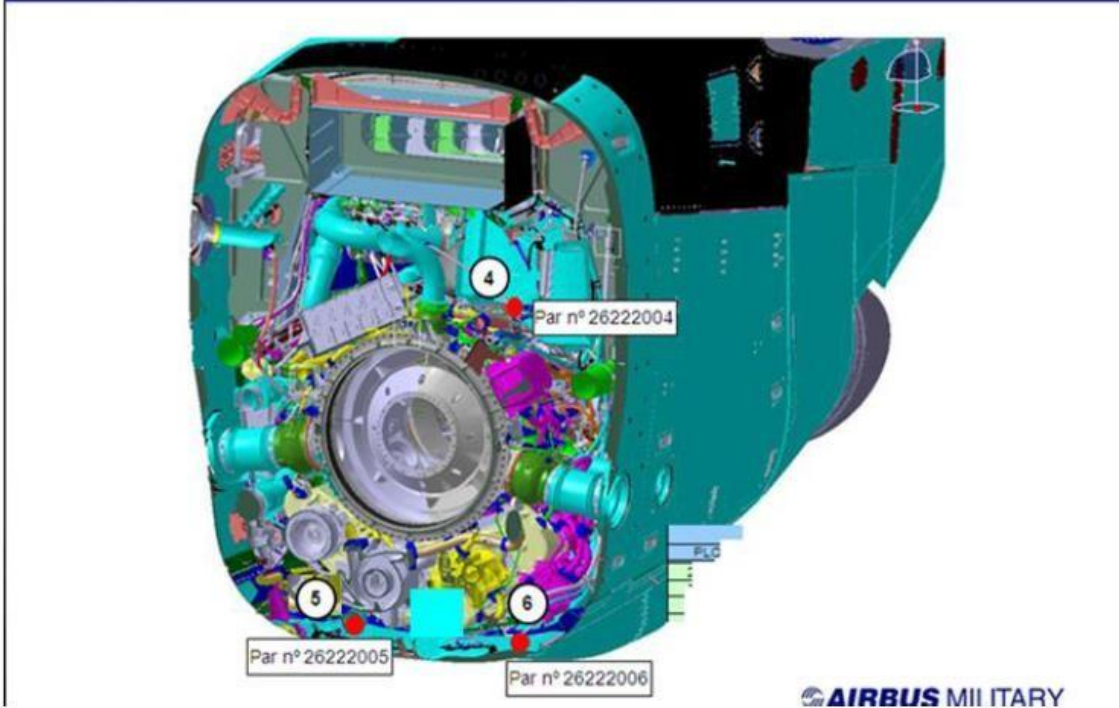
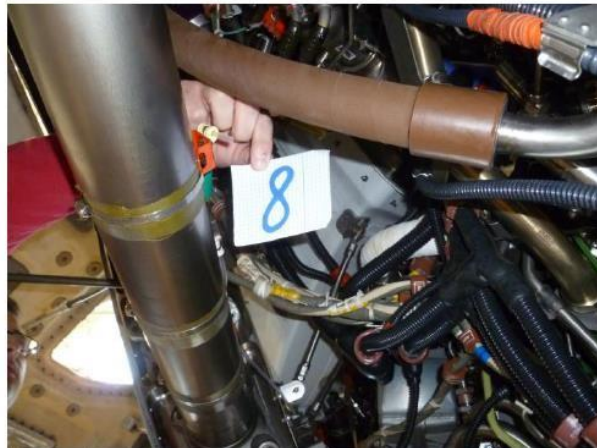


Figure 20. Section B sensors entry positions

Section C-C (Offset 2800 mm.)



Section C-C (Offset 2800 mm.)

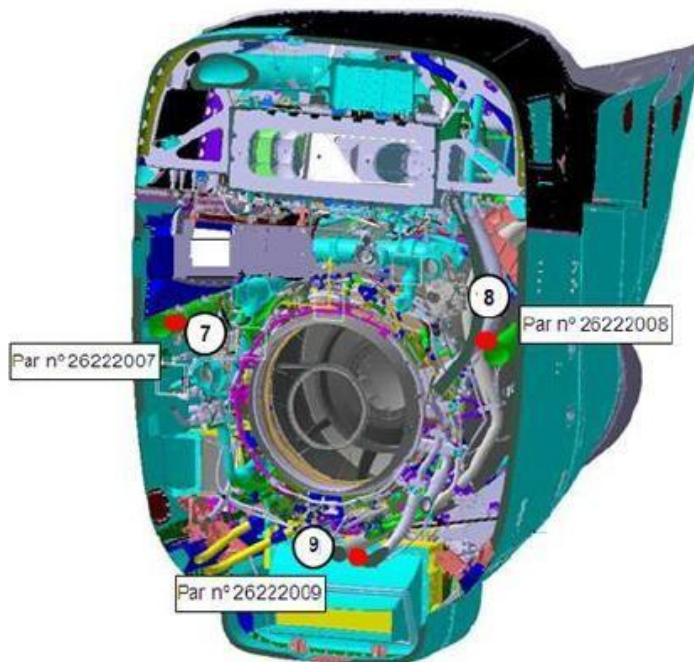
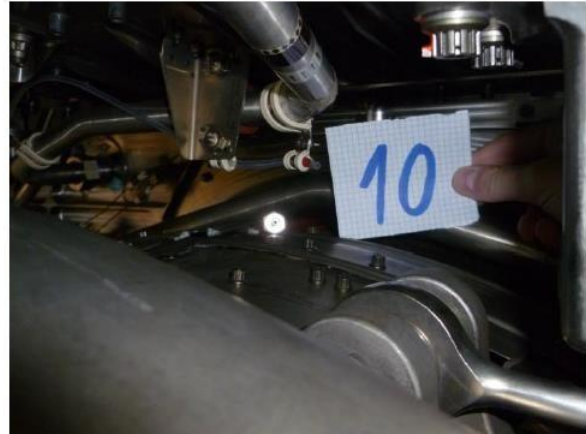


Figure 21. Section C sensors entry positions

Section D-D (Offset 3600 mm.)



Section D-D (Offset 3600 mm.)

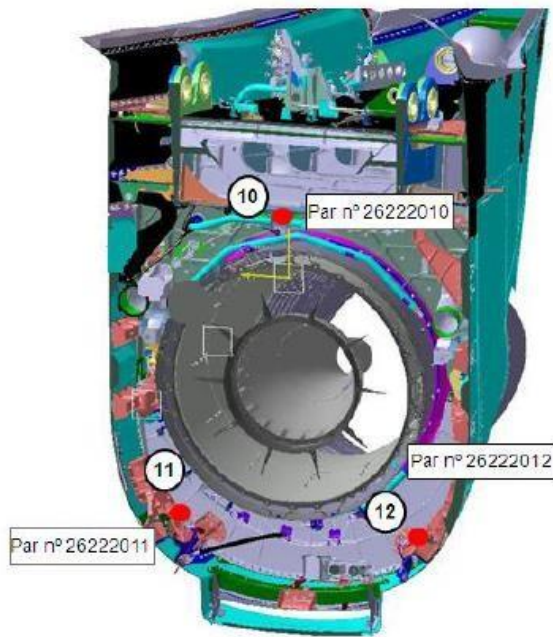


Figure 22. Section D sensors entry positions

II. 4. Flight test data

The flight test, that we will use to calibrate the model in (Eq. 10), was performed in Seville and consisted on a simple procedure for the chief pilot to activate the fire extinguishing procedure, which release the extinguishing agent based on a Halon compound. The extinguishing system is designed to be capable to extinguish a fire in the most critical condition (i.e, the agent bottle at lowest temperature and highest dynamic pressure or ventilation in the engine cowl) which is:

- 150 ft (Low altitude cruise).
- Mach 0.45.
- ISA – 70°C.
- Bottle temperature = -55°C.

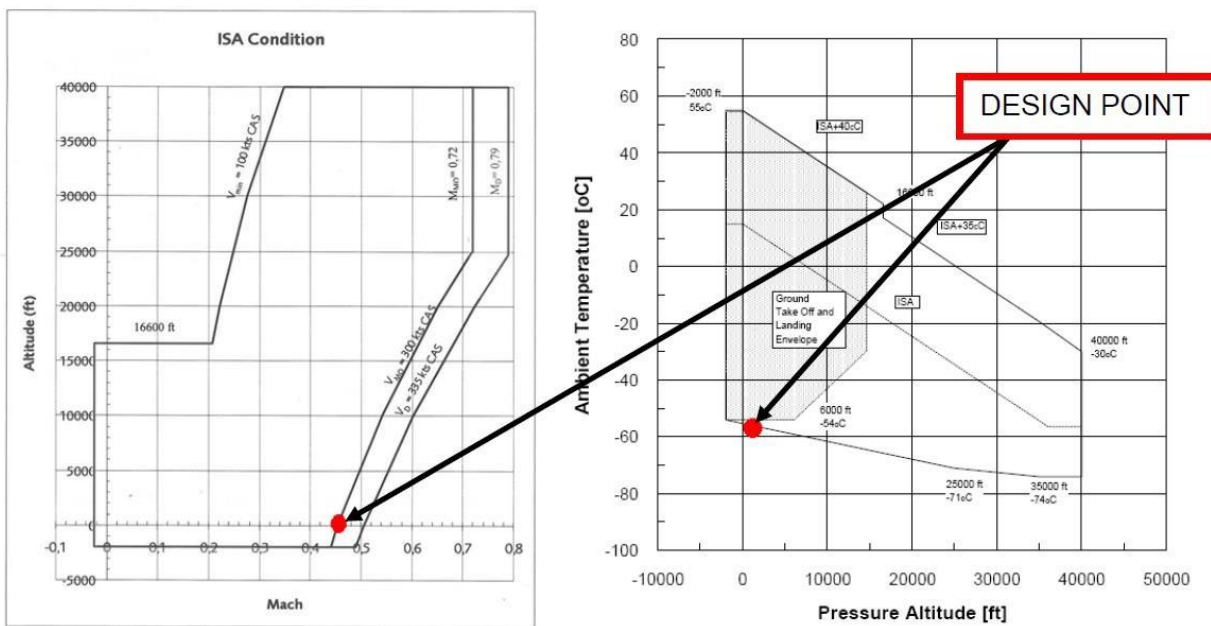


Figure 23. Engine Fire extinguishing design point within A400M flight operational envelope

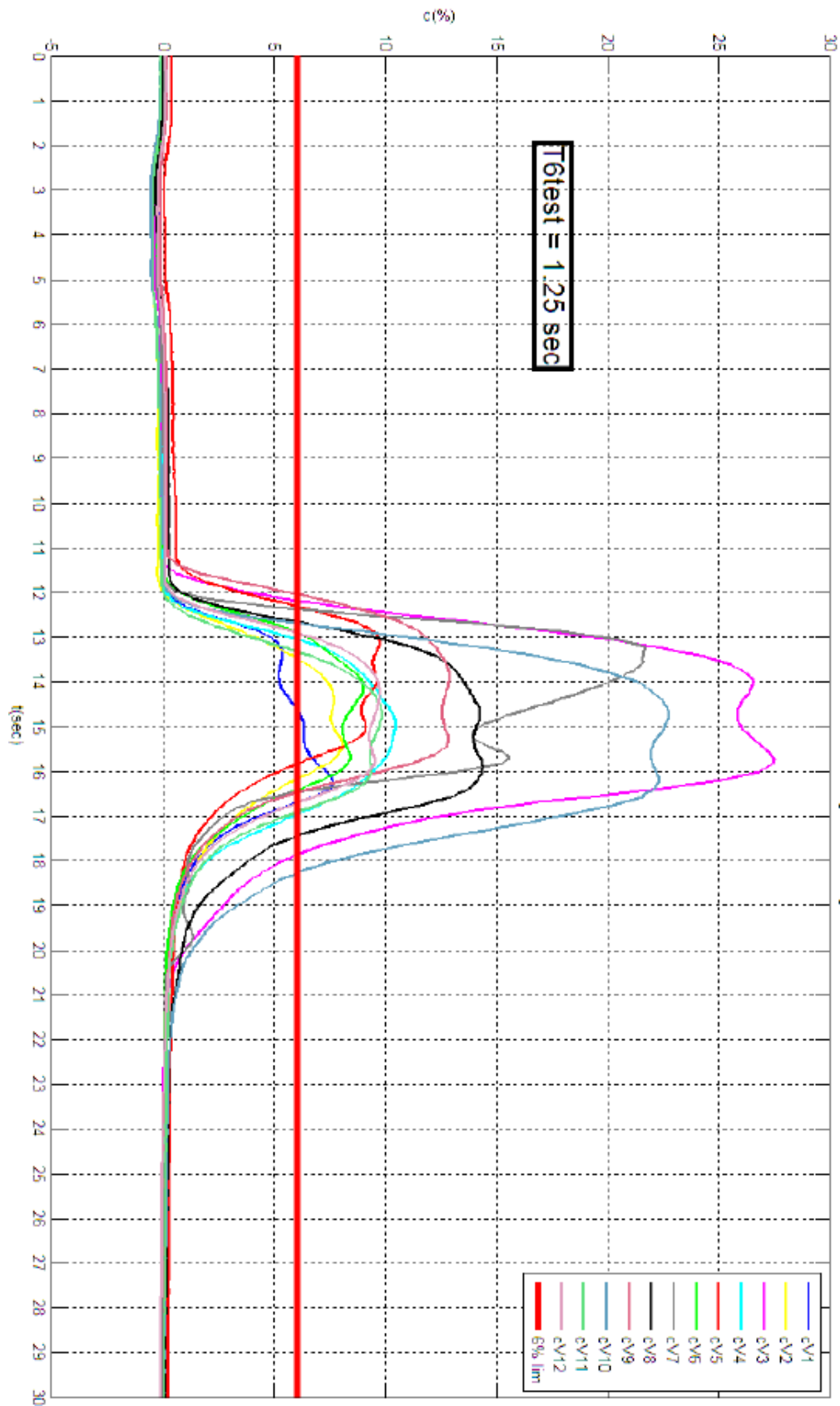


Figure 24. Flight test results. Volumetric concentration for each position time evolution

One important comment to highlight is related with the ambient temperature. The flight tests were performed in Seville during winter period, then the temperature was set at ISA-7,4°C which corresponds to 7,6°C. The design point temperature at ISA – 70°C (i.e. -55°C) was not possible to get, this ambient condition is only possible in the artic pole for which no resources to perform the campaign were get. Nonetheless, the results are valid for our model calibration purposes.

II. 5. Model calibration

The model parameters calibration will be done as per a longitudinal flow line according to the offsets defined. The sensors entry 2, 4, 8 and 10 are located in an almost longitudinal axis, then, the defined offsets are sufficient for the location purposes:

Sensor configuration 1	Offset (m)	Maximum Volumetric concentration (%) at t = 15 sec
2	1,200	7,5
4	2,000	10,5
8	2,800	14,5
10	3,600	23,5

Table 2. Sensor volumetric measurements at t = 15 sec. The t = 15 sec is selected to fix a common reference time for model parameter obtaining.

During the testing condition, it is possible to consider that the reaction term ($|x|^{\sigma}u^p$) is more relevant than the non-linear diffusion (Δu^m). This assumption is sensible as the discharging time is qualitatively fast. Under the assumption, Section 2.6.1 in [2] provides a solution of the form:

$$u = |x|^{\sigma/(1-p)}(1 - p)^{1/(1-p)}(t - \tau)^{1/(1-p)} \quad (Eq. 11)$$

Which is used, together with the table 2 data, to determine the values for σ and p . Previously, the data in table 2 is represented in the following figure:

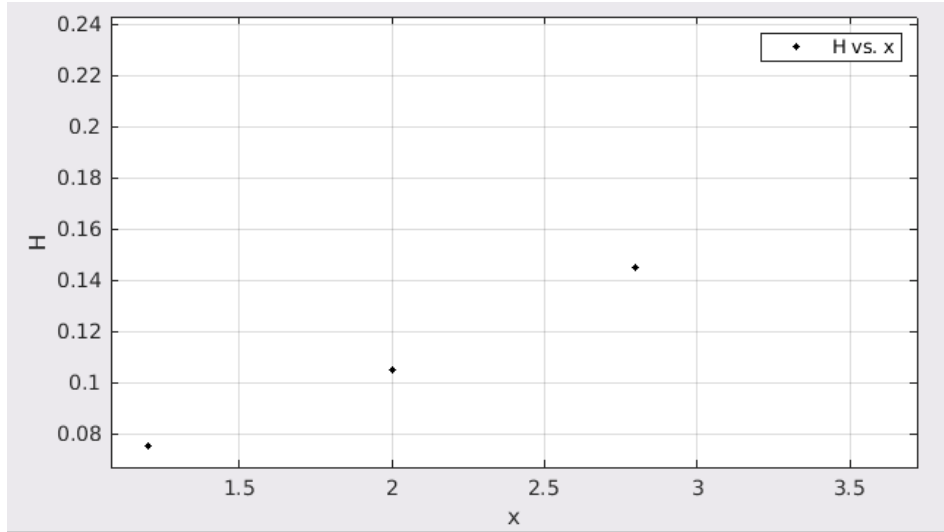


Figure 25. Halon concentration (H) expressed per unit, as function of the offset (x in meters).

Figure 25 data is adjusted to a potential law of the form:

$$u = 0,1461|x|^{0,3277}$$

Which can be compared to the expression (Eq.11) that adopts the specific form according to data in the figure 24.

$$u = |x|^{\sigma/(1-p)}(1-p)^{1/(1-p)}(15-12)^{1/(1-p)}.$$

Where the discharge time is considered at $t = 15 \text{ sec}$ and the beginning of the discharge process is set at $\tau = 12 \text{ sec}$. Then, we have:

$$(1-p)^{1/(1-p)}(15-12)^{1/(1-p)} = 0,1461.$$

after resolution:

$$p = 0,78$$

And:

$$\sigma/(1-p) = 0,3277$$

$$\sigma = 0,072$$

It is particularly relevant to observe that the model calibration provides a value for $p \in (0,1)$ and $\sigma > 0$, which was a priori assumption to model the saturation in the media due to the increasing population of the extinguishing agent (see Section II.2 of this memory).

Under the assumption that the reaction predominates over the diffusion, Section 2.6.1 in [2], provides the following condition to be met among the different parameters:

$$m\sigma + 2(1-\sigma)p + \sigma < 2$$

We obtain:

$$m < 6,67$$

For simplification purposes, we admit the following value for m :

$$m = 2$$

The existence of global solutions requires a certain condition to be met for the involved parameters (see Theorem 2.6.2.1 in [2]):

$$p < \text{sign}_+ \left(1 - \frac{\sigma(m-1)}{2} \right)$$

This condition is met, ensuring then the existence of solutions:

$$0,78 < \left(1 - \frac{0,072(2-1)}{2} \right) = 0,964$$

Therefore, the solution describing the behavior of the halon concentration exits as per the model (Eq. 10) along the line given by the sensor configuration 2-4-8-10. This solution adopts the form:

$$u = |x|^{0,3277} 0,00102 (t - 12)^{4,5} \quad (\text{Eq. 12})$$

Where:

$$0 < u < 1$$

Is the concentration of halon expressed per unit;

x is expressed in meters;

t is expressed in seconds.

Our next intention is to obtain the propagation front that results when considering the diffusion carried by the PME. For this purpose we consider the results as per Theorem 2.6.2.2 in [2]. Particularly, the positivity of the solution (i.e. the existence of halon concentration) is provided in the frame:

$$u(x, t) > 0, \quad \text{when} \quad |x| < c_2(x)t^\beta$$

Where,

$$c_2(x) = c_{supp} |x|^{\frac{\sigma(m-1)}{2(1-p)}}$$

And,

$$c_{supp} = \frac{(-\alpha + \beta)^{\frac{\sigma(m-1)}{2(p-1)}}}{\left(\frac{(m-1)\beta}{2m}\right)^{\frac{1}{2}}} = 0,775$$

$$\alpha = \frac{\sigma + 2}{\sigma(m-1) + 2(p-1)} = -5,63$$

$$\beta = \frac{p - m}{\sigma(m-1) + 2(p-1)} = 3,33$$

After compilation of results, we have:

$$u > 0, \quad \text{whenever} \quad |x| < 0,738 \cdot t^{3,92}$$

Therefore, the shifting front is given by the expression

$$|x| = 0,738 \cdot t^{3,92}$$

And represented in the following figure:

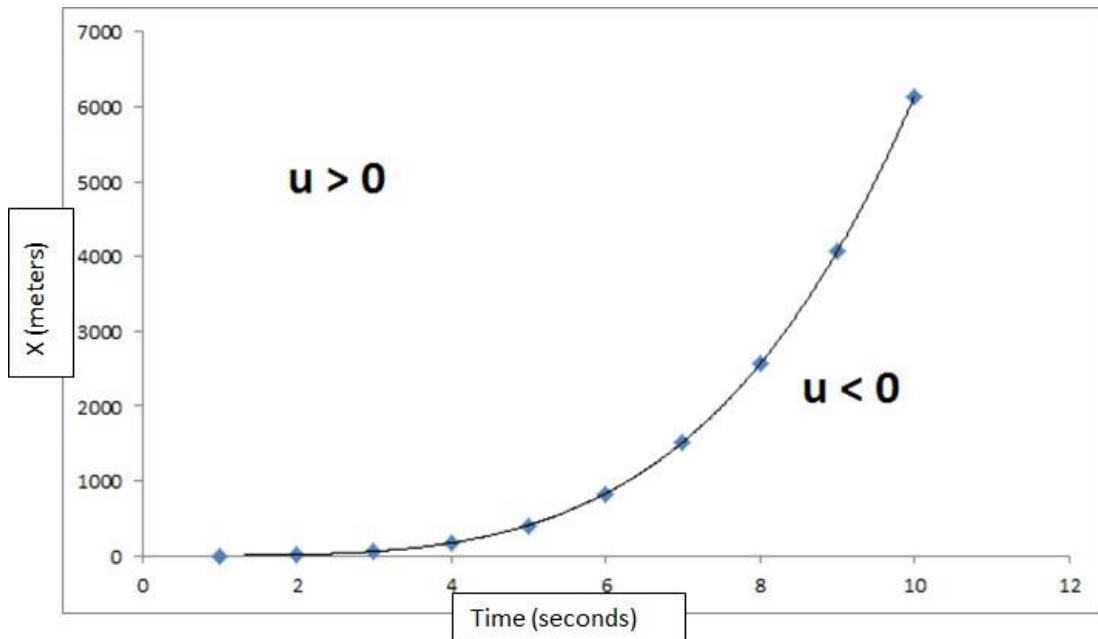


Figure 26. The propagating front, represented by the continuous line, is the effect of the diffusion and absorption while moving along the flow line characterized in Table 2.

Based on the results compiled in Figure 24, it is possible to determine the requested time to ensure that the halon concentration reaches the complete domain. For this purpose, we consider the engine cowl domain:

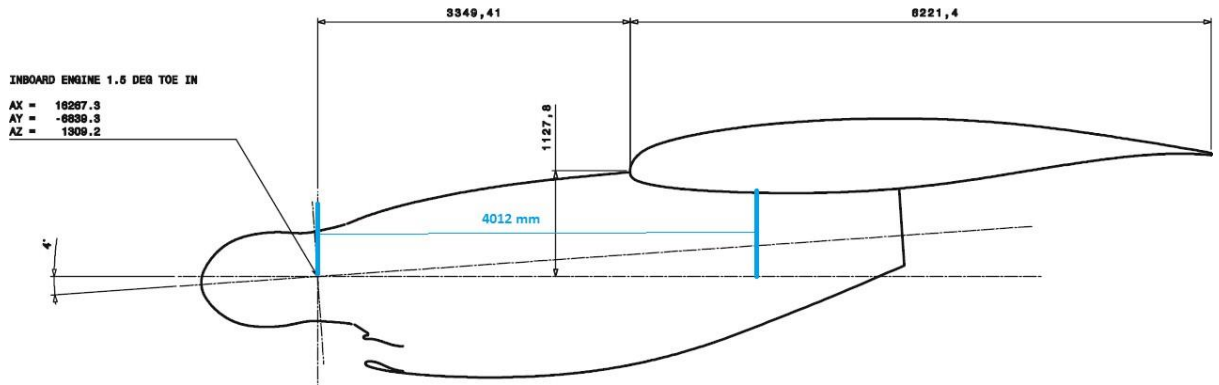


Figure 27. Engine cowl geometry. The blue line represents the length of the flow line characterized by the data in Table 2.

When the diffusion and reaction have made the halon concentration to propagate along the engine cowl, we have

$$|x| = 4,012 \text{ m}$$

And the time required to ensure the propagation has reached the entire engine cowl is given by the graph in Figure 26:

$$t = 1,4 \text{ seconds}$$

Note that this time obtained via the results of Theorem 2.6.2.2 in [2], matches perfectly with the flight test data compiled in Figure 24. Indeed, according to this figure, the discharge process reaches all domain areas in 1,3 seconds. In this short period, all sensors are measuring a certain quantity of concentration and, in the half of them, the extinguisher established concentration reaches the level of 6% (represented by the horizontal red line in the following figure) which is considered as a sufficient value to extinguish any engine fire (see the requirements CS 25.1195(b) & (c) in [9]). Therefore, we can ensure that for the assessed value of $t = 1,4 \text{ seconds}$ the propagating extinguisher front is well established and positivity of solutions can be shown.

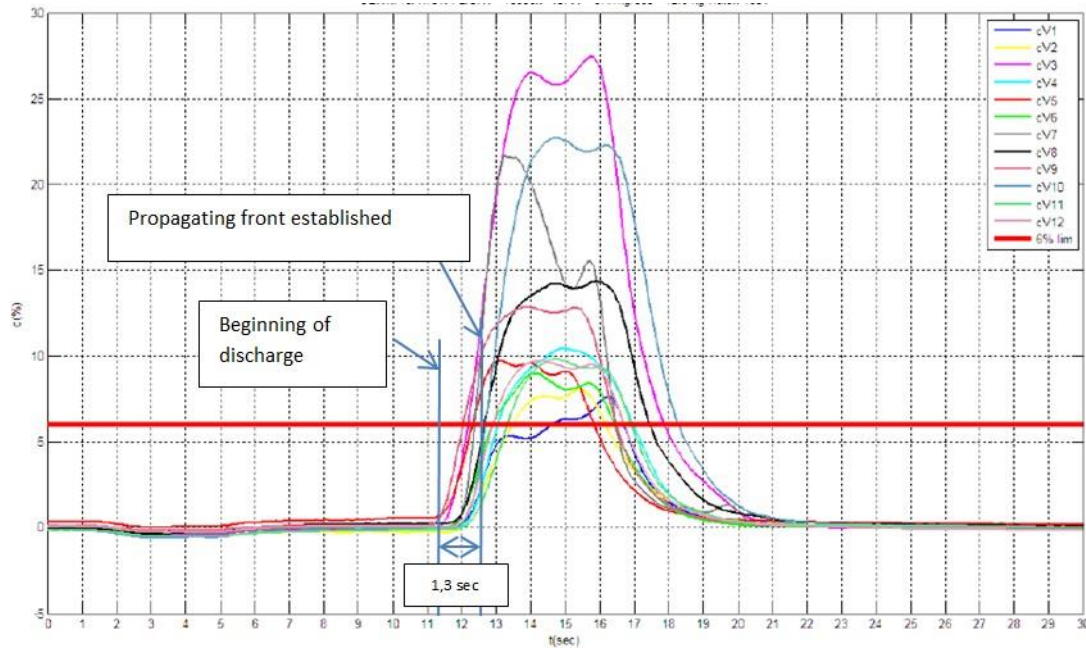


Figure 28. Representation of the beginning of the discharge process and the propagating front established.

As pointed, the requirements CS 25.1195(b) and (c) in [9] establish that a minimum level of 6% of halon is required to extinguish a fire. We can determine the minimum time required to get the 6% value thanks to the following expression from (Eq. 12):

$$\Delta t = \left(\frac{u}{|x|^{0,3277} 0,00102} \right)^{1/4,5}$$

This expression is tailored for $u = 0,06$ and $|x| = 4,012 \text{ m}$. Then, we have:

$$\Delta t = 2,24 \text{ seconds}$$

This value obtained, thanks to the solutions in Section 2.6.1 of [2], matches with the flight test data in Figure 28. According to this data, at $t = 2,24$ seconds, the sensors 2-4-8-10 are measuring above 6%.

The same process can be repeated for other sensor configuration. Let consider, now, the measuring line given by the following table:

Sensor configuration 2	Offset (m)	Maximum Volumetric concentration (%) at t = 15 sec
1	1,200	6,2
4	2,000	10,3
7	2,800	14
10	3,600	22

Table 3. Sensor volumetric measurements at t = 15 sec. The t = 15 sec is selected to fix a common reference time for model parameter obtaining.

The data in Table 3 can be represented as per the following figure:

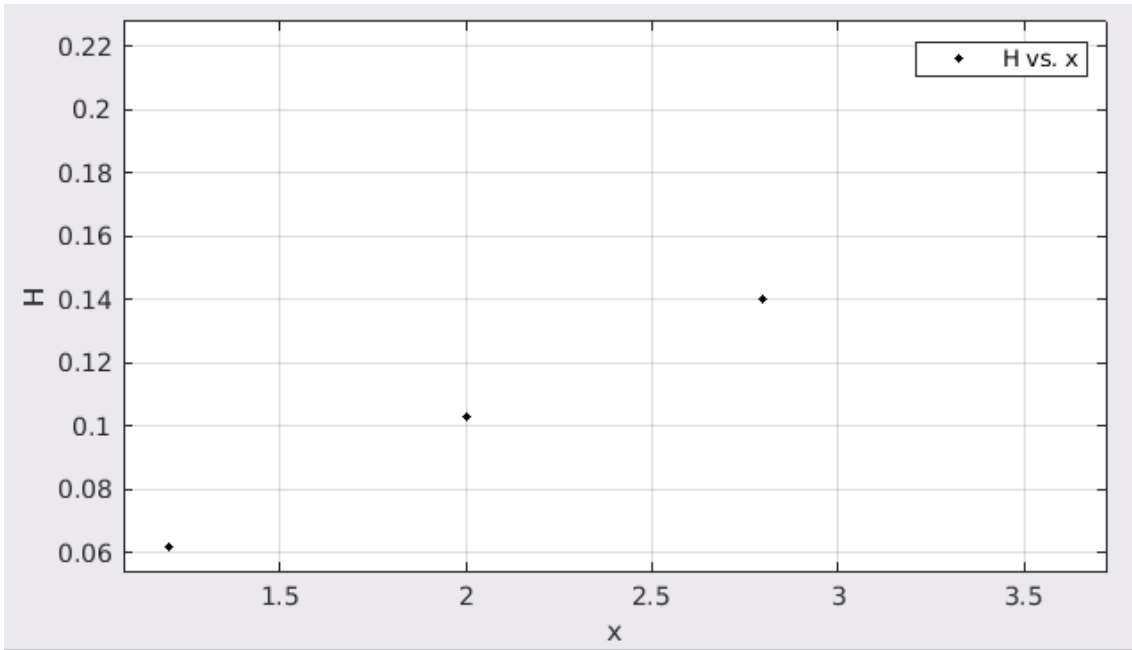


Figure 29. Halon concentration (H) expressed per unit, as function of the offset (x in meters) for the set of sensor configuration in Table 3.

The data is adjusted to the following power law:

$$u = 0,2551 |x|^{0.4345}$$

Which can be compared to the expression (Eq.10) that adopts the specific form:

$$u = |x|^{\sigma/(1-p)}(1-p)^{1/(1-p)}(15-12)^{1/(1-p)}.$$

Where the discharge time is considered at $t = 15 \text{ sec}$ and the beginning of the discharge process is set at $\tau = 12 \text{ sec}$. Then, we have:

$$(1-p)^{1/(1-p)}(15-12)^{1/(1-p)} = 0,2551$$

after resolution:

$$p = 0,76$$

And:

$$\sigma/(1-p) = 0,4345$$

$$\sigma = 0,10$$

Under the assumption that the reaction predominates over the diffusion, Section 2.6.1 in [2], provides the following condition to be met among the different parameters:

$$m\sigma + 2(1-\sigma)p + \sigma < 2$$

We obtain:

$$m < 7,32$$

For simplification purposes, we admit the following value for m :

$$m = 2$$

We check, now, the parameters condition to ensure the existence of global solutions as per Theorem 2.6.1.1 in [2]:

$$p < \text{sign}_+ \left(1 - \frac{\sigma(m-1)}{2} \right)$$

This condition is met, ensuring the existence of solutions

$$0,76 < \left(1 - \frac{0,1(2-1)}{2} \right) = 0,95$$

Therefore, the solution describing the behavior of the halon concentration exits as per the model (Eq. 10) along the line given by the sensor configuration 1-4-7-10. This solution adopts the form:

$$u = |x|^{0,4345} 0,00261 (t - 12)^{4,2}$$

Where:

$$0 < u < 1$$

Is the concentration of halon expressed per unit;

x is expressed in meters;

t is expressed in seconds.

As we did before, our next intention is to obtain the propagation front that results when considering the diffusion carried by the PME. For this purpose we consider the results as per Theorem 2.6.2.2 in [2]. Particularly, the positivity of the solution (i.e. the existence of halon concentration) is provided in the frame:

$$u(x, t) > 0, \quad \text{when} \quad |x| < c_2(x)t^\beta$$

Where,

$$c_2(x) = c_{supp} |x|^{\frac{\sigma(m-1)}{2(1-p)}}$$

And,

$$c_{supp} = \frac{(-\alpha + \beta)^{\frac{\sigma(m-1)}{2(p-1)}}}{\left(\frac{(m-1)\beta}{2m}\right)^{\frac{1}{2}}} = 0,717$$

$$\alpha = \frac{\sigma + 2}{\sigma(m-1) + 2(p-1)} = -5,52$$

$$\beta = \frac{p - m}{\sigma(m-1) + 2(p-1)} = 3,26$$

After compilation of results, we have:

$$u > 0, \quad \text{whenever} \quad |x| < 0,757 \cdot t^{4,075}$$

Therefore, the shifting front is given by the expression

$$|x| = 0,757 \cdot t^{4,075}$$

And represented in the following figure:

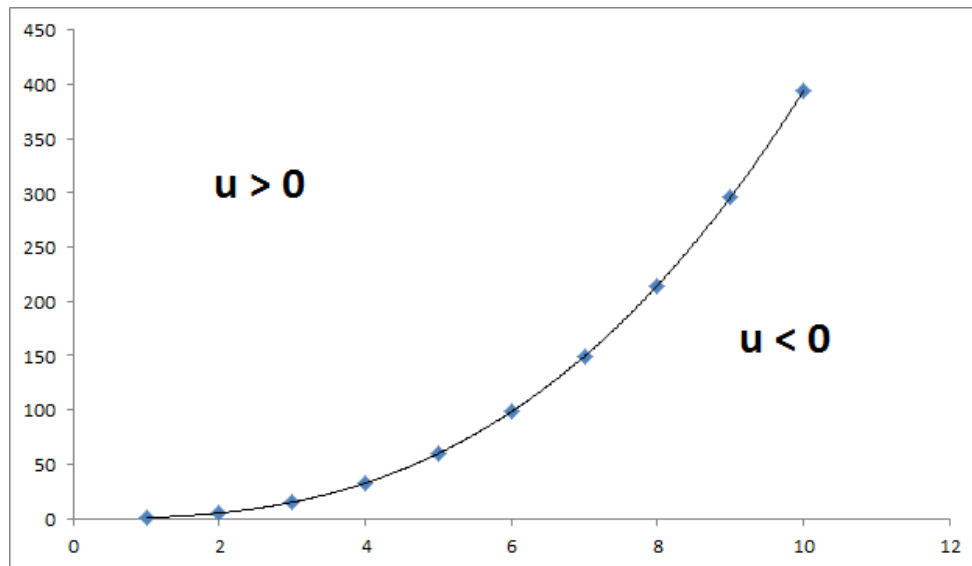


Figure 30. The propagating front, represented by the continuous line, is the effect of the diffusion and absorption while moving along the flow line characterized in table 3.

III. Conclusion

The main objective that has scoped our study has been to model in engineering making use of advanced mathematical principles. It has been shown, for the two models involved and dealt in Sections I and II of this report, that solutions exist and such solutions have been obtained and tailored for a real scenario. The governing equations, extensively studied in [2], have been calibrated making use of testing activities in Airbus aircraft platforms. Once the set of equations has been derived and made particular, the solutions obtained in [2] have been applied with success. At this point, we can conclude that our approach provides a set of solutions for each of the models derived that can be used to understand, assess and predict during any design activity.

The main added value of our approach is that the results are based on an analytical concept. This implies that any solution is valid provided it is applied within the correct scope. As no numerical mesh-type models are given, it is not necessary to introduce efforts for assessing the correctness of the numerical exercise via errors propagating principles, complex calibration and interpretation of results.

Additionally, the work performed along this memory permits to answer the following questions frequently asked by the design engineers.

- For the inerting system model (Section I), these questions can be formulated as:
 - How is the oxygen time evolution in the fuel tank? The answer to this question has been provided along Section I.6 of this document for an Airbus A320 aircraft.
 - What is the required time to ensure an inert fuel tank ullage? The answer to this question has been provided along Section I.7 of this document for an Airbus A320 aircraft.
- For the fire extinguishing model (Section II), the key questions can be summarized as:
 - What is the required time to ensure that the propagating extinguisher is capable of extinguish an engine fire? The answer to this question has been provided along Section II.5 of this document for an Airbus Military A400M aircraft.
 - How is the extinguisher propagating front in areas of the engine nacelle? The answer to this question has been provided along Section II.5 of this document for an Airbus Military A400M aircraft

We stress the fact that the work performed has permitted to answer the above reflected questions. In addition, we shall highlight that the simple questions have led to a set of novelties in the PDE theory, i.e. we have dealt with equations not previously treated permitting to ensure an academic path for our work [2].

We, finally, conclude that our objectives have been fulfilled for both the industrial and the academic perspectives.

References

1. National Transportation Safety Board (1996). *In-flight breakup over the Atlantic Ocean Trans World Airlines Flight 800, Boeing 747-141. Ref N93119*. Washington D.C.
2. Díaz Palencia, J. L. (2020) *Non-linear reaction and diffusion models in partial differential equations, with applications to aerospace and biomedical technologies*. Tesis Doctoral CEU. Madrid.
3. Bird, R.B.; Stewart W.E. and Lightfoot E.N. (1960). *Transport Phenomena*. John Wiley & Sons. NY. p 780.
4. Summer S.M. (1999). *Mass loading effects on fuel vapor concentration in an aircraft fuel tank ullage. Ref DOT/FAA/AR-TN99/65*. Washington D.C.
5. Burns, M.; Cavage, W.; Hill, R. and Morrison, R. (2004). *Flight-Testing of the FAA Onboard Inert Gas Generation System on an Airbus A320. DOT/FAA/AR-03/58*. Washington D.C.
6. Pesman, G. J. (1950) *Analysis of Multiengine Transport Airplane Fire Records*. National Advisory Committee for Aeronautics Research Memorandum. Washington D.C.
7. Gann, R. (2007) *Advanced Technology for Fire Suppression in Aircraft. NIST Special Publication 1069*. U.S. Department of Commerce. USA.
8. Standard Ref: Def Stan 00-970 (2017) *Design and airworthiness requirements for service aircraft*.
9. EASA (2006) - *Certification Specification for Large Aeroplanes CS-25 Amdt 2*.
10. Wikiwand. *TWA Flight 800 accident*. Recovered 24/01/2020. https://www.wikiwand.com/en/TWA_Flight_800.
11. FAA (2008). *Advisory Circular Ref. 25.981-1C. Fuel Tank Ignition Source Prevention Guidelines*.
12. Khan, S.; Grattan, K. and Finkelstein (2007) L. Mathematical Modelling. 6.11. Application of modelling in Engineering and Technology. *Education, Engineering and Economics* 395-404.

ANNEX I

function CRD

```
xinit = linspace (0, 60, 10000);
options = bvpset('RelTol', 10^(-6), 'Abstol', 10^(-6), 'Nmax', 10000,
'Stats', 'off');
solinit = bvpinit (xinit, @fguess);
sol = bvp4c(@dEqs, @res, solinit, options);
f = deval(sol, xinit);
plot(xinit,f(1,:), xinit,f(3,:))
xlim([0 0.02])
ylim([0 0.025])
xlabel('xi') % Etiqueta el eje horizontal
ylabel('f_1, f_2') % Etiqueta el eje vertical
legend('f_1=u', 'f_2=v') % Pone una leyenda
```

function F = dEqs(x, f)

```
%Differential equationsco
%The Function F is the vectorial representation of the equations (1.286)
and (1.290) in [2] with n = 0.568; m = 0.025; (a+c) = 0.075 and delta =
epsilon = 10E-4.
```

```
F = [f(2); (-0.075*f(2)-(1-f(1))*f(3)^(0.586))*100000; f(4); (-
0.075*f(4)+f(3)*f(1)^(0.025))*100000; f(6); (-0.075*f(6)-(1-
f(5))*f(7))*100000; f(8); (-0.075*f(8)+f(7)*1^(0.025))*100000];
```

function r = res(fa, fb)

```
r = [fa(1)-0.8; fa(3)-0.2; fb(1)-1; fb(3); fa(5)-0.8; fa(7)-0.2; fb(5)-1;
fb(7)];
```

function finit = fguess (x)

```
finit = [heaviside(-x);0; heaviside(-x); 0; heaviside(-x);0; heaviside(-
x); 0]
```